DEVELOPMENT OF OMNIDIRECTIONAL

COLLINEAR ARRAYS WITH BEAM STABILITY

FOR BASE STATION AND MOBILE APPLICATIONS

A thesis submitted in fulfilment of the requirements for

The degree of Master of Engineering

Robert A. Daly

School of Electrical and Computer Engineering

College of Science Engineering and Health

RMIT University

November 2013

RMIT UNIVERSITY

Development of omnidirectional

collinear arrays with beam stability

for base station and mobile applications

II

Robert A. Daly

RMIT University

Development of omnidirectional

Collinear arrays   with beam stability

For base station and Mobile applications

III

A thesis submitted in fulfilment of the requirements for

The degree of Master of Engineering

Robert A. Daly

School of Electrical and Computer Engineering

College of Science Engineering and Health

RMIT University

2014

Declaration

I certify that except where due acknowledgment has been made; the work is that of the author alone; the work has not been submitted previously in whole or in part to qualify for any other academic award; the content of the thesis is the result of work which has been carried out since the official commencement date of the approved research program; any editorial work, paid or unpaid, carried out by a third party is acknowledged.

Robert Andrew Daly

21/11/2013

V

ACKNOWLEDGEMENTS

GLOSSARY

AUT	Antenna under test
CDMA	Code division multiple access: mode of transmission
CPW	Coplanar waveguide
CST	Computer Simulation Technology: Company name
COCO	Coaxial collinear
BER	Bit error rate: data integrity parameter
dBd	Decibel power ratio relative to a dipole used to qualify antenna gain
dBi	Decibel power ratio relative to an isotropic radiator used to qualify directivity
dBc	Decibel power ratio below carrier level used to qualify PIM
D.C	Direct Current
Ɛr	Dielectric constant real
EM	Electromagnetic
GCPW	Grounded coplanar waveguide
MIMO	Multiple input multiple output
MMIC	Monolithic microwave integrated circuit
PIM	Passive intermodulation
GRP	Glass reinforced plastic
PIP	Peak Instantaneous Power
PET	Polyethylene terephthalate: A polymer used for flexible printed circuit substrate
RFID	Radio frequency identification
TEM	Transverse Electromagnetic
TDMA	Time division multiple access: transmission
UHF	Ultra high frequency 300-1000 MHz
VSWR	Voltage Standing Wave Ratio
WIFI	wireless delivered internet service

Table of Contents

VIII

IX

List of Tables

X

List of Figures

XI

List of Appendices

Abstract:

Since the 1800's, inventors have considered electromagnetic radiation as a medium for communications between ship and shore and base to mobile. Generally, these were narrow band services, supported by simple series fed arrays. These arrays are limited in bandwidth by an inherent tapered phase profile which exhibits an undesirable vertical beam angle shift with excessive change in frequency. This performance is not suitable for the modern broad band networks. Antennas that are suitable for these networks are the centre fed and corporate fed arrays. These antennas are relatively expensive and complex with a coaxial architecture to allow for the feed network to be routed up the core away from the dipoles. With a symmetrical tapered or linear phase profile, the radiation pattern remains on the horizon over at least 10% bandwidth.

This thesis aims to presents the development of an antenna which has a unique compact planar architecture, and has achieved the performance required for broad band communications channels in the 900 MHz band. With low cost; volume manufacture, PIM and PIP considered.

A major achievement in this work has been the development of a planar passive coupled dipole array with coplanar feed network presented on a single sided low cost flexible PCB. In this format, the array can be re produced accurately at a fraction of the cost of the conventional sleeve dipole arrays. Major challenges in the implementation of such a solution, are in the substitution of a coaxial feed network with planar alternatives and still maintain symmetrical phase profile stability and a reasonable power rating. Due to PCB processing limits for track spacing, the array has been designed with a main transmission line track spacing of 0.638 mm resulting in a higher impedance of 86 Ohms. At this track spacing, the main transmission line can withstand a 2.1 kV ionisation test allowing for a PIP value of 1 Kw. To compliment this planar array, a specially designed planar dipole; matched to the new feed network scheme. With slots to augment the radiation pattern for improved directivity and reduced azimuth ripple, and notches to stagger tune the dipole to cover a broader than otherwise band and compensate for the reactance associated with close proximity to the slotline tracks. This dipole meets broad bandwidth and omnidirectional pattern specifications similar to cylindrical sleeve dipoles, while still maintaining inter-stage isolation.

To further compliment the array attributes, a robust coaxial cable connection to the thin and flexible substrate employs a novel passive coupler transition circuit. The proposed transition is

1-14

electromagnetically coupled to source and ground terminals of the array, eliminating the need for soldering, resulting in low loss, low PIM "Passive intermodulation" typically <-148 dBc, This coupler also provides the impedance transformation from 70 Ohms to 50 Ohms

An omnidirectional six element "coplanar waveguide (CPW)" fed collinear array was assembled from the planar feed network, dipole elements and passive coupler components. Most research in the area of printed antennas is focused on small low gain antennas. This research presents a high gain antenna printed array supporting six elements with a centre fed network, having a total length approximately 1.8 meters. This large array has the unique attributes of wide band, less than 1 degree beam tilt over a frequency range of 850 to 960 MHz (for a measured reflection coefficient magnitude greater than 14 dB), with low measured passive intermodulation below -140dBc "Decibel power ratio relative to transmit carrier". The prototype collinear array can also withstand a wind loading of 240 km/h.

The resulting planar collinear antenna array meets all of the electrical specifications for low power base station applications, including operation in the desired frequency band, high gain, and extremely stable radiation pattern. A gain of 10 dBi has been achieved with omnidirectional radiation.

Chapter 1

Since the discovery of electricity and electromagnetic radiation in the 1800's, inventors have been actively exploiting this phenomenon as a medium for communications. The radio stations used in modern networks need reliable infrastructure which enables contact to all stations in order to transfer data and telephony. An antenna with this capability is the collinear array. Depending on its feed arrangement, the radiation pattern remains stable in shape within the band of operation. This thesis presents an antenna which meets these requirements in a unique planar architecture. The challenge in this design is the substitution of coaxial feed network with planar alternative, and still maintains effective inter-stage isolation and phase stability. It is designed to be low cost, with low passive intermodulation and provides a zero beam tilt pattern. In the industry these attributes are normally dominated by complex and expensive products. This cost reduction has been achieved by creating an array of dipoles and feed networks on a single sided flexible printed circuit. Both "coplanar waveguide (CPW)" and slot line feeders have been successfully integrated on this architecture. Some research has been active in the area of printed antennas, most focus on small low gain antennas. This new research is into a high gain antenna which is able to support six elements with a centre fed network. All components in this design have been optimized to provide a highly efficient performance with structural integrity.

1.1 Introduction

With radio networks expanding and the introduction of multicarrier digital radio systems with increased density some new problems arise, namely passive inter-modulation and peak instantaneous power. As radio networks become more sophisticated, they call for a higher standard in antenna construction to deliver the enhanced performance offered by the new systems [1].

The omnidirectional array antenna has three major methods of feeding as listed Table 1-1. The simplest is the series fed array where each element feeds through the residual current to the next element until a point of diminishing return is reached. Series feed networks are limited in operational bandwidth by frequency dependent beam tilt.

A more complex approach is the centre feed network, which is actually two series feed networks back-to-back with 180° offset in phase. The differential phase relationship, results in almost complete cancellation of beam tilt in the far field. To prevent aperture blockage, feed cables are shielded from the dipoles. This normally restricts the design to heavier tubular constructions that allow the cables to rout internally. The broadest band feed network of the three is corporate feed. In this configuration, the same power level and phase profile is applied to each element. The corporate feed has the advantage of broadband performance and a high power rating as each element shares the load of the applied power. Losses in corporate feed networks are usually higher than for a centre fed array due to extra cabling used in the design. This loss can directly affect the antenna efficiency and result in the gain of the antenna being lower relative to its overall length.

Historically, array antennas for cellular base station applications are hand assembled. This is to ensure reliable construction to meet the requirements of the new cellular systems, and enables independent low maintenance service. Conventional centre fed and corporate fed omnidirectional arrays can be complex in design and have many fasteners and soldered junctions. These attributes not only make manual assembly a lengthy and expensive process, but also are likely to contribute to the generation of PIM which is realised as noise in the receivers pass band. PIM affects both analogue and digital systems equally [2].

The multi-carrier environment of modern cellular systems brings to light another phenomenon known as PIP "peak instantaneous power". PIP is a function of multiple carriers combining into one antenna and can result in premature equipment failures. The issues of PIM and PIP are crucial points of concern for current base station array antennas as the availability of tower space is limited. The economical alternative is to combine multiple

1-17

transmitters/services into one antenna, resulting in higher incidences and consequences of PIP and PIM.

Table 1-1 Characteristics of the three conventional array feed types

Feed type	Advantage	Disadvantage
Series fed array	• Low cost • Simple construction • Light weight • Lower wind loading • Axis symmetric omnidirectional	• Frequency dependent beam tilt • Narrow band • Sharp gain response • No invert mounting due to tilt • Max gain limited by mechanical stability and progressive phase errors • Unpredictable coverage
Centre fed array	• Zero beam tilt • Can be invert mounted • Broad band • Beam tilt can be adjusted • Flat gain response • Can support combined transmitters • High continuous power rating • Highly predictable coverage	• Heavy weight • Relatively expensive, • Prone to vibration fatigue over time • High wind loading • Large radome diameter • Complex construction • Feed network must be routed inside antenna • High parts count • High labour costs
Corporate fed array	• Zero beam tilt • Can be invert mounted • Broad band • Beam tilt can be adjustable • Supports combined transmitter's high continuous power rating • Flat gain response • High gain arrays are possible over a wide band • Highly predictable coverage	• Heavy weight • High wind loading • Relatively more expensive than centre feed • Large radome diameter • Complex construction • High feeder losses • Feed network must be routed inside antenna • High parts count • High labour costs

1.2   Problem statement

The advances in communications equipment have resulted in a need for more bandwidth to allow for high speed data, digitally encoded cellular networks such as CDMA systems.   The antennas needed for these networks must be capable of supporting broad bandwidths. Maintaining phase stability is the challenge as phase instability manifests itself as shift in the vertical beam angle. This is known as beam tilt and will be discussed in section 1.2.1

There are some operational challenges for base station antennas in this new age of communications. The challenges relate to the integration of services into a finite spectrum. At some point the frequencies combinations allocated can mix together and generate a third order product of 2A-B and is known as PIM "Passive intermodulation". This subject will be discussed in section 1.2.2 yet another problem related to bandwidth is PIP "Peak instantaneous Power. PIP is generated as two or more transmitters are combined to utilize one antenna. The more transmitter power sources involved the higher the probability of signal peaks combining and generating a potentially catastrophic power surge known as Peak instantaneous Power which results in voltage spike. This phenomenon will be discussed in section 1.2.3

1.2.1   Beam tilt

When mobile radio systems were first introduced 50 years ago, the systems were quite basic and narrow band by today's standards. Most had single frequency requirements that were easily supported by simple series fed collinear array designs. Later, networks required the base stations to support more traffic and broader bandwidths, and to allow for duplex communications and multiple transmitters into one antenna. The frequency dependent tilt that is experienced by series fed antenna arrays to these broader bandwidth systems is seen in Fig 1-1.   Zero tilt is seen at the design frequency; however significant tilt may be experienced at the upper and lower band edges. This led to the introduction of higher performance antenna systems, such as the corporate fed and centre fed arrays. These arrays are capable of cancelling out the frequency dependent tilt.
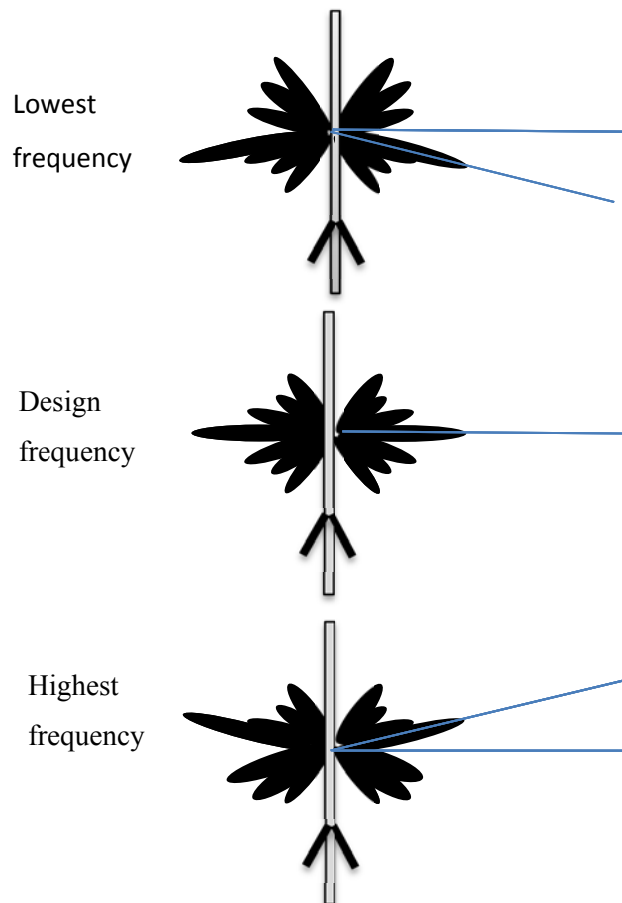
Fig 1-1 Frequency dependent beam tilt in series fed array

Beam tilt can be a significant problem for high gain series fed arrays. As the gain of an array is increased (i.e. increasing the number of array elements), the effect of the beam tilt is pronounced where the maximum tilt exceeds the 3dB beam width, causing the tilted frequency beam to appear in a null of the un-tilted frequency pattern. A tilt value of 7° is typical for a series fed array at the lower edge of an 8% bandwidth.

Clearly, the series fed array is only suitable for narrow band base station services [3]. Mounting antennas inverted to one another is an option to conserve tower space and stop series fed array tilting out of service. Series fed antennas when mounted in this way, tilt in opposing directions at the band edge frequencies, whereas as zero tilt antenna remains in service over a broad band as shown in Fig 1-2.

ries

s in

ays remain

at

ncy

of
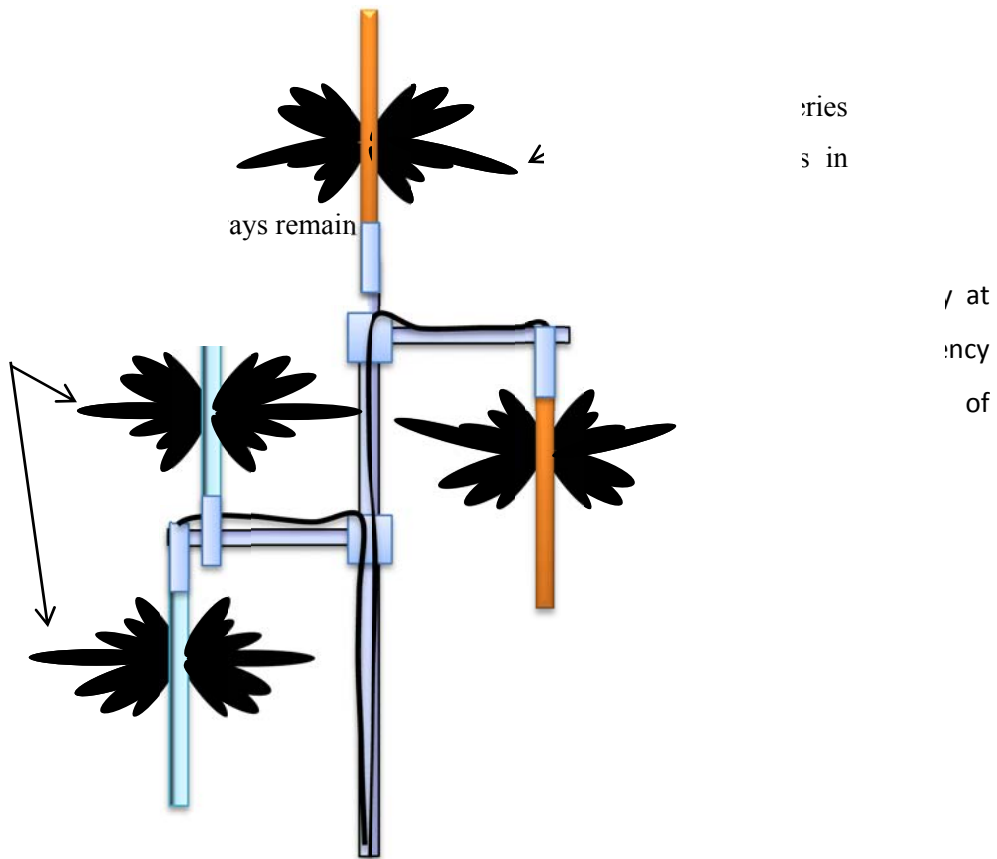
Fig 1-2 Zero tilt array vs. series fed array when invert mounted

It is apparent that series fed antennas when operated away from the design frequency can provide a narrow band of useable down tilt. This may be desirable in a narrow band service, where a single channel transmitter is location on high terrain and may over shoot the fringes of the coverage area as shown in Fig 1-3. Fig 1-4 exhibits how a slight tilt has improved the coverage for an elevated terrain site.
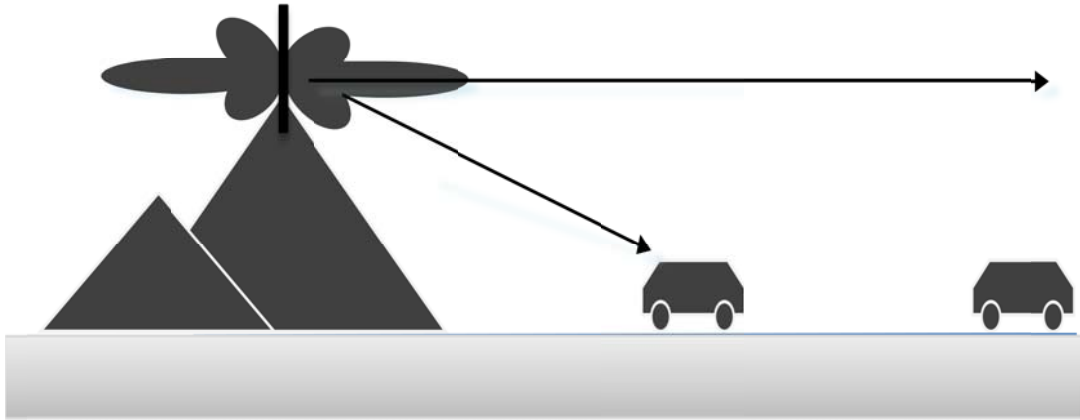
Fig 1-3 A base antenna that has overshot the fringe area
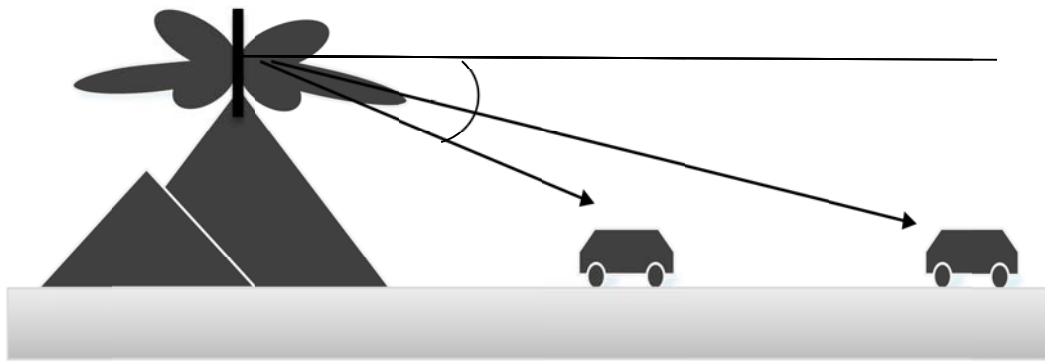
Fig 1-4 The series fed base antenna corrected using beam tilt to cover the fringe area

Operating a series fed antenna array offset from the design frequency tilts the main lobe.

The level of tilt determined by the manipulation of Eqn. (1.1)

$$\psi = kd \cos \theta + \beta_\theta = kd \cos \theta_0 + \beta = \vartheta \Rightarrow \beta = -kd \cos \theta_0 \qquad (1.1) [4]$$

$\psi = relative\ phase\ between\ elements$

$\beta = \text{Progressive } phase\ lead\ current\ exicitation\ difference\ between\ elements$

$d = Separation\ distance\ between\ sources$

$\theta = reference = 90° for\ broadside\ radiation$

ϑ = beam tilt angle

Alternatively down tilt can be set to a particular value for a number of reasons in a radio network, for example, interference suppression or simply to enhance the coverage in a restricted area as seen above. Down tilt can also be used as a method used to attenuate crosstalk from adjacent cells allowing for frequency reuse [5], [3] as shown in Fig 1-5.
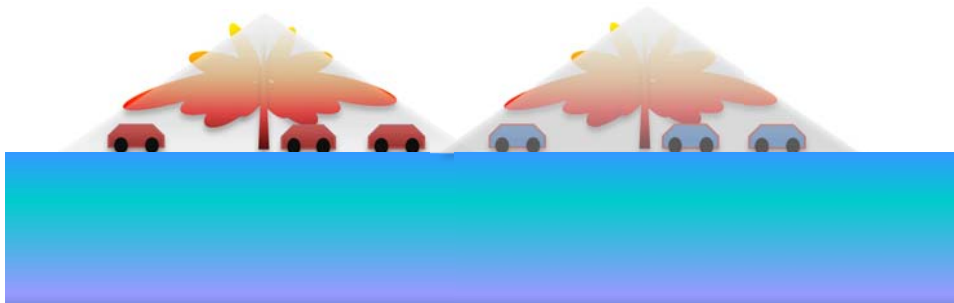
Fig 1-5 Beam tilt in base station arrays to allow for frequency reuse

In a cellular networks, pattern shaping including beam tilt is an option to firstly limit the size of the cell and secondly increase the carrier to noise C/N ratio by up to 10 dB [3], [6]. In some applications, mechanical beam tilt is used [3]. Fig 1-6 shows how mechanical down tilt is used

independently of electrical tilt. The rear lobe tilts up, resulting in a beneficial null being directed close in behind the antenna.

In Fig 1-7 it is shown that electrical tilt is effective when used with omnidirectional arrays as the entire azimuth pattern is tilted down to the required angle. For unidirectional arrays where down tilt is used to fine-tune the cell coverage, electrical tilt will also down tilt the rear lobe which may not be desirable. Electrical tilt can be controlled remotely by mechanical actuators attached to phase shifting elements within the array [1]. Others methods are in the form of a rheostat, an arc shaped conductor element with a contactor to tap at variable phase lengths on the transmission line. Patents protect most of these tilt mechanisms [7], [8].

Omnidirectional   Unidirectional
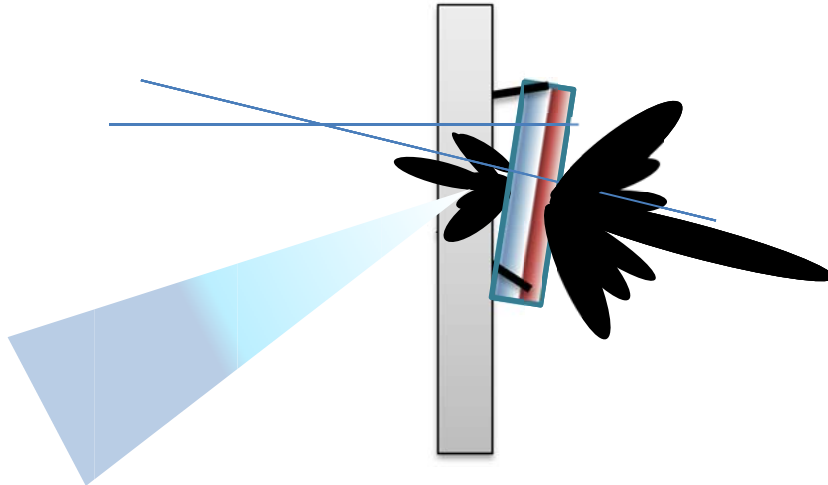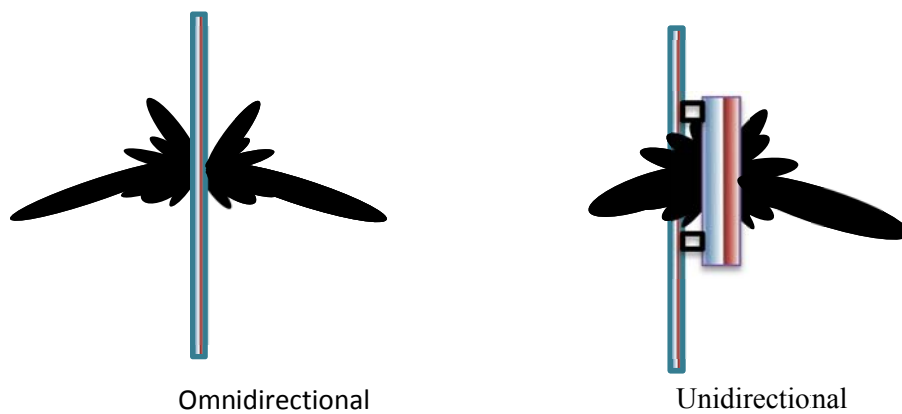
Fig 1-7 Electrical beam tilt in omnidirectional and unidirectional antenna arrays

The characteristics of the antenna pattern in conjunction with terrain path loss can be employed to predict coverage. Fig 1-8 and Fig 1-9 illustrate how effective this mapping is, the former showing a coverage mapping for Newland Hill SA for a zero tilt base station [9], and the latter with a 5° down tilt applied. An increased area for frequency reuse is indicated in Fig 1-9.
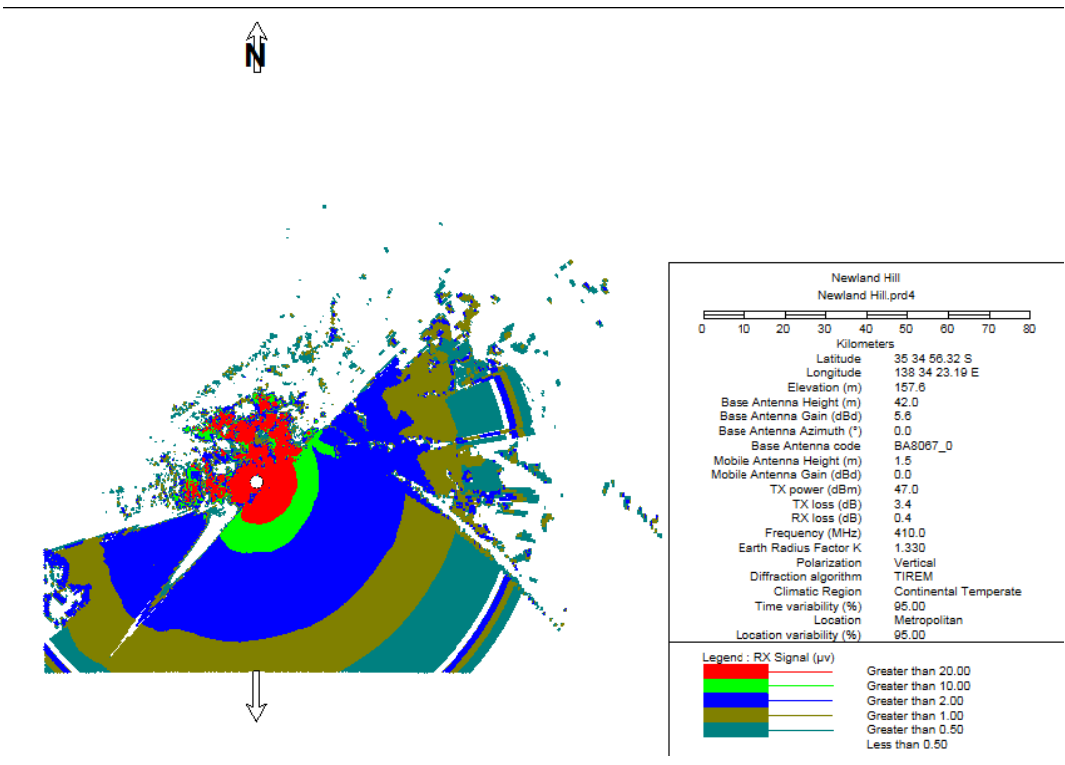
Fig 1-8 Field coverage prediction map with no beam tilt [9]

Reuse of a channel could be allowed in this region
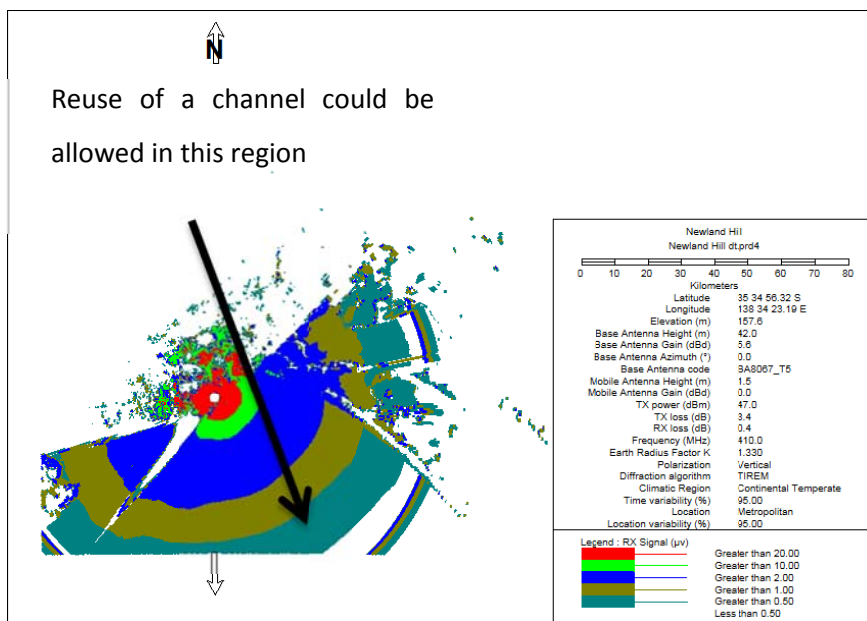
1.2.2   PIM "Passive intermodulation"

Passive intermodulation (PIM) is caused by the mixing of two or more carriers resulting in higher order products. PIM can occur in solder joints and loosely braided copper [10] [11] [12]. Ferromagnetic materials such as ferrites also generate PIM. Any plating containing nickel is likely to cause PIM. Loosely fitting tubes that are only partially soldered can cause PIM. The most concerning mixes are third order products as they are most likely to appear within the operational frequency band of the system, no amount of filtering will eradicate PIM. The 3rd order emissions are at higher amplitude than the other products (such as the 5th and 7th order) as shown in Fig 1-10. The 3rd order products are generated under the conditions 2a-b and 2b+a, fall close to the mix frequencies associated with the system TX channels denoted

a and b. If the carrier levels are stronger than the normal expected receive level, the 3rd order product can break through the receiver noise threshold, as indicated in Fig 1-10   This intermodulation "noise" will increase bit errors in a digital system reducing the network capacity. It will desensitise the receiver channels in a conventional duplex system.

$$2a - b$$
$$3a - 2b$$
$$4a - 3b$$
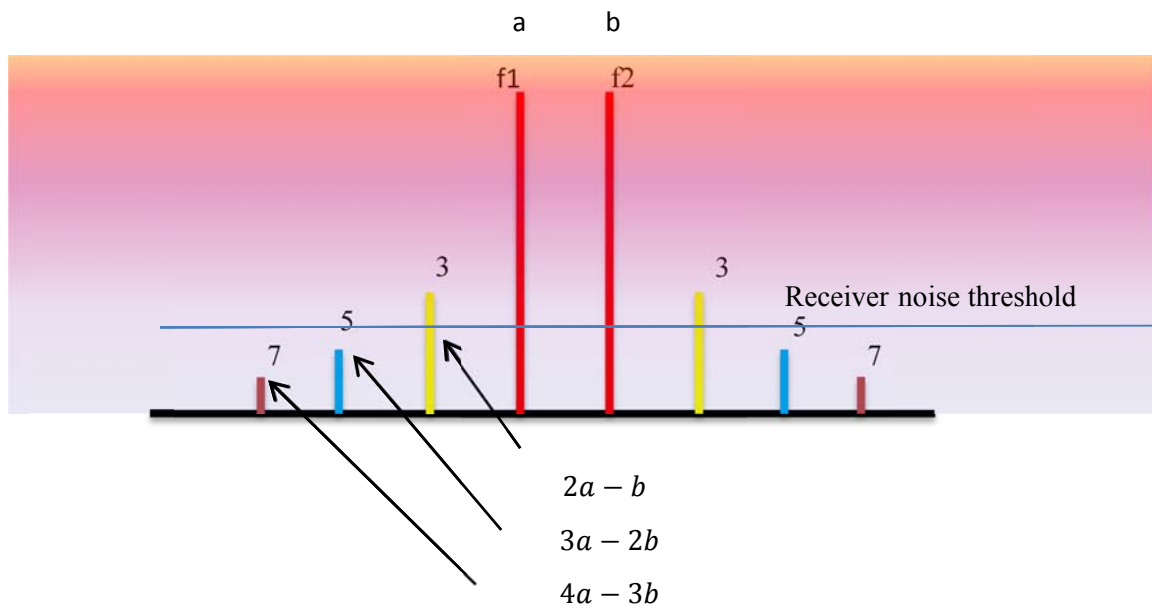
Fig 1-10 Intermodulation products

A conventional soldered coaxial cable interface to the dipole is historically most susceptible to PIM in an array design. Designing this interface with what is known as PIM mitigation

1-27

techniques should result in minimizing PIM. PIM mitigation can take the form of semi rigid coaxial lines, keeping the assembly clean and free of metal particles. The measurement of devices immunity to the generation of PIM is done using a test set that excites the potential for PIM in a device. To be effective the test set itself must have high PIM immunity. Shown in Fig 1-11 is such a test set. It comprises of all the components necessary to couple two transmitters into one output that produces the intermodulation carrier. A receive band pass filter is used to detect only this product, and reject the fundamental carriers from the transmitters. Some notch reject filters are added to the transmit output which further suppress the fundamental carriers from reaching the receiver. To measure PIM levels of -150 dBc, the test set must be capable of measuring -160 dBc. The intermodulation product is such a low level; a low noise amplifier is needed to increase the resolution.
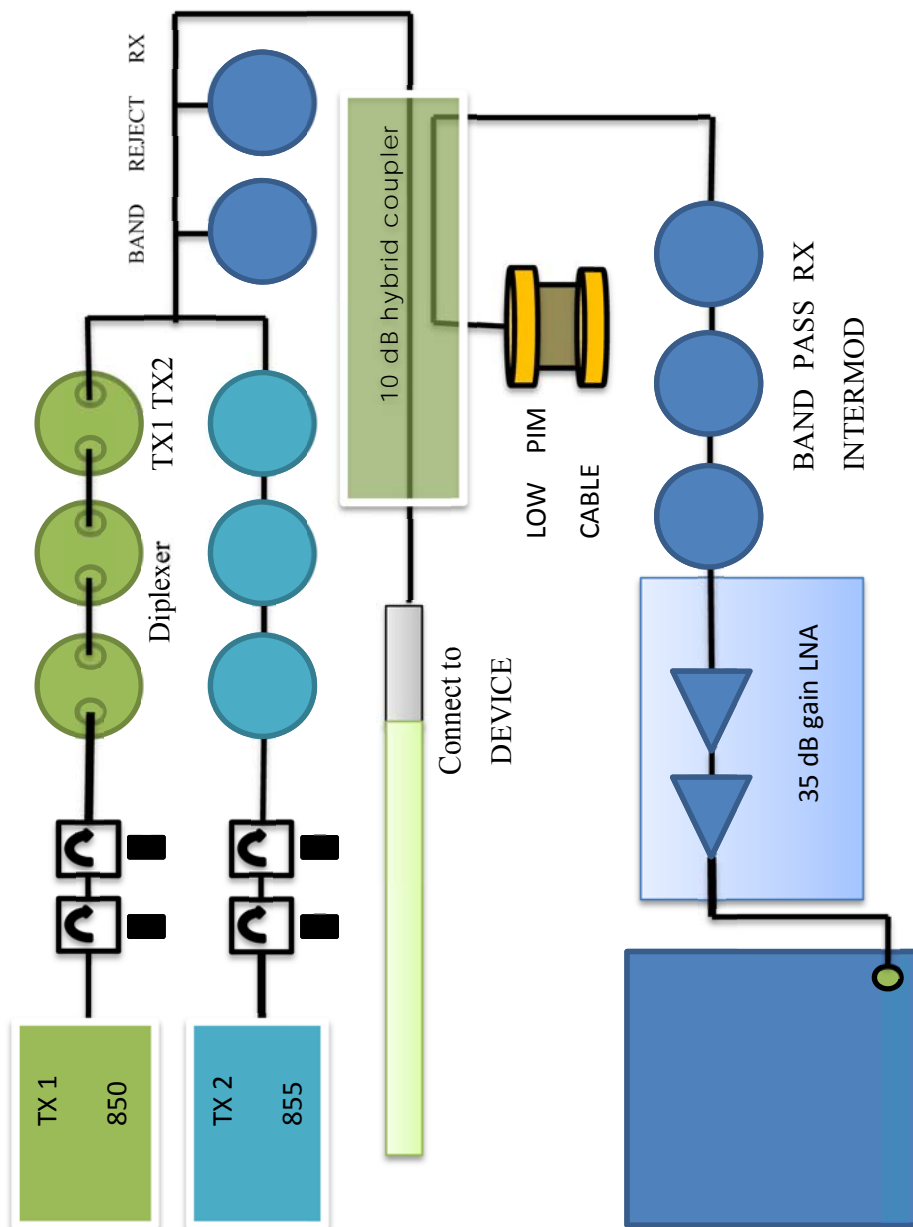
Fig 1-11 PIM test setup

1.2.3 PIP "Peak Instantaneous Power"

With advanced radio networks using multi-carrier digital schemes, there is a statistical chance that multiple transmitter carrier powers can combine in-phase to generate a high voltage gradient within an array combiner/feed network [2]. This voltage is capable of destroying the insulation components in an array, including coaxial cable dielectrics and insulators.

For all base station arrays that support multiple carrier systems, electrical acceptance testing should also include a non-destructive high pot test at a peak level of approximately 2.1 kV [2].

1-29

This test involves applying a high voltage to the components in order to detect and highlight faulty solder joints, intermittent contacts, moisture and contaminated dielectrics. Failure to detect these quality points can result in early system failure.

For non-destructive device testing, the applied voltage is gradually increased towards the peak voltage whilst monitoring the leakage current as shown in Fig 1-12. If the current exceeds a pre-set threshold or an arc occurs before reaching the test voltage the device has failed and the applied voltage resets. The voltage spike associated with PIP is not readily detected by conventional power meters. It is normally seen as noise affecting the bit error rate (BER). The measurement of PIP is not practical, and prevention is preferable. Eqn. 12 can be used to calculate the potential value for PIP based on the power, modulation index and the number of transmitters in use at a transmitter site.

$$PIP = 2 \times 10^{\left[\frac{20\log_{10}(N) + 10\log_{10}(P_{ca}) + M}{10}\right]}$$ (12)

M = modulation Peak to Average ratio dB

P_{ca} = Power per channel at antenna port in watts

N = Number of channels in use
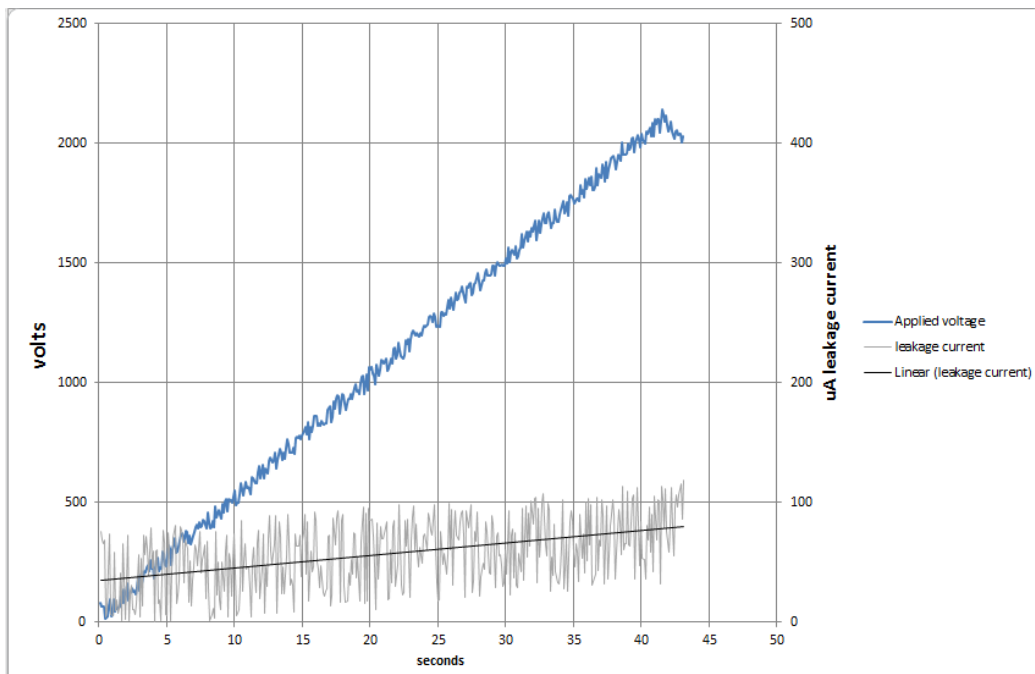
Fig 1-12 Non-destructive ionisation test

1.3 Aims of the thesis

This thesis will present research into a new cost effective and environmentally friendly option for base station antennas that will not only eliminate radiation beam tilt with change in frequency, but also substantially reduce the PIM potential by using a single copper layer on a printed flexible substrate. A passive coupling technique is employed to distribute power to the antenna elements, allowing for a more compact architecture and expansion to a greater number of elements for a higher gain if required. Other planar omnidirectional arrays with zero beam tilt found in the literature are not as adaptable.

A comprehensive set of electromagnetic simulations and optimisations are presented to achieve the highest performance possible from the printed planar array. Another feature is the entirely passive coupled input, meaning the base station array has no DC continuity to the interfacing connector. Electromagnetic coupling of the ground and source lines of the input connector is employed for improved mechanical stability, and to provide a gradual transition from the coaxial mode of the connector to the "Coplanar waveguide (CPW)" Quasi TEM "Transverse electromagnetic". The design has less environmental impact than antennas designed using aluminium or brass tube sections with many solder connections.

The outcomes from this thesis are expected to spawn further research in the area of high specification antennas using printed circuit based construction. This novel type of feed network is not restricted to omnidirectional base station antennas, and may find applications for smart antennas and patch arrays with the implementation of spatial diversity.

1.4   Thesis objectives

This thesis investigates a solution to the problem of frequency dependent beam tilt in an omnidirectional array, in a form that is suitable for high volume manufacturing and low cost. The array will provide a VSWR and radiation pattern performance, which meets or exceeds the currently available centre fed antennas.   The feed network will make use of planar transmission lines to form a compact and efficient centre feed network with gable phase profile [13] suitable for a centre fed omnidirectional array.   The feed network will be well isolated from the radiation element.   The array will be flexible in such that the addition of more antenna elements to the array is possible without exceeding a fixed radome diameter of 63 mm.   The array will provide sufficient mechanical stability with enhanced PIM and PIP performance by using passive coupling to the input, as opposed to a directly soldered connection.   The outcomes of this new research will contribute to the development of highly efficient planar feed networks for collinear array antennas for current and next generation communications systems.

1.1.1   Chapter overview

CHAPTER 2 outlines the design and performance of a planar feed network for a zero tilt collinear array. The implementation of a "Coplanar waveguide (CPW)" main line with compact parallel slot transmission lines to connect to the dipoles is described.   The motivation and techniques used in developing this feed network are explained, with the objective of maintaining a minimal width to the array.

CHAPTER 3 details the design of a new broadband planar dipole to suit the coplanar feed network described in Chapter 2.   The planar dipole is shown to have the broadband performance of a cylindrical dipole of similar width, enabled by the use of edge slots and notch features in the printed element.

CHAPTER 4 introduces a passive coupled "Coplanar waveguide (CPW)" to microstrip transition circuit that provides a rigid interface to the input connector of the collinear array. The coupler covers the 850 – 960 MHz band and provides a gradual transition from the "Coplanar waveguide (CPW)" modes to the microstrip mode. Mechanically, this transition is novel as it allows a flexible substrate to interface with a rigid laminated PCB providing an efficient coupling to the antenna without DC continuity. It also offers enhanced mechanical stability suitable for the direct connection of a coaxial cable or connector. In conjunction with the solder free printed circuit based array, the DC isolation helps provide exceptional PIM and PIP performance. A special low PIM cable transition is also developed and used to interface to the attached cable.

CHAPTER 5 explains the integration of the sub-assemblies to realise the complete printed collinear array with frequency independent beam direction, and presents a discussion on the simulated and experimental results. The power handling and mechanical performance of the array are also examined. Methods of providing a fixed beam tilt in the array are also investigated.

CHAPTER 6 provides a summary of the key conclusions from the research, and suggests avenues for future investigation.

1.5 Specifications

The specifications in Table 1-2 and Table 1-3 are based on the expected performance of a conventional collinear array antenna with consideration given to the lower temperature substrate of the prototype and reduced power rating.

Table 1-2 Proposed electrical specifications of the collinear array prototype

ELECTRICAL SPECIFICATIONS	
Frequency band	850-960 MHz
HPBW	10.5 degree typical
Gain	10 dBi
Side lobe suppression typically:	-10dB
Azimuth pattern stability	+/- 0.8 dB over 360° 10% bandwidth
Tilt	0 degree +/- 1 over 10% bandwidth
With the option to offer up to	4° down tilt.
Power rating:	100 Watts Maximum at 26° C
VSWR:	<1.5:1 over 10% bandwidth
Connector interface:	7/16 Din jack
PIM:	-150 dBc test two carrier @ +47dBm
Peak Instantaneous Power:	1 KW

Table 1-3 Proposed mechanical specifications of the collinear array prototype

The wind loading characteristics based on array length	
Projected area	$1270 \; cm^2$
Lateral thrust @160 km/h	160 N
Wind gust rating	>240 km/h
Torque @ 160 km/h	73 Nm
Length:	1850mm
Radome OD:	76mm
Mounting:	89 mm diameter
Weight:	2 kg

1.5.1 Limitations

There are several commercial limitations for the printed collinear array for base station applications. The major ones are listed below:

1.   The proposed array will be suitable for low power telemetry and cell extension applications where the applied power <100 watts, based on the printed materials used for the feed network and antenna elements.

2.   It is restricted in diameter to a standard off the shelf radome with inner diameter of 63 mm.

3.   Printed track spacing is governed by the PCB processing tolerance, which sets a minimum conductor track spacing of 0.5 mm.

1.6 Literature review

In section 1.6.1, discussions on self-choking function of sleeve dipoles. This function, related to dipole array antennas. The next sections 1.6.2 to 1.6.8 describe the applications, the regulations and the details of the three different feed methods for the collinear array antenna. In section 1.7 the limitation related to all base station antennas.

1.6.1 Self-choking related to dipole array antennas

Each dipole in an array is related to the next through mutual coupling. The mutual coupling effects can be minimised by suppressing the induced currents between the elements. The effectiveness of this choking can be seen in the radiation patterns where an improvement is pattern side lobes are reduced.

The dipole isolation is tested by feeding one dipole whilst measuring the level of that signal across the terminals of another dipole in the array. Mutual coupling is always present in an array of dipoles. Its effects are reduced by inter element choking ("High impedance barriers that act to cancel surface currents between the dipoles")
The use of a cylindrical dipole in an array has an infamous function of "self-choking". This function helps to prevents out of phase radiation from distorting the radiation pattern. A typical dipole to dipole isolation > 25dB is achievable with an element spacing of 0.81λ as shown in Fig 1-13.
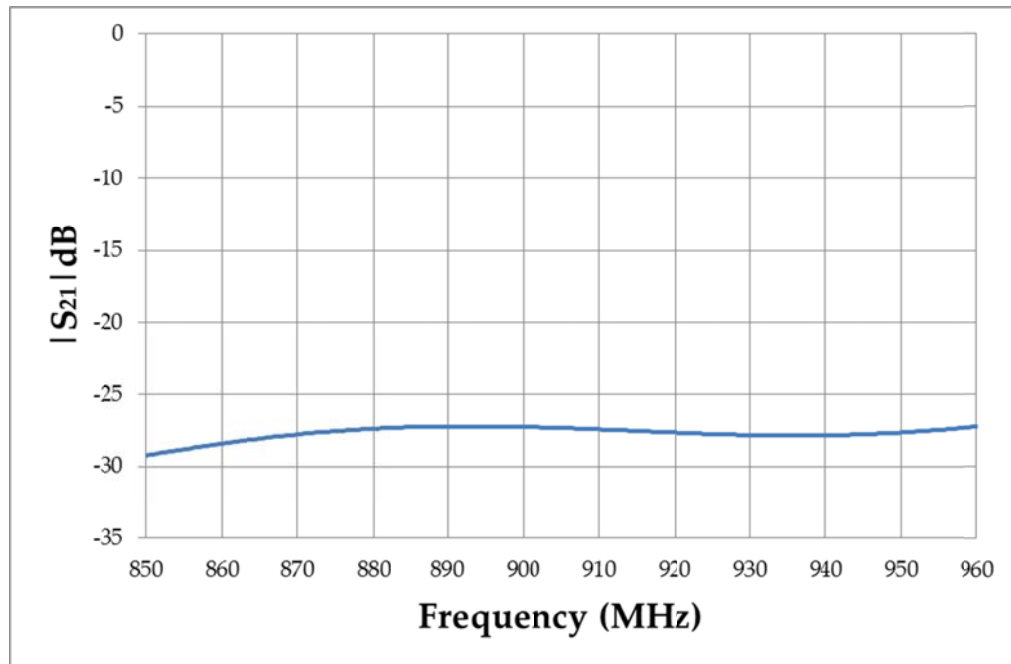
Fig 1-13 The typical response for inter element isolation

The choke action of the dipoles is controlled by the internal $\lambda/4$ long cylinder cavity where the low impedance short circuited bulkhead is reflected and inverted to form very high impedance which is presented at the open end of the choke [7], creating a quiet zone. as shown in Fig 1-14(a). The planar dipole also provides a narrow band self-choke function, which is slightly less effective than the cylindrical version, as shown in Fig 1-14 (b). This function appears in a planar form as the dipole arms reach $\lambda_g/4$. Currents that make their way on the inside arms of the choke are cancelled out by the high impedance presented at the open end of the dipole as shown back to back in Fig 1-15 , where the impedance and current relationship is found.

1-37

a)

Quiet zone

(b)

Fig 1-14(a) Cylinder and (b) planar choke analogue showing the self-choke function

Current level
after choking

Current level
before choking

Equivalent circuit

λ/4

Non-
radiating

λ/4

High Z

High Z

Low Z

Low Z
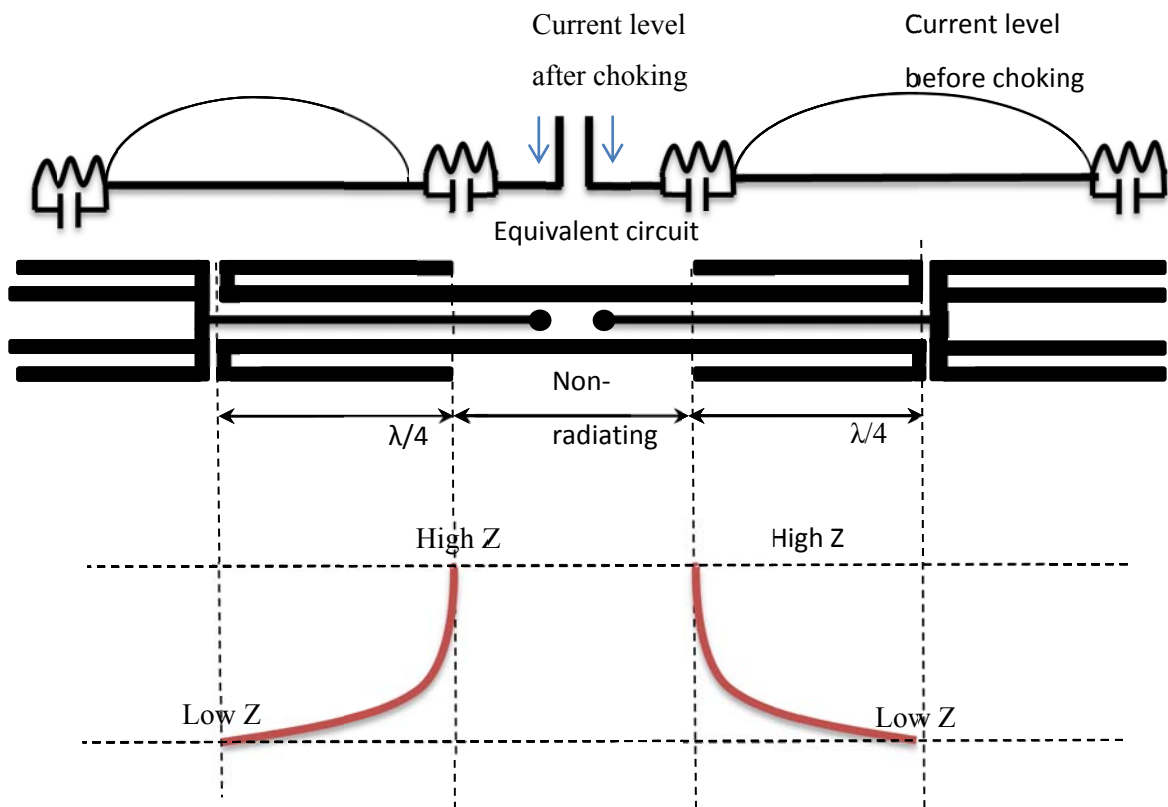
Fig 1-15   Back to back choke impedance to odd mode on two-element conventional sleeve dipole

1.7 Antennas for base station applications

Most of the literature for this type of antenna is in the form of patents from the 1980's when there was fierce competition to supply antennas for the utilities and car phones applications in the VHF and UHF bands. These patents were filed by major commercial entities of that time. Most have now specialised in the cellular base station arrays. Some have merged, and some are no longer trading. Hence, the public literature is scarce and there has been very little development of this type of antenna since this time. Antennas manufactured today are mostly adaptations of the earlier designs.

The omnidirectional collinear array antenna has been the critical component of mobile radio since the 1930's [14]. The broad omnidirectional pattern with narrow elevation beam width is most suitable for mobile communications base stations. In some applications, the azimuth pattern is shaped to suit specific requirements of the network [3]. The collinear array antenna finds applications for military command posts, aircraft traffic control, marine sea phone and emergency beacons, and public mobile radio. However, they are most widely used for cellular mobile telephone services and Wi-Fi broadband internet services.

1.7.1 Antenna specifications regulation

As this is a performance sells market, antennas gain and power ratings are in many cases over stated. For example some manufacturers claim a two-element array has a gain of 3dBd and a four-element antenna has a gain of 6dBd. This is incorrect as aperture size, internal losses such as phase delay error, VSWR and resistive losses all restrict the realised gain. To help address this problem, a standard TIA329 [15] is in place to regulate the industry. It standardises how pattern measurements are performed, and presents a standard gain antenna design that can easily be fabricated and used as a common reference for all antenna specifications linked to a set formulae. At frequencies above 600 MHz, a pyramidal horn is used as the gain standard. Below 600 MHz, dual dipole flat panel arrays covering each segment of the band are used. Many companies are now promoting their products with reference to TIA329 gain standards and conditions.

Power ratings are another perceived indicator of superiority in the industry. These figures are usually estimates based on the power handling of the coaxial cables considered the most at risk part of the design. Antennas with highly reactive matching circuits are likely to produce damaging standing wave hot spots resulting dielectric stress and melting well before reaching the power limit of the cable.

1.7.2   Characteristics of the collinear array antenna

The main objective of the collinear dipole array antenna is to provide an advantage in the form of gain over that of a single dipole by compressing the available power into a narrow beam directed into the coverage area. The total power radiating from a single dipole is congruent with that of a high gain array. Collinear array antennas classified as broadside have pattern maximum occurring at right angles to the centre axis of the array. Omnidirectional collinear arrays distribute this energy radially. A maximum lobe occurs at θ = 90 degrees when each dipole element is fed on the same phase front (in phase), and has a symmetrically tapered or equal amplitude current distribution applied.

The omnidirectional collinear array in its practical form is an array of dipoles which are positioned in a linear pattern most commonly in the vertical plane at a spacing of less than a guided wavelength. At this spacing, the resultant radiation pattern provides a maximum gain at zenith. At larger spacing's, extra lobes appear (grating lobes) which reduce the amount of power available at the main lobe [13].

Symmetrical aperture tapering methods such as binomial and Dolf-Tchebyscheff [13] can reduce the side lobe level from collinear arrays to below 20 dB; however this results in a reduction in directivity. Specific applications such as mono pulse radar and adaptive beam antennas require high side lobe suppression to reduce backscatter ghosting [16]. To realize such low side lobes requires additional attenuation and variable phase shifters at each feed source. An acceptable side lobe / gain balance can be achieved when an array has an element spacing of 3/4 λ or less. A collinear array energised by a travelling wave, must consider some fundamental rules and constraint, including a consistent element spacing of less than a wavelength and an element length equal to or below $\lambda/2$. A non-compliant design in most cases will

result in unpredictable performance and severe pattern distortion. Self-radiation of the feed network is a common cause for pattern distortion [3].

The advantage of the increased gain is delivering intelligible communications over a wide coverage area, especially where repeater stations are used. Repeater stations rely on high performance antennas to receive the weakest signals and rebroadcast these signals to the fringe of the radio horizon, which maybe 125 km radius from the repeater depending on frequency. The repeaters are normally duplex with frequency splits of up to 10 MHz. It is most important in these systems to cover the same geographic area with reception and transmission. Most repeaters will be located on elevated sites high above the coverage area. A series fed array may not be able to provide this level of performance due to beam tilt with change in frequency, as shown in Section 1.3.

1.7.3   Series fed arrays

The series fed array is a very simple design. In most cases the same element geometry is repeated throughout the array, leading to lower manufacturing cost. An omnidirectional series fed collinear array schematic shown in Fig 1-16. The gradient colouring of the arrows represents the current amplitude taper over the length of the array. Most series fed arrays have very high input impedance, as impedances combine in series at the input. Series fed arrays also have a progressive phase error, which limits the pattern stability over frequency.
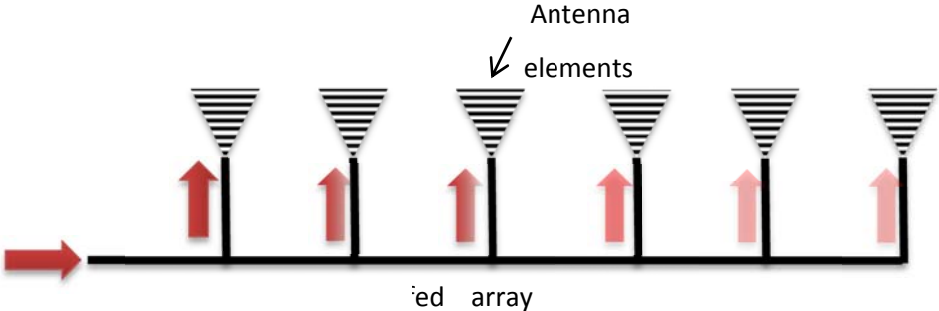
Fig 1-16 Schematic of a series fed array

A series collinear array antenna can be realised using several sections of resonant wire lengths of $\lambda/2$ to up to $5\lambda/8$ long separated by a phase shifting devices such as coils or meanders, as seen in Fig 1-17. The meandering sections of this array create a phase shift such that the second half cycle of the wave is absorbed, leaving only the positive half cycle to radiate [17] whilst the non-radiated energy is dissipated as heat. Applications for these meander type collinear arrays include narrow band VHF base station antennas and mobile mounted antennas for military and utilities. Analysis of this type of array has only ever been approximated [17]; the complexity of such modelling is the antenna elements and phasing sections are interdependent impedance transformation elements. That is, the radiation function and the matching functions are inseparable.
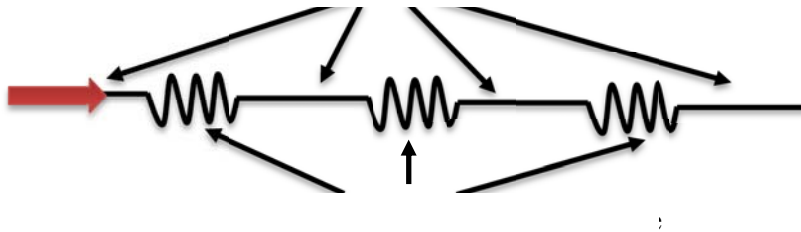
Fig 1-17 Meander type collinear array

A series fed array can also be realized using sections of coaxial cable interconnected in transposition as shown in Fig 1-18 [18]. This array functions by routing the applied energy inside the coaxial cable non-radiating sections in each half cycle, leaving the exposed sections to radiate on the positive half cycle. This ensures that only the positive part of the cycle is able to radiate, resulting in a single major lobe and smaller side lobes. There is extensive literature on the numerical analysis of this type of array antenna [19]. The feed point impedance for this antenna increases with the addition of more elements. The design is suitable for narrow band commercial products in the UHF 400 MHz band.

1-42
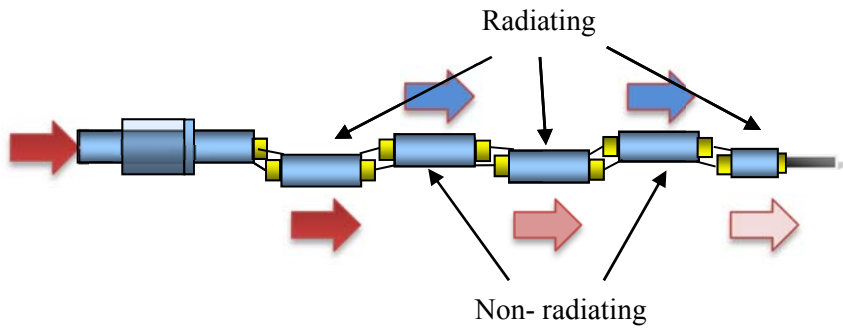
Fig 1-18 Transposed cable antenna array

Another coaxial cable based antenna known as a suppression collinear array [20] is shown in Fig 1-19. The suppression collinear array creates an alternating radiator element/suppressor structure consisting of resonant/low impedance radiator sections, and non-resonant/high impedance suppressors at the design frequency. This array feed point impedance is high (typically > 300 Ω) and requires a complex matching circuit such as dual stub tuning at the input. As the impedance is highly reactive, these antennas have a very narrow impedance bandwidth, typically around 3% [21]. The antenna finds application as a narrow band base station antenna in the 400-1000 MHz band.
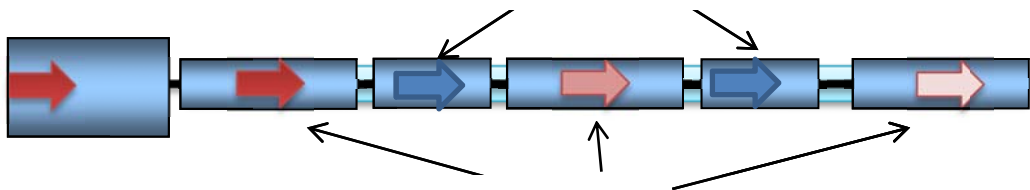
One of the most common series fed antennas is the annular slot fed coaxial sleeve dipole array, also known as COCO ("Coaxial Collinear"), as depicted in Fig 1-20. It comprises of a number of welded dipole assemblies mounted one above the other. A coaxial cable with outer shield removed is inserted, forming an array of annular slots between the dipole bulkheads of each assembly which feed each adjacent sleeve dipole. The elements are field isolated from one another by the integral $\lambda/4$ choke in the dipole sleeve. As the feed lines between dipole elements are coaxial cables, the

1-43

element spacing is governed by the velocity of propagation as calculated in equation (1.2) [22]. This propagation delay determines the electrical length of the cable used in the antenna impedance matching circuits as well as the element spacing. A spacing of 0.7λ is ideal for low side lobes [13]. The metal element components provide a high degree of thermal dissipation making this design suitable for higher power applications. As the element diameter is much greater than that of the coaxial cable, this antenna can provide a broadband VSWR response. The feed point impedance is also lower than previous examples mentioned above.

$$V_p = \frac{c}{\sqrt{\mu\varepsilon}}$$ (1.2)

where:

c = velocity of light = 3×10^8 m/s

μ = permeability of dielectric

ε = permittivity of dielectric
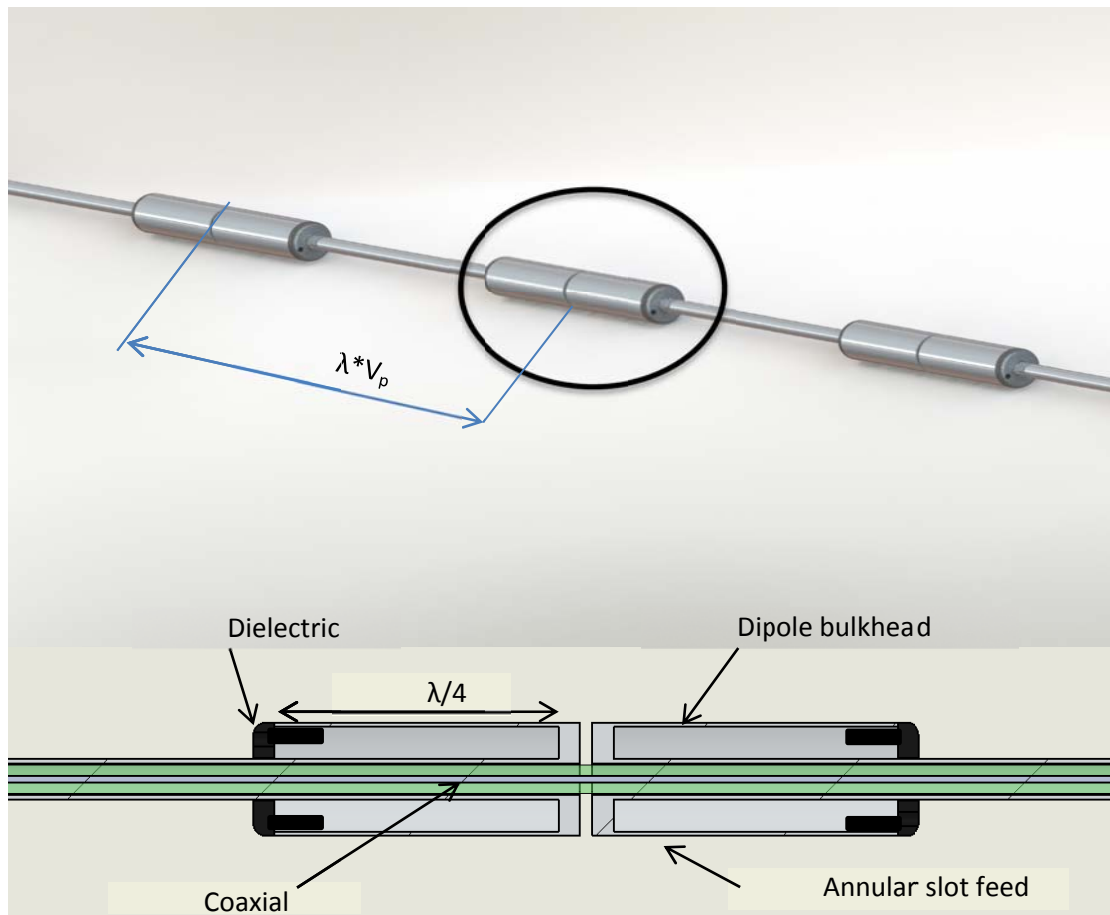
Fig 1-20 Series fed annular slot fed collinear array: section view

The use of printed circuits for collinear array allows for more degrees of freedom for impedance matching, as extra open circuit stubs can be integrated to compensate for excessive reactance [23].   The basic structure shown in Fig 1-21 is a typical PCB representation of a coaxial dipole type collinear array using microstrip transmission lines [24] [25].   An example of a commercially available series fed array antenna is the COL85-870 [9]. This antenna is a meander phase shifted array of five radiating elements on a low cost flexible substrate. The substrate carries the planar form radiating elements and the meander elements, manufactured with the precise positioning offered by PCB technology. The planar antenna elements are attached to the choke element, which also houses the matching circuit. The antennas are relatively lightweight, broadband (with VSWR < 1.5:1 over an 8% bandwidth), and have a gain of 6 dBd. The antenna is specifically designed to minimise the generation of PIM typically < -150 dBc. In Fig 1-22 a typical application for this series fed array is shown, generating a bidirectional pattern.

1-45
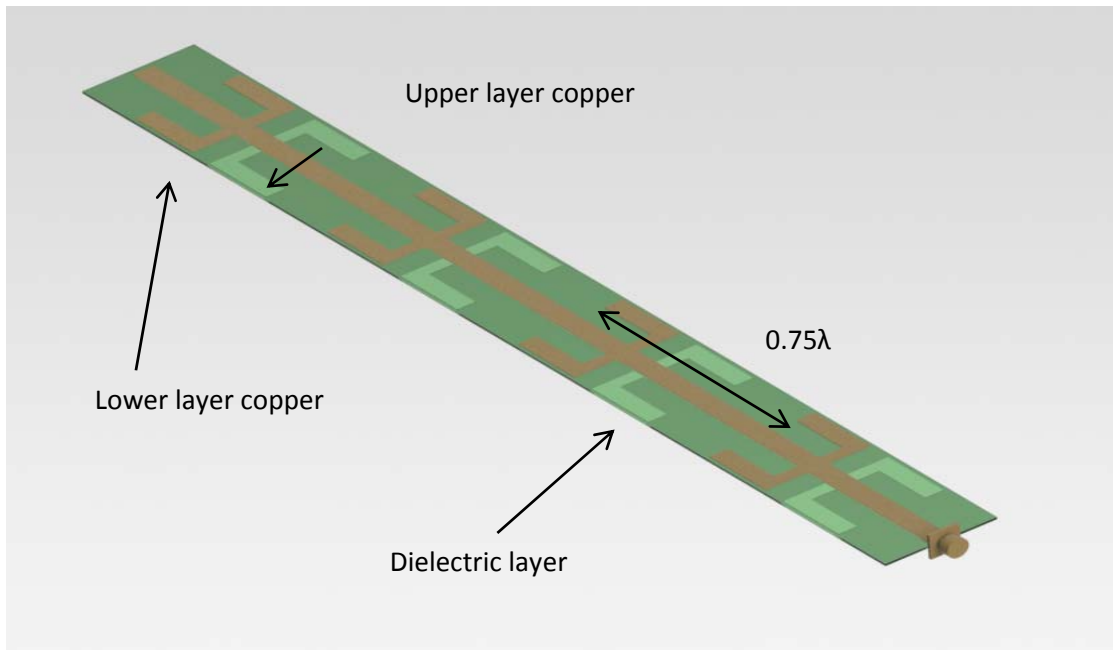
Fig 1-21 Planar double-sided PCB series fed array [24]

Fig 1-22 Series fed arrays configured for bidirectional coverage

1.7.4　**Centre fed array antenna**

The cancellation of beam tilt incurred by series fed arrays is the main objective of implementing a centre fed array. A centre fed array is fundamentally two series fed arrays mounted back to back and fed in phase, producing a differential current distribution in each series sub array. This arrangement effectively cancels the beam tilt with change in frequency. Tilt occurs in both main beams simultaneously, but in the opposing direction, forming a "gable phase profile" [13] as shown in Fig 1-23. The main beam of the centre fed array now remains stable with change in frequency rather than abruptly tilting.
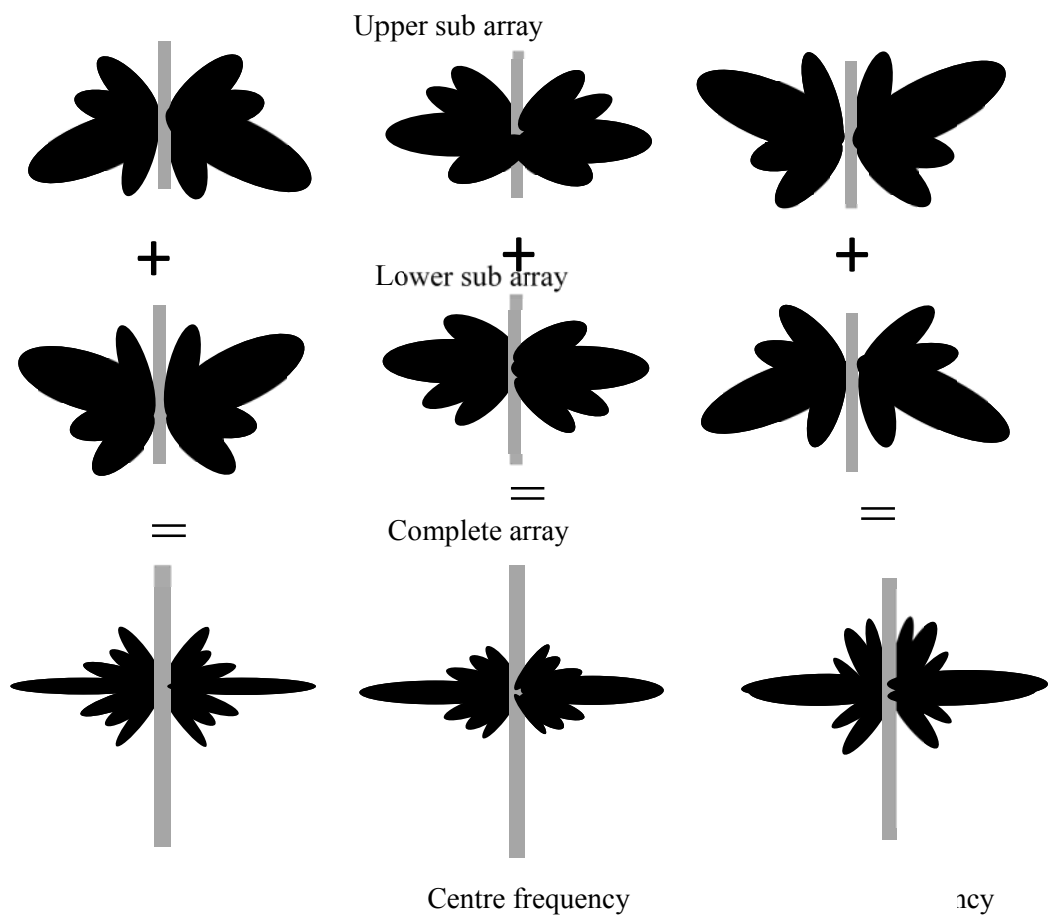
Fig 1-23　Pattern behaviour of an omnidirectional centre fed dipole array

The majority of conventional centre fed dipole arrays for base station applications have a pattern bandwidth of 8% for six radiating elements. As the cables in a centre fed array are in the same plane as the dipoles, they are likely to be source of spurious

1-47

radiation unless isolated from the radiating surfaces. There should also be good isolation between each sub array. If not properly isolated, out of phase energy radiating from the feed or the mounting tube can lead to the distortion of the radiation pattern.

To satisfy the requirement of feed isolation, array design is often restricted to using the more expensive coaxial sleeve dipole with a hollow core [7]. The most complex part of this array is the power divider and impedance matching circuit. Impedance matching for the array must be located as close as possible to the feed point, in order to provide balanced broadband matching and minimize the phase errors. If the feed point is at the centre of the array with differential current distribution to the sub arrays, the amplitude remains constructive over a larger number of elements. Mutual coupling and electrical spacing's exceeding λ_g limit the bandwidth of centre fed arrays. Outside of the operating band the end lobe levels significantly increase and the main lobe starts to tilt, as out of phase currents become dominant. Commonly, two routing configurations are used for centre fed arrays. In the case of the unidirectional array in Fig 1-24, the series arrays are fed from the side. For the omnidirectional case in Fig 1-25, the feed is routed inside the shielding. Coaxial choke elements at the base of the array prevent coupling back to the tower and feed cable.

The Marconi-Franklin array [26] as shown in Fig 1-26 was one of the first collinear array antennas, which was re-designed to be centre fed array [27]. The antenna is formed by partially stripping the braid off a coaxial cable, forming a coaxial dipole. By bending periodic meanders in the line the current distribution truncates and forms resonant and non-resonant elements over the length of the array at the design frequency. The array relies on cable surface currents for the excitation.

1-48

twork
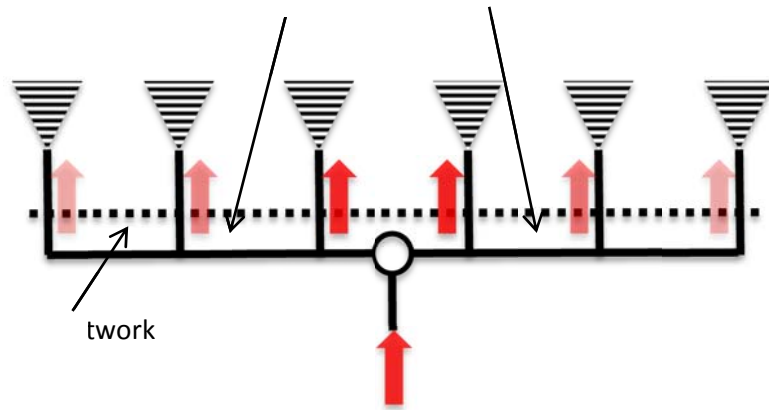
Fig 1-24 Schematic of unidirectional centre fed array with a side feed

λ /4 current choke

Feed network shield
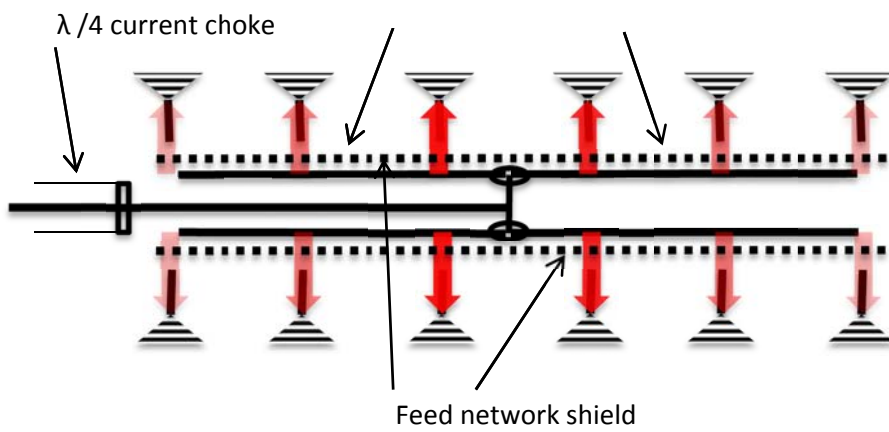
Fig 1-25 Schematic of an omnidirectional centre fed array with a routed feed

1-49
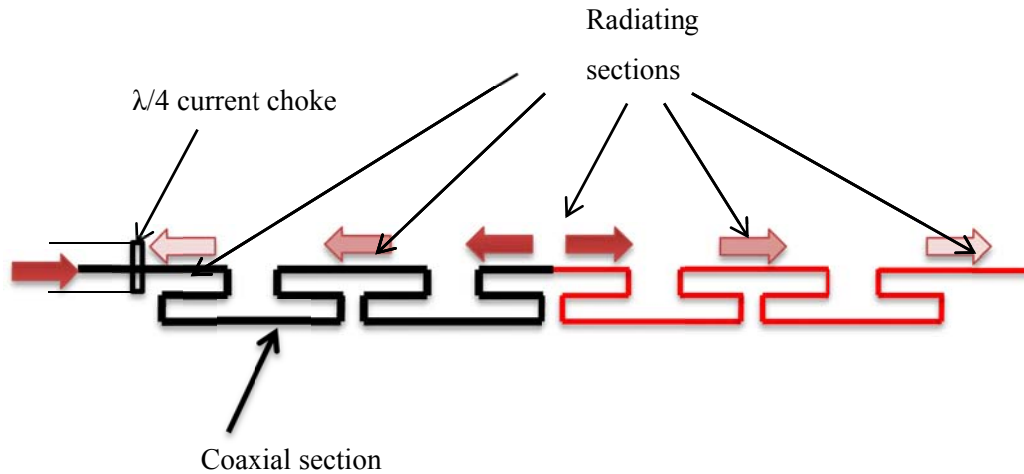
Fig 1-26 The Marconi- Franklin antenna [27]

Another form of centre fed array is the suppressor collinear antenna as shown in [20]. Although this is a very early design (1955), it is still the concept used for many of today's centre fed base station antennas products Fig 1-27. Its operation is similar to the series fed suppressor collinear antenna, except it takes advantage of the standing waves generated either side of the feed point.
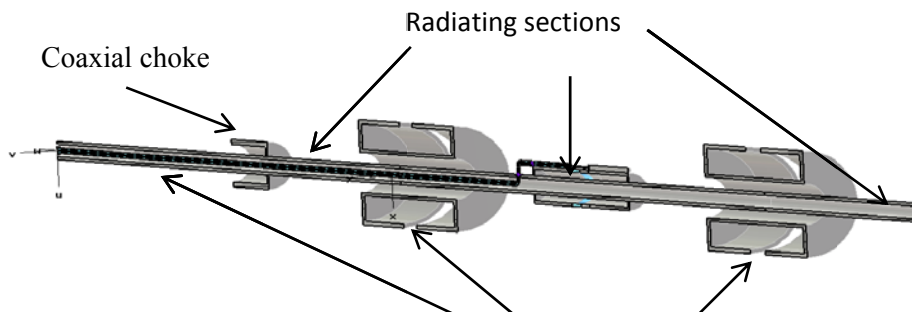
Fig 1-27 Centre fed suppressor collinear antenna

Many current antennas are based on these earlier welded metal tube designs, which are at high risk of causing PIM and failing to meet the more stringent base station specifications. A typical commercially produced centre fed array with adjustable

1-50

beam tilt is shown in Fig 1-28 [7], [28]. The cylindrical dipoles sleeves are welded to a series of support tubes and an air dielectric coaxial transmission line runs to the centre feed point. This antenna is an adaptation of the annular slot fed sleeve dipole array described in Fig 1-20. In the centre fed version, the coaxial cable feed is isolated before reaching the mid-point in the array. A tapping point from the inner conductor through to an insulated capacitive cylinder is coupled to the outer conductor of the secondary coaxial feed line. The inner conductor of the main feed line is then shunt fed onto the upper inner tube. The sub arrays are fed back to back; hence the phase relationship is 180° as required for differential phase distribution [13]. A shorting ring placed $\lambda/4$ from the feed point shunts the central dipole assembly tube back onto the outer of the main feed line in order to reduce the feed point impedance and provide static protection.

1-51

Sleeve dipoles

Impedance matching

Shorting ring

Capacitive coupling ring
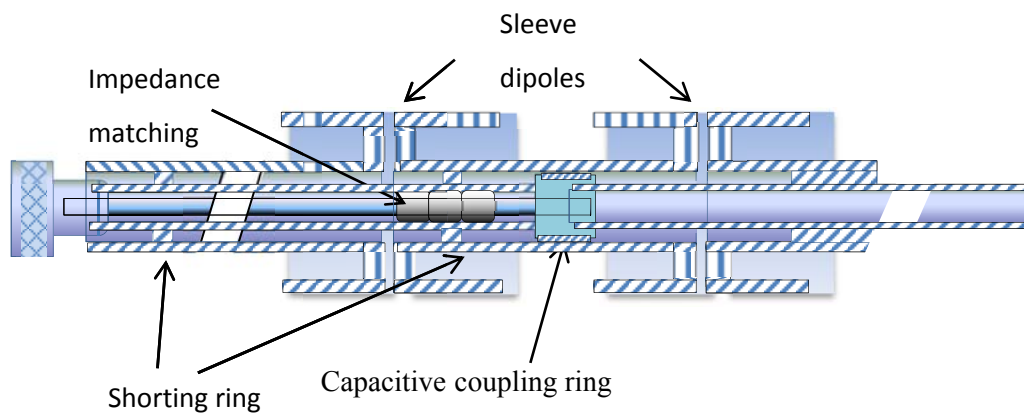
1.7.5   **Corporate fed collinear arrays**

Corporate fed antennas selected for applications such as MDS (Multi-point distribution) Wi-Fi [3] have specific pattern shaping. Some installations require a bi-directional radiation pattern, for example to cover narrow corridors such as tunnels, subways and roads [29]. Others require sectored coverage such as in a cellular network.

In Fig 1-29 a schematic for a typical corporate fed array is presented. The corporate fed array feed network consists of two-way power dividers which provide a cascaded binary distribution network. To be classed as corporate fed the feed line sections must provide the same electrical phase length from the input source to each antenna element regardless of the mechanical position of the elements in the array [13]. This may lead to very long feed runs, especially where the cable enters at the base.

ders
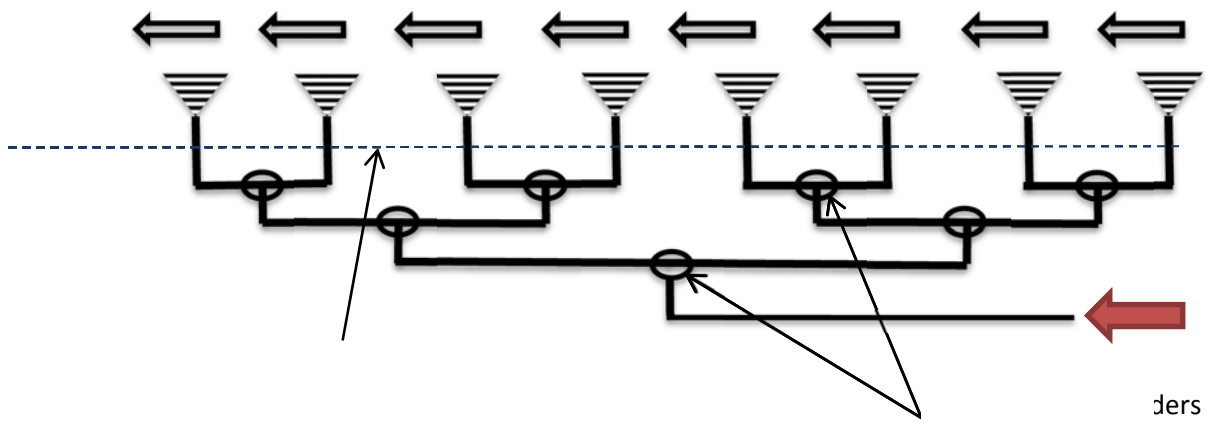
Fig 1-29 Schematic of a corporate fed array

Corporate fed arrays are commonly configured as unidirectional integrated panels [30]. This type of antenna array can approximate omnidirectional coverage by sectorial arrangement, shown in Fig 1-30. A synthesised omnidirectional coverage is achieved if three sector arrays are aligned such that the -10dB beam width points merge and the arrays fed in phase, as shown in Fig 1-31.

Fig 1-30 A cluster of 120° panel array antennas

3 x 120°
spaced
panel array
antennas
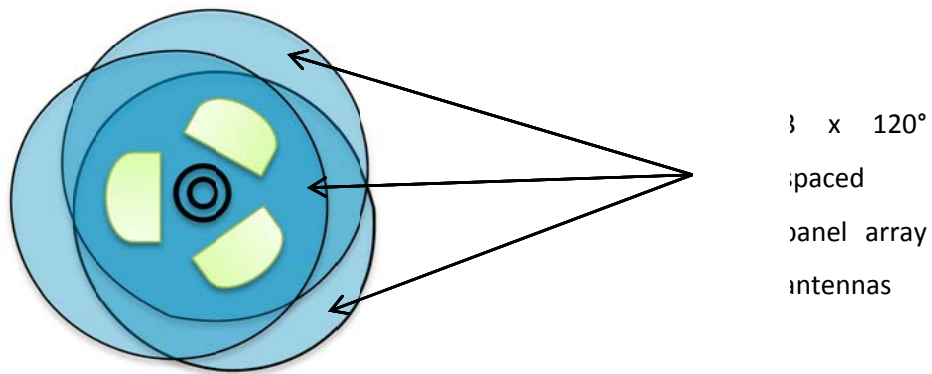
Fig 1-31 Tri-sector arrangement of corporate fed panel arrays in a cellular network

An omnidirectional exposed folded dipole array with the antenna elements positioned concentrically [9] is shown in Fig 1-32. This array provides broadband VSWR performance (typically 26%) with narrow elevation patterns and a nominal gain of 6 dBd. The feed network for this array is complex, consisting of an internal harness made from low loss coaxial cable.

Fig 1-32 Corporate fed folded dipole array (RFI BA80-67) [2]

One of the latest developments in omnidirectional corporate fed arrays is the CC807-11 series array [2] shown in Fig 1-33. The dipole radiators are unique in that they are PCB sheets of half wave dipoles wrapped around metal forms creating broadband lightweight cylindrical elements. The feed cable harness is routed inside the central support mast to prevent detuning of radiating elements, and has an operating band of 746-870 MHz. This array is designed for high power and low PIM, with a typical PIM value of < -150 dBc.

1-54
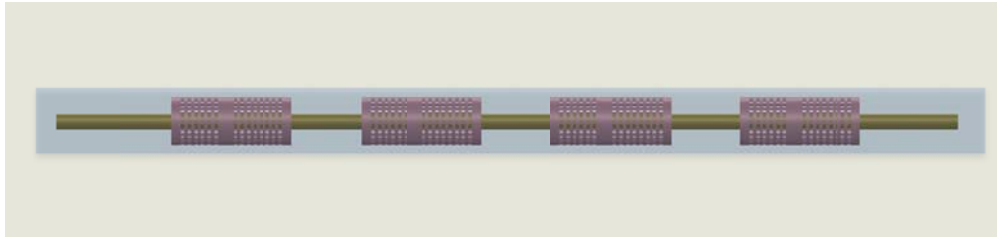
Another form of corporate fed sleeve dipole array is shown in Fig 1-34 [31]. The feed network is created using a custom aluminium extrusion with independent shafts to form the air dielectric multi-transmission line feed network. A Wilkinson power divider used to split the power equally to each of the corporate feed lines, and improve the current balance leading to lower side lobes and clean patterns. The antenna has relatively large diameter dipoles, which include a matching stub. The stub is in parallel with the feed point, formed by folding back the grounded element end to the centre of each dipole. The whole assembly inserted into a heavy-duty radome and exhibits a bandwidth of 18%.

Dipole end folded back forming a high impedance feed point

Air dielectric feed lines are part of the aluminium

A section of the feed tube with coaxial channels
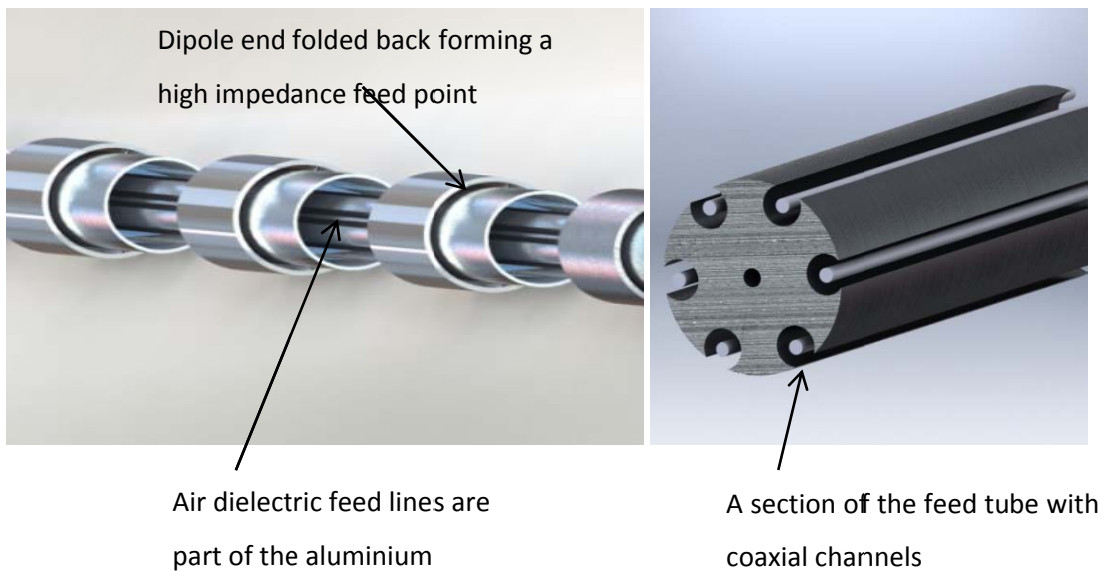
The corporate fed arrays can provide beam tilt by using a delay or line stretcher, integrated in either the power divider arms or as a phase offset in the transmission line sections. A phase shift distributed at all branches maintains low side lobes and impedance matching in the tilted pattern. Another method is to used phase shifters and attenuators as bulk components [32]. The phase shifters control the phase offset and the attenuators level the amplitude independent of the phase. This levelling has the effect of reducing the side lobe levels. [16].

Although corporate fed arrays can be broad band, they lack freedom in designing for a particular gain. Most noticeable is extending from eight elements to sixteen elements in order to increase gain from 11 dBi to 13 dBi respectively. The doubling of the aperture leads to excessive losses in the antenna system due to the extensive coaxial cable harness. Printed circuit based array antennas are now more widely use in base station applications [3]. The main advantage comes from the highly repeatable geometry and lower labour costs involved. The physically smaller size of components at higher frequencies makes printed circuits an obvious choice, as with increased frequency the components need precise tolerances that can render hand assembly ineffective.

1.7.6   Planar omnidirectional arrays

Available literature suggests that planar centre fed omnidirectional collinear array antennas do not appear to be as popular as series fed, perhaps due to the more complex feed requirements. Some non-coplanar (two layer printed circuit) centre fed arrays where a coaxial cable is included from the base of the array up to the centre are more prevalent. This example is presented as a triple band [33]. So-called coplanar centre fed collinear arrays of two elements have also been reported [34]. This design also contains non-coplanar components that would need to be hand fitted during assembly, likely incurring a significant labour cost. "Coplanar waveguide ("Coplanar waveguide (CPW)")" feeding geometries commonly require air bridges to equalise ground potential. These thin conductors bridge the ground tracks in order to cancel out higher order modes at discontinuities such as bends and transitions to connectors [35].

1-56

The antennas in [34] are a logical embodiment for a two-element centre fed array based on coplanar wave-guide. However, issues associated with the current distribution and amplitude were raised but not resolved. Also, the direct air bridge connection from the inner conductor of the "Coplanar waveguide (CPW)" to the active conductor of the second dipole elements as shown in Fig 1-35 does not allow for further expansion of the array design to more elements.
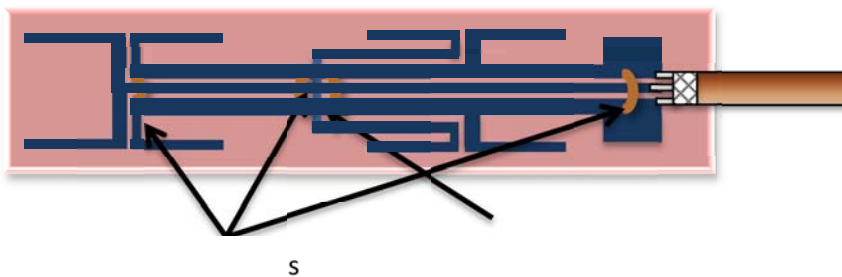
Fig 1-35 "Coplanar waveguide (CPW)" based planar centre fed array [34]

A four element series fed uniplanar collinear array is described in [36], and is depicted in Fig 1-36. The array uses electromagnetically coupled dipole elements through an aperture in the ground tracks. This feed comprises of a "Coplanar waveguide (CPW)" transmission line with periodically slotted finite ground tracks to feed the dipoles in series. The distance between slots appears to be at λ_g intervals. The measured VSWR bandwidth is quite narrow at 2%, and impedance matching is achieved using a single series transformer integrated into the "Coplanar waveguide (CPW)" feed line. Expansion to more array elements is possible due to passive coupled architecture. The antenna array was fabricated on a 200 micron thick Rogers R4003 substrate, providing a low cost array implementation for the 10 GHz band.

1-57

Ground track slots feed the
passive dipole strips

Integrated Series
transformer
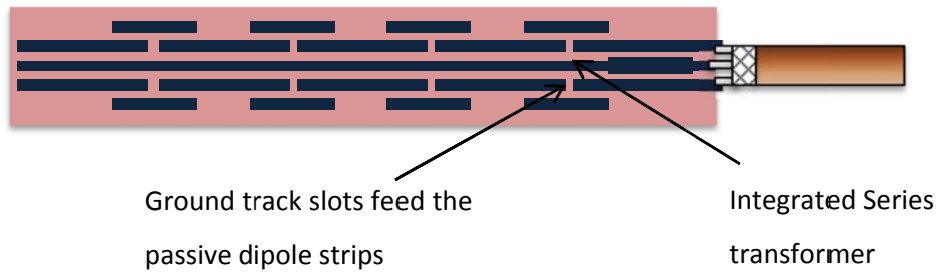
Fig 1-36 CPW based planar series fed array [36]

1.8   Design limitations in all base station antennas

In order to support subscribers with a high quality and reliable network, the latest technological advances and system implementations such as "Time division multiple access (TDMA)", "code division multiple access (CDMA)" and "wide band code division multiple access (WCDMA)" are offered by telecommunication carriers, making economical use of broad bandwidths, spatial diversity and frequency reuse [3]. The base station antennas deployed in these systems must not hinder the exceptional performance offered by these new technologies.

With the introduction of these advanced techniques, a number of challenges for antenna designers arise. A highly concentrated spectrum leads to new phenomena such as PIM (Passive intermodulation) and PIP (Peak instantaneous power). Many of the current base station antenna designs have not considered these phenomena, and as such may not meet these new specifications. An antenna deployed in cellular networks must also be able to sustain relentless mechanical stresses of wind loading and vibration, and be impervious to moisture. The combination of multiple transmitters at a single base station site results in high peak powers. Antennas used in these highly concentrated radio sites are heavily scrutinized for construction and power handling.

A growing trend in network delivery is taking shape, where closer spaced lower power base station sites are deployed [3]. This is driven by environmental factors, as the lower powered sites will consume less energy. Lower power sites are also less likely

1-58

to generate PIM and PIP. This presents an ideal situation for printed circuit based antennas as high volume, lower power rated antennas at a fraction of the cost of the conventional base station arrays.

There are numerous flexible substrates that may be employed into printed base station arrays. PET is low cost and is readily available substrate from PCB processing companies in Asia. The material is Bo PET ("Biaxial-oriented polyethylene terephthalate (Bo PET)" has been available in several forms for some time. Originally by DuPont, development of advanced materials based on PET starting in the 1950s; NASA first used it in 1960 for the Echo 1 satellite project where it found applications in the materials used for manufacture of the inflated reflective sphere. These flexible PET substrates originated from the research into alternative low cost flexible PCB substrates and materials. It is a lower cost alternative to Kapton and Polyamide for flexible interconnects, although Kapton and Polyimide can operate at much higher temperature than PET [37]. PET is now widely uses in ("radio frequency identification (RFID)" tags and labels and in multi-layer, low profile PCBs found in current electronic equipment. Despite its low cost, its RF properties of 125 micron thick, 35 micron copper clad PET are very good, with a permittivity ε_r = 2.8 – 3.0 and loss tangent of 0.0013 making it suitable for high frequency applications.

Prior to PET substrates, the production of flexible substrates in lengths greater than 500 mm would have proven too costly for antenna array applications. There are only a small number of PCB manufacturers capable of processing these longer PET flexible substrates. New techniques have significantly improved the registration accuracy in processing long PCB's. This was motivated by the need to commercially produce a longer than standard length PCB's for other antenna products. Six-meter long elements designed for some VHF high gain series fed collinear arrays antennas [9].

Another substrate that is becoming more available is LCP (liquid crystal polymer) [38] . It has better thermal properties than PET, but is more expensive and minimum order quantities are required to produce it economically. RFID tag applications may increase demand for LCP, making it a more cost effective proposition in the future.

1-59

Shown below in

Table 1-4 are typical specifications for base station antennas available to industry. Most of these designs are based on the earlier developments in antenna design.

Table 1-4 typical base station antenna specifications

	antenna type	Frequency	gain	Return Loss	Az	Elev.	power rating	PIM	Length	diameter	connector type
example ant											
CAN 008H	fed sleeve dipole	824-960 MHz	10 dBi	-14dB	360	8.5deg	300W	-150 dBc	2700	50mm	7/16 DIN
SC420-hf1lnf-dm	unknown	806-869 MHz	9.6 dBi	-14dB	360	11deg	500W	-138 dBc	2604	64mm	N jack
BMR8-O-B1	fed dipole array	806-869 MHz	10.1 dBi	-14 dB	360	8.5deg	500W	none spec	2440	168.3mm	7/16 DIN
1110-5	center fed array	896-940MHz	11.1 dBi	-14 dB	360	6 deg	500W	none spec	3400	65mm	N jack
4168.11.33.00	unknown	870-960 MHz	11dBi	-14dB	360	6 deg	500W	-150 dBc	3000	78mm	7/16 DIN
COL807-08	fed dipole array	746-870 MHz	10.2dBi	-14dB	360	9deg	500W	-150 dBc	2900	76mm	7/16 DIN

Chapter 2   "Coplanar waveguide (CPW)" feed network with centre feed

Traditionally, centre fed array networks consist of a number of ridged coaxial conductors arranged to provide a feed to coaxially mounted cylindrical metal dipoles [7]. In this chapter a novel planar feed architecture is introduced, with performance equivalent to these commercial coaxial systems in terms of achieved bandwidth, phase stability and system losses. The planar feed network has the added advantages of relatively low fabrication cost, and adaptability to support beam tilt. This feed network will also be more repeatable when manufactured in large batches due to maturity of printed circuit technology. With no soldered connections in the array, passive intermodulation [10] will be significantly lower than coaxial implementations. As the feed network is flexible, it is less likely to be compromised by mechanically induced vibration. An innovative "Coplanar waveguide (CPW)" discontinuity similar to the geometry of [39] is used to distribute symmetrical linear amplitude and phase profiles along printed slotlines to centre feed the collinear antenna array elements.

The performance of the array is numerically characterized and validated using commercial electromagnetic solver CST Microwave studio [40].

2.1   Structure of the planar centre feed network

This section overviews the structure and operation of the planar centre feed network. The implementation of a planar structured feed network for a centre fed collinear array (as seen in Fig 2-1) uses a finite ground "Coplanar waveguide (CPW)" as the primary feeder. The second layer of the network is a symmetrical set of slotlines, which feed the array elements. The critical requirements for this type of feeding system are phase and amplitude must have mirror symmetry through the centre axis of the array. This is known as a linear phase profile [13]. Even though the phase delay of the individual sub arrays changes with frequency as in series fed array, the mirror symmetry of the ports have an opposing phase error which cancels mutual phase shift effects in the array.   In the proposed network, the excitation of the array is provided by a novel "Coplanar waveguide (CPW)" discontinuity [41]. This simple yet effective circuit in conjunction with the second layer of slot lines creates a series parallel power divider with balanced ports. Effectively the array network consists of two dual port series feed arrays back-to-back.

2-61
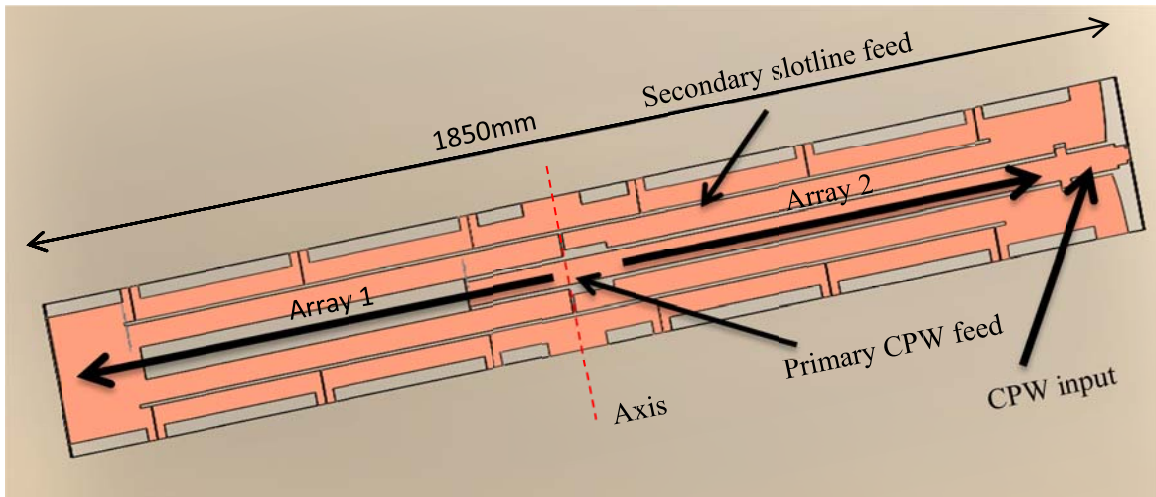
Fig 2-1 The basic architecture of the planar array feed network

The initial section of the feed network shown in Fig 2-2 utilises an input "Coplanar waveguide (CPW)" line that extends to the centre of the array. The slotline transmission lines are formed in close proximity to the ground tracks of the "Coplanar waveguide (CPW)", a novel technique used to reduce the overall width of the feed network when compared to other planar structured arrays [36], [34].

Conventional "Coplanar waveguide (CPW)" ground tracks are typically double the width of the source tracks (or larger) based on this paper [35] [42]. The proposed feed network has a more compact finite ground "Coplanar waveguide (CPW)" transmission line. This transmission line will require evaluation, as it no longer conforms to the standard closed form equations available for conventional "Coplanar waveguide (CPW)". A short circuit slotline stub is used after the final antenna ports to ensure appropriate phasing of the antenna elements.
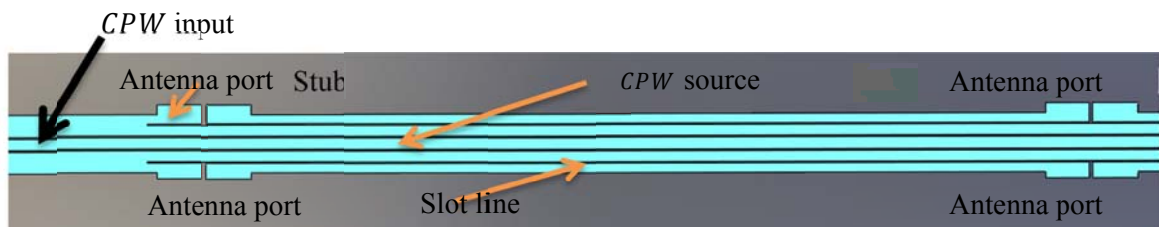
Fig 2-2 CPW input with slot lines feeding the antenna ports

2-62

2.1.1 The feed network component impedance control

The impedance of "coplanar waveguide (CPW)" transmission line is primarily set by the width of the source track and the spacing between the ground and the source track. For finite ground "Coplanar waveguide (CPW)", the ground track width also plays a role. Narrower gaps and wider source track results in a lower impedance line.

The impedance of a slotline is controlled by the gap spacing. The narrower gap between conductors results in lower impedance. In the case of the proposed feed network, the antenna ports are equal in impedance to the feeding slotlines to ensure maximum power transfer.

A series transformer is used to transform from the main line impedance to the series parallel combination feed point impedance of approximately 127 Ω. In the proposed network, the series impedance matching transformer is created by expanding the "Coplanar waveguide (CPW)" ground track spacing, creating a section of relatively higher impedance as shown in Fig 2-3. The transformer is used to match the slotline discontinuity junction to the main "Coplanar waveguide (CPW)" line. The "Coplanar waveguide (CPW)" transmission line continues past the slot discontinuity and terminates in a shunt stub to a virtual ground.
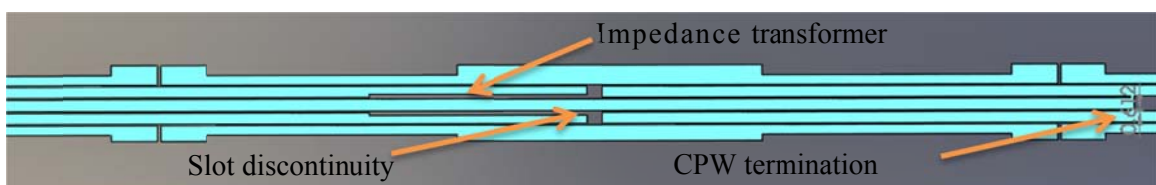
Fig 2-3 The centre feed point comprising of a CPW with series impedance transformer

The slotline feeds comprise of the "Coplanar waveguide (CPW)" ground track and an extra track running in parallel which also electrically supports the slotline output ports to the dipoles. The slotlines route to the extreme ends of the array as shown in Fig 2-4, where they eventually return to virtual ground via a shorted stub.

2-63
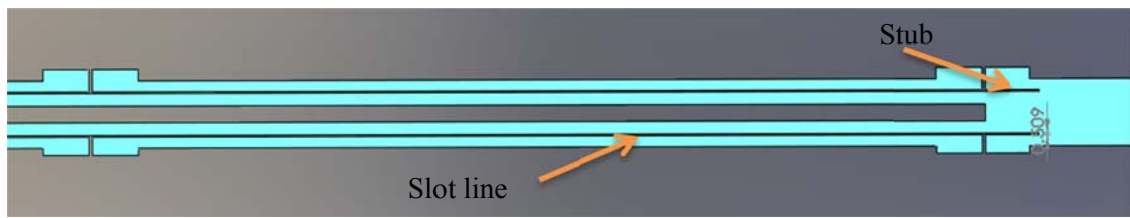
Fig 2-4 The end of the feed network showing the slot lines and the return to virtual ground

2.1.2   Feed network component phase control

This feed network is based on the well-established theory related to phased arrays; where each port is inter connected using λg delay lines. The "Coplanar waveguide (CPW)" transmission line is terminated in a λ/2 short circuit stub ("Coplanar waveguide (CPW)" termination as seen in Fig 2-3). The λ/2 stub is primarily used to transform the short circuit back to the discontinuity, thereby providing a phase reference for the upper array.   Short circuit stubs are also placed at the far end of the slot line transmission lines to terminate the slot line to virtual ground.

2.1.3   Feed network current distribution

The finite ground coplanar transmission line in the proposed configuration has quasi TEM ("Transverse electromagnetic") [43] mode propagation until its arrival at the ground track discontinuities. This behaviour is evident from analysis of the surface current vectors as shown in Fig 2-5(a) the symmetrical current vectors are seen on a section of the main "Coplanar waveguide (CPW)" transmission line. A section of the feed network is presented in Fig 2-5(b) containing both the "Coplanar waveguide (CPW)" and the pair of parallel slotlines shows similar current vectors on the "Coplanar waveguide (CPW)" line, and opposing vectors for the slotlines on either side.   At the slot discontinuity in Fig 2-5(c), the current is transverse to the transmission line, indicating a distinct mode change at this point where the energy is coupled to the slot lines.
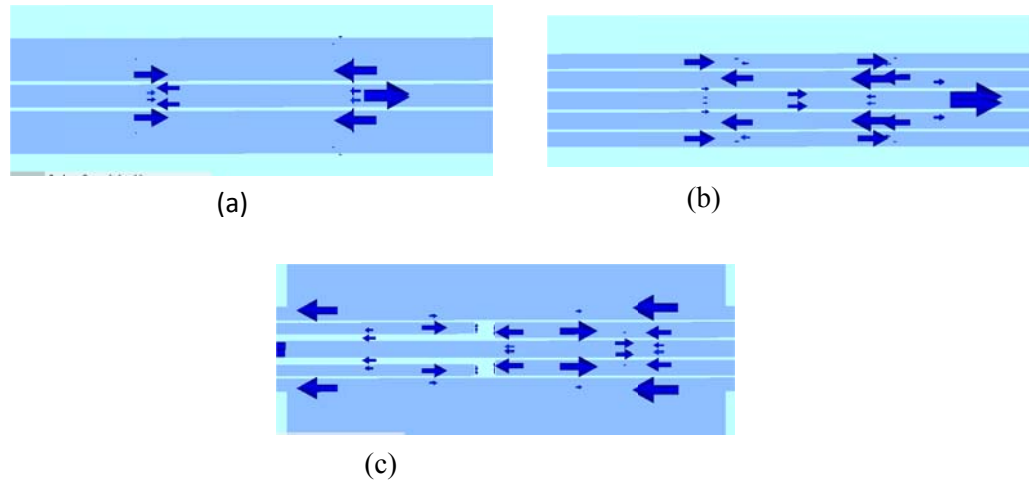
Fig 2-5 Surface current vectors

(a) the main CPW (b) CPW with a pair of slotlines (c) the CPW discontinuity

2.1.4   Relationship to a coaxially fed architecture

The proposed planar feed network has a similar current distribution and antenna port coupling to the commonly implemented coaxial counterparts. The cross section of the coaxial feed network in [7] is very similar to the planar feed network.

Coaxially constructed networks are fully enclosed in the body of the array they feed; as such prevent the feed network cabling from de-tuning the radiating sections. The proposed planar feed network takes advantage of "Coplanar waveguide (CPW)" high cross talk [35] to provide a similar level of protection. A major advantage over coaxial architectures is the open conductor scheme allowing for easy inspection during assembly. The planar structure can be realized on a single sided, flexible, low cost printed circuit material. This added flexibility also reduces the incidence of stress fractures found with conventional solid tube welded components.

2.2   Requirements and limitations for the planar centre feed network

This section highlights the important requirements for a planar centre feed network used in a collinear array, and the limitations imposed by the structural configuration.

The substrate for the planar centre feed network is selected based on electrical performance and low cost.   An extremely thin substrate is effective at reducing transmission losses. However as the substrate becomes thinner, a 50 Ω characteristic impedance "Coplanar waveguide (CPW)" normally used for a feed network would require a very close ground spacing or an exceptionally wide source track.   A thicker substrate enables lower impedances to be achieved more readily; however it would introduce phase delay that reduces antenna element spacing and lowers the directivity.   Using a wider "Coplanar waveguide (CPW)" source track width is not an option in the proposed array due to the structural and mechanical constraints that limit the width of the array.   The final configuration of the collinear array formed with this feed network will utilize a radome with   an internal diameter of 63 mm. This limits the track widths used within the design of the feed network, as the slotlines and antenna elements of the collinear array also need to fit within this diameter.   A very small ground gap is also undesirable due to the PCB manufacturing process.   As the printed feed network is 1850 mm long, a step and repeat fabrication process is employed.   The tolerance of this process is 0.5 mm [37]; making very small gap spacing's unrealisable.

The planar feed network must be sufficiently supported to prevent fracture in the copper cladding that may occur under severe vibration.   The prototype array has two "D" shaped foam mouldings that fit either side of the PCB sandwiching it concentrically within the radome, as explained in Section 5.1.2.   The foam material used is high density polyethylene, which was tested for RF suitability and was found to be inert.   Due to the cellular consistency, the effective dielectric constant of this material is ε_r = 1.04, which is close to that of air.   The planar nature of "Coplanar waveguide (CPW)" does not offer the same level of thermal dissipation as metal coaxial components.   This will impact on the power rating that can be specified for this antenna.

The substrate selected for the printed feed network is a relatively low cost Polyester (PET) which is 0.125 mm thick, with 0.035 mm of copper cladding.   This substrate material is

commonly used for other base station antenna products [9]. The material specifications: ε_r of 2.8 and loss tangent of 0.0013 at 1 GHz. The film substrate can withstand a temperature of 150°C, which is sufficient for the specified maximum power of 100 Watts as demonstrated in a live power test in chapter 5.6.2.

2.3 Feed network design for a planar collinear array

The calculations for the feed network are for fundamental line transformers with substrate loading. The dimensions for the transmission line track widths and slot lines have been initially calculated using conventional transmission line formulae (found in any basic transmission line text – and hence were omitted from the thesis), and these baseline values were used as a starting point for the EM model using CST Microwave studio and CST design studio [40]. As there are areas of the feed network where some cross coupling is evident, no conventional formula can accurately calculate the line widths. Optimisation with a goal of a specific impedance value has been an effective way to determine these parameters. The line lengths are governed by the radiating element spacing, and the series transformer lengths.

The design of the planar feed network for a centre fed collinear array starts with the characterisation of the main feed line geometry. Then the realisation of the transmission and discontinuity components of the feed network can take place. The use of electromagnetic simulation software is essential to design an open architecture feed network of this type. Extensive parameter sweeps and optimization has been used to develop these interactive transmission lines.

2.3.1 Theoretical design of the feed network

The highest realized gain for a collinear array occurs with very close spacing between the antenna elements on opposing sides of the array. Implementing the planar feed structure describe in Section 2.1 would require smaller transmission line gaps than what is allowed for in step and repeat PCB processing. To realize a 50 Ω "Coplanar waveguide (CPW)" for the main feed line requires a source to ground track spacing of 0.125 mm. The PCB processing limitation has a minimum track spacing of 0.5mm [37].

An impedance of 85Ω is selected for the finite ground "Coplanar waveguide (CPW)" to allow for wider physical track spacing as discussed in Section 2.2. To find the optimum geometry, a parametric simulation is performed using [40]. The variables for this simulation are source track width, and ground track gap spacing with ground track width fixed. At this impedance, a track spacing of 0.638 mm is possible.

The secondary slotline feeds are also set to a minimum gap size of 0.5 mm. This results in a line impedance of 127Ω. An advantage of this wider track spacing (higher impedance) is an increase in the break over voltage related to PIP (Peak Instantaneous Power) [10], as discussed in Section 1.2.3.

The design of the feed network has to preserve a symmetrical distribution of the applied energy. Each of the line lengths are phase matched to ensure the antenna ports receive the same phase signal. An amplitude taper is expected as the four sub arrays are series fed, and as such energy is lost at each consecutive antenna port. Each antenna port must present balanced port impedances, the energy is balanced in each sub array to ensure a uniform distribution. Line lengths are selected which are related to a wavelength at the design frequency of 903 MHz. An impedance schematic of the feed network is shown in Fig 2-7. It indicates the impedance and line length of each branch of the feed network to ensure maximum efficiency.

127Ω slot line, length λg

Slot line

Termination stubs:
Impedance 127Ω; length 0.053λ.

Upper section

Lower section

Slot line

Termination stubs:
Impedance 127Ω;
length 0.053λ.

Typical
Port
impedance
129Ω

85 Ω CPW
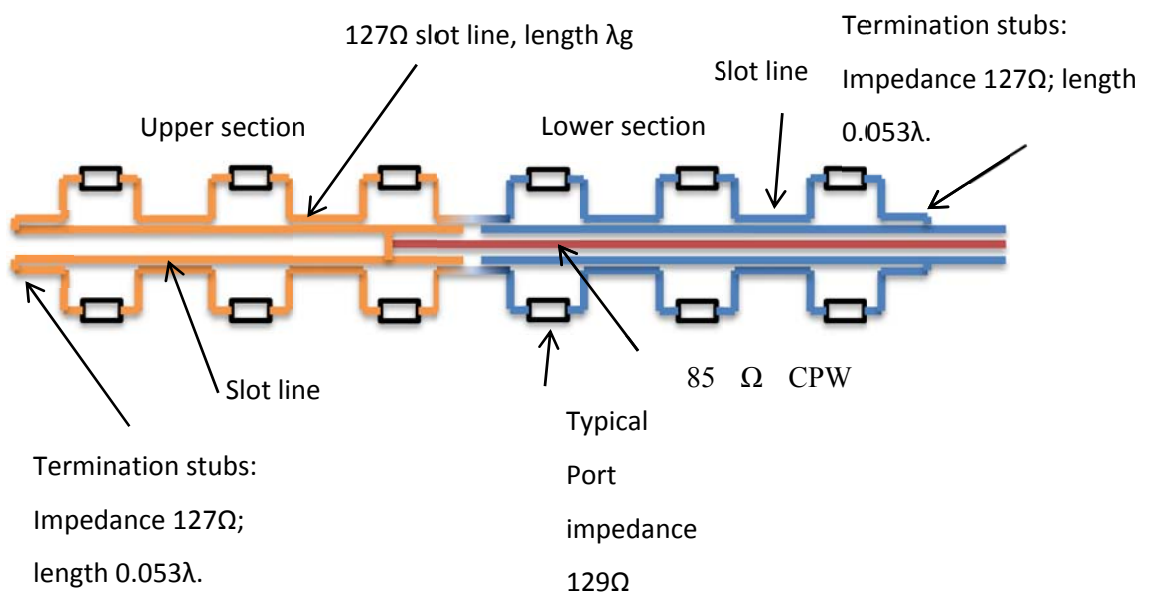
Fig 2-6 The line and terminal impedances of the planar centre feed network

The 13 port feed network (one input and 12 outputs) consists of two sets of parallel sub arrays in mirror symmetry as shown in Fig 2-7, each sub array has 3 antenna ports represented as a complex impedance block with a real component of approximately 129 Ω. The ports are linked in series using line sections L1 with a length of λ_g, and line section L2 with length $\lambda_g/2$. Both L1 and L2 have an impedance of 127Ω, as does L3 which is a return path to virtual ground for each sub array. L4 provides a return path to virtual ground for the main "Coplanar waveguide (CPW)" line. The network is considered as a series resistive circuit with each sub array presenting an impedance of ≈ 380Ω at 903 MHz, when the four sub array impedances are combined in parallel and the "Coplanar waveguide (CPW)" discontinuity impedance component is considered, the result is an impedance of 120Ω. Due to minimum track spacing for PCB fabrication, the main feed impedance has been raised to 85Ω with a track spacing of 0.65mm (L5), determined using the impedance calculation formula for finite ground "Coplanar waveguide (CPW)" given in [35]. A series transformer of 100 Ω (line L6) is used to transform from this to the feed line of 85 Ω (L2). A further $\lambda_g/4$ transformation of 75 Ω (L7) is required to reach the 70 Ω input impedance of the passive coupler circuit as described in Chapter 4. The passive coupler circuit is designed to transform from the 70 Ω "Coplanar waveguide (CPW)" to a 50 Ω microstrip where the feed network can be connected to the base station equipment.
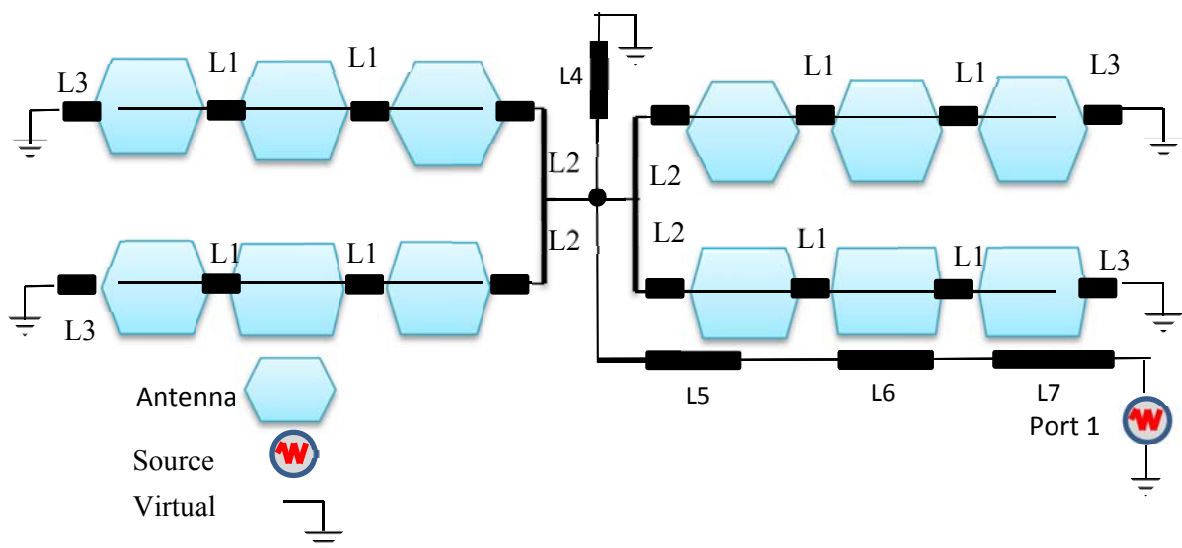
Fig 2-7 the theoretical feed network schematic

A circuit model of the complete planar feed network based on the schematic in Fig 2-7 is analysed with respect to phase and amplitude at each of the antenna ports. The results are provided in the following section.

2.3.2   Circuit model results

The input reflection coefficient magnitude of the circuit model schematic in Fig 2-7 is shown in Fig 2-8. The result is well inside the 14 dB reflection coefficient magnitude specification over the region of interest from 850 – 960 MHz. The transmission loss characteristics of ports 2 to 7 are shown in Fig 2-9, and the phase characteristics of these ports are given in Fig 2-10. Similarly, the transmission loss and phase response characteristics for ports 8 to 13 are shown in Fig 2-11 and Fig 2-12 respectively. The circuit model port characteristics are identical for the two halves of the feed network, as well as ports on opposing sides of the structure due to symmetry. The transmission loss responses exhibit < 1 dB difference at any particular frequency across the band. The circuit model does not consider the parallel coupling component that will be present due to the close proximity of the transmission lines. These differences must be considered in an electromagnetic model and compared to the circuit model results.
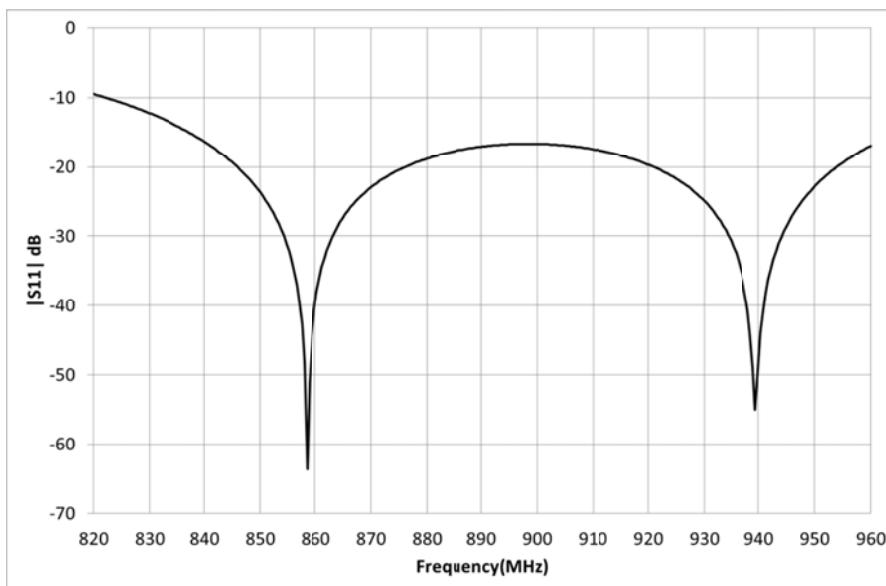
Fig 2-8 Input reflection coefficient magnitude (circuit model)

2-70
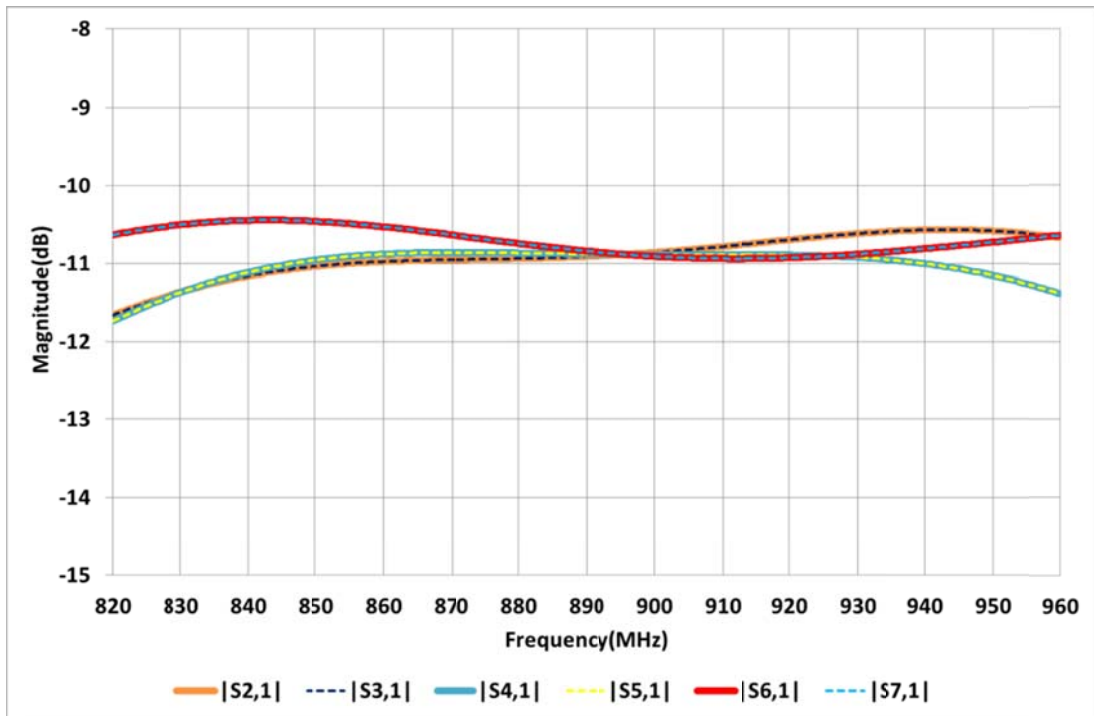
Fig 2-9 Transmission loss characteristics of ports 2 to 7 (circuit model)
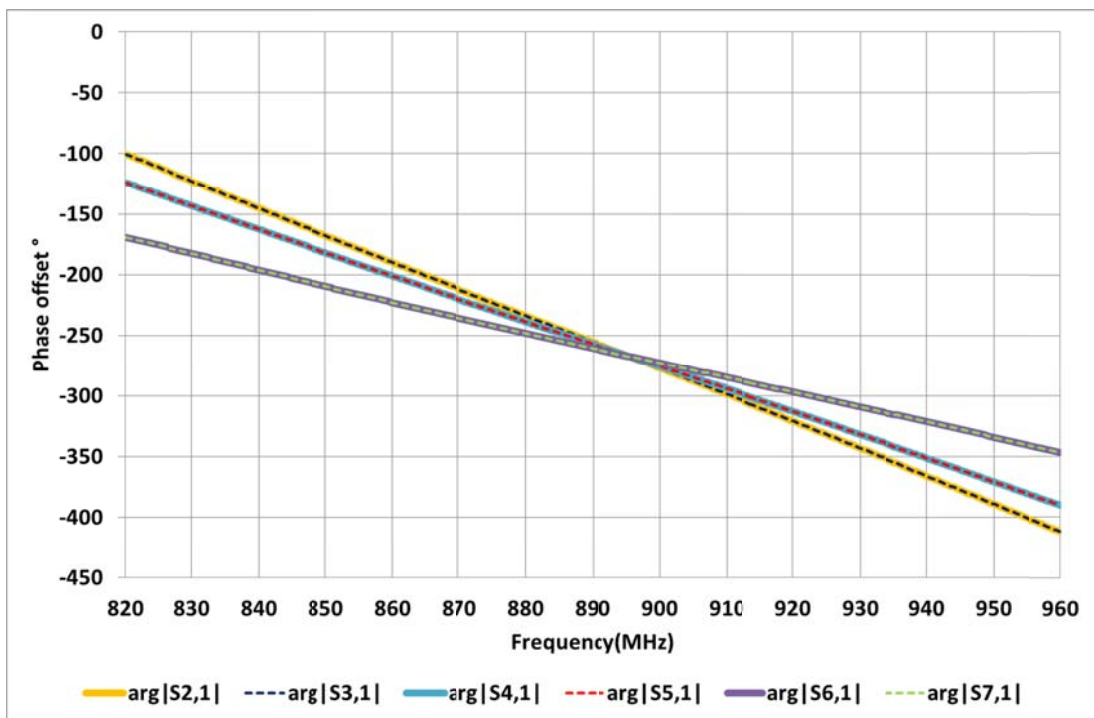
Fig 2-10 phase response for ports 2 to 7 (circuit model)

2-71
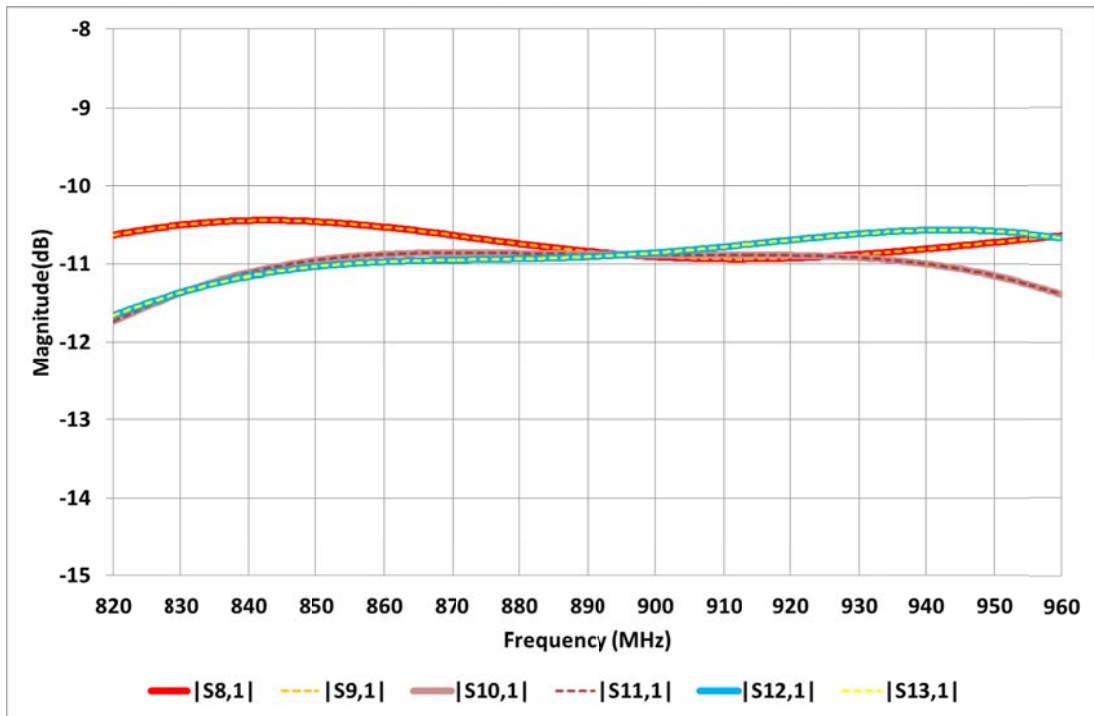
Fig 2-11 Transmission loss characteristics of ports 8 to 13 (circuit model)
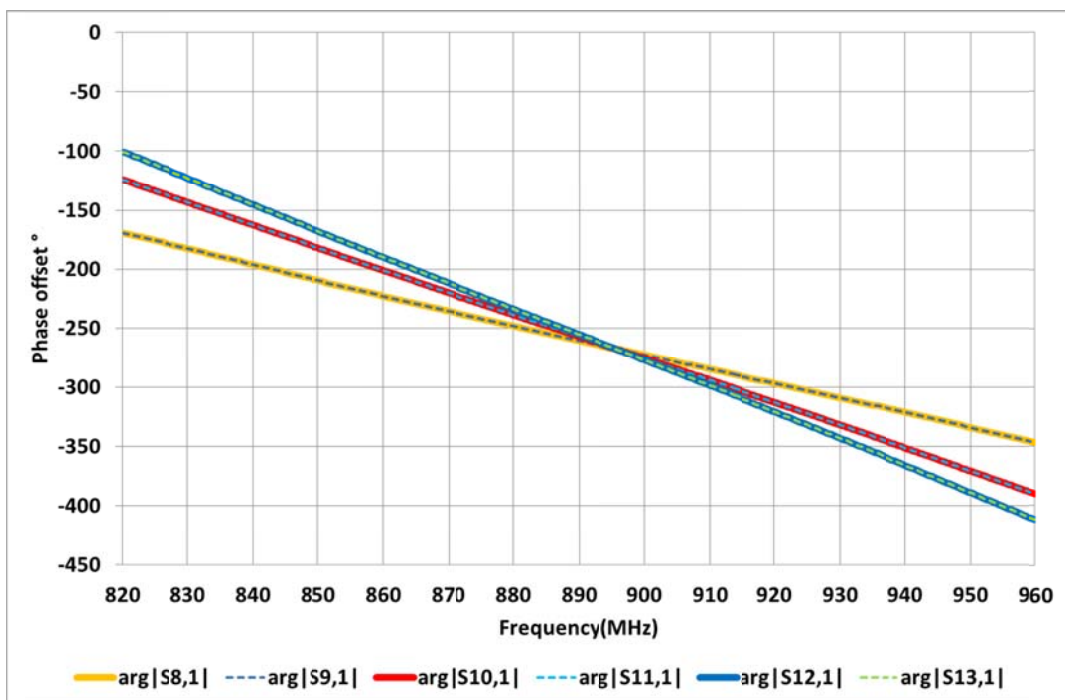
Fig 2-12 Phase response for ports 8 to 13 (circuit model)

2-72

2.3.3 The finite ground "Coplanar waveguide (CPW)" and secondary slot transmission line

In this section the coplanar transmission line dimensions are determined. As previously mentioned, these lines dimensions are selected to satisfy the PCB processing constraints on gap width, and overall array width limited by the mechanical constraints of the radome. In Fig 2-13 depicts the proposed geometry for the 85 Ω "Coplanar waveguide (CPW)" line.
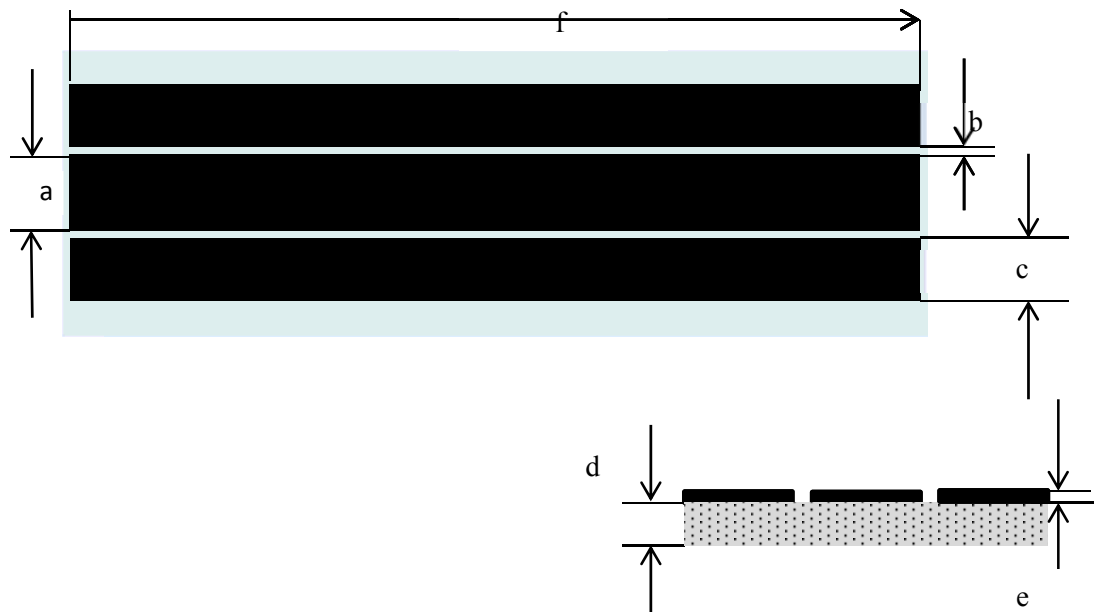
Fig 2-13 Geometry of CPW transmission line model

Parameters: a - source track width = 3.8 mm; b - ground track gap = 0.638 mm; c - ground track width = 3.0 mm; d - substrate thickness = 0.125 mm (ε_r = 2.8); e – metal cladding = 35 um (Cu); f - sample length = 293 mm.

A two port simulation is conducted in CST Microwave Studio to confirm that the desired characteristic impedance of the "Coplanar waveguide (CPW)" line has been achieved. The result of this test as shown in Fig 2-14, indicate that the line has a characteristic impedance of 85 Ω over the pass band of 850-960 MHz.
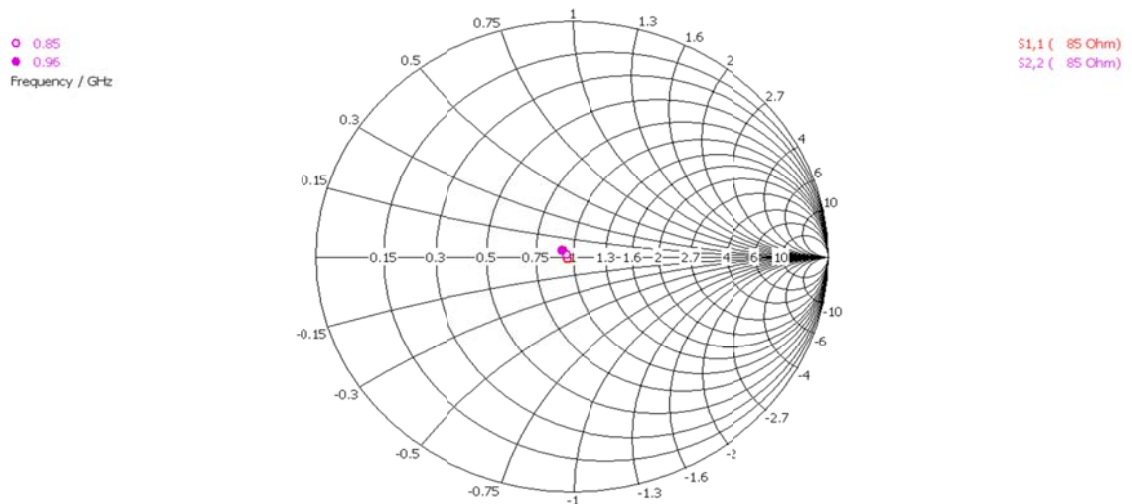
Fig 2-14 Port Impedance of the 85Ω CPW (Smith chart normalised to 85Ω)

To characterize the slot line impedance, a two port simulation is also conducted to confirm that the 127Ω characteristic impedance of the slotline has been achieved. A model is created using the parameters as shown in Fig 2-15. The results of this simulation shown in Fig 2-15 indicate that the line impedance of 127 Ω has been achieved.
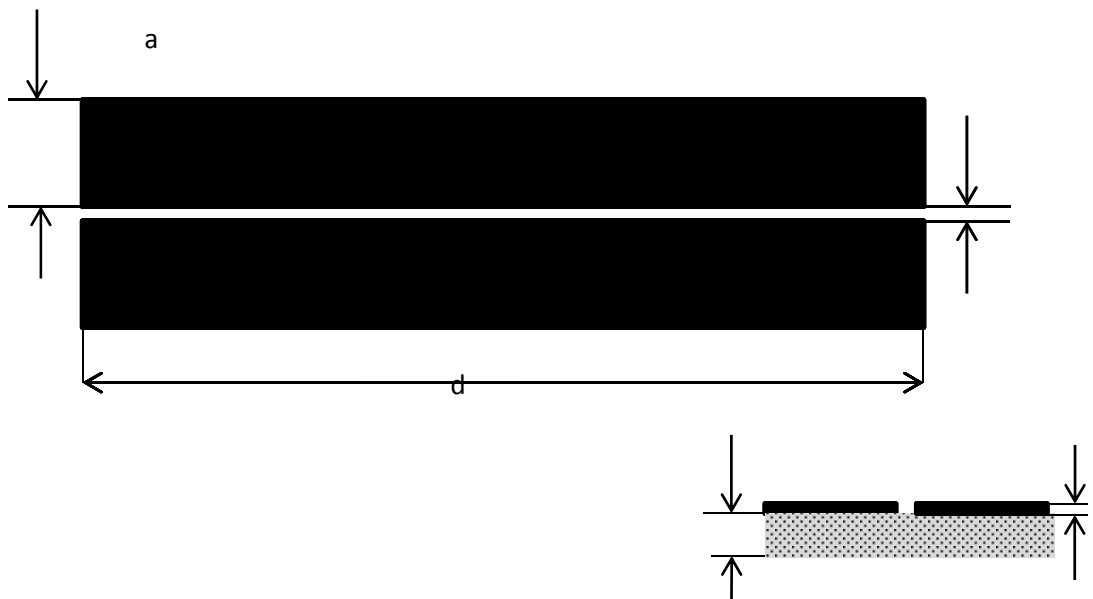
Fig 2-15 Geometry for 127Ω slot line model

Parameters: a- conductor width = 3 mm; b – gap = 0.5 mm; c - substrate height = 0.125 mm (ε_r = 2.8); d - sample length = 100 mm; e – metal cladding = 35 um (PEC).
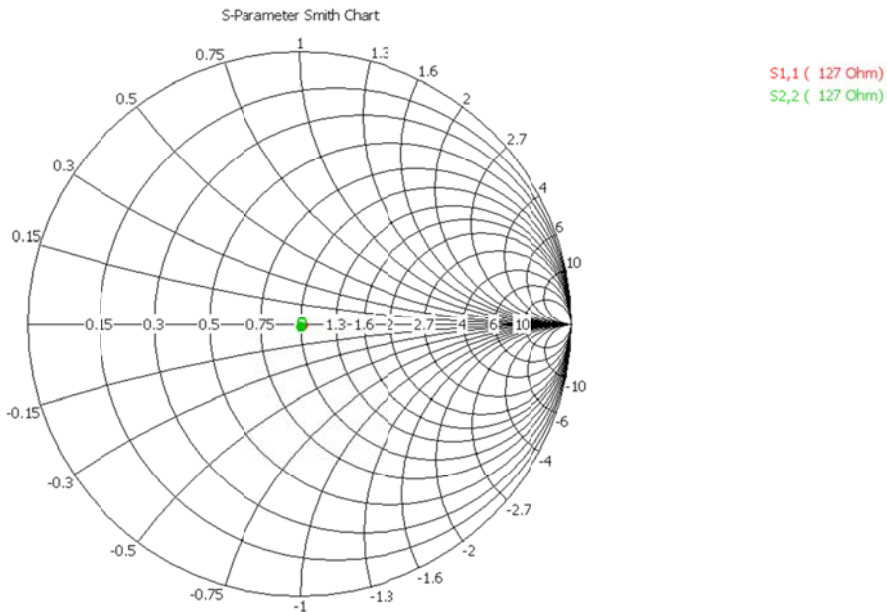
Fig 2-16 Impedance of the 127Ω slot line (Smith chart normalised to 127Ω)

2.3.4   Close proximity of the transmission lines

As the "Coplanar waveguide (CPW)" and slotline are in close proximity, it is necessary to characterize the coupling and losses associated with this. As the "Coplanar waveguide (CPW)" ground tracks are not conventional in that they have a finite width ground plane, there is expected to be some influence on the properties of the slotline.   Adding to this complexity is the exploitation of the ground track of the "Coplanar waveguide (CPW)" to form one conductor of the slot line.

To investigate this hypothesis, a model comprising of the "Coplanar waveguide (CPW)" and the two parallel slotlines is created, as shown in Fig 2-17. There are five ports used in this model. It was not possible to feed the "Coplanar waveguide (CPW)" section directly with a wave port, as its width would exceed that of the "Coplanar waveguide (CPW)" ground tracks, interacting with the closely spaced slotlines. To alleviate this, Port 1 is connected to the "Coplanar waveguide (CPW)" input via a short coaxial cable with the characteristic impedance of the "Coplanar waveguide (CPW)" line. The measurement plane is shifted forward in order to de-embed the coaxial line phase component.

2-75

A wave port is connected to each end of the slotline, Ports 2 to 5. As the slot line is actually part of the "Coplanar waveguide (CPW)" geometry, the ports are arranged to limit mode interaction. This is achieved by adding a 90 degree bend to the output ports such that the slot line ports and "Coplanar waveguide (CPW)" ports have 90 degree opposed measurement planes as shown in Fig 2-17.   Each 90° elbow extension has the same electrical length. The series $\lambda_g/4$ matching transformer is used to transform the feed point impedance measured at the "Coplanar waveguide (CPW)" discontinuity to the main "Coplanar waveguide (CPW)" line impedance. The slots in the ground tracks of the "Coplanar waveguide (CPW)" are designed to transition to an odd mode and couple energy to the close proximity slotlines, channelling the energy to Ports 2 to 5. With Port 1 as the source, the properties of interest are the phase and amplitude measured at each subsequent port with respect to Port 1 and the reflection coefficient magnitude measured at Port 1 as the "Coplanar waveguide (CPW)" ground track width, short circuit stub, and slotline track width are altered.
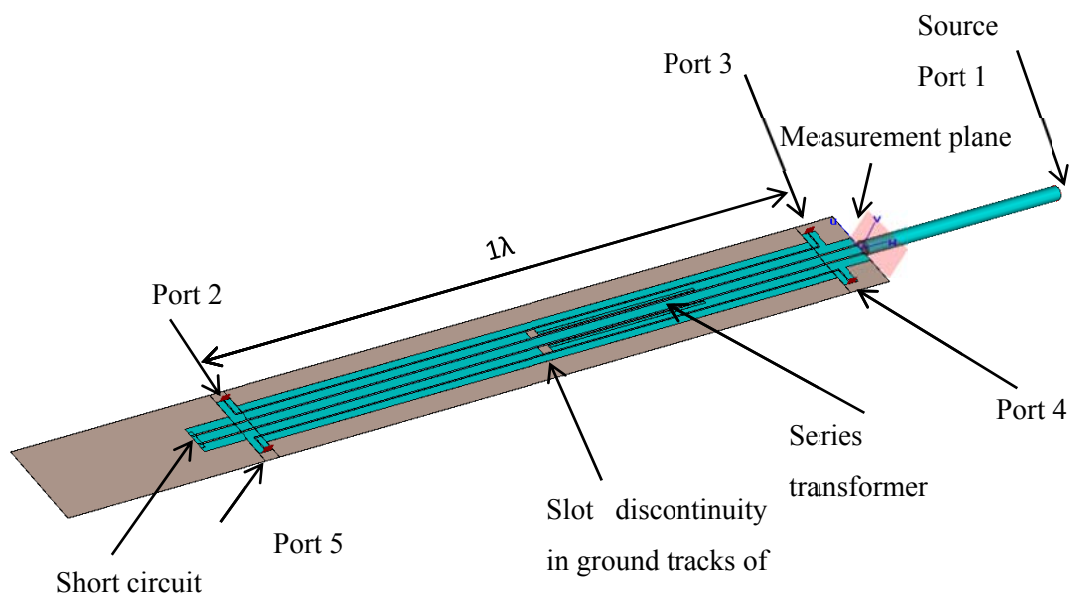
Fig 2-17 Schematic layout for the 5 port feed network evaluation

As there is lateral symmetry in the design, the amplitude and phase shift from input to output should be identical at the parallel ports. There is expected to be a slight phase and amplitude shift when comparing the non-parallel ports as the feed network has included a series transformer and a short circuit stub which break the lengthwise symmetry. The following sections detail simulations conducted to analyse the power divider section of the feed network in isolation.

2-76

2.3.4.1 Power divider characteristics with change in "Coplanar waveguide (CPW)" stub length

Fig 2-18 shows the dimensional reference for the "Coplanar waveguide (CPW)" stub component of the feed network. The stub, which is ideally $\lambda/2$ long, is used to provide a phase reference and limited impedance matching. As it is an extension from the feed point, it is important to characterize this component in terms of phase and amplitude as the stub length is varied from 160-175 mm.
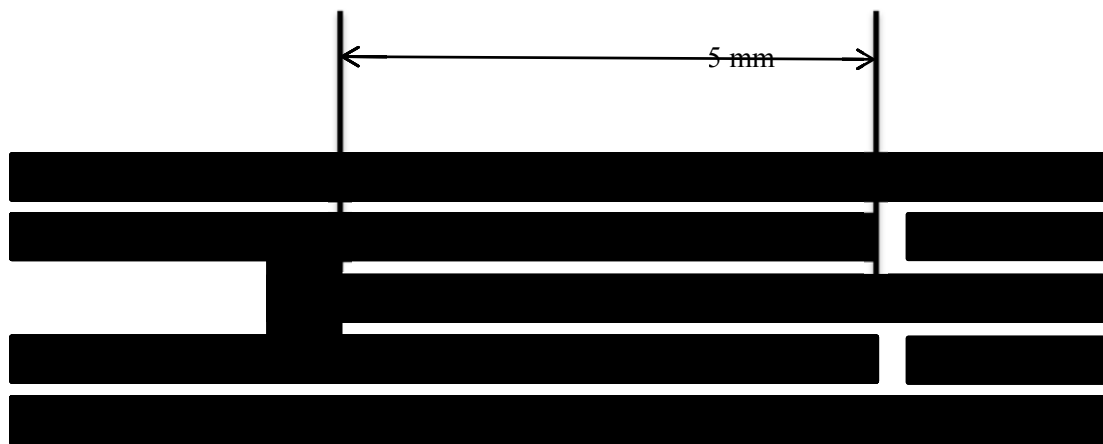
Fig 2-18 CPW termination stub length reference

The maximum phase error at the output ports of the power divider section with respect to the source input as the "Coplanar waveguide (CPW)" stub length is varied is presented in Fig 2-19. The results indicate that a stub length change of 15mm has very little influence on the phase response, producing a phase difference of less than 1.5 degrees at the output ports. The stub length of 171 mm was selected (dotted black trace) as it exhibits the least overall impact on the phase over the desired band from 850-960 MHz. In Fig 2-20 the input reflection coefficient magnitude of the power divider section indicates that the stub length can tune the input matching without impacting on the phase response. The dotted line corresponds with the final stub length of 171 mm.
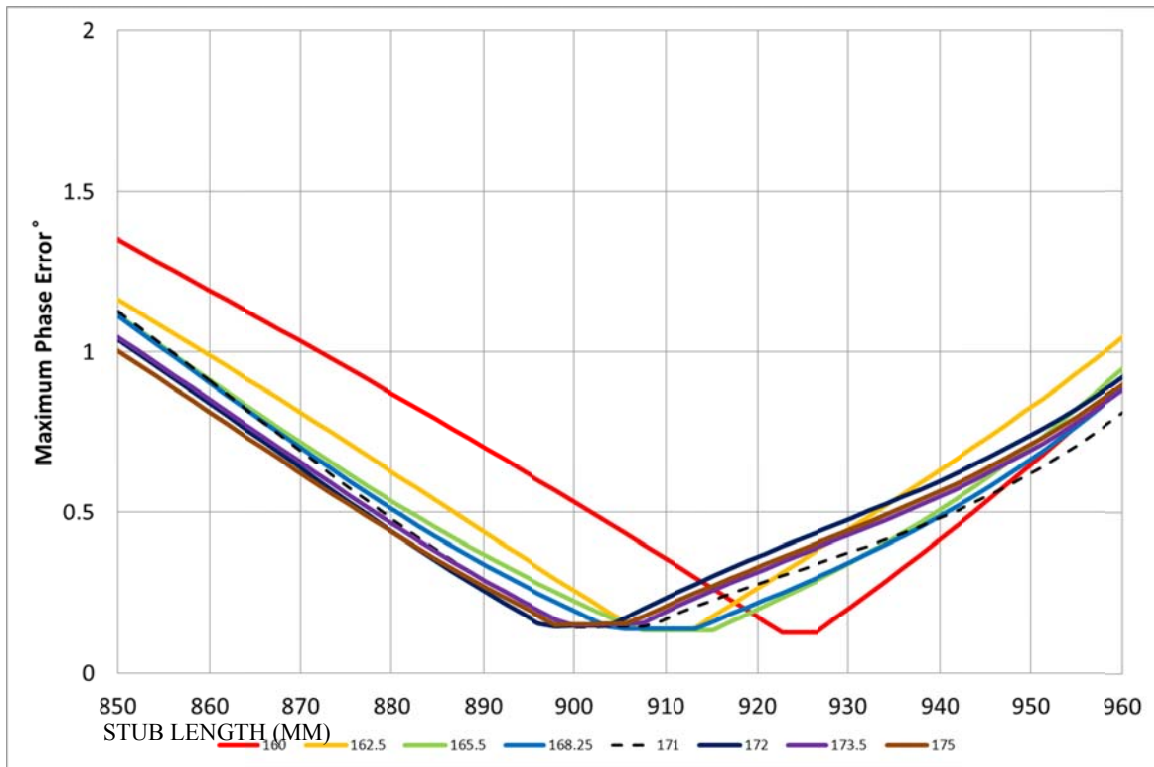
Fig 2-19 Maximum port phase difference with variable CPW stub length (in mm)
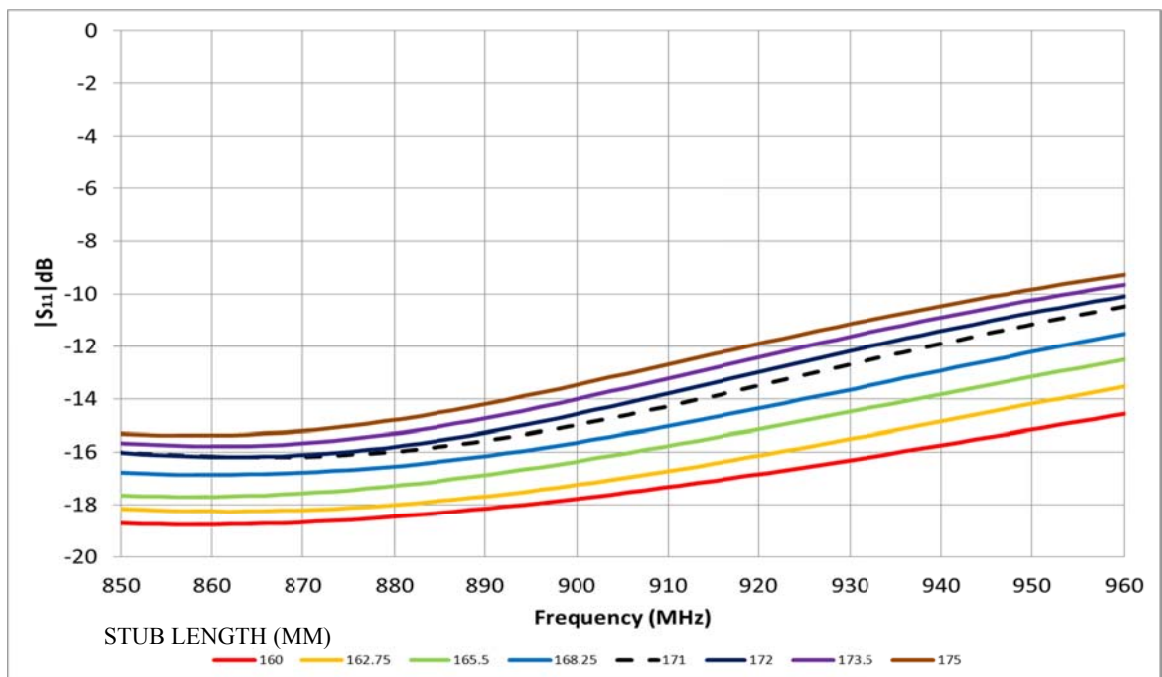
Fig 2-20 Reflection coefficient magnitude with variable CPW stub length (mm)

2-78

The relative signal magnitude at each output port is presented in Fig 2-21. The signals at each of the output ports had a maximum difference in level of less than 0.5 dB The available power at the input is split four ways, and a transmission level of 7 to 8 dB is seen at the output ports. This level of loss is typical of a four way splitter.
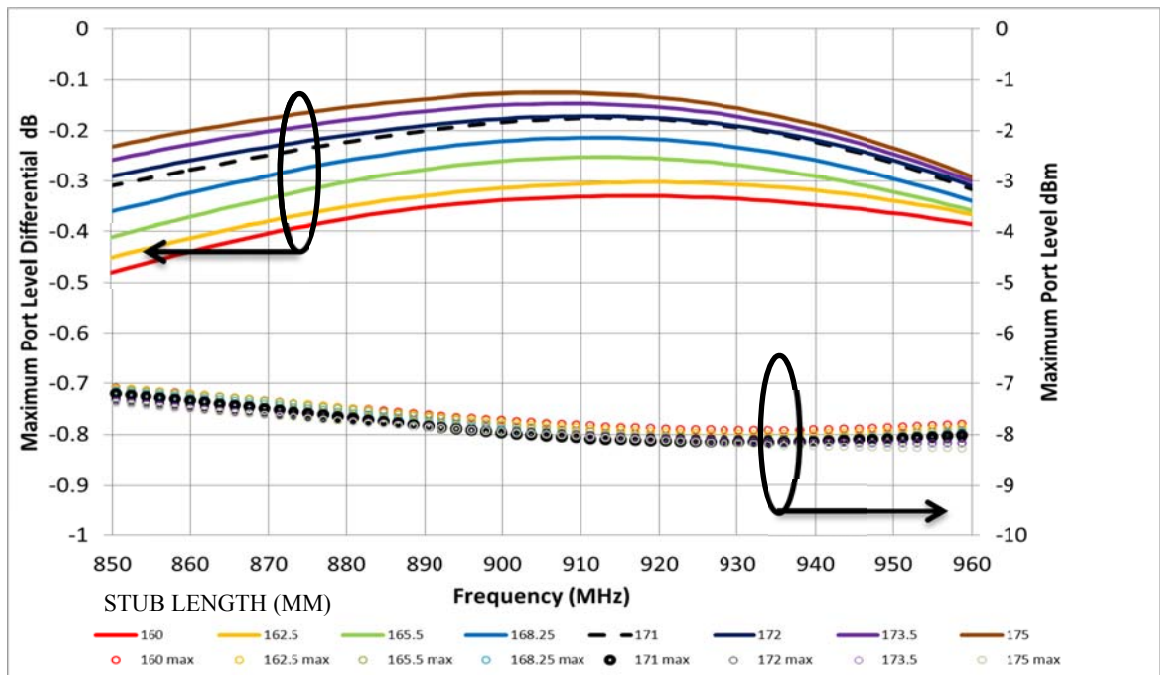
Fig 2-21 Maximum port magnitude difference with variable CPW stub length (mm)

2.3.4.2 Power divider characteristics with change in "Coplanar waveguide (CPW)" ground track width

Shown in Fig 2-22 is the ground track width reference used to characterize the effects of this parameter on the feed network performance. The "Coplanar waveguide (CPW)" ground track width is parametrically adjusted whilst monitoring the reflection coefficient magnitude, and transmission phase and amplitude at each port.

2-79

Ground track width

Fig 2-22 CPW ground track geometry reference

The maximum phase error at the output ports of the power divider section with respect to the source input as the "Coplanar waveguide (CPW)" ground track width is varied from 2 to 4 mm is presented in Fig 2-23.
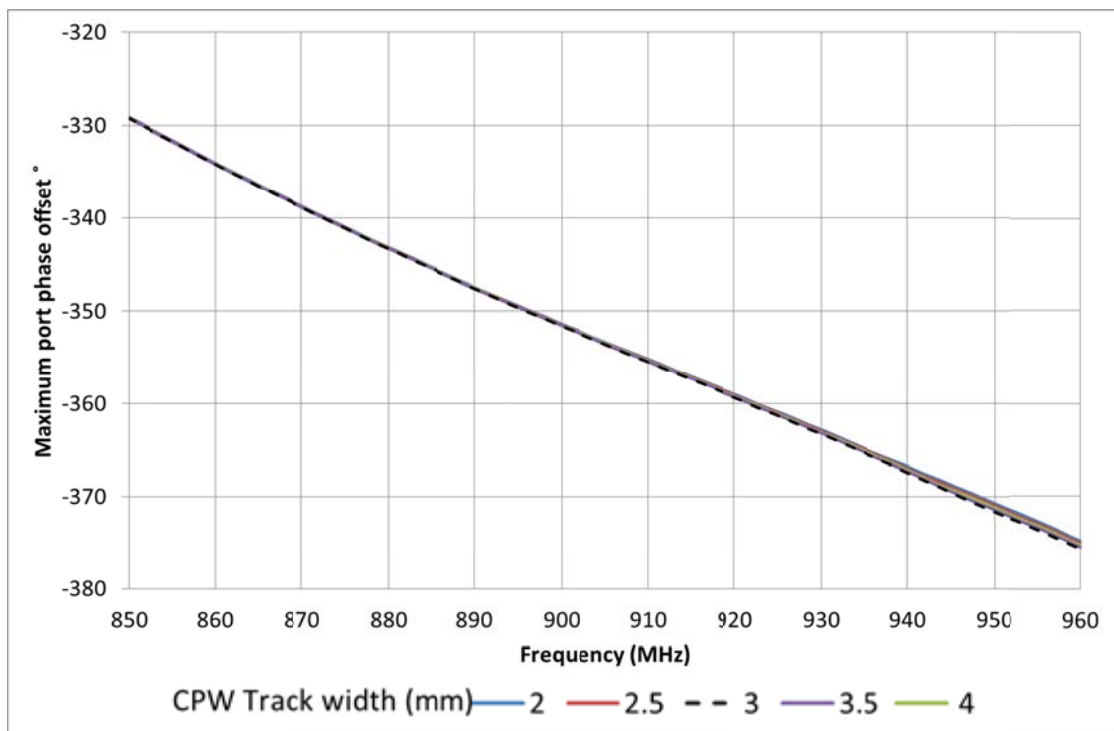
Fig 2-23 Maximum port phase offset with change in CPW ground track width

The "Coplanar waveguide (CPW)" ground track width has an influence on the phase response as it can define the level of coupling between the "Coplanar waveguide (CPW)" and the slotlines. A smaller phase differential is seen from lower values of the "Coplanar waveguide

2-80

(CPW)" ground track width, producing a phase difference of less than 1.5 degrees at the output ports for a 2mm width. However, the results shown in Fig 2-24 indicate that a narrower ground track width causes an increased signal magnitude variation at the output ports. In Fig 2-21 the input reflection coefficient magnitude of the power divider section increase for lower values of the "Coplanar waveguide (CPW)" ground track width.
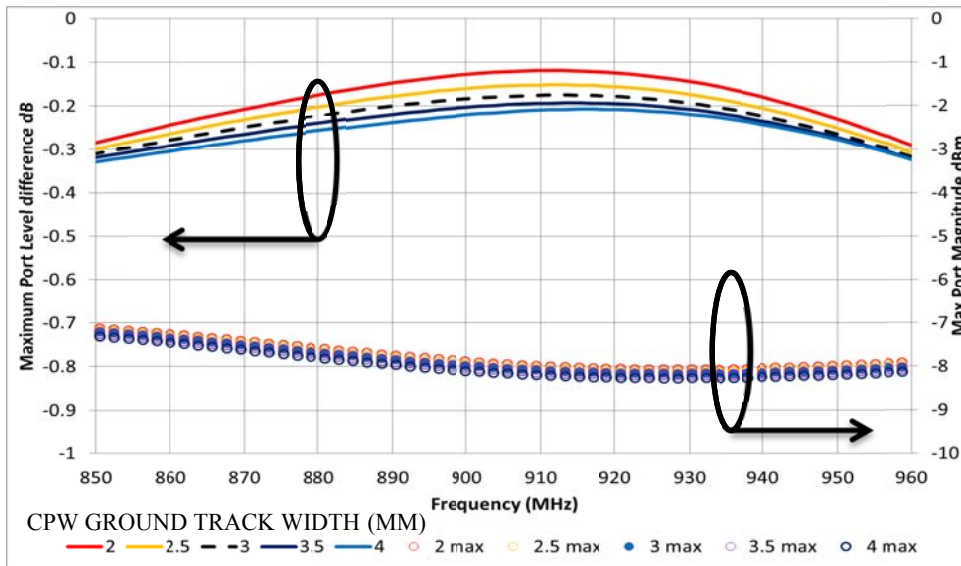
Fig 2-24 Port level with change in CPW ground track width (in mm)
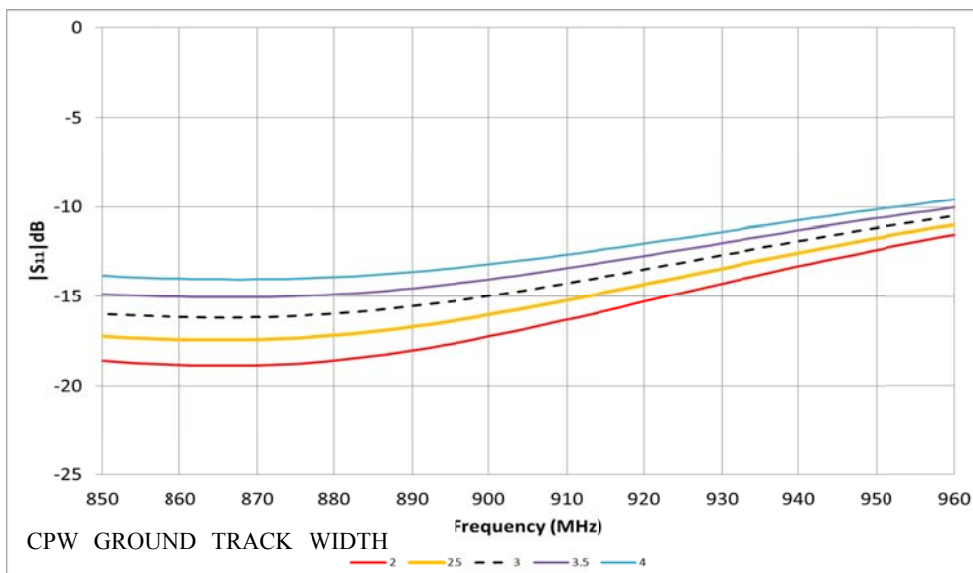
Fig 2-25 $|S_{11}|$ vs. frequency with change in CPW ground track width (in mm)

2.3.4.3 Power divider characteristics with change in "Coplanar waveguide (CPW)" discontinuity gap width

In this section the "Coplanar waveguide (CPW)" discontinuity as depicted in Fig 2-26 is analysed. The maximum phase error at the output ports of the power divider section with respect to the source input as the "Coplanar waveguide (CPW)" ground discontinuity gap width is varied from 1 to 7.75 mm is presented in Fig 2-27 The "Coplanar waveguide (CPW)" discontinuity gap width has a slight influence on the phase response typically <2.0 degree of phase variation over this range as shown in Fig 2-27. A greater discontinuity gap width also causes an increased signal magnitude variation at the output ports, as shown in Fig 2-28. However these values are still small, remaining below 0.6 dB In Fig 2-29, larger discontinuity gap widths are seen to reduce the input reflection coefficient magnitude of the power divider section, as a more significant discontinuity is presented to the propagating signal.

Finite ground CPW

Slot

Ground

Source

Ground

Ground discontinuity width =1 to 7.5mm
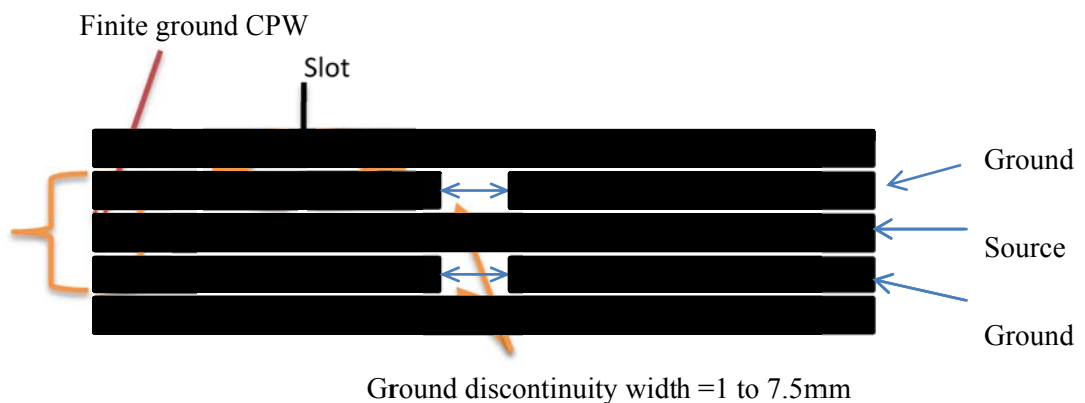
Fig 2-26   CPW discontinuity planar power divider
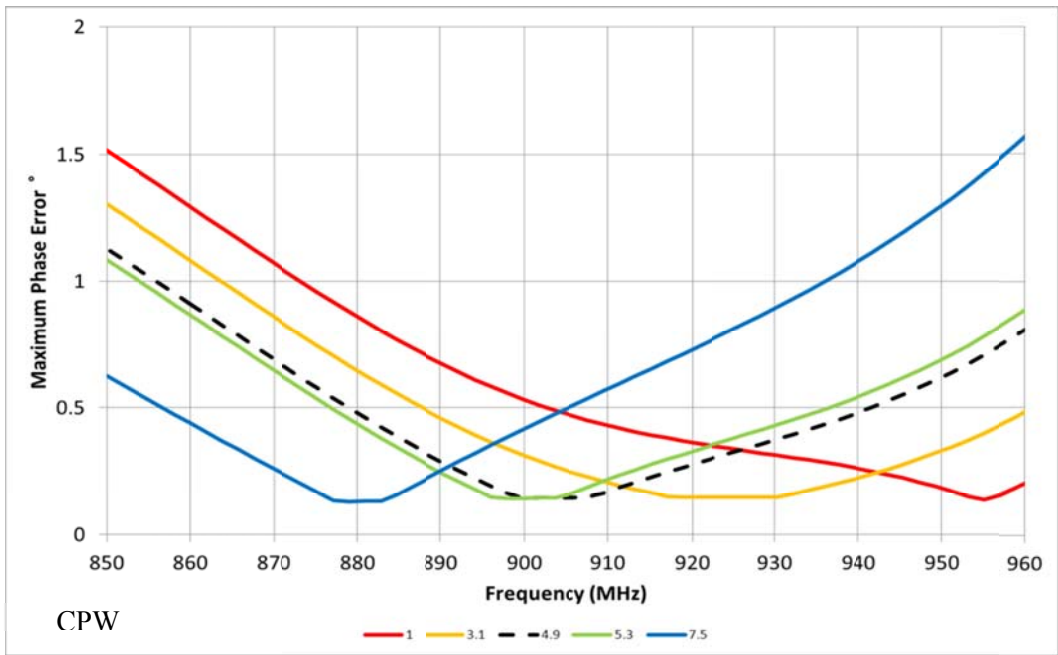
Fig 2-27 Port phase with change in CPW discontinuity gap width (in mm)
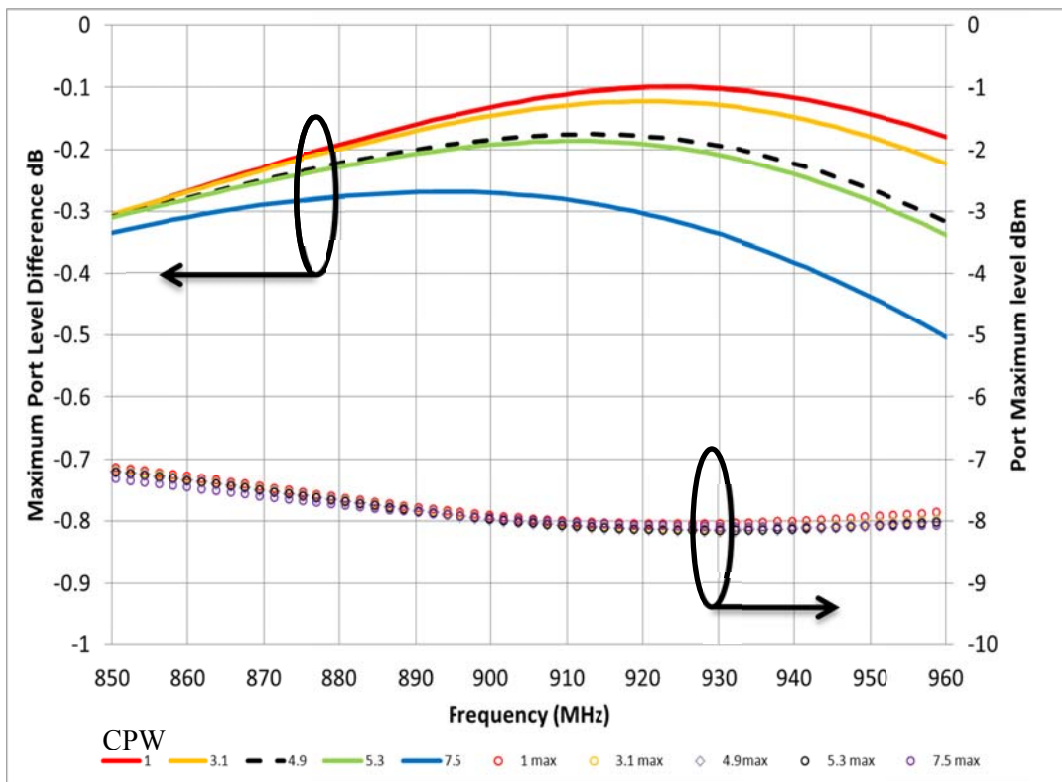
Fig 2-28 Port level with change in CPW discontinuity gap width (in mm)
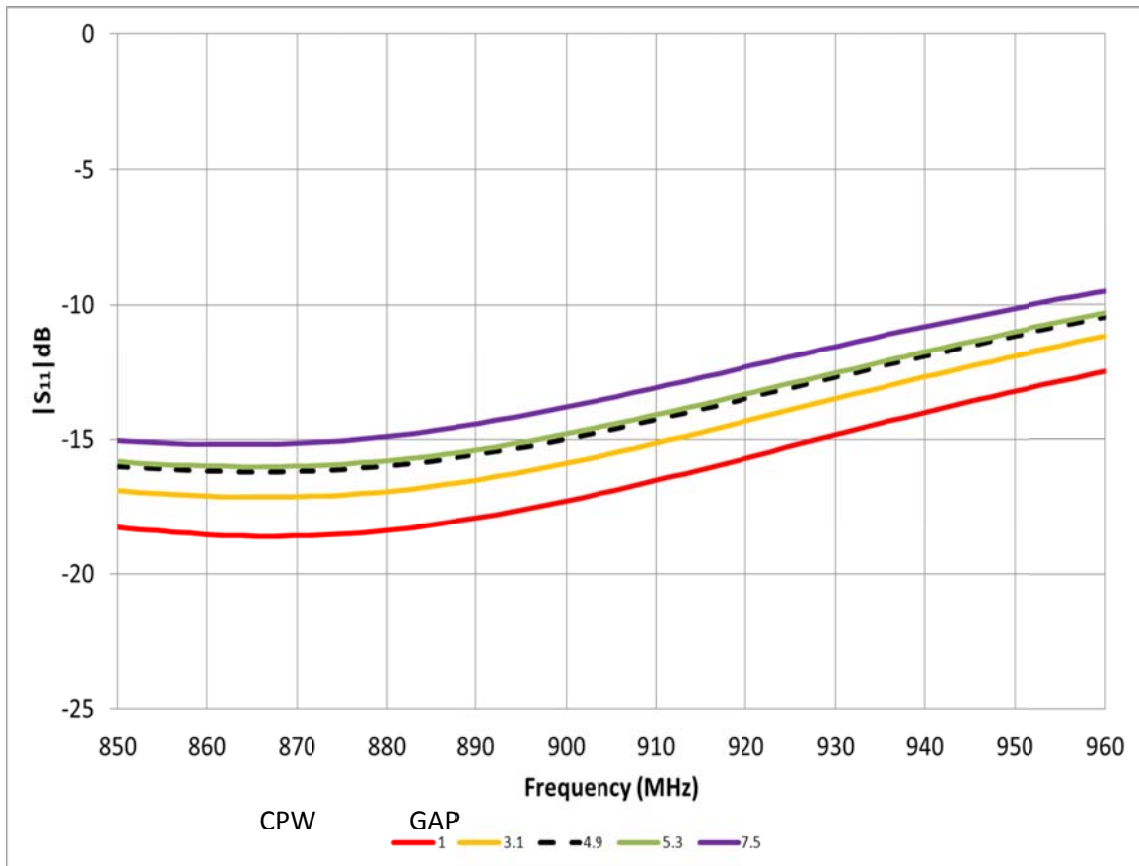
Fig 2-29 Reflection coefficient magnitude of feed network with change in CPW discontinuity gap width (in mm)

2.3.5 Antenna port T-junctions

The antenna port T-junction is actually a short section of slot line that is tapped off the secondary slot line. For the analysis of the antenna port T-junctions, an entire sub-array feed network consisting of three series fed antenna ports is considered, as seen in Fig 2-30 . The S parameters are recorded at each iteration of slot line gap width to determine the amplitude and phase profile across the series sub-array.

It is expected that the phase slope seen at each port will be different either side of the design frequency, but coincide at the design frequency. This is typical of a series fed array. As the sub array is a conventional series fed network, the phase is in advance above the design frequency and lags below the design frequency. Each of the four sub-arrays in the complete feed network will have the same amplitude and phase profile as they have identical structure. Each sub-array on either side of the final feed network is fed back to back; therefore the two

2-84

phase profiles will be in direct opposition. This is the profile required of a centre feed array network.

The phase and amplitude are measured at each of the three antenna ports with respect to the input at port one. Each sub array comprises of a slotline and three antenna ports with an impedance of 129 Ω. The variables analysed are the antenna port gap, slotline track and the slotline stub length.
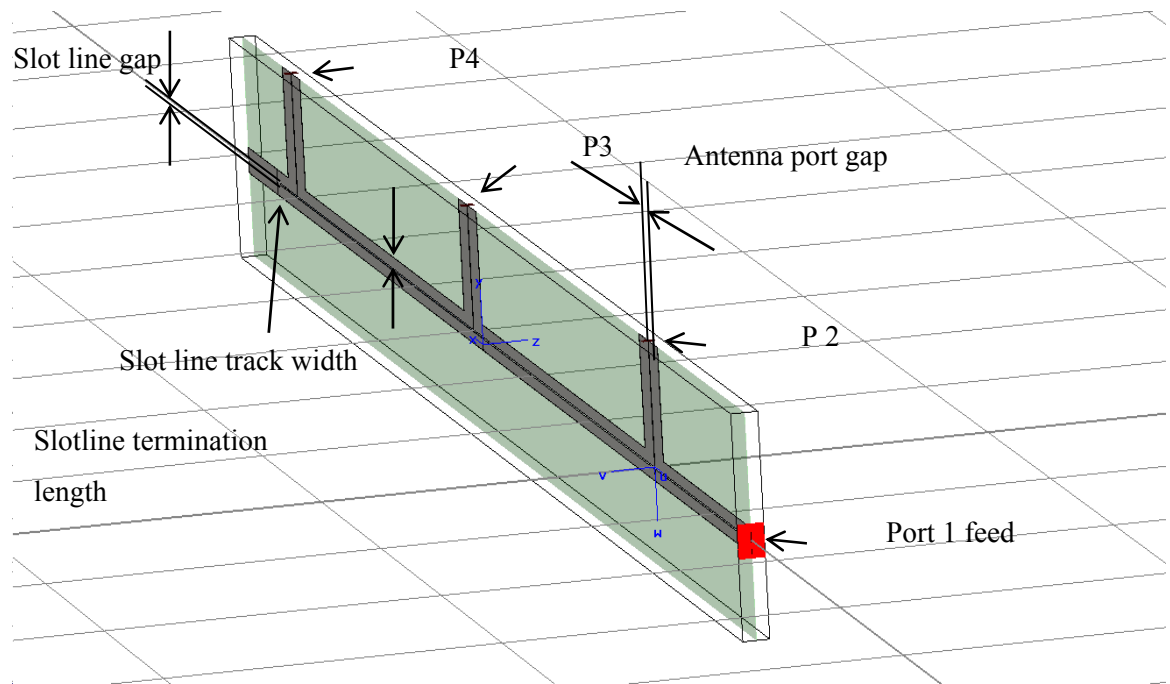
Fig 2-30 Schematic of the three element slotline sub-array feed network with variable parameters

Note: The following results are for just the slotline connected to the dipole ports. These results will not represent cross coupling.

The results presented in Fig 2-31 to Fig 2-34 depict the phase variation across the frequency band of 850-960 MHz for the three antenna ports of the series sub-array for antenna port slotline gaps of 0.2 to 0.7 mm. The anticipated phase slope seen at each port being different either side of the design frequency, but coincide at the design frequency of approximately 910 MHz was observed. The maximum phase taper across the sub-array at the upper band edge (960 MHz) was around 65 degree at a gap of 0.2 mm, extending to about 75 degrees at 0.7 mm.

The results show that relatively consistent and flat responses are observed for Ports 2 and 3 As Port 4 is in close proximity to the termination stub, it experiences a more rapid change in the S-parameter transmission magnitude than the other ports. A maximum amplitude variation between all antenna ports of around +/- 1.5 dB is observed across the entire frequency band. The dipole gap spacing of 0.5 has been selected in the final arrangement as it satisfies the minimum track spacing and has the least variation in amplitude response over the pass band.
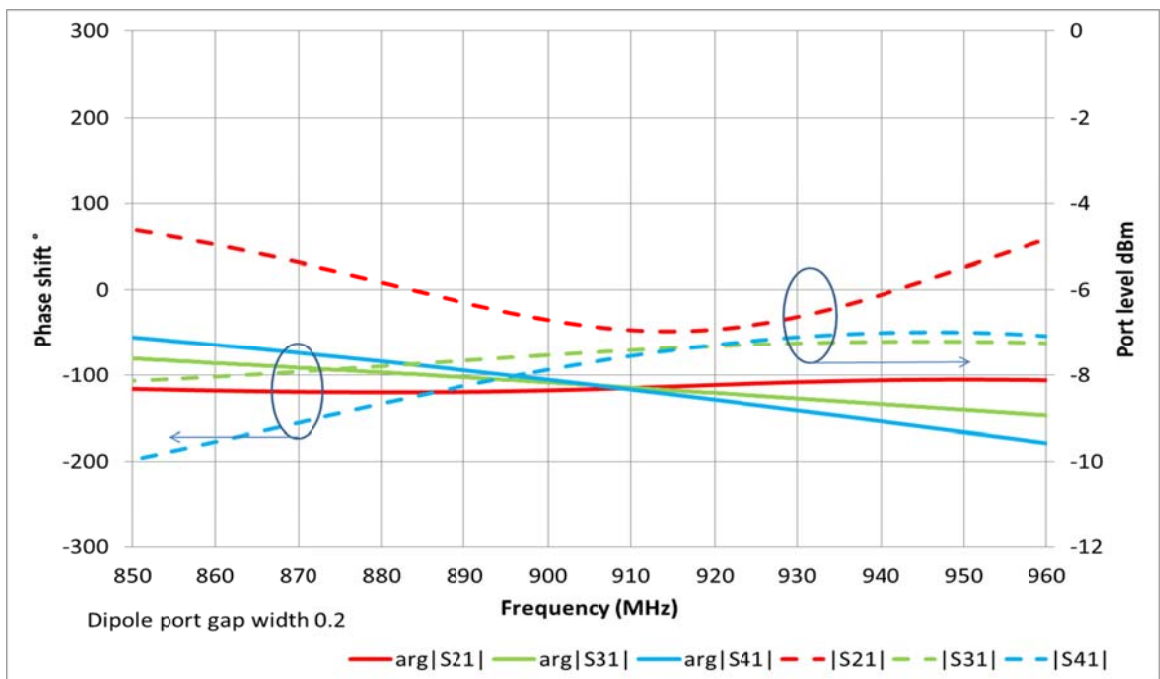
Fig 2-31 Port characteristics where the dipole port gap width is 0.2mm (EM) model
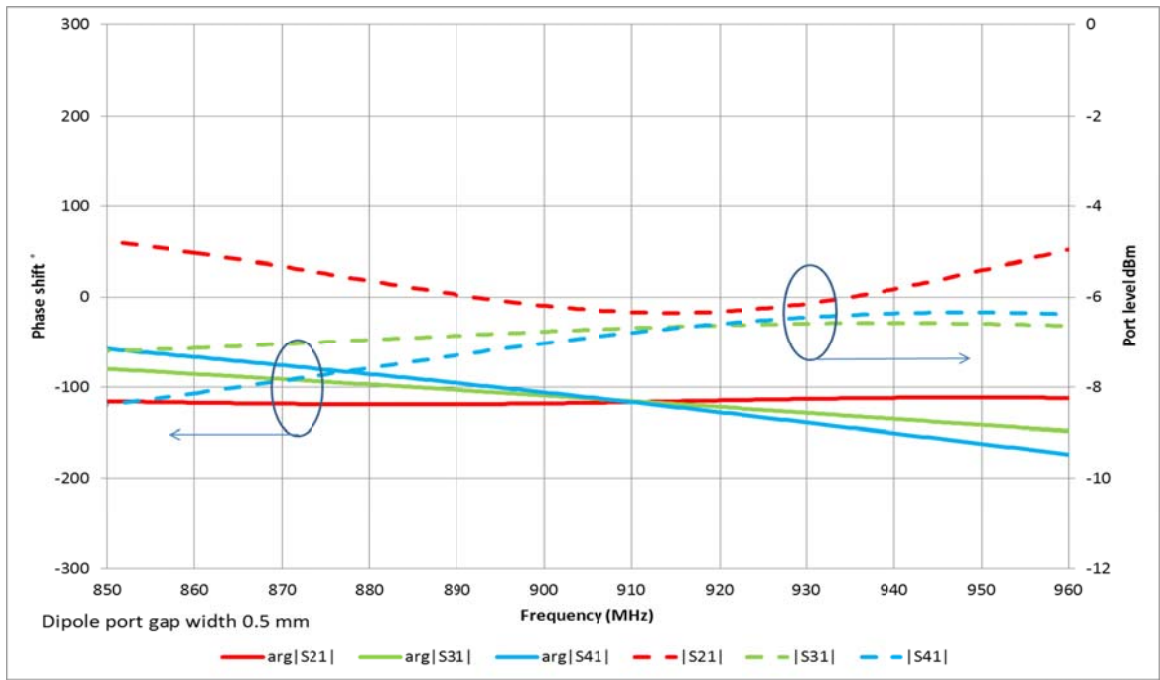
Fig 2-32 Port characteristics where the dipole port gap width is 0.5mm (EM) model
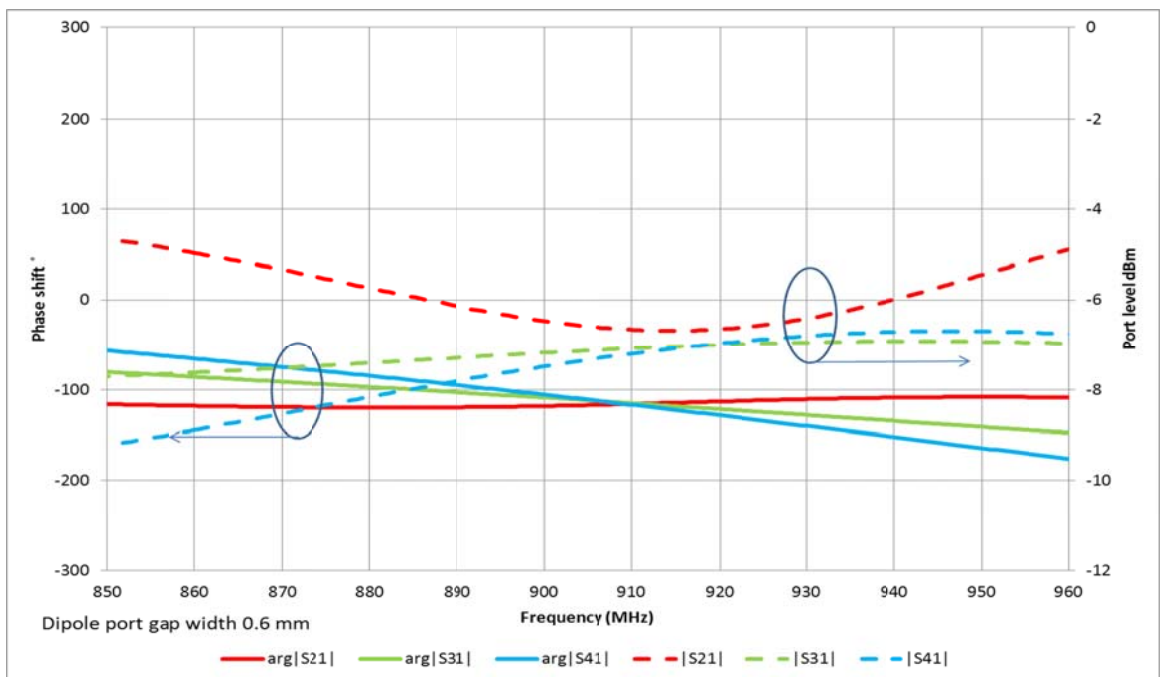
Fig 2-33 Port characteristics where the dipole port gap width is 0.6mm (EM) model

2-87
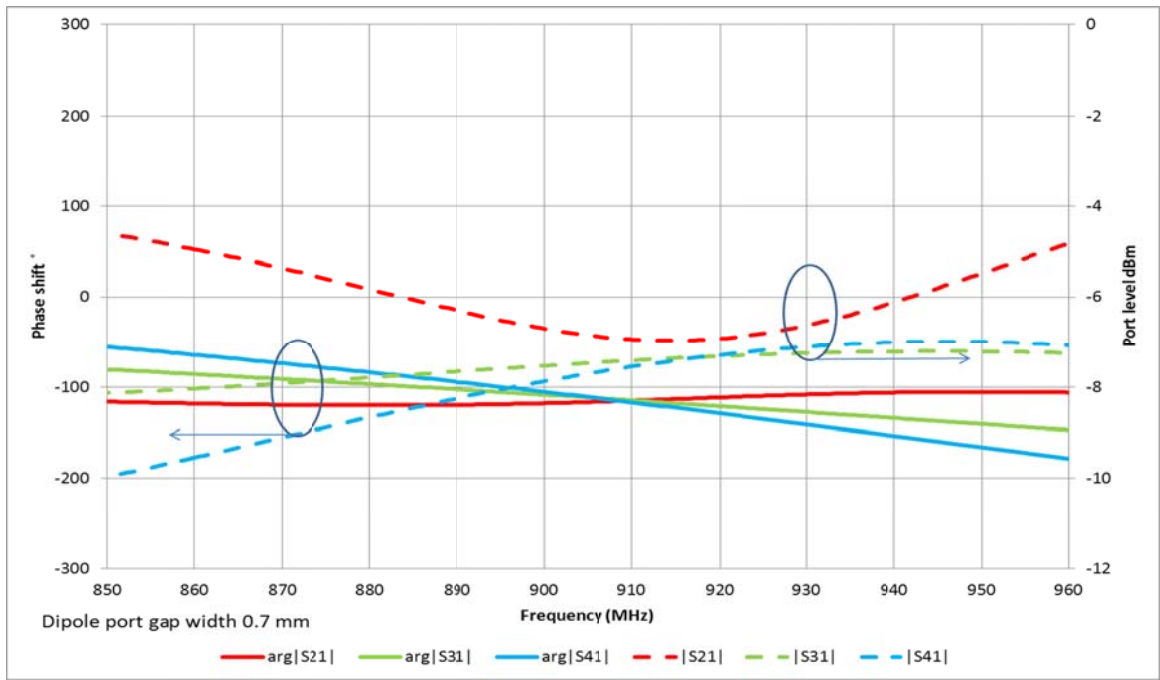
Fig 2-34 Port characteristics where the dipole port gap width is 0.7mm (EM) model

2.3.6   Phase compensation slotline termination

A phase compensation slot line termination is employed at the end of each sub-array to balance the behaviour of antenna ports at the extreme end to the characteristics of the inner antenna ports. To evaluate the effectiveness of this termination, the four port model seen in Fig 2-30 was used with parametric control of the slot line termination length. The transmission performance is analysed as the stub length is varied in length from 1 to 17 mm. The results are presented in Fig 2-35 to Fig 2-37.
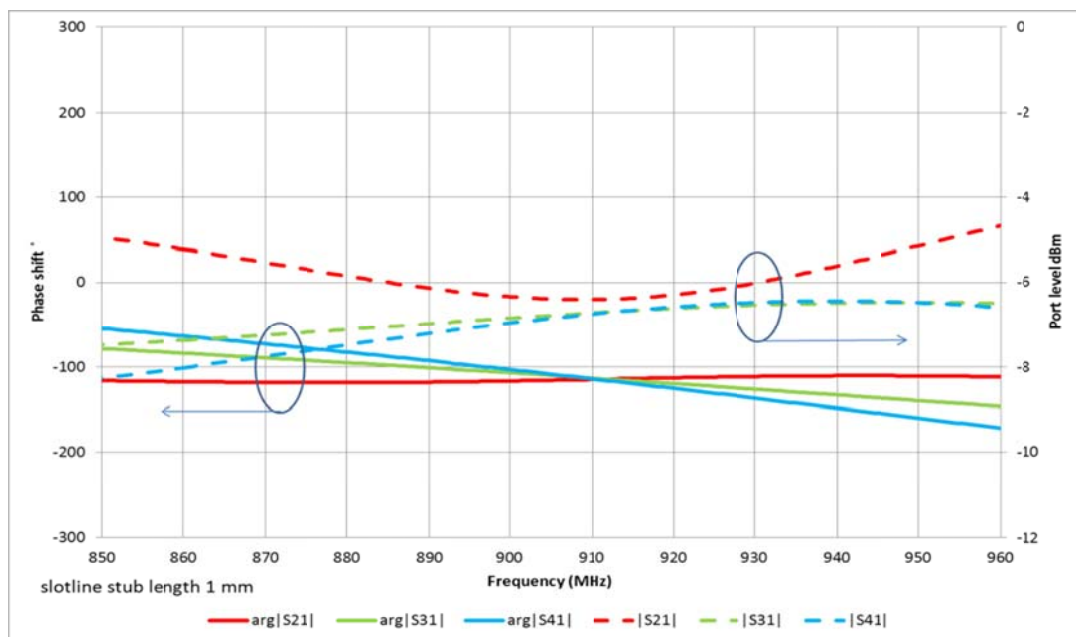
Fig 2-35 Port characteristics where the slot line stub length is 1 mm (EM) model
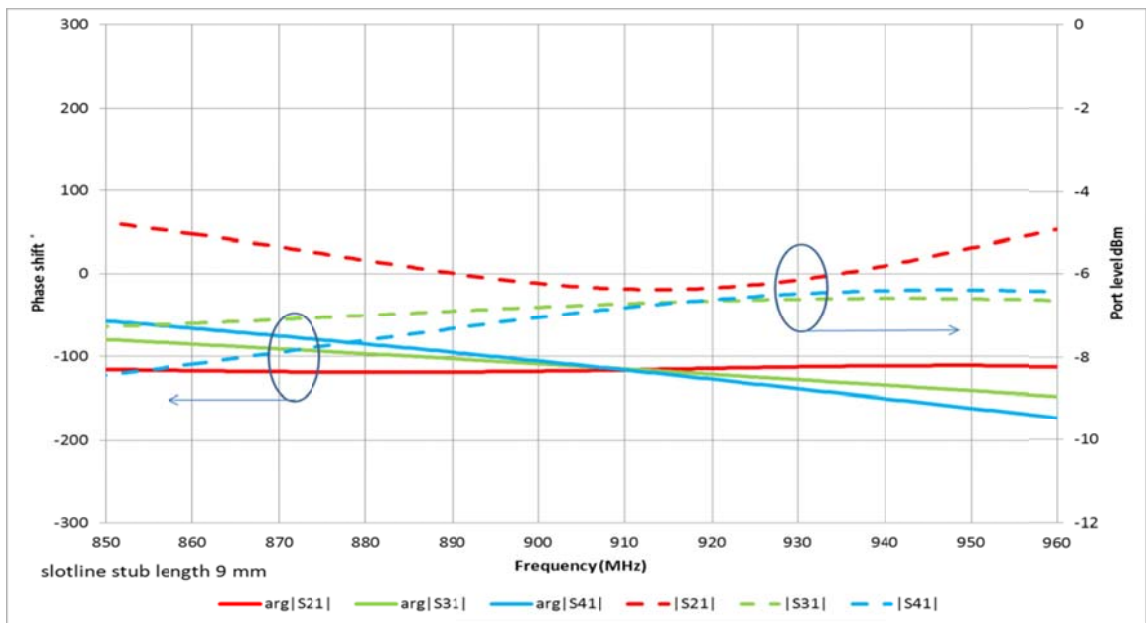
Fig 2-36 Port characteristics where the slotline stub length is 9 mm (EM) model
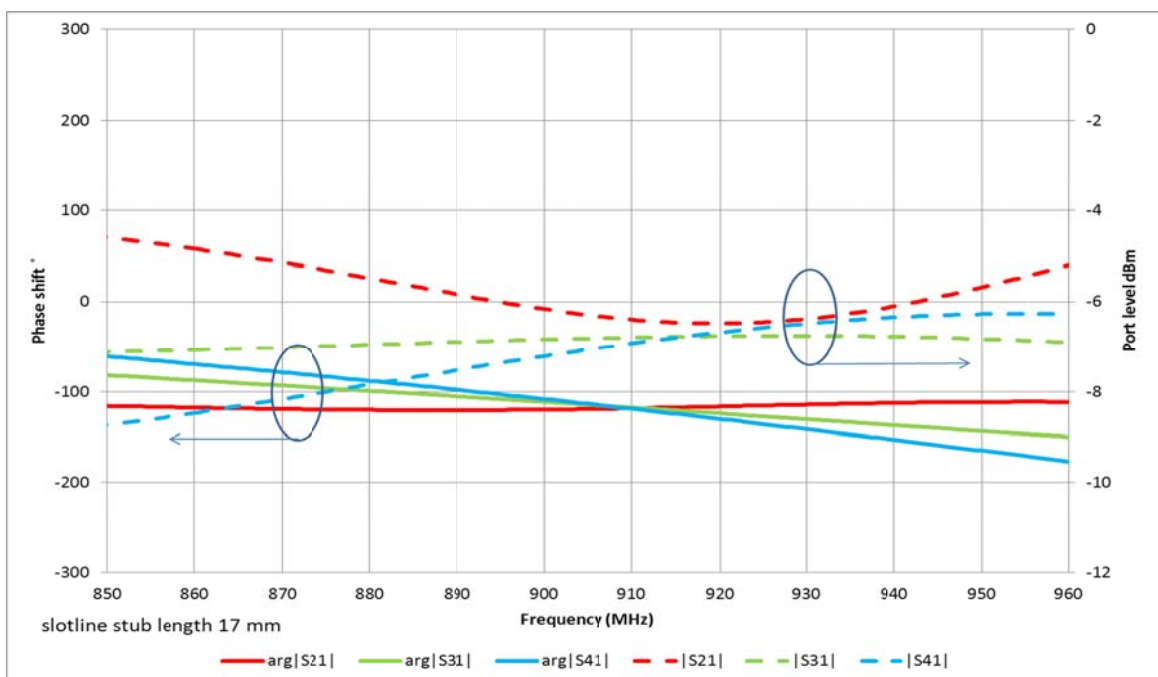
Fig 2-37 Port characteristics where the slotline stub length is 17 mm (EM) model

The result of the parametric sweep of the slotline stub length indicates minimal impact on the phase and amplitude. These stub lengths (1 to 17 mm) represent a very small phase shift of approximately 1 to 18 degrees. As the feed to the network is in series, the phase shift in each

2-90

port is related and minimizes the effective control of phase. The slotline stub of 17mm has been selected as it provides similar feed point geometry to that of the other ports.

2.3.7 Parametric sweep of the slotline track width

As the "Coplanar waveguide (CPW)" and slotline transmission lines are in close proximity, the effects of the width of the slotline track must be evaluated with respect to feed network performance. The four port model seen in Fig 2-30 was again used, this time with parametric control of the slot line track width. The transmission performance is analysed as the track width is varied from 2.4 to 4 mm. The results are shown in Fig 2-38 to Fig 2-40.
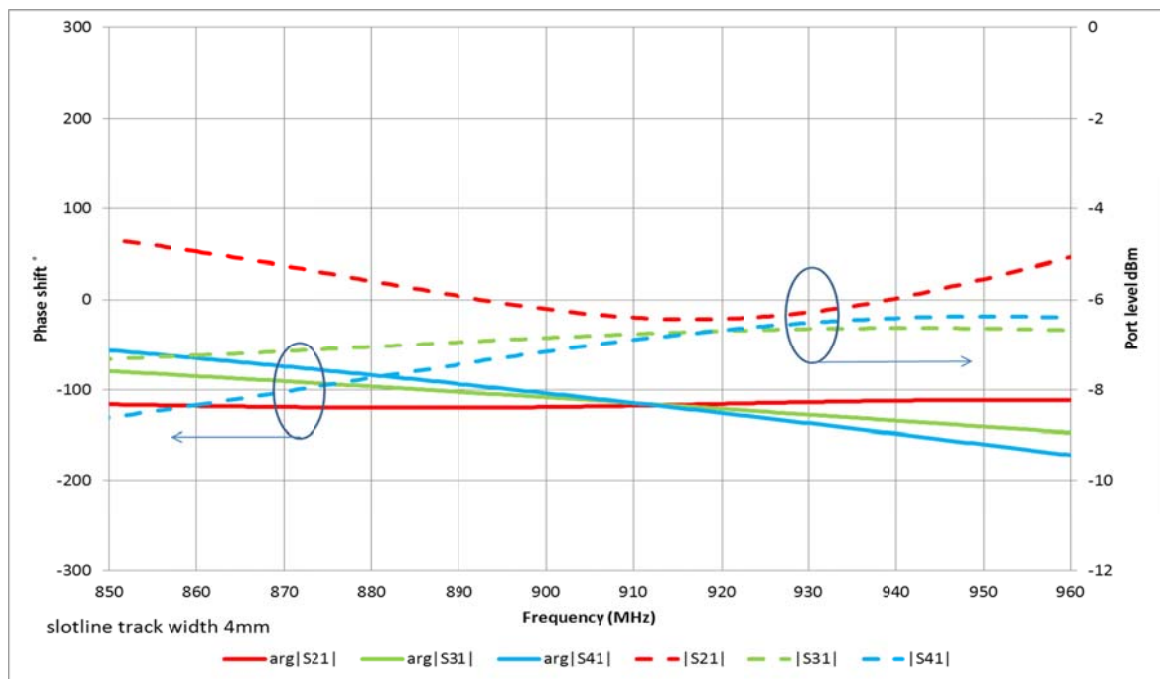
Fig 2-38 Port characteristics where the slotline track is 4mm wide (EM) model
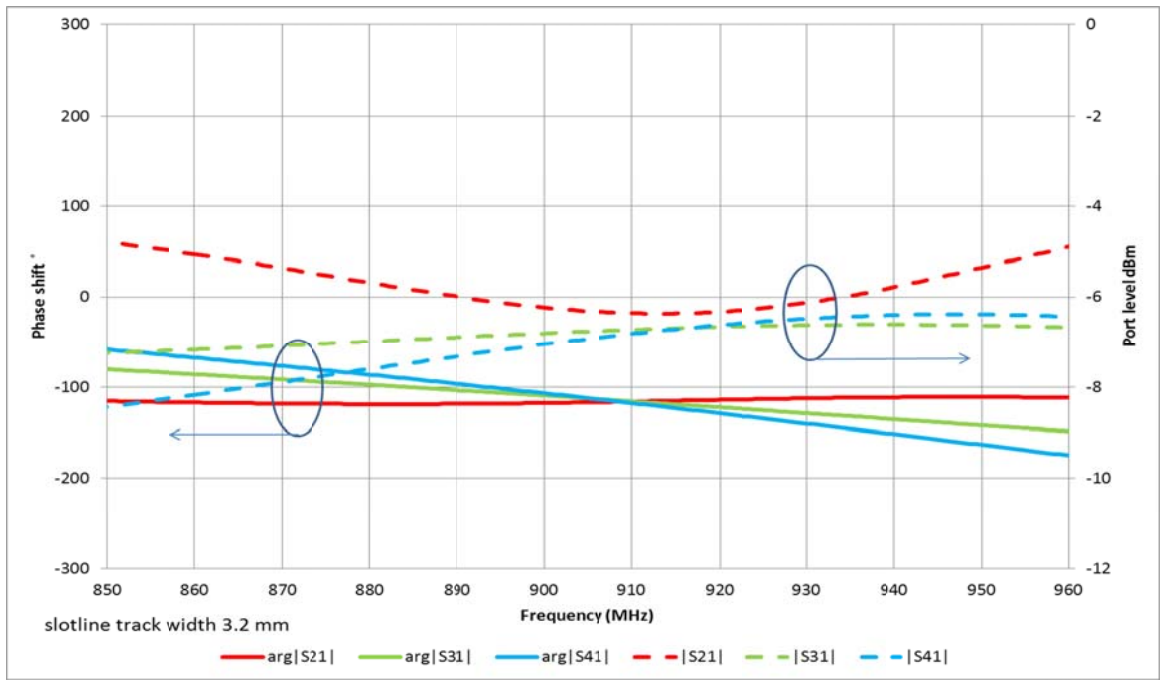
Fig 2-39 Port characteristics where the slotline track is 3.2mm wide (EM) model
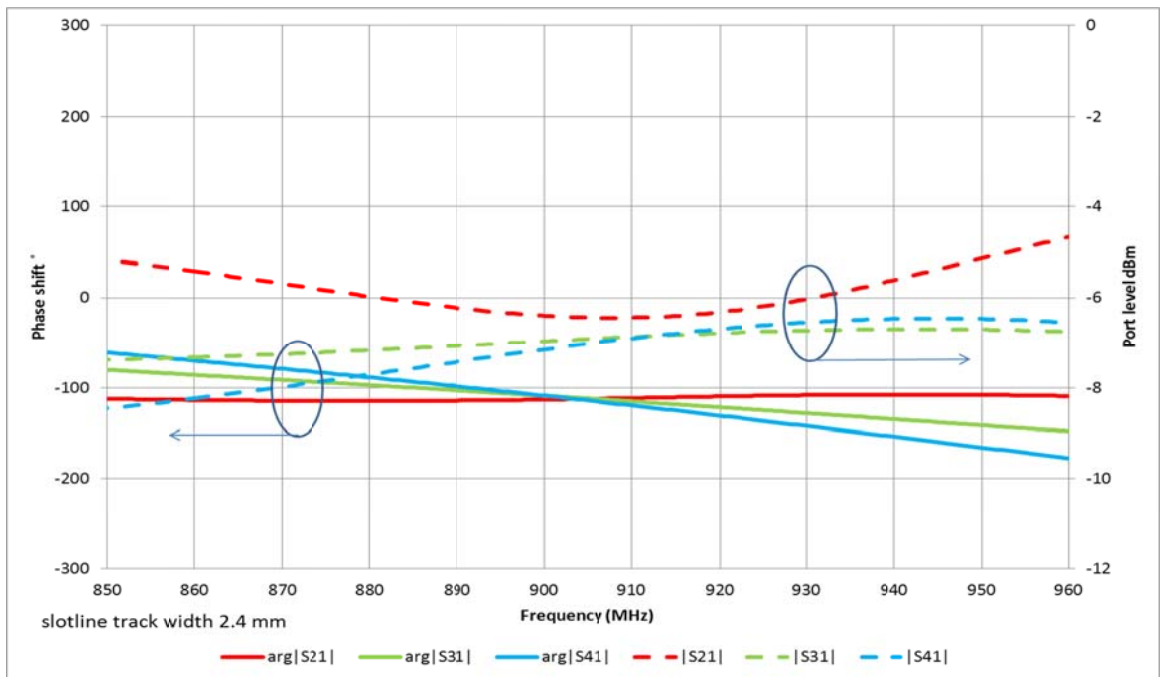
Fig 2-40 Port characteristics where the slotline track is 2.4 mm wide (EM) model

From the analysis of these results, the slotline track width has a negligible impact on the network performance. The most noticed effect is a slight shift in the zero tilt cross over

2-92

frequency. A 4.2mm slotline track width produced a zero degree relative phase at 913 MHz, whereas a track width of 2.4 mm has a zero phase frequency of 905 MHz. This phase error is not critical as any mutual phase offset is cancelled out as both sides of the complete feed network have a phase tilt in opposition to each other. The "Coplanar waveguide (CPW)" ground track width selected is 3.5mm as it is close to the "Coplanar waveguide (CPW)" ground track width.

2.4   Electromagnetic simulation of the planar centre feed network

A detailed electromagnetic (EM) model of the entire feed network was created and analysed using CST Microwave Studio. The antenna ports in this feed network were defined as wave ports to allow the phase and amplitude response to be analysed including coupling effects. The radome and other peripheral mounting structure used (as explained in Chapter 5) are not included in order to reduce the computation time. The port arrangements for the array are shown in Fig 2-41 only one side of the network has ports assuming mirror symmetry.
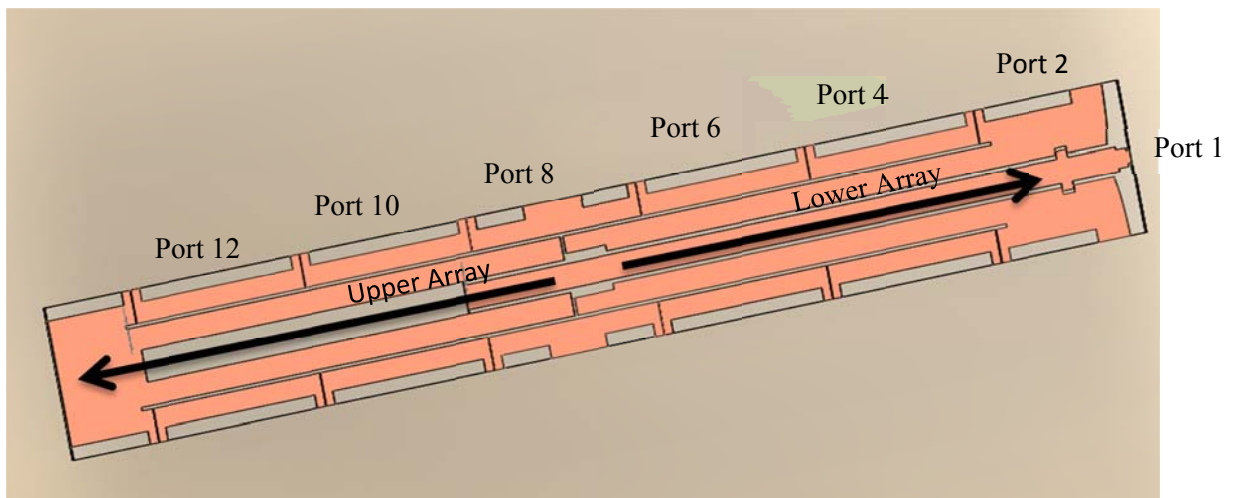
Fig 2-41 The CPW array feed network port configuration

2.4.1   Electromagnetic model results

The transmission loss characteristics and the phase response from the EM model are depicted in Fig 2-42 and Fig 2-43 . As a certain amount of cross coupling between the "Coplanar waveguide (CPW)" and the slotlines was expected the response of the EM model differs with that of the circuit model, showing a slight asymmetry between the two halves of the feed network. The phase response is typical of a feed network for a centre fed array, where a relatively constant gradient is evident. The worst case phase difference between the antenna ports is 100 degrees, which occurs at 880 MHz. This phase error is tolerable as each sub array is fed back to back cancelling out the frequency dependent phase error. The circuit model simulation exhibits a similar phase error. The amplitude response exhibits undulation across the frequency band of interest as a result of cross coupling. The port amplitude difference is approximately 7 dB in the case of the EM model; whereas the circuit model was 4 dB The differences in amplitude are most likely the result of cross coupling between the "Coplanar waveguide (CPW)" main line and the slotlines.
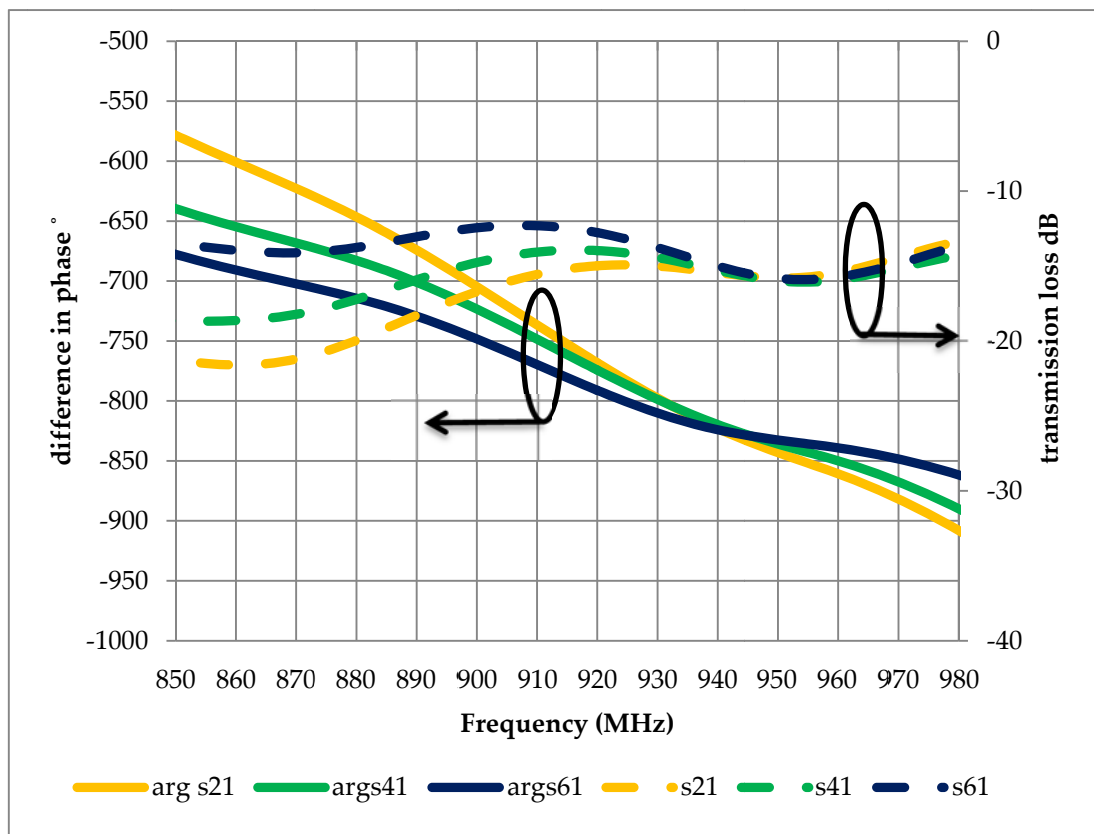
Fig 2-42 Phase and amplitude of the lower array ports (EM model)
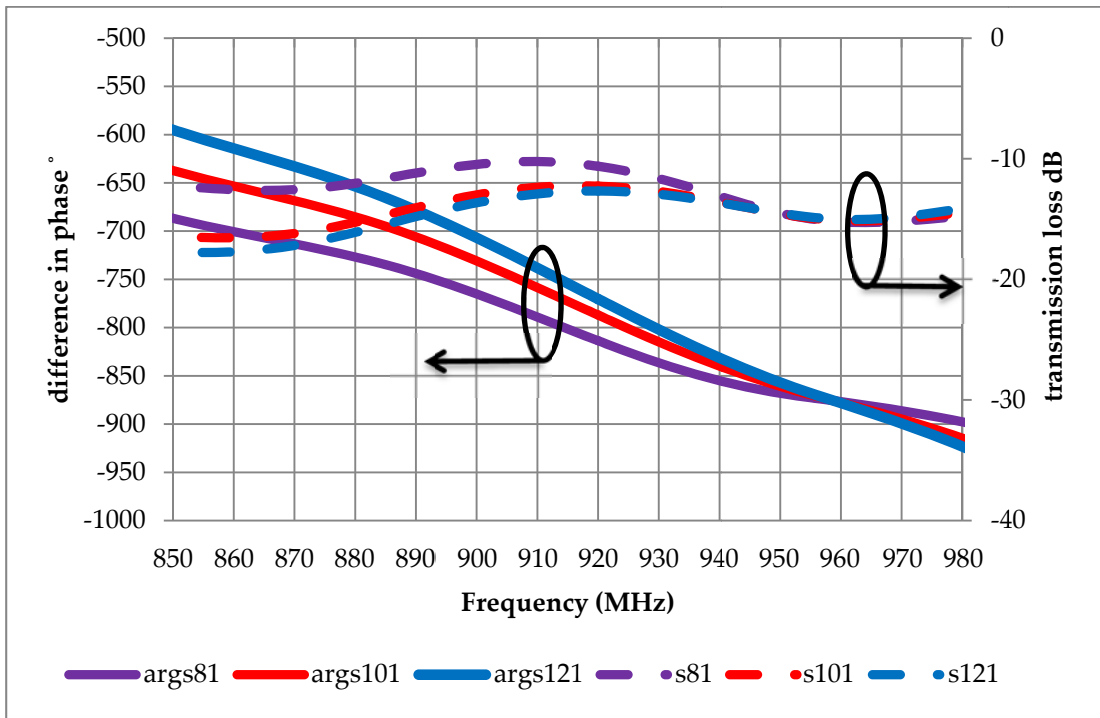
Fig 2-43 Phase and amplitude of the upper array ports (EM model)

Note: Figure 2.42 and 2.43 are the results from EM simulation of the upper and lower array ports including the "Coplanar waveguide (CPW)" feed. These models will present cross coupling.

The $|S_{11}|$ of the EM model is presented in Fig 2-44   the feed network exhibits a 10 dB reflection coefficient magnitude bandwidth commencing at approximately 872 MHz. This is inside the final bandwidth specification of 850 – 960 MHz. However, as mentioned previously these results are generated with no radome or peripheral mounting components included in the model. These components act as a dielectric loading to the feed network and have been shown to shift the response approximately 40 MHz lower in frequency. The final antenna port spacing allowing for dielectric and radome loading was one wavelength, or approximately 290 mm at 910 MHz.
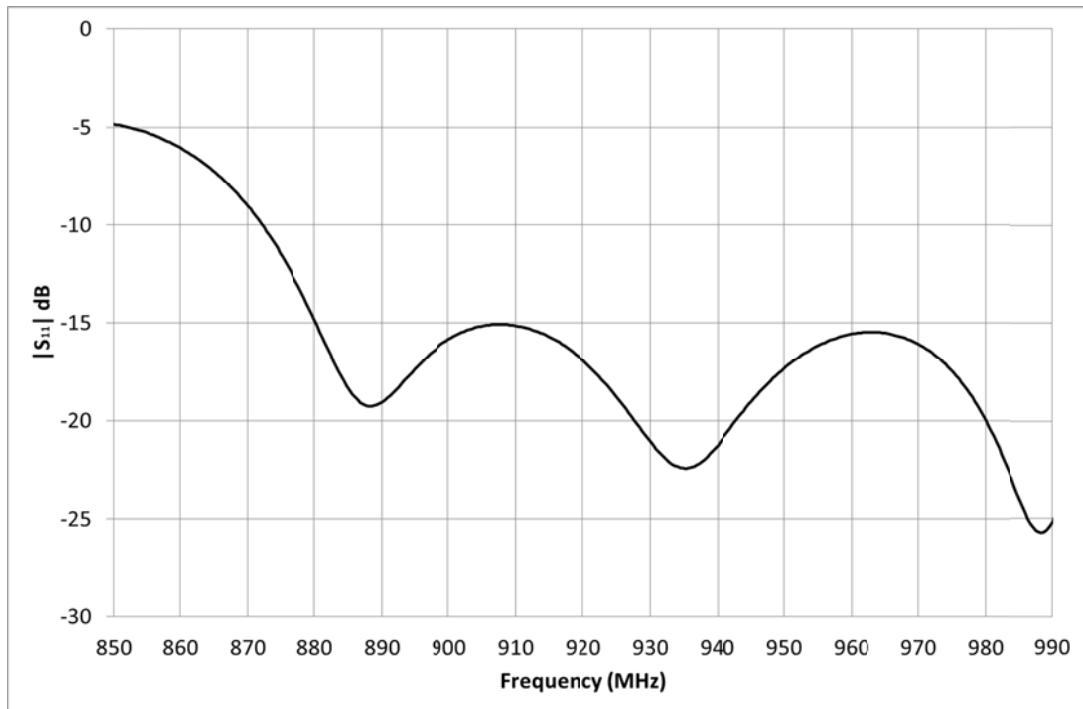
Fig 2-44 $|S_{11}|$ of the planar feed network (EM model)

2.5   Summary

A feed network suitable for a centre fed collinear array was introduced in Section 2.1 which satisfies the dimensional and electrical requirements of this project.   The feed network characteristics have been analysed as a planar multi-port network with the aid of [40]Design studio for a circuit model simulation, and [40] microwave studio. By designing the "Coplanar waveguide (CPW)" main feed line at high characteristic impedance, the overall width of the array can be reduced, meeting the mechanical constraints set forth.

The limitations of the "Coplanar waveguide (CPW)" feed network have been discussed in Section 2.2.   The printed network has low effective thermal dissipation when compared to state-of-the-art metal tube construction, and hence is suitable for low power base station applications. The minimum track spacing of 0.5mm imposed by standard reel to reel printed circuit processing is accounted for in the design.

A [40]Design studio circuit model of the feed network has been created in Section 2.4 and port characteristics were analysed. This model has been used as to benchmark performance and

2-96

was further developed with associated electromagnetic models of particular sections of the feed network.

In Section 2.4, an electromagnetic model of the entire feed network was generated. All electrical expectations for the feed network were achieved, including low transmission loss, operation in the desired frequency band, and relatively stable phase profile. The linear phase profile has been verified by experimental testing of the complete base station array in Chapter 5.3.

Chapter 3   A broadband printed dipole element for a collinear array

3.1   Introduction

In this chapter, the development path from a conventional cylindrical dipole to the novel planar dipole element for a printed collinear array is described. The characteristics of the printed dipole element fed in series by a slotline transmission structure are investigated and validated using numerical simulation in CST Microwave Studio.

A standard dipole is a simple assembly with two $\lambda/4$ wires or tube elements on either side of the source. A single dipole on its own has relatively a small proportion of the available radiated energy directed at the horizon due to the wide elevation beam width of its omnidirectional pattern, which limits its application. To increase this radiation level, the pattern shape must be compressed in the elevation plane. This is achieved by creating a vertical array of a number of dipoles, as discussed in Chapter 1. The complexity in creating a conventional omnidirectional array of vertically oriented dipoles for base station applications lies in the routing of the feed lines/cables to each dipole element. To preserve the omnidirectional performance, the array geometry must be as close as possible to axis symmetric. To achieve this, the feed network is normally routed in the core of the array, with the dipoles mounted concentrically as sleeves on a cylindrical support pipe. This is the most common implementation for conventional omnidirectional base station arrays. Increasingly, array antennas are being designed using printed circuit technology and as such, the dipole elements are normally planar and integrated with the feed network. The advantage of this direction is lower cost, high repeatability, and a reduction in the number of soldered connections leading to less passive intermodulation. Specialised designs are required to mask the transmission lines from the radiating elements. For omnidirectional collinear base station arrays, these advantages are countered by the complexities associated with feeding the array elements and processing a high aspect ratio printed substrate.

This chapter introduces a high performance planar dipole which is suitable for printed omnidirectional collinear arrays. To prove that this new topology has more control over

3-98

impedance and has a more uniform radiation pattern characteristic than currently available planar dipoles, a number of investigative tests are conducted. Section 3.1 presents a review of broadband planar dipoles, and explains how the planar dipole is the analogue of a cylindrical dipole in terms of current distribution and radiation pattern. Section 3.3 includes the capabilities of planar dipoles for impedance matching and self-choking to prevent out of phase radiation, and the ability to reduce aperture blockage.

The unique structure of the proposed planar dipole for printed omnidirectional collinear arrays is introduced in Section 3.3, along with an explanation of the bandwidth enhancement techniques applied to the geometry in the form slots and notches. The enhancement techniques are analysed and validated with the aid of electromagnetic simulations [40]. The model of the proposed planar dipole element is analysed separately from the array in order to characterize the feed point impedance and bandwidth characteristics.

The dipole performance when in an array configuration is also discussed. The current distribution resulting from series feeding and the effect of mutual coupling on the array pattern stability are analysed. The requirements for the use of this dipole element in an omnidirectional array are also detailed. A summary of the investigations and results are presented in Section 3.4.

3.1 A review of existing broadband and planar dipoles

For conventional dipoles, bandwidth can be primarily controlled by the geometric length to diameter ratio. Smaller ratios i.e. Fat dipoles have lower Q factor (and hence broader bandwidth) but also result in reduced cross-polar performance as there is less distinction between E and H plane geometry. The resonant length for these dipoles is shorter than for thin dipoles.

Dipole bandwidth can also be increased by introducing slots and notches into the element [44], in this example as shown in Fig 3-1 the dipole is fed at across A and B by a slot line with a gap spacing of 0.5mm. This example comprises of two sets of elements fed in parallel by a short section of slot line. Finding the right balance between match and band position will

result in a broad impedance bandwidth. The slots are used to create a dual band response. A parasitic element placed in front of one of the dipole arms, further increased the bandwidth This dipole without parasitic element can achieve a bandwidth of 22% 1.65 to 2.05 GHz with a reflection coefficient magnitude of -10dB.With the addition of a parasitic element, the bandwidth is 50% 1.66 to 2.71 GHz. The radiation pattern for this arrangement is directed forward with front to back ratio of approx. 10 dB this results in a realized gain > 6dB The asymmetry is the direct result of placing the parasitic element in front of one of the elements and slightly towards the feed gap.

A

Arrangement for 50% bandwidth asymmetric radiation

B

Arrangement for 22% bandwidth symmetrical radiation

Fig 3-1 The broad banding technique used for [44]

Parasitic elements were considered in the proposed design, these would have resulted in an increase of >10mm in the array width. These geometric obstacles delay the propagation of current around the dipole perimeter, independent of the physical length of the element. This increases the inductance which cancels out the capacitance. The net effect is to reduce the reactance that is impacting on the bandwidth. Dipoles treated in this way usually will have a lower resonant frequency. **The bandwidth of a dipole is increased by introducing a disturbance to the Q of the dipole. This element being closely coupled modifies the resonance to form a second resonance. Careful adjustment of the geometry can yield a broad response in terms of reflection coefficient.**

3-100

The bi-conical dipole shown in Fig 3-2(a) can achieve a multi octave bandwidth as its geometry is able to occupy a large volume within the radian sphere. In this configuration, the feed point impedance remains relatively constant with change in frequency [16]. The large volume geometry restricts its use to heavy duty applications such as broadcast panel antennas. The planar analogue of the bi-conical dipole is the bowtie dipole, shown in Fig 3-2 (b). This dipole does not have as broad bandwidth performance as the bi-conical dipole, as radian sphere occupation is only possible with a >60° dual triangular element [16] in only one plane.

(a)   (b)

Plan   view
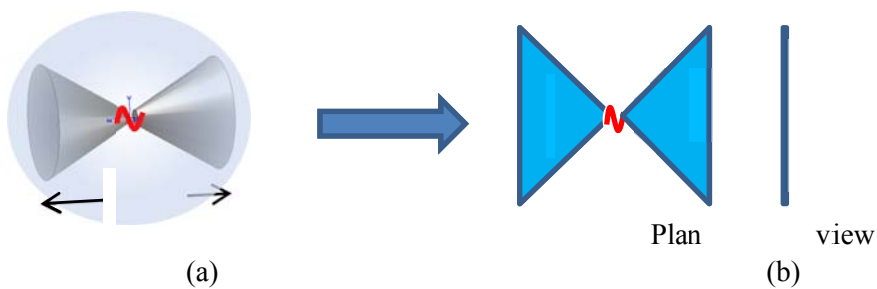
Fig 3-2 (a) Biconical dipole (b) Bowtie dipole [16]

Another form of dipole which is commonly used in base station arrays is the sleeve dipole, shown in Fig 3-3 [31]. This dipole design has low frequency resonant elements which are not active at higher frequencies, resulting in a dual resonant response [16]. By careful selection of tube diameters and lengths this can approach a broad band response. A comparison between dual band and broad band tuning of sleeve dipole is shown in the inset of Fig 3-3. In this case the two stronger resonant responses are merged together forming a flatter, broadband response. This effect is similar to broad band-pass filter tuning.

3-101
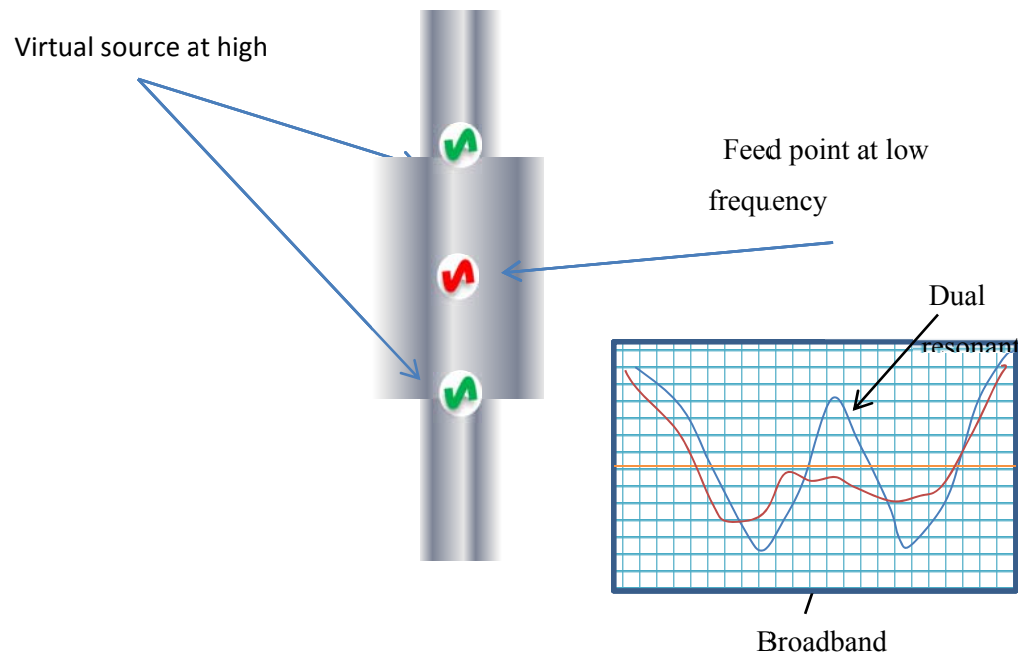
Fig 3-3 Sleeve dipole with virtual high frequency source:

Inset - synthesized broad band response

Planar dipoles found in the literature are generally the 2D analogue of cylindrical structures, fabricated on low cost printed circuit material. All are designed to minimize the azimuth distortion in order to provide the best omnidirectional performance possible from a planar element. Some examples of these dipoles can be found in [24] [33] [34]. These arrays all have "H" shaped dipoles. This shape creates a safe path for the feed network of either microstrip or "Coplanar waveguide (CPW)" to be routed where there is no masking of the radiation pattern. The geometry of the "H" shaped dipole is such that the radiating elements are spaced out on either side of the feed network. In this arrangement, the radiation pattern from each element is directed away from the feed network and combined with a 180 degree phase relationship producing a slightly oval omnidirectional performance.

 The major difference between these dipole designs and the proposed dipole design is in the integrated element matching and broad banding approach. The proposed dipoles are slot fed

and passive coupled which provides broad band performance with a balanced current distribution.

It is well known that radiating surfaces of an antenna are highly reactive and feed cables that are routed in close proximity to them will radiate out of phase. This cable radiation can cause destructive interference to the primary antenna pattern. The planar array architecture in [24] attaches a section of coaxial cable to a grounded section in the planar geometry to remove the potential difference between the feed cable ground and dipole element ground. This allows the cable to be routed behind dipoles with minimal interaction.

Much of the previous research concentrates on implementing broad band matching circuits rather than directly increasing the impedance bandwidth of the dipoles (for example [36]). The use of planar dipole elements allows for more flexibility in the creation of lumped constant components within the dipole geometry. These can be created using strategically positioned tags and notches within the dipole geometry. The proposed broadband planar dipole structures in this Chapter are fed using "Coplanar waveguide (CPW)" primary feed line. The feed network discussed in Chapter 2 is designed to isolate the main feed network from the dipoles by coupling to a secondary set of slotline transmission structures. The planar dipole elements are tapped off in series using a short section of slotline.

3.2 Design considerations for an omnidirectional collinear array dipole element

As elements are added to an array, mutual coupling of the adjacent dipoles effectively lowers the resonant frequency of all the dipoles in the array. Both the cylindrical and planar dipoles typically are shorter than a half wave as the array size increases up to about 8 dipoles. Another factor that must be considered is radome loading. E.g. A fiberglass radome with a 6mm wall has enough loading to reduce the dipole resonant frequency by 25MHz at 850 MHz. Knowing the loading effects and offsets can significantly reduce simulation task as it can be treated as a post process [41].

The proposed array dipoles are designed to suit their position in the array and as such, the dipole elements at the far ends of the array are different. This is due to the inside dipole arm being loaded by the previous dipole and the outside dipole arm exposed to free space

conditions. Increasing the length of the central conductive support above the dipole, will then expose the dipole to similar loading as the inside elements.

3.2.1   The transition from cylindrical to planar topology

To allow the dipole to be used in planar type arrays and take advantage of a printed circuit process, the element must undergo another transition phase from cylindrical to planar, as shown in Fig 3-4. Planar elements are an advantage as they can be fabricated as a printed circuit using highly repeatable processes. This topology is suitable for integrating matching circuits into the dipole. The first change is feeding a monopole above a coaxial sleeve (Fig 3-4a), to a feed through cable form that can be routed to feed multiple series fed elements (Fig 3-4b). The cylinder elements are then replaced with planar elements as shown in Fig 3-4c. Finally, the coaxial cable is replaced with a "Coplanar waveguide (CPW)" transmission line (Fig 3-4d). The dipole and feed are now suitable for fabrication onto a PCB. The next stage, and the subject of the thesis, is to further enhance the antenna performance. This is done by providing a centre feed function for the planar array. To achieve this, the dipoles are fed by passive coupled slot lines. The method allows for energy to be coupled off the main "Coplanar waveguide (CPW)" line in a controlled way. In Fig 3-4e, the passive coupled dipole is fed via two slot lines energised by the "Coplanar waveguide (CPW)" discontinuity discussed in detail in Chapter 2.
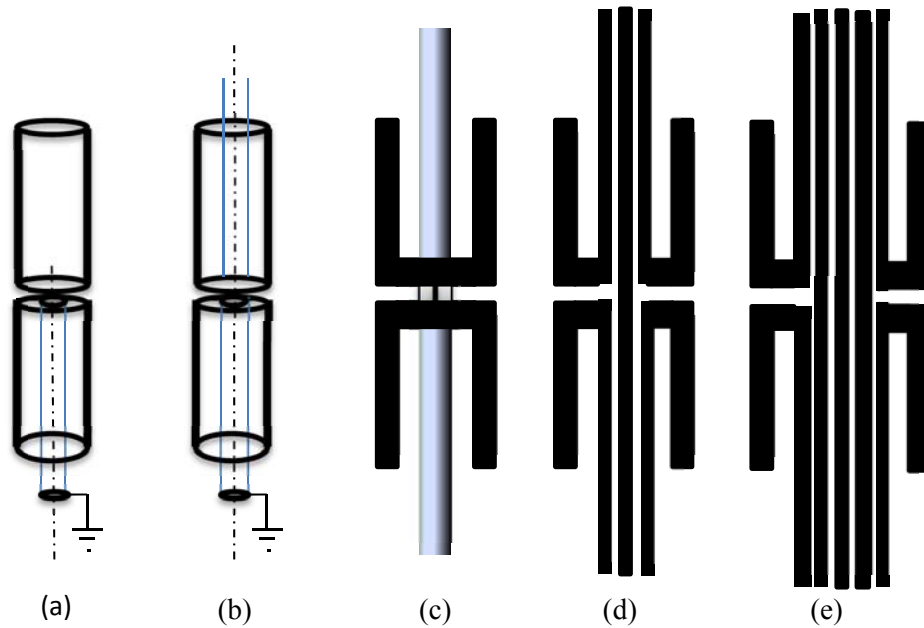
Fig 3-4 Cylindrical to planar element evolution

(a) A cylindrical dipole – centre fed

(b) A cylindrical dipole – series feed through

(c) Cylindrical dipole planar analogue – series feed through

(d) CPW fed planar dipole

(e) The proposed slotline fed planar dipole topology

A model of a conventional cylindrical dipole and a planar dipole was created as in Fig 3-5. The planar dipole is supposed to be an alternative to the cylindrical dipole. As the planar dipole has less volume, it will normally fall short in bandwidth when compared to a cylindrical dipole. To increase the bandwidth of a planar dipole, the Q must be reduced. This can be done by introducing a second parasitic element or small notches in the forcing resonance at two frequencies, spreading the band.

There is a broader response than the equivalent conventional cylindrical dipole, as seen in the results in Fig 3-6. The width of the dipole has been increased to give the dipole the equivalent flat plate area of a cylindrical dipole.

i.e. a cylindrical dipole of 31mm diameter is the electrical equivalent to the area of 62mm wide planar dipole of the same length [16].
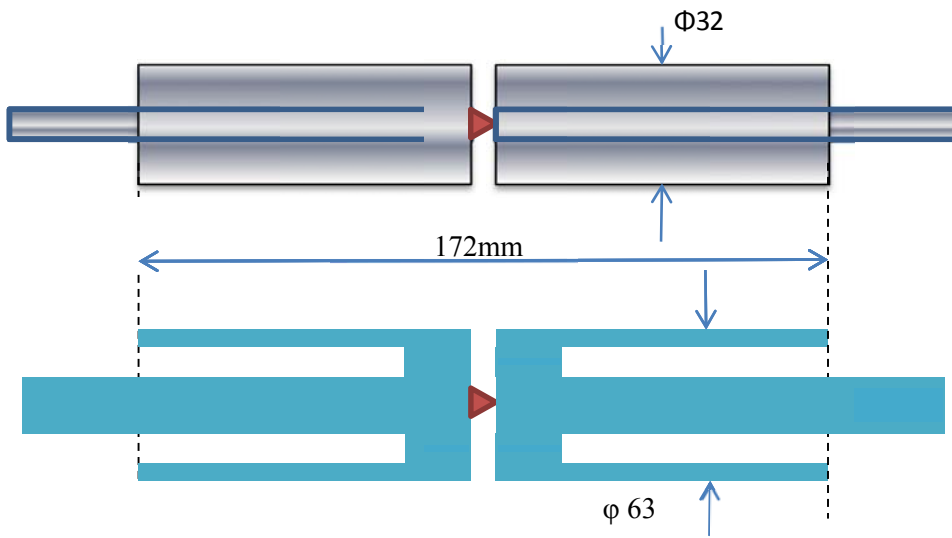
Fig 3-5 A cylindrical sleeve dipole and the analogue planar dipole
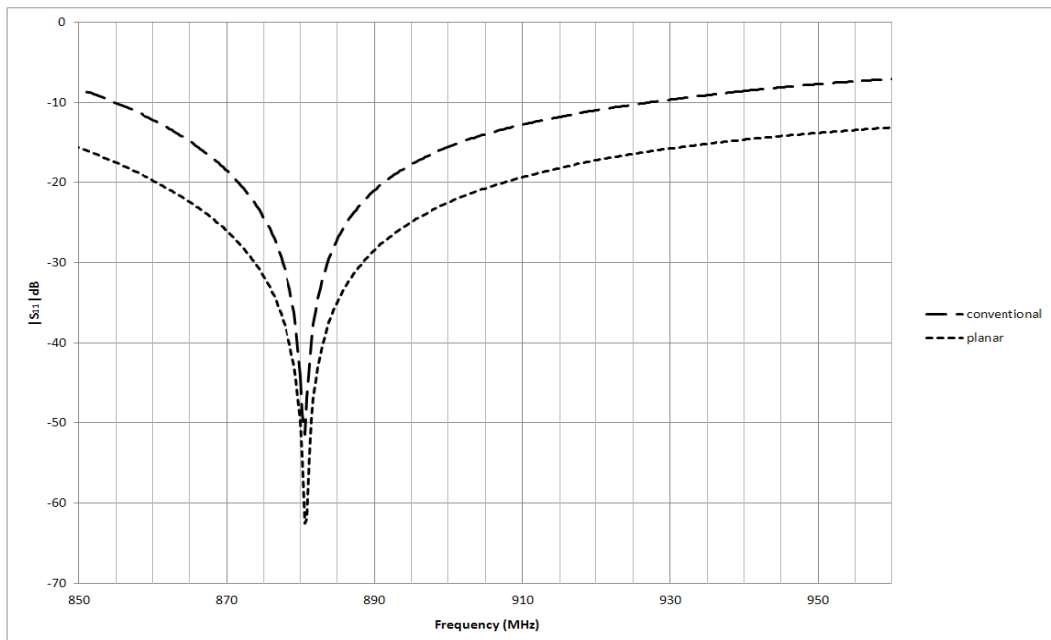
Fig 3-6 $|S_{11}|$ for the conventional cylindrical dipole compared to the planar dipole

3.3   The proposed planar dipole

The structure of the proposed dipole is designed to integrate with a linear array feed network as described in Chapter 2. The width of the final planar dipole collinear array is limited by the mechanical dimensions of the proposed radome. This restricts the distance the dipole can be away from the main feed structure, (a) in Fig 3-7, and defines the azimuth pattern omnidirectional performance. If the spacing is too large, the azimuth pattern becomes more oval shaped rather than circular (for an omnidirectional array). The dipole gap spacing (b) determines the feed point impedance for the dipole, which sets the characteristic impedance of the slotline (c). Slots placed in the ends of the dipole arms (d) are used to help reconstitute the omnidirectional azimuth pattern.   Planar elements naturally have a compressed omnidirectional azimuth pattern due to their 2D structure. The slots are placed parallel to the leading edge of the dipoles. To broaden the dipole impedance, notches (e) are removed from the tips of each dipole arm. To provide inter-element choking of the dipoles, the inside arm length of the dipole (f) is adjusted to cancel out the currents that may be induced onto the transmission sections between the dipoles. This dipole is coupled to a "Coplanar waveguide (CPW)" main feed network. A slot line transmission line (c) is formed between the "Coplanar waveguide (CPW)" ground tracks (g) and a second track running in parallel. This is used to feed the dipoles as a second layer transmission network and prevents cross talk from the main "Coplanar waveguide (CPW)" feed coupling directly to the dipoles, suppressing any undesirable radiation. The dipole length (h) has been selected to resonate at the centre frequency of 903 MHz, taking into account the radome loading and mutual coupling. The dipole starting geometry is based on a conventional half wave dipole. The dimensions are then adjusted to compensate for dielectric loading and mutual coupling effects with CST microwave studio [40]. The final dimensions were optimised with the assistance of numerical simulation (CST microwave studio) [40].

3.3.1   Proposed planar dipole structure

As the slotline transmission lines feeding the proposed dipole are balanced, the planar dipoles maintain a balanced current distribution, leading to an efficient array pattern which is comparable to the cylindrical form. A comparison of the surface currents is made between the conventional coaxial collinear series feed element in planar form [34] and the proposed feed in Fig 3-8. In Fig 3-8(a), a large portion of the available current is coupled to the dipole, leaving less available for subsequent dipoles along the series feed. The currents on the dipole arms are also asymmetric. A section of the proposed topology shown in Fig 3-8(b) displays much more evenly distributed currents. Only a controlled portion of the energy is coupled off the main feed network, allowing the subsequent dipoles to have more evenly matched amplitude in the series fed array. In this situation, the currents in the array will be viable over a longer distance enabling a large number of elements. The extra slotline tracks between the dipole and main feed line effectively separate the current paths, preventing out of phase interference from main feed.

3-107

(h)

(b)

(e)

(f)

(g)

(c)
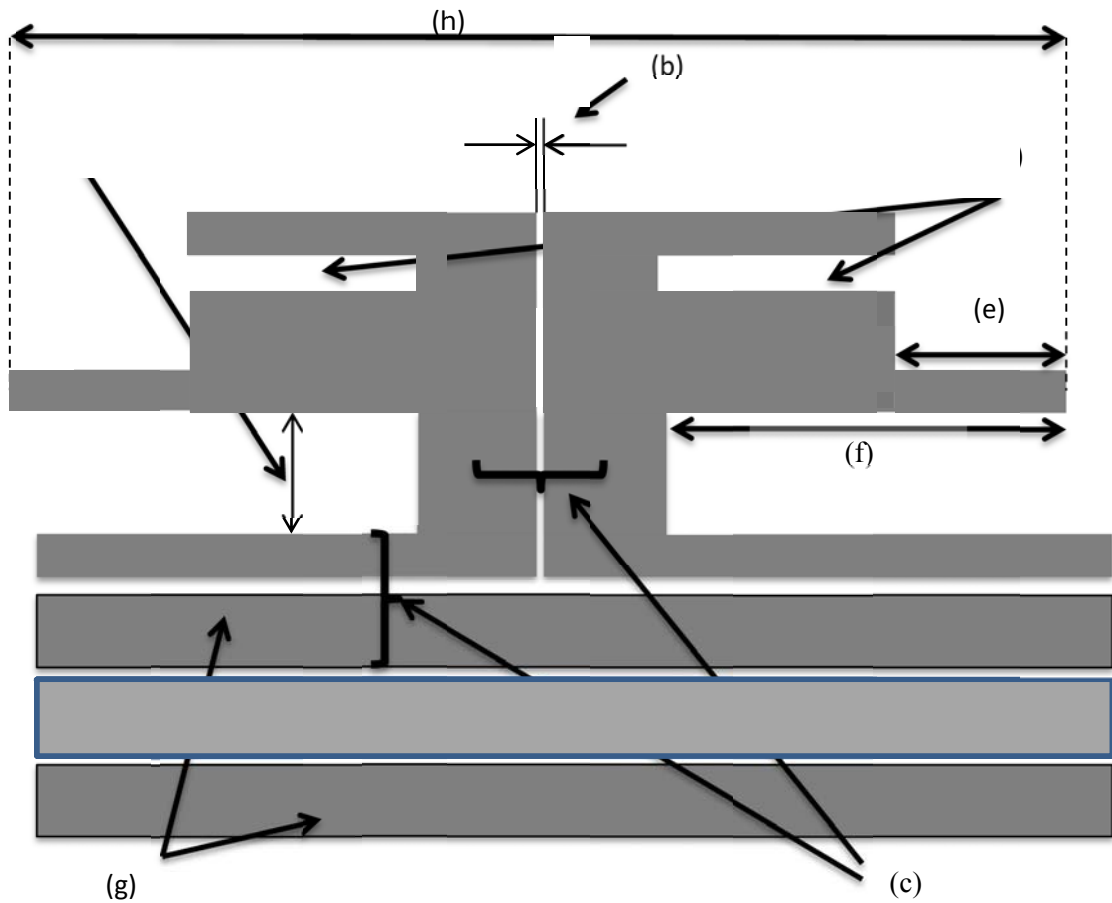
$\cdot \lambda/4*Vp$

Fig 3-7 Proposed planar dipole schematic and interface to feed network (with parameters)
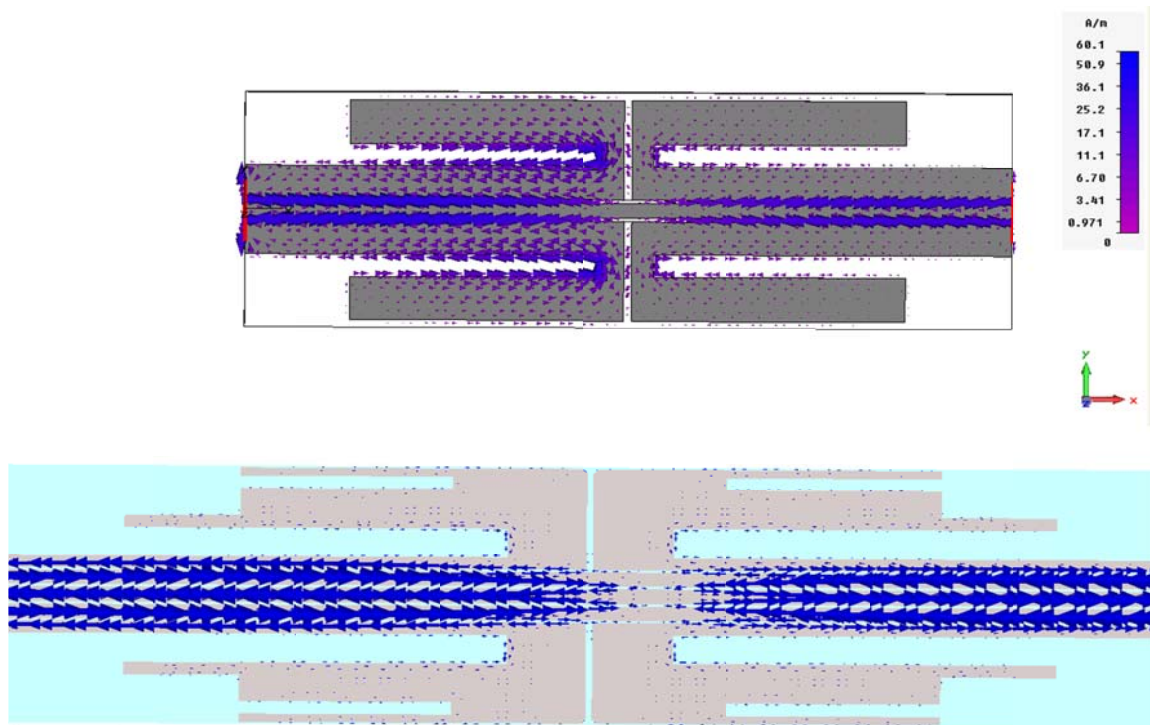
Fig 3-8 Current distribution for dipoles with different CPW feed methods

(a) Planar dipole fed directly from "Coplanar waveguide (CPW)"

(b) The proposed method of feeding a planar dipole with slotlines coupled from a "Coplanar waveguide (CPW)"

3.3.2 Proposed planar dipole characteristics

The final topology for the proposed planar dipole is shown in Fig 3-9. This dipole is from the upper section of the final collinear array antenna; hence the centre track of the "Coplanar waveguide (CPW)" cannot be seen. The planar dipole is designed to work over a bandwidth of at least 10%.
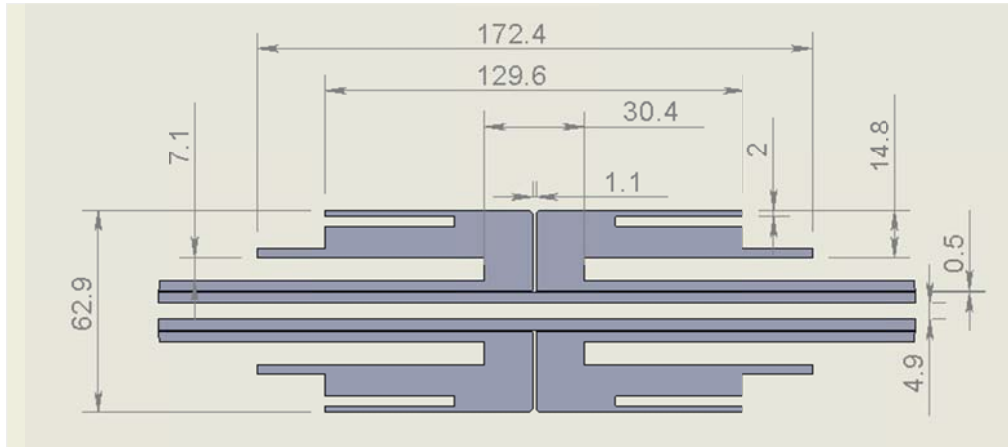
Fig 3-9 Final dimensions of the proposed planar dipole (in mm)

The structure was simulated in CST microwave studio, and the $|S_{11}|$ results are depicted in Fig 3-10. The proposed dipole achieves a 15 % bandwidth centred at 916 MHz, which meets the specification to cover the 850-960 MHz band.

The key to broad band performance over and above a standard dipole is in reactance cancellation. The main reactive impact for this dipole comes from its close capacitive coupling to the feed network strips. This affect is cancelled out by introducing some method of increasing the inductance without adding to the capacitance. This is done by placing notches and slots in the perimeter of the dipole to make it look electrically longer than its physical size. The effectiveness of the techniques used improve the performance of the planar dipole are also evaluated using Fig 3-10. The structure where either the dipole slots or notches are filled in Fig 3-10 (a) is compared to the proposed dipole Fig 3-10 (b).

3.3.3   The planar dipole optimisation method

The dipole starting geometry is based on a conventional half wave dipole. The dimensions are then adjusted parametrically to compensate for dielectric loading and mutual coupling effects. The broad band performance of the radiation pattern of the complete array is monitored during this process. with CST microwave studio [40] optimisation and parametric sweep. A parametric sweep is used to define useful geometric limits for the optimiser. Parametric sweep of the slot depth and notch filling in Fig 3-10 and notch depth is shown in Fig 3-12

3-110

(a)

(b)
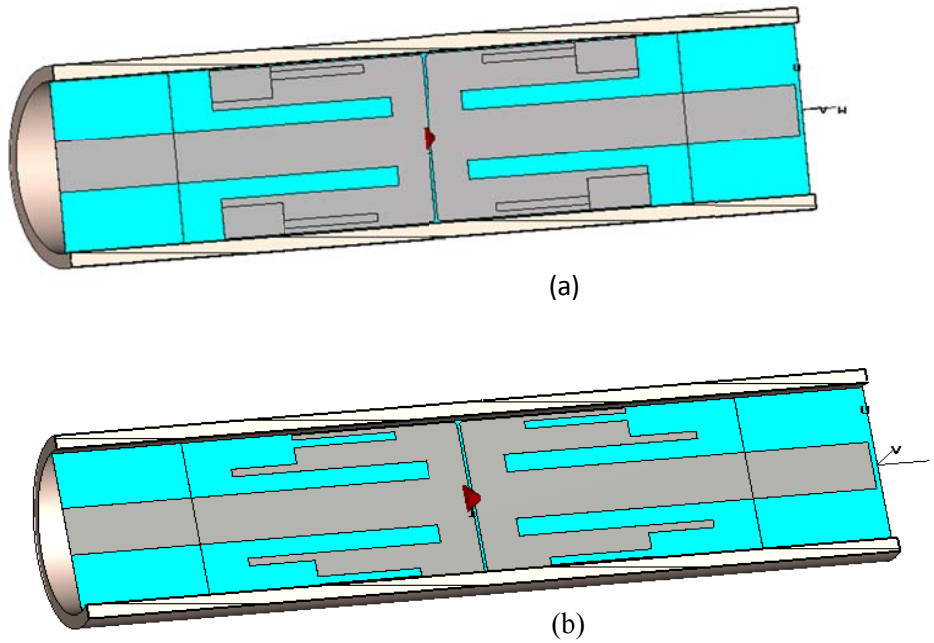
Fig 3-10 The comparison models used (a) slots and notches filled in (b) no filling

The $|S_{11}|$ performance seen in Fig 3-11 is virtually unchanged with and without the augmentation slots, except for a slight variation in bandwidth from 16.5 % to 15 %. The benefit of the slots is evident in the azimuth pattern performance. If the dipole notches are removed, a large shift in $|S_{11}|$ performance is observed as shown in Fig 3-11. To recover the desired frequency coverage, the dipole length needs to be made shorter. These notches are to compensate for reactance associated with the close proximity of the dipoles to the slot lines edge track [23]. In Fig 3-11, the notched dipole has 15% bandwidth, whereas the same dipole with the notches filled has only 12.4% bandwidth.
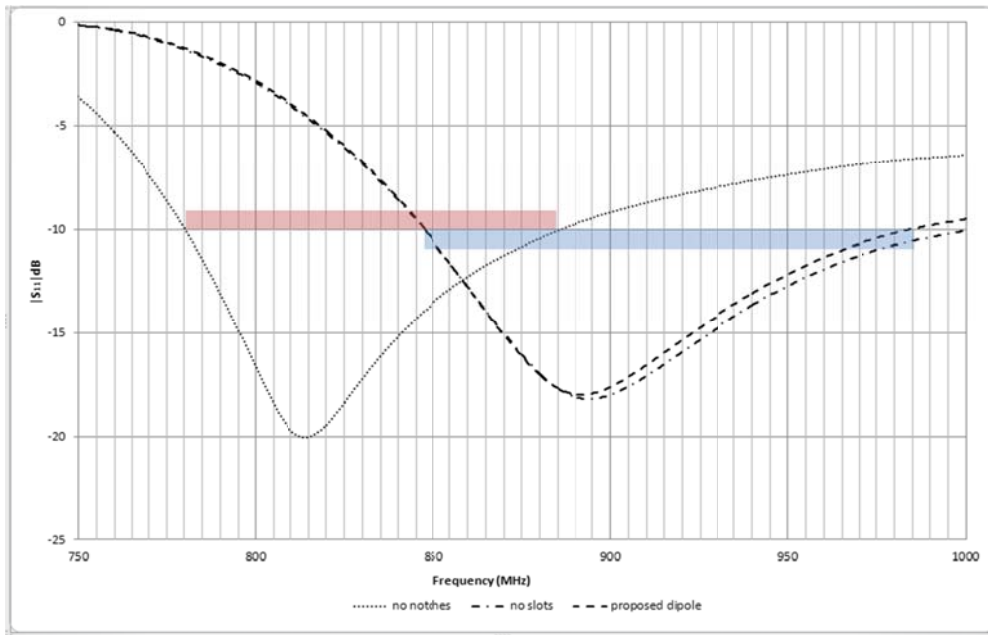
Fig 3-11 $|S_{11}|$ of the proposed dipole with and without notch and slot elements

The dipole notches are placed in the tips of the dipole arms to fine tune the correlation between the required pattern pass band performance and the $|S_{11}|$ band position. As shown in Fig 3-11, the reflection coefficient magnitude performance of the notched dipole element case falls directly over the desired pass band of 850-960 MHz, depicted by the blue band. Where the notches have been removed, the reflection coefficient magnitude performance occurred somewhat lower in the band as depicted by the red band. The effect of notch depth between these two extremes is shown in Fig 3-12 , where the $|S_{11}|$ characteristic is more sensitive to longer length notches.

3-112
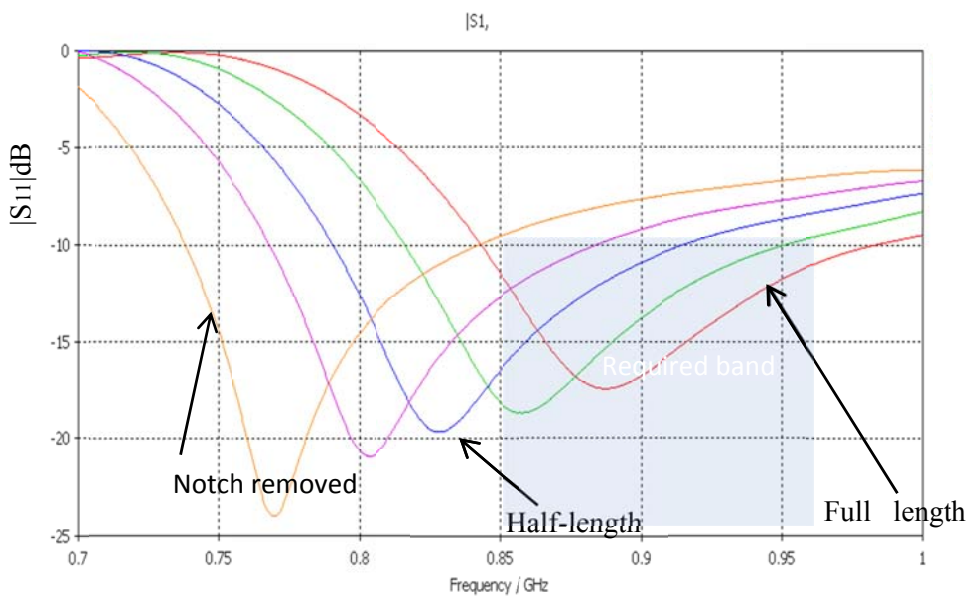
Fig 3-12 The $|S_{11}|$ of a proposed planar dipole as the notch depth is adjusted

3.3.4   Planar dipole inside radome

Factors such as mutual coupling and reflections make it difficult to analyse the dipole performance when in the array.   A model of the dipole is created to analyse the single element performance of the final construction.   The model is shown in Fig 3-13; with a waveguide port placed across the slot line to feeds the dipole independently.   The radome, substrate and part of the feed network are also included to provide realistic loading.

Substrate is 0.125 mm thick PET with $\varepsilon_r = 2.8$ and $\tan\delta = 0.0012$

ıe   Radome with $\varepsilon_r = 4.2$ $\tan\delta = 0.012$
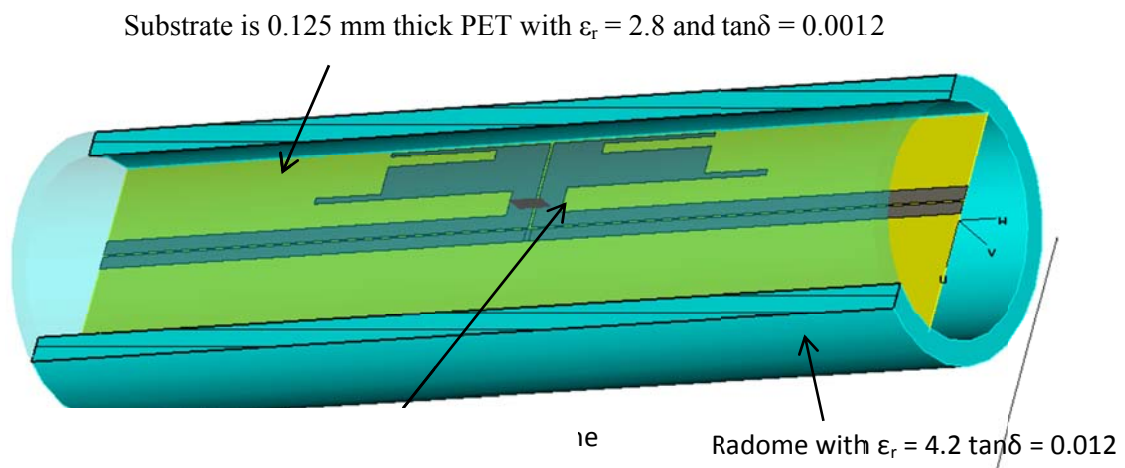
Fig 3-13 Single element planar dipole with radome loading

Referring to Chapter 2, a feed network port impedance of 129Ω is assumed. The impedance results given in Fig 3-14 show that the mean feed point impedance of the dipole is close to 129Ω, Smith Chart is normalized to this value. The $|S_{11}|$ of the radome loaded planar dipole is shown in Fig 3-15, where there is a minimum reflection coefficient magnitude of >10 dB with 10% bandwidth.
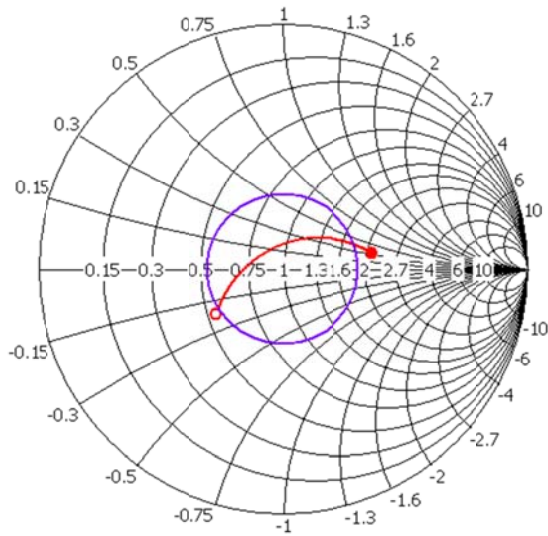
Fig 3-14 Feed point impedance of a planar dipole mounted inside 76mm diameter radome
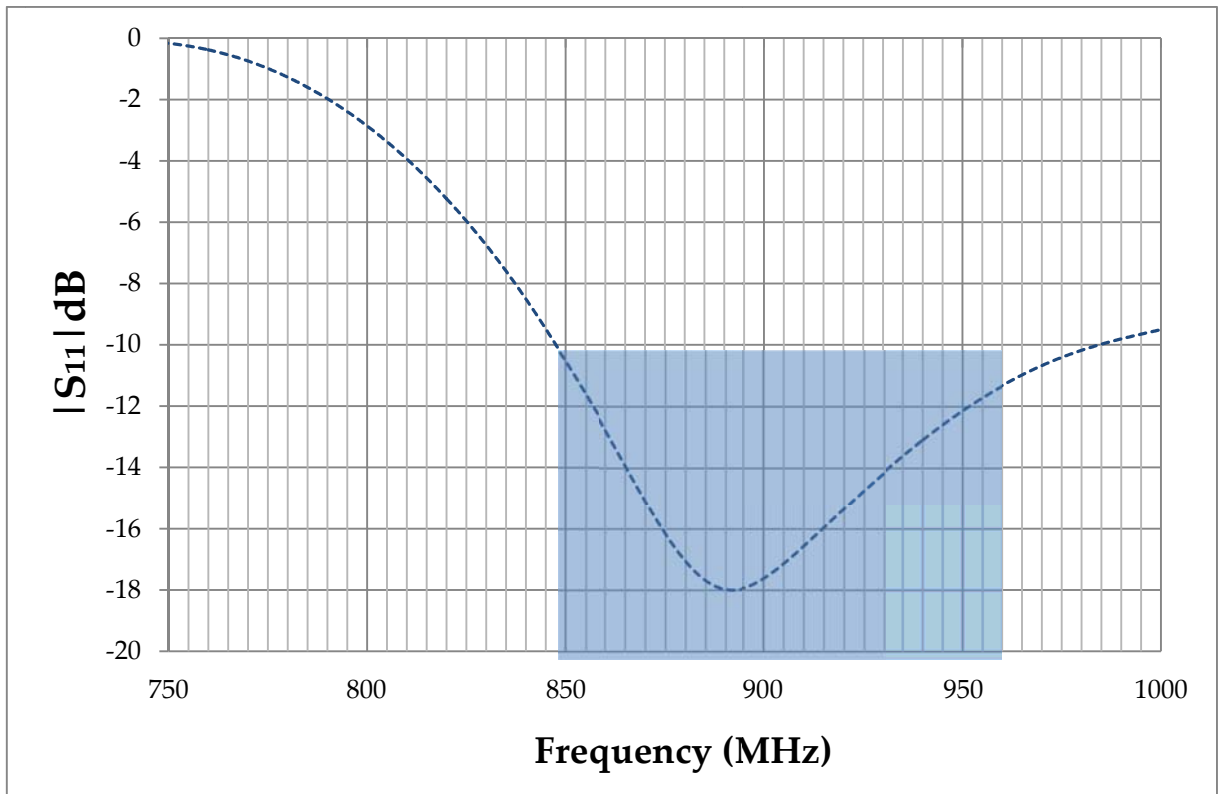
Fig 3-15   Normalised planar dipole reflection coefficient magnitude impedance (reference is 129Ω)

The E-field current distribution was analysed at the extremities of the desired frequency band, and the results are shown in Fig 3-16 and Fig 3-17.   At the lowest frequency of 850 MHz, the

3-114

longer current path around the outer edges of the dipole can be seen. At the higher frequency of 960 MHz, the current activity is more confined to the geometric length of the dipole. This characteristic highlights how the dipole geometry has been modified to present the broader response.
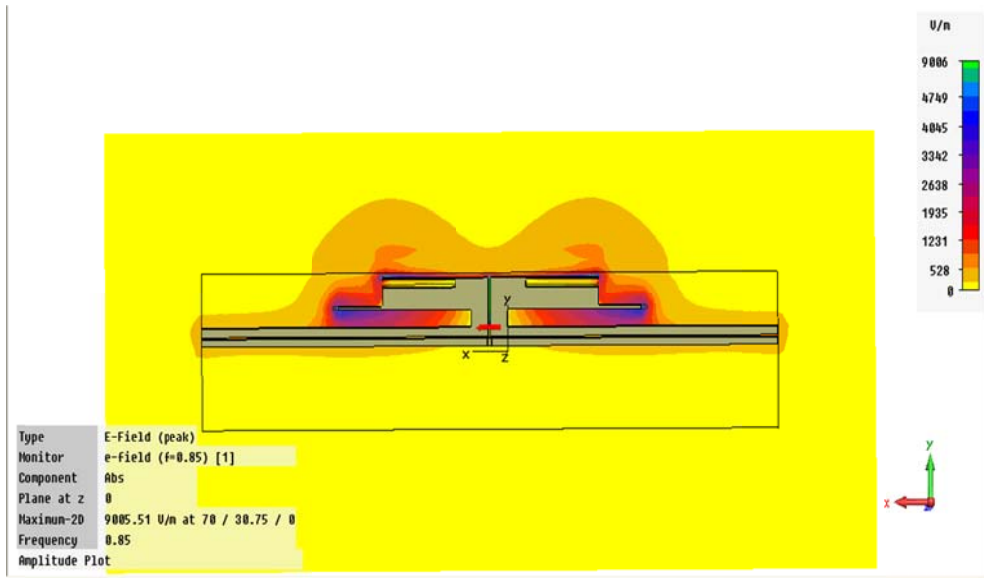
Fig 3-16 E field current distribution at lowest frequency= 850MHz
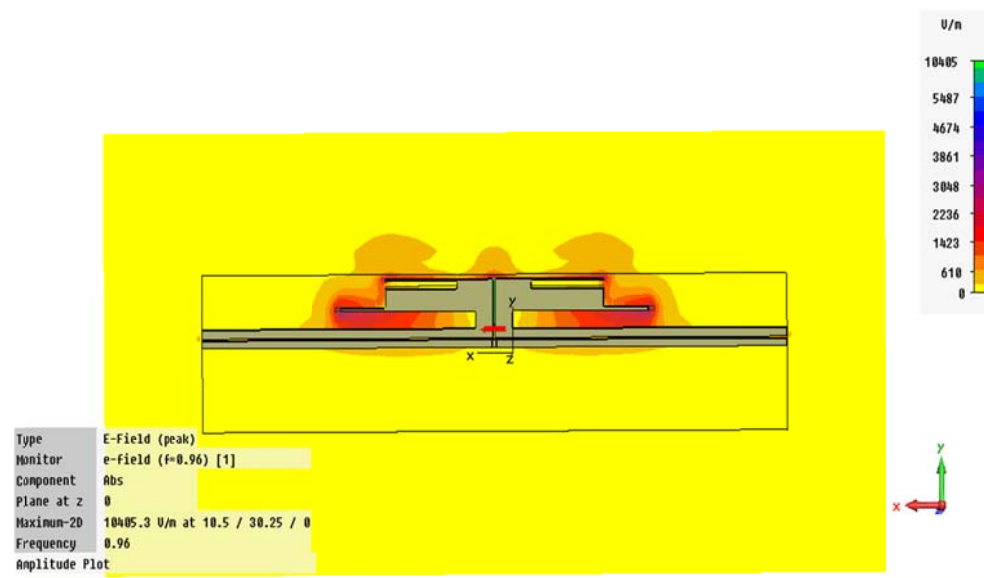
Fig 3-17 E field current distribution at the highest frequency = 960MHz

3-115

3.3.5   Dipole performance in the array

When antenna elements form an array, mutual coupling of the adjacent elements effectively lowers the resonant frequency.   As a consequence, the planar dipoles must be shortened in length when arranged in the final collinear array to maintain the coverage of the desired frequency band.

The proposed dipole design has a slotline feed, hence there are no extra balancing devices required. This type of feed insures equal current distribution leading to efficient radiation from the array. The proposed array dipoles are designed to suit their position in the array and as such, the dipole elements at the far ends of the array are different than those in the middle. This is due to the inside dipole arm being loaded by the previous dipole and the outside dipole arm exposed to free space conditions for elements at the end of the array. Increasing the length of the central conductive tracks of the feed network exposes the end dipoles to similar loading conditions as the inner elements.

3.3.6   Radiation performance of the planar dipole array elements

Radiation properties of the dipole element and feed network design are the main controls on pattern shape in an array situation. A squinted dipole pattern will influence the squint in the array; and incorrectly phased elements will introduce major pattern distortion independent of the dipole performance. If the dipole does not choke currents sufficiently, the out of phase currents become dominant and greatly influence the radiation pattern distortion.

The radiation patterns of the proposed planar dipole array elements a seen in Fig 3-18a elevation and The azimuth pattern in Fig 3-18(b) shows a maximum distortion of 1.6 dB peak to peak. This distortion is typical of a planar collinear array element with a width approaching a $\lambda/4$. The individual array element gain is approximately 3.2 dBi.

3-116
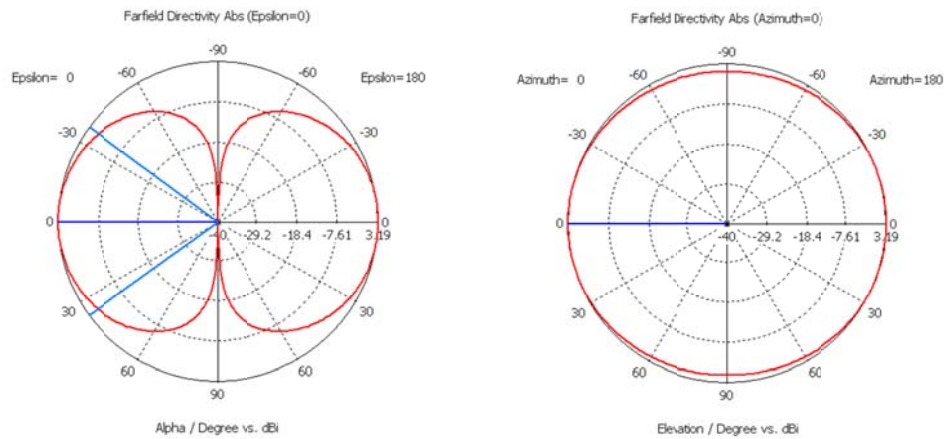
Fig 3-18 The typical (a) elevation and (b) azimuth radiation pattern of dipole

3.4 Summary

Within an electromagnetic modelling environment, the operational parameters of the novel planar dipole element proposed for use in a collinear array have been analysed. The transition from a cylindrical dipole to a planar dipole was discussed, and then further developed to allow for use in the collinear array proposed in this thesis. It was shown how this planar dipole is related to coaxially constructed dipoles in terms of current choking, and an example of the proposed dipole with its balanced feed displays evenly distributed currents. The planar dipole structure is also effective at choking off surface currents.

The proposed planar dipole is designed to meet the broad bandwidth and omnidirectional pattern specifications outlined in Chapter 1 by implementing augmentation techniques, namely slots and notches. The slots are used to compensate for reactance associated with the close proximity of the dipoles to the edge of the slotline feed [23]. The slots augment the radiation pattern to improve directivity and reduce azimuth ripple, and to lesser extent assist in impedance matching. The proposed planar dipole with notched tips was shown to be capable of a 15% bandwidth for VSWR < 2:1, whereas the conventional planar dipole shape is only capable of a 12% bandwidth. It was shown that this planar dipole design meets the bandwidth required for base station application, and is similar to a cylindrical dipole in terms of impedance and radiation pattern performance. A study of the current distribution showed that the dipole is active at its extremities for the lower frequency and more active closer to the feed point at the higher frequencies. Individual planar collinear element sections displayed an azimuth ripple of 1.6 dB and a maximum gain of 3.2 dBi.

3-117

Chapter 4   Robust Coplanar wave guide to microstrip transition

4.1 Introduction

A passively coupled "Coplanar waveguide (CPW)" to Microstrip transition with DC isolation operating in the band from 850 – 960 MHz is presented. The transition is specifically designed to solve a mechanical stress fracture risk associated with the soft solder attachment of a coaxial cable to the "Coplanar waveguide (CPW)" transmission line feed of an array antenna. The transition provides a low loss connection to the "Coplanar waveguide (CPW)" fed antenna array, with a robust launching platform for a microstrip line/coaxial connector interface. The added advantage of passive coupling is a reduced number of solder connections and a gradual transition to the "Coplanar waveguide (CPW)". Significantly, this transition is unique in that it is totally DC isolated, leading to improved PIM performance.

In Section 4.2, a literature review details research relating to broad band "Coplanar waveguide (CPW)" to Microstrip transitions, all of which are fabricated on the same dielectric layer and using a common ground plane or a common source connection. In Section 4.3 the proposed passive coupling circuit is introduced. The unique performance capabilities are discussed. The proposed transition is unique as it provides an impedance transformation, DC isolation and enhanced PIM protection by using passive coupling. Section 4.4 details the simulated performance of the transition, along with a parametric investigation of key structural features. Section 4.5 explains the physical test setup required to accurately characterise the proposed transition. Measured results are presented, and compared to the simulations. In Section 4.6 the assembly of the transition is explained, along with an analysis of tolerance effects in construction. A summary of the investigations is provided in Section 4.7.

4.2 Literature review of broad band "Coplanar waveguide (CPW)" to microstrip transitions

The vast majority studies into "Coplanar waveguide (CPW)" to Microstrip transitions are found to be based on uniform thickness homogenous substrates.   These transitions are of great interest to the research community as they allow for a low loss controlled transition for module interconnections up to 40 GHz.

"Coplanar waveguide (CPW)" can pose difficulties when interfacing with a coaxial cable via conventional connectors. A close pitch track spacing in most cases makes it difficult to attach a connector or cable without the risk of short circuit. A low loss transition to non-coplanar transmission line can be a better option for mechanical and electrical interfaces.

The design shown in Fig 4-1 is a transition with strong electromagnetic field coupling. The transition has capacitive surface patches to couple the active lines of the "Coplanar waveguide (CPW)" and the Microstrip [45]. The ground plane is common to both "Coplanar waveguide (CPW)" and Microstrip. This transition has a relatively low reflection coefficient magnitude (< -10 dB) from 3.2 GHz to 11.2 GHz, and a transmission loss of 0.2 dB

(a)　　　　(b)　　　　(c)

Microstrip interface

CPW interface

a) Microstrip interface

b) Transition area

c) CPW interface
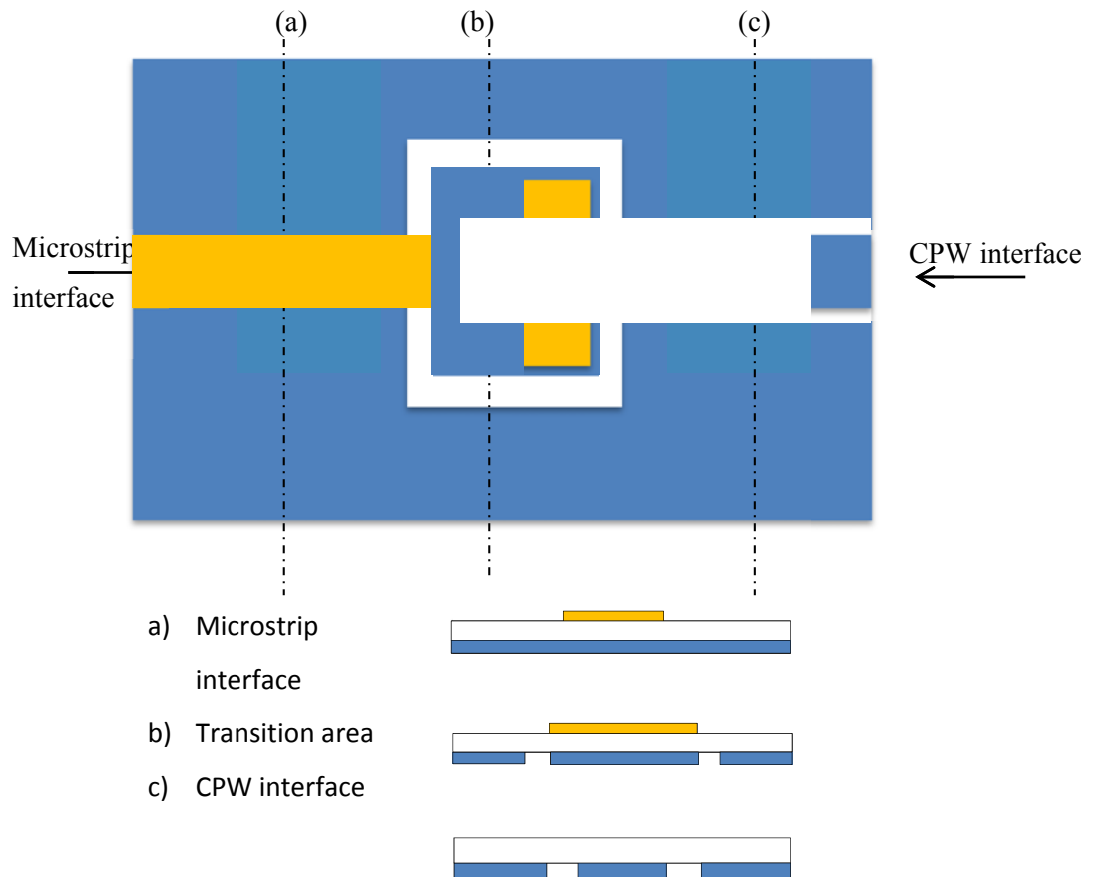
Fig 4-1 Capacitive coupled CPW to microstrip transition [36].

The "Coplanar waveguide (CPW)" to microstrip transition shown in Fig 4-2 has an electromagnetically coupled ground and a common source track. This transition has a transmission attenuation of 0.3 dB at 5 GHz and 1 dB at 7.8 GHz, with a reflection coefficient magnitude of 15 dB from 2.8 - 7.5 GHz [46] and is proposed for use in flip chip *"monolithic microwave integrated circuit (*MMIC)" applications.
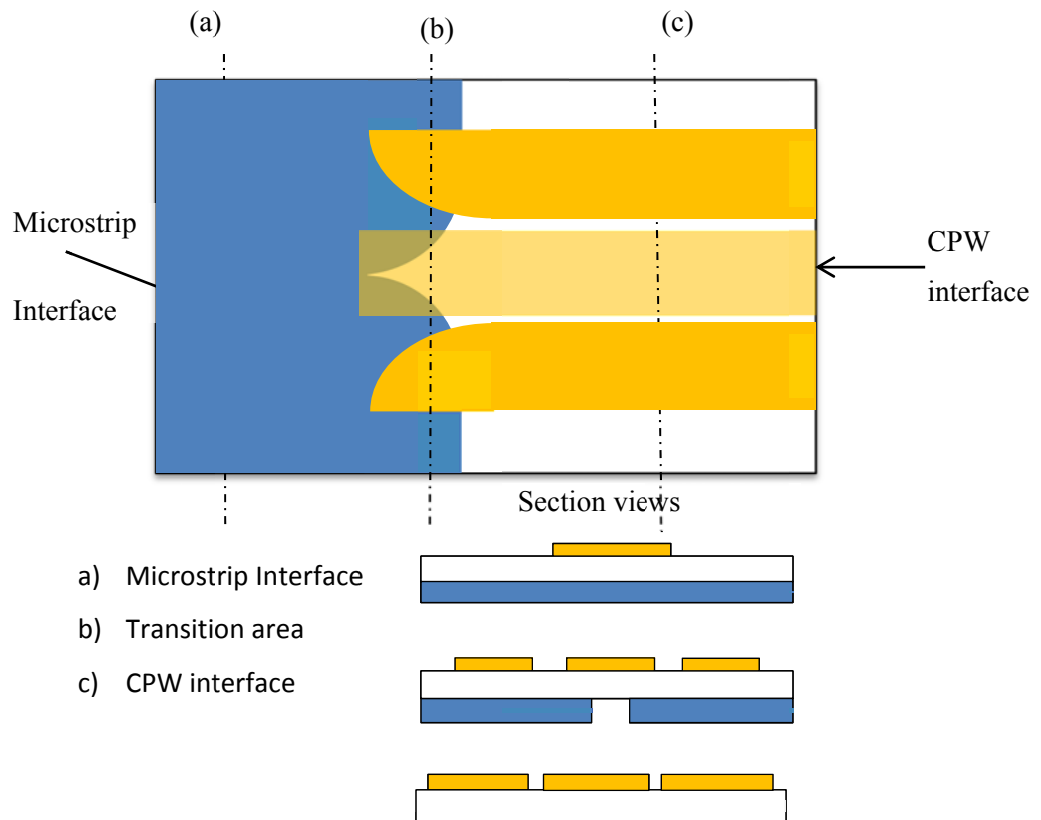
Fig 4-2 A transition with common source track and electromagnetically coupled ground [37]

In   Fig 4-3, a transition design with stepped grounded CPW (GCPW) sections is shown which also has a common microstrip and "Coplanar waveguide (CPW)" signal conductor [47]. The interface is a conventional microstrip line, and the transition is made through a GCPW transformer to "Coplanar waveguide (CPW)". The presented performance is not clear, the reflection coefficient magnitude is approximately 10 dB, the insertion loss < 1 dB over a bandwidth of 38%.

(a)   (b)   (c)

Micro strip

CPW interface

a) Microstrip interface

Section views

b) GCPW Transition area

c) CPW interface
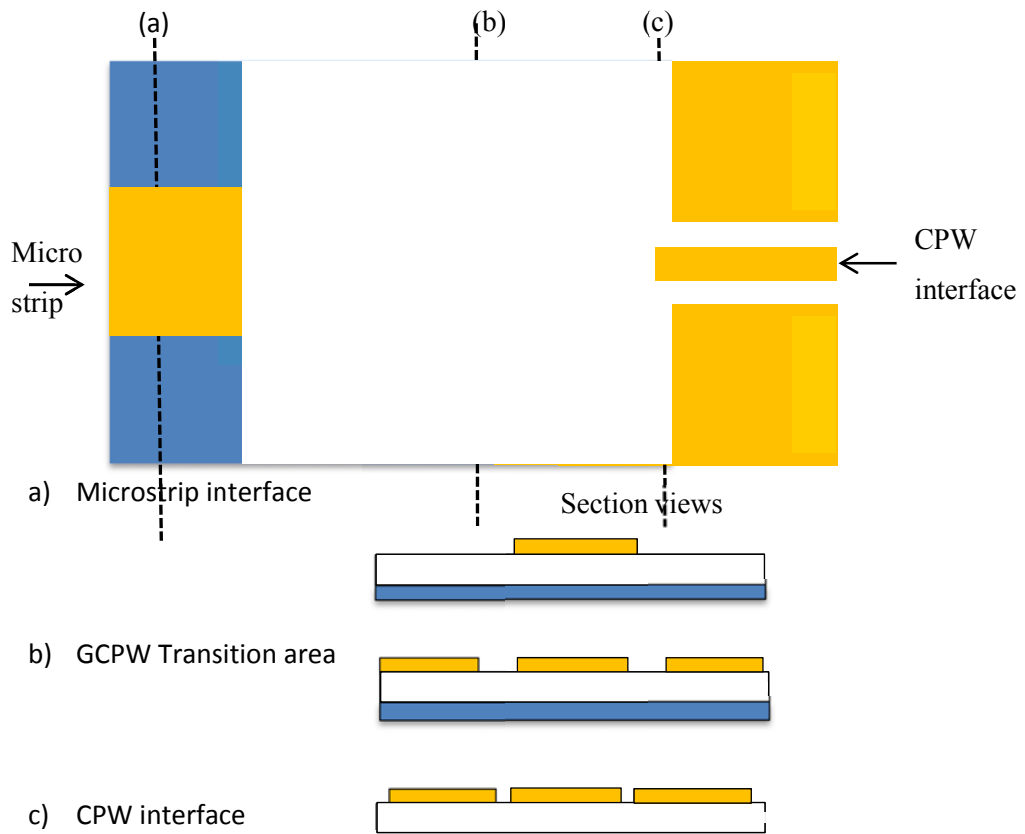
Fig 4-3 A transition with common source track and electromagnetically coupled ground [38]

A tapered ground "Coplanar waveguide (CPW)" to Microstrip transition is shown in Fig 4-4. Tapering of conductor tracks is well known broad-banding technique. This transition is an improvement over the previous design as it has a modified ground track and source track introducing a more gradual transition from one mode to the other [48].

(a)   (b)   (c)

Microstrip

interface

CPW
interface

Section views

a)   Microstrip interface

b)   GCPW Transition area

c)   CPW interface
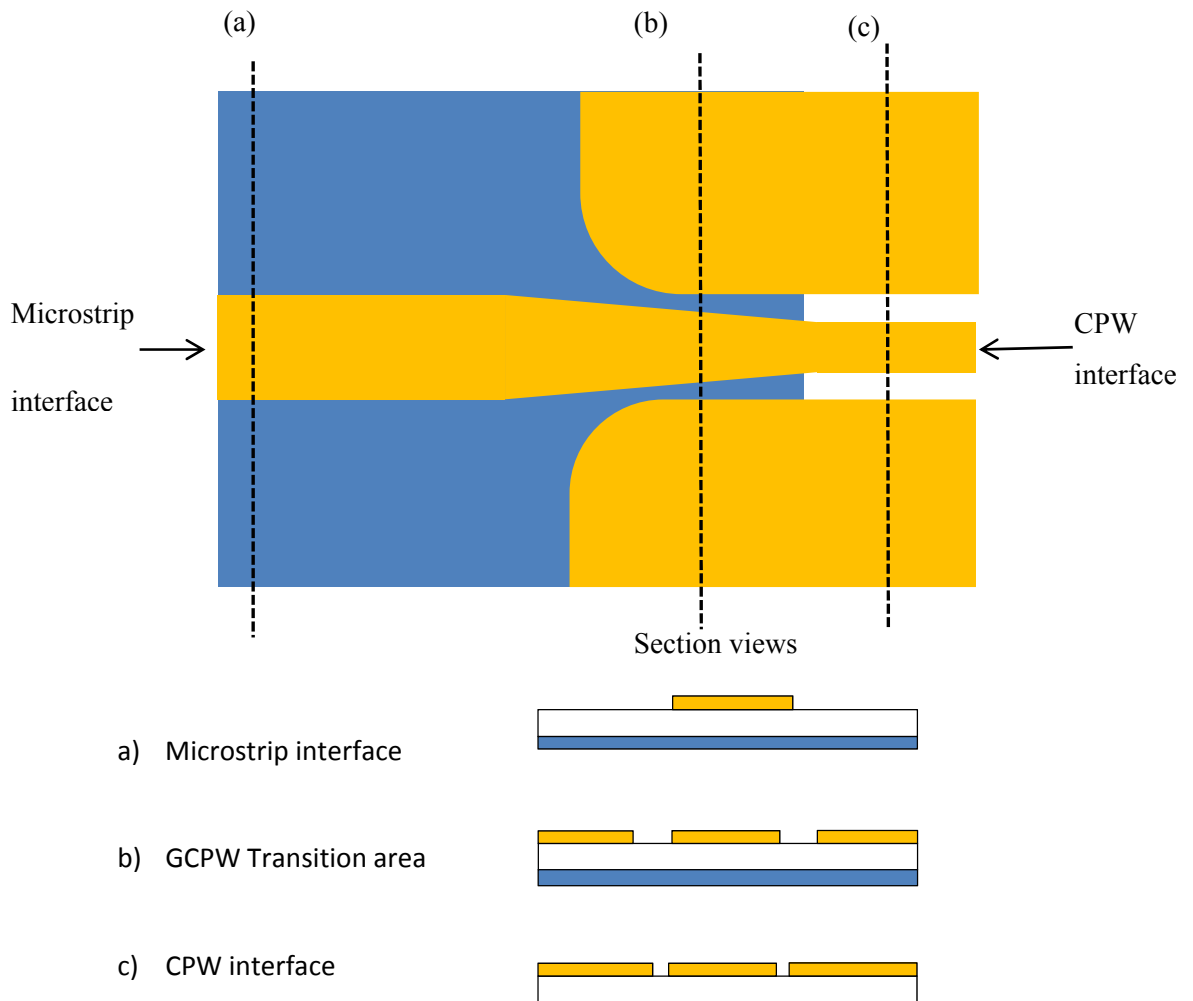
Fig 4-4 A transition similar to Fig 4-2 but with tapered conductors [39]

The transition depicted in Fig 4-3 uses electromagnetic coupling for the source of the Microstrip line. The "Coplanar waveguide (CPW)" source track is at ground potential at the transition. The Microstrip coupling has fan stub and the "Coplanar waveguide (CPW)" has a return to ground [49]. The reflection coefficient magnitude is 10 dB with insertion loss of 0.3 dB at 5 GHz and 1 dB at 7.5 GHz. This transition uses an RT/Duroid substrate with a permittivity of 10.2 to reduce the physical size of the transition. As the source track of the Microstrip is DC isolated from the "Coplanar waveguide (CPW)", this type of transition avoids the need for DC blocking capacitors in some applications. The fan stub meshing with the fan

shaped aperture provides the gradual transition from "Coplanar waveguide (CPW)" to Microstrip over a broad band exhibiting similar results to the previous transition with a tapered geometry.
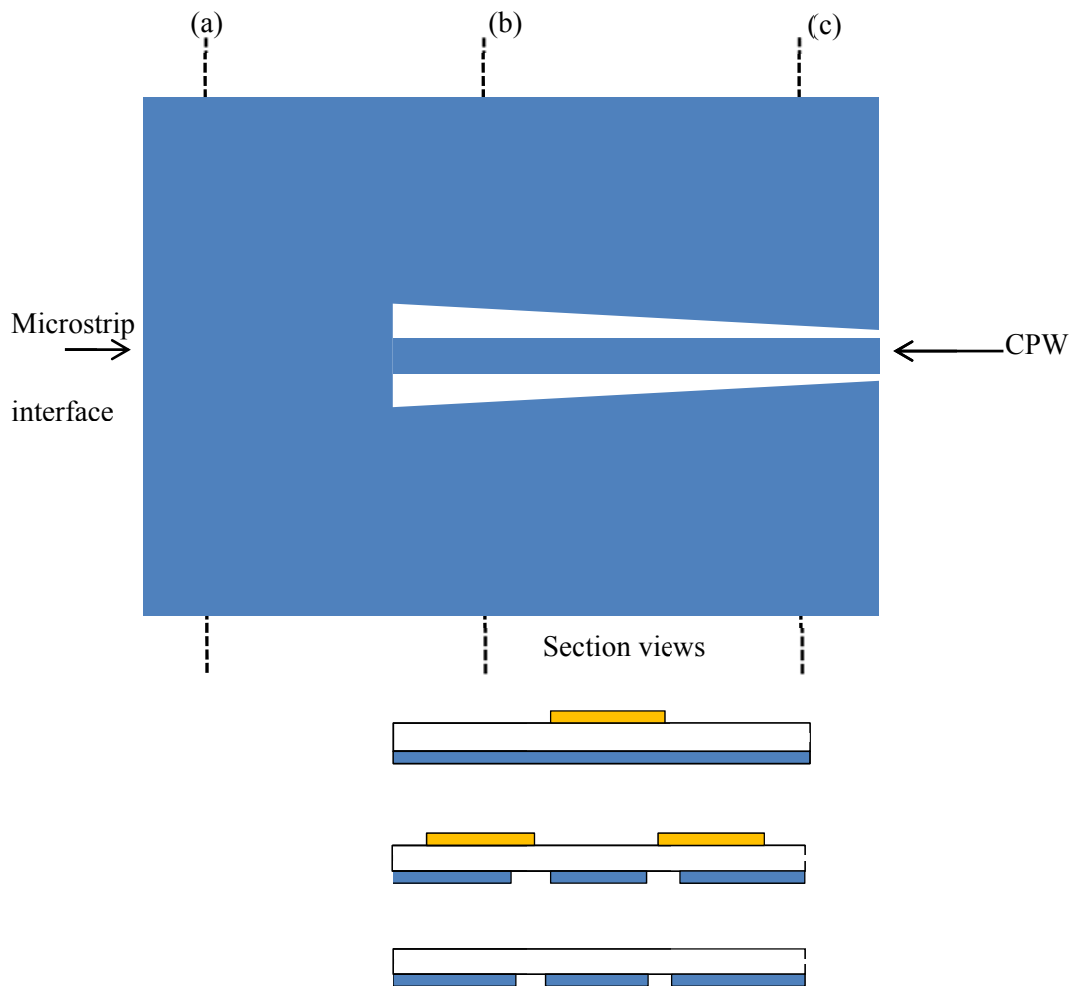
Fig 4-5 An electromagnetically coupled CPW to Microstrip transition, common ground [40]

The "Coplanar waveguide (CPW)" to Microstrip transitions shown in Fig 4-6 are examples of: (a) a straight-stub transition with a bandwidth of 20%; and (b) a radial stub transition with a bandwidth of 25%. Both transitions have a reflection coefficient magnitude of 17 dB and an insertion loss of 0.18 dB in the range near 85 to 110 GHz [50]. The transitions have electromagnetically coupled ground plane, and share the source conductor. The metal tracks are gold flashed and deposited on a silicon wafer substrate.
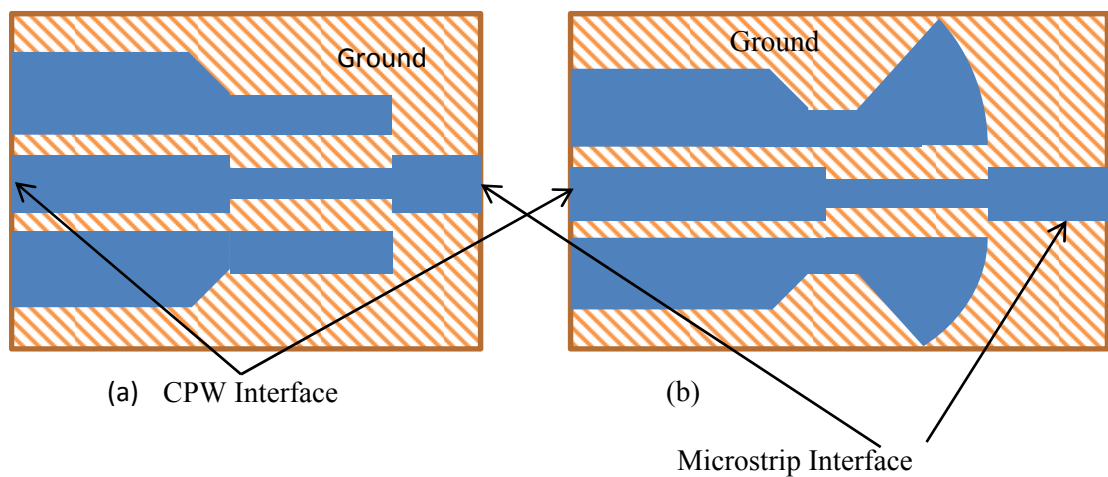
Fig 4-6 These are examples of state of the art performance coupler circuits [50]

(a) straight-stub transition (b) radial-stub transition

A very simple transition is shown in Fig 4-7, where both the "Coplanar waveguide (CPW)" and Microstrip have continuity in ground and source tracks [51]. Via are used to complete the connection between the "Coplanar waveguide (CPW)" ground tracks and the Microstrip ground. The source tracks are directly connected. As there are no resonant circuits involved, this coupler works over a very large bandwidth (0.04 GHz up to 25 GHz). The insertion loss is typically around 1.5 dB at 20 GHz and the reflection coefficient magnitude is 15 dB Values of insertion loss and reflection coefficient magnitude are not stated at the lower frequencies.
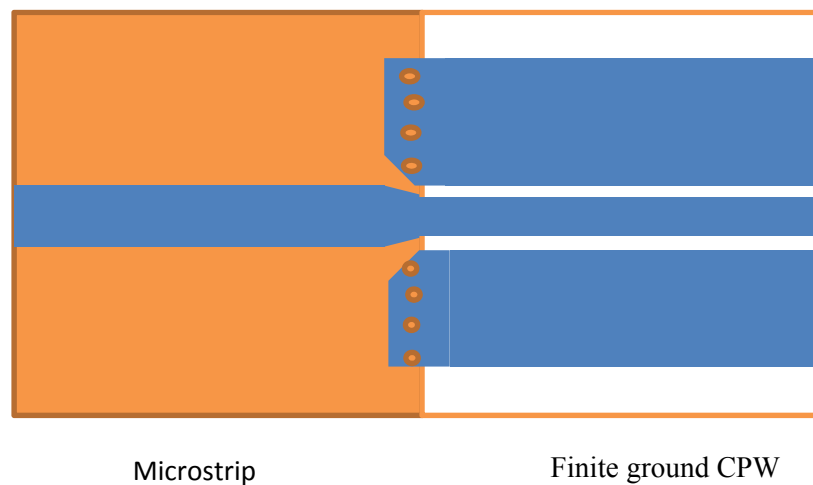
Fig 4-7 Example of directly connected CPW to Microstrip transition [42]

4.2.1 Performance goals for the "Coplanar waveguide (CPW)" to Microstrip transition

The desired coupler will make a transition from a flexible PCB collinear array to a substantial coaxial cable and low PIM connector. As per other couplers described, the proposed transition will be passive (i.e. has no DC continuity) and has a resonant structure to fine tune the coupler pass band performance. The following specifications are required:

Table 4-1 The performance specifications for the passive coupler

Bandwidth:	850 to 960 MHz (minimum)
Insertion loss:	0.25 dB
Reflection coefficient magnitude:	> 15 dB
PIM:	≥ -140 dBc minimum, ≥ -150dBc ideal with 7/16 DIN connector
Power:	100W maximum
Array port:	CPW (approx. Z_o = 69 Ω)
Equipment port:	7/16" DIN connector via RG142 double shielded cable.

4.3 The structure and operation of the passive coupling circuit

This section introduces a passive coupling transition from Microstrip to "Coplanar waveguide (CPW)" lines, where a heavy duty connector or cable can be attached to a robust, rigid Microstrip PCB. The design is unique, as both the source and ground of the "Coplanar waveguide (CPW)" transmission line are effectively DC isolated from the coaxial connector assembly. The shape of the "Coplanar waveguide (CPW)" coupling pads is the result of the analysis of [46], and other literature on "Coplanar waveguide (CPW)" to microstrip couplers.

Strong capacitive coupling was found to be required in order to couple the ground currents effectively from the array to the microstrip ground. The geometry of the coupling probe is based on the analysis of [45]. The dimensions of the final coupler were restricted by the available width of the radome. It is well known that smooth transitions are required to enhance the bandwidth achieved hence the curved geometry.

There is no solder processing required on the "Coplanar waveguide (CPW)" side of the transition, with the coaxial cable only attached to the more robust Microstrip side of the transition. In the specific application for the "Coplanar waveguide (CPW)" fed collinear array proposed in this thesis, DC continuity is specifically avoided to improve the PIM performance of the entire assembly. A schematic of the proposed "Coplanar waveguide (CPW)" to Microstrip transition is depicted in Fig 4-8. The transition consists of two substrates: the 125 μm PET flexible substrate (ε_r = 2.8) of the "Coplanar waveguide (CPW)" collinear array presented in this thesis; and an Arlon AD250C [52] substrate (ε_r = 2.5 and tanδ = 0.0014). This rigid Arlon fibreglass composite material is more suitable to support a coaxial cable or connector interface (via a Microstrip line) than the flexible PET, and also provides stable electrical properties, low PIM and high operating temperature allowing for high temperature soldering. The two materials are laminated together with no direct electrical connection between the two transmission lines.
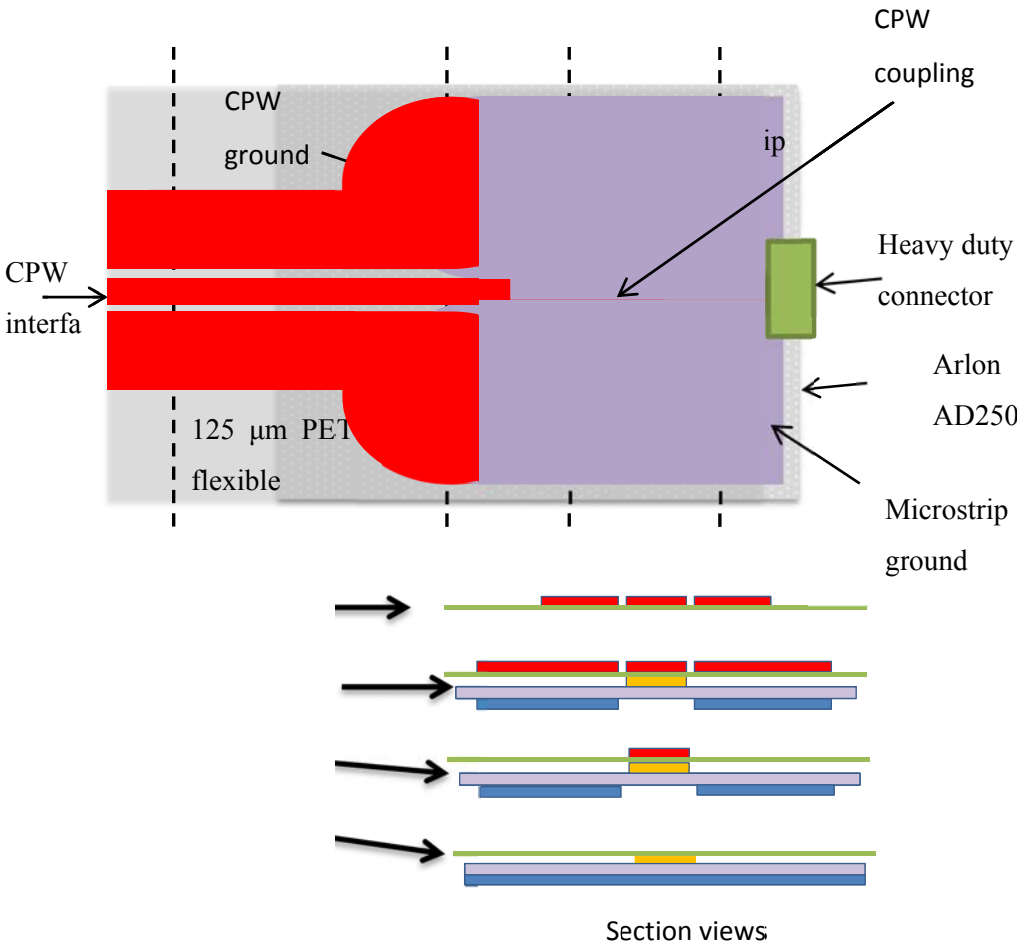
Fig 4-8 Schematic layout of the proposed passive CPW to Microstrip transition

The broad band performance of this transition is facilitated by a gradual change in the ground plane geometries of the Microstrip line and "Coplanar waveguide (CPW)". The tapering of the ground planes gradually changes the "Coplanar waveguide (CPW)" modes to the Microstrip modes over the λ/4 wavelength of the transition. The optimum slot depth in this transition is 13.75mm. This tapered shape maximises the bandwidth during the transition from "Coplanar waveguide (CPW)" to Microstrip as seen in the lower plan view of Fig 4-9. The flaring of the "Coplanar waveguide (CPW)" and Microstrip grounds are overlapped to form low Q capacitive coupling plates. The shape of the transition plates was optimised using [40]. The optimum microstrip probe length is 32.5mm for a "Coplanar waveguide (CPW)" probe length of 38mm. The slot length and microstrip probe length have been selected based on the highest average Reflection coefficient magnitude response and the minimum loss through the transition.
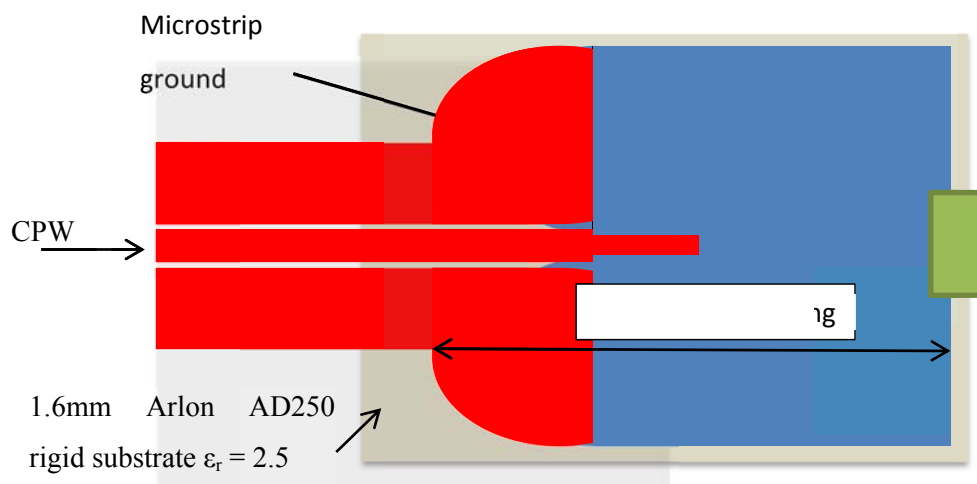
Fig 4-9 The layout of the coupling transition bottom layer showing coupling pad alignment

The specially designed edge connector is presented in Fig 4-10 allows a coaxial cable to be soldered directly to the Arlon Microstrip line with more substantial mechanical strength and electrical connection than when directly soldered to a "Coplanar waveguide (CPW)". Unlike most microwave connectors which are fabricated with individual dielectric supports and separate inner conductor components, this edge connector was specifically designed to include the attaching cables dielectric and inner conductor as part of the assembly thereby reducing the manufacturing parts count and cost. The connector mounting grooves are designed to slide onto the Arlon AD250 substrate [52], and precisely set the height of the

4-128

attached cable such that the inner conductor passes through at the surface of the Microstrip track. The braid of the cable can be securely soldered into the body of the connector. The Arlon PCB is recessed to allow for the length of the connector to be inset into the PCB, increasing the alignment accuracy and mechanical strength.

)
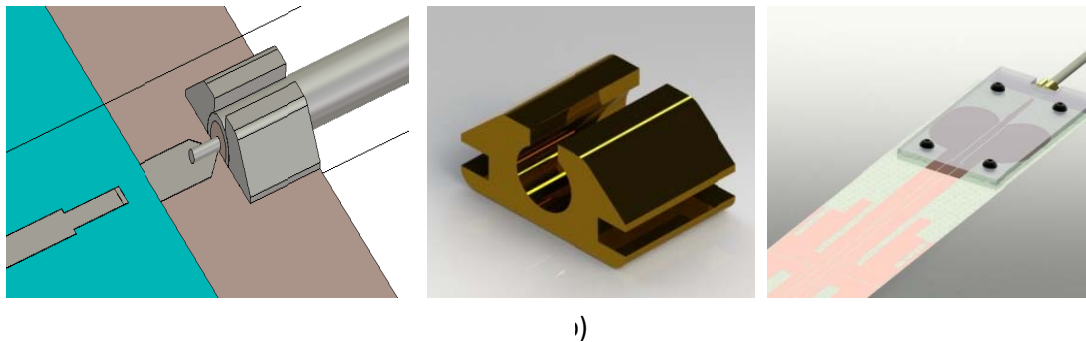
Fig 4-10 low pim edge connector application

(a) Low PIM edge connector model (b) a fabricated edge connector (c) the application of the connector to the passive transition to the collinear array

4.4   Broadband passive transition performance

Traditionally "Coplanar waveguide (CPW)" to microstrip transitions and couplers are used to provide low loss interconnects for microwave modules. This proposed coupler provides this performance with complete DC isolation, as well as solving a mechanical issue when interfacing "Coplanar waveguide (CPW)" using a cable or connector.

A parametric model of the passive coupler in the back-to-back configuration was created to optimise the geometry. This is a well-known method to characterise transitions that are not 50 Ohms as shown in [53]. The transition structure in Fig 4-11 was simulated using CST electromagnetic software [40]. The back-to-back test fixture comprised of two identical Microstrip to "Coplanar waveguide (CPW)" transitions connected as a mirror image about a section of "Coplanar waveguide (CPW)" equivalent to that used in the collinear array feed of section Chapter 2.5.

mmetry
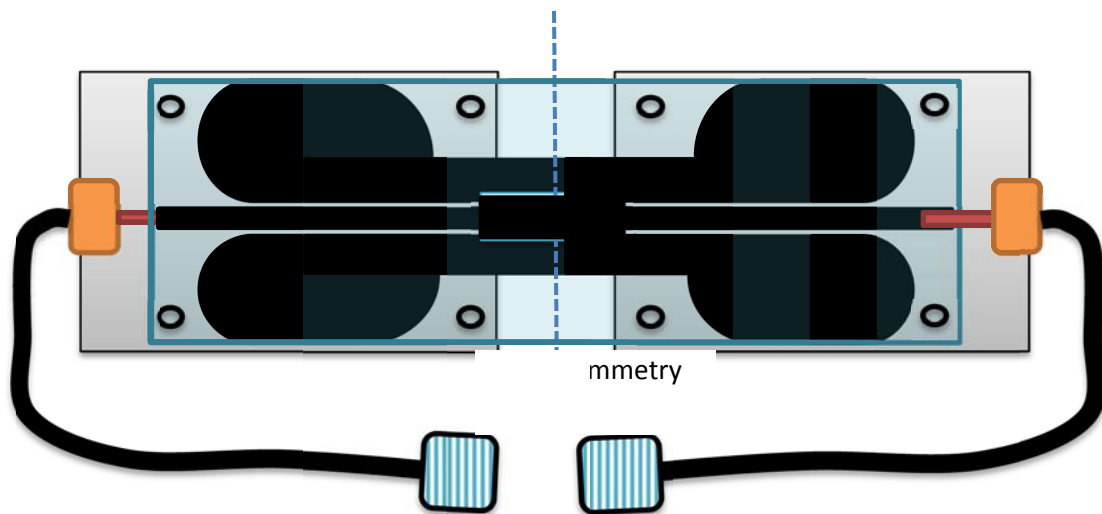
Fig 4-11 Back to back coupler test fixture

A parametric sweep of the slot depth located between the coupling plates as shown in Fig 4-9 was conducted. Minimum insertion loss is achieved over a wide band for a slot depth of 13.75mm is observed from Fig 4-12. This configuration results in an insertion loss of 0.1-0.2 dB and a minimum and reflection coefficient magnitude 29 dB. From these results, the slot depth is seen to have a minor influence on the insertion loss, but greatly affects the reflection coefficient magnitude.

The effect associated with the Microstrip probe length (as seen in Fig 4-8) is shown in Fig 4-13. This is a critical component in the matching and efficiency of the coupling coefficients. A Microstrip probe length of 32.5mm provides a minimum insertion and reflection coefficient magnitude values.

Small variations in the "Coplanar waveguide (CPW)" probe length (depicted in Fig 4-8) generate gradual changes in insertion and large changes in reflection coefficient magnitude, An optimal value of 38 mm produces a minimum insertion and reflection coefficient magnitude of 0.2 dB and 29dB respectively when combined with a Microstrip probe length of 32.5mm and slot depth of 13.75mm.
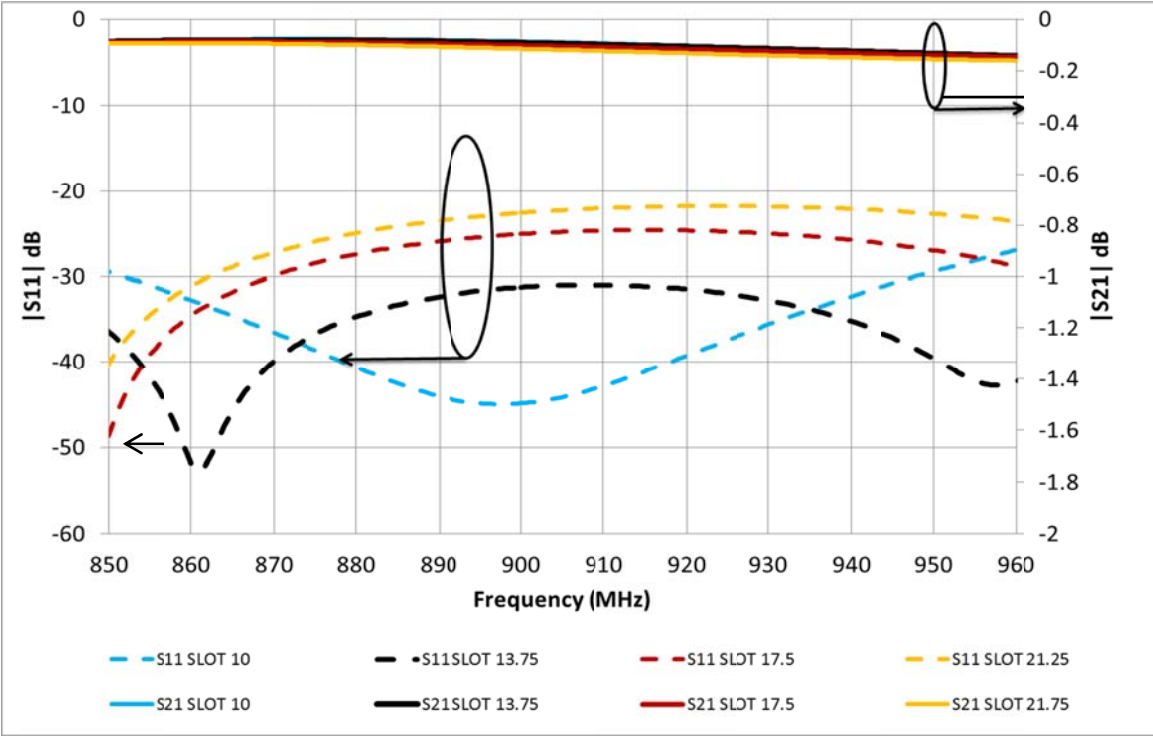
Fig 4-12 Back to back coupling test with parametric slot depth
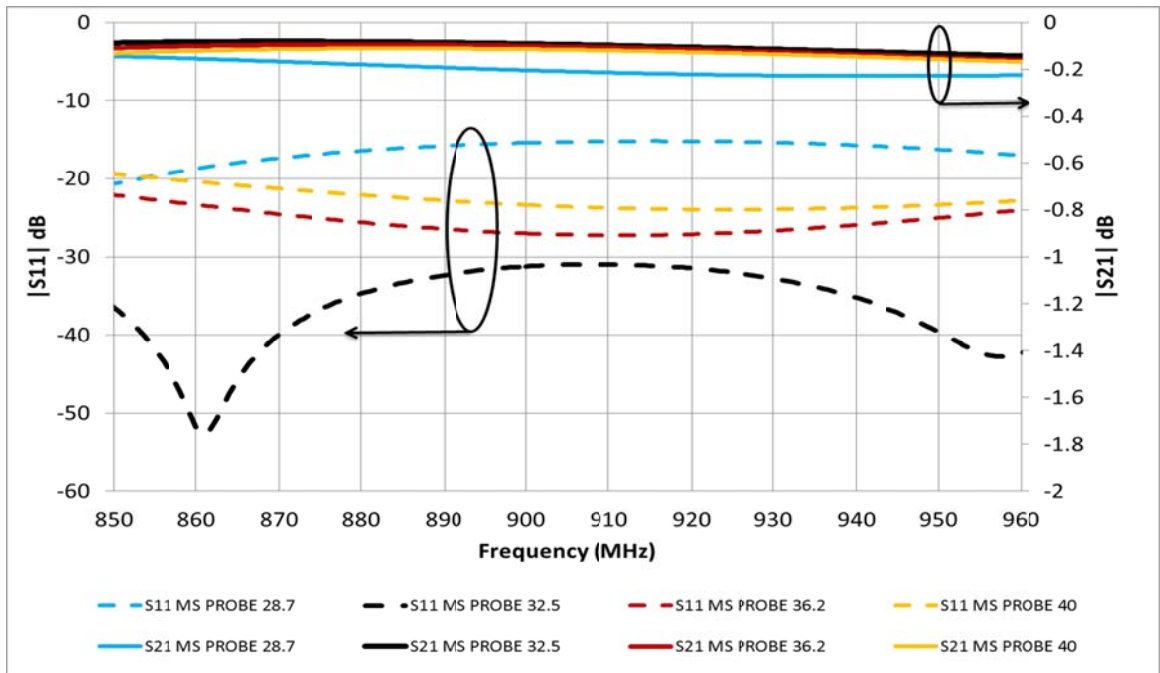
Fig 4-13 A parametric sweep of the passive coupler with various Microstrip probe lengths

4.5 Back to back transition measurement

The back-to-back transition was measured from 850 - 960 MHz, with two 100 mm long coaxial cables used to connect to an Agilent 5070B network analyser to characterise the S-parameters. A comparison to the modelled results (with coaxial cable sections included) is provided in Fig 4-18. By halving the insertion loss measured in the back–to-back transition, a single passive coupler exhibited an insertion loss of around 0.3 dB, with a reflection coefficient magnitude greater than 15 dB. The worst case measured insertion loss is 0.4 dB at 850 MHz The measured reflection coefficient magnitude response is different to the modelled response, although it remains within the specification outlined in Section 4.1.1. The increased loss most likely caused by the PCB registration and alignment accuracy in the fabrication of the prototype passive coupler.
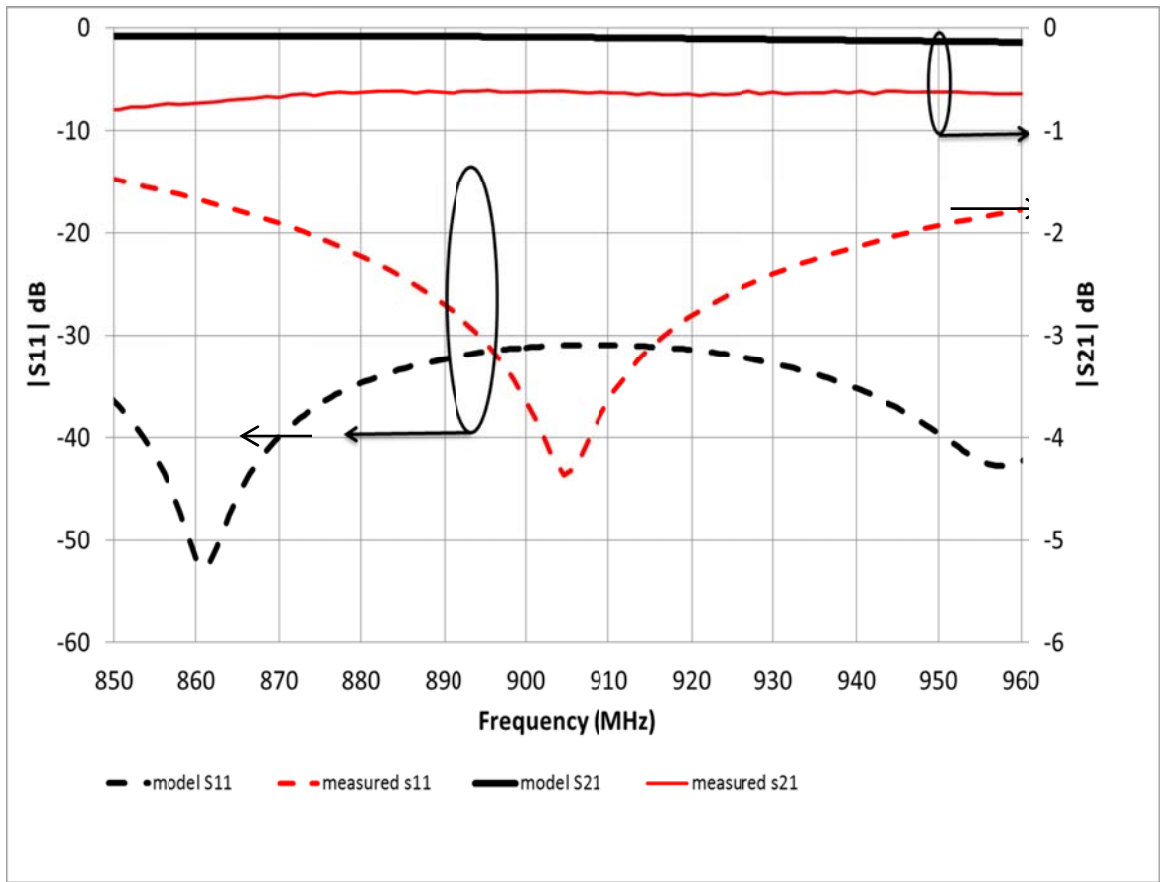
Fig 4-14 Modelled and measured S parameters of transition characterised back to back

The performance of the coupler is comparable to similar transitions presented in the literature. A comparison is provided in Table 4-1. However, this coupler also has the added advantage of total DC isolation, allowing the transition to function with arbitrary substrates at each interface whilst maintaining low insertion loss and high reflection coefficient magnitude.

Table 4-2 Comparison the proposed passive coupling transition to references (measured back-to-back results)

	Proposed coupler	[50]	[51]	[46]
Frequency	850-960 MHz	85-110 GHz	0.04-25 GHz	2.8-7.5 GHz
Transition	CPW -> microstrip	GCPW -> microstrip	CPW -> microstrip	CPW -> microstrip
Insertion loss	< 0.5 dB	0.18dB	< 1.5 dB @20 GHz	1 dB
Reflection coefficient magnitude	15 dB	17 dB	15 dB	15 dB
Ground tracks	Passive coupled	Passive coupled	Direct connection	Direct connection
Source tracks	Passive coupled	Direct connection	Direct connection	Passive coupled

4.6   The passive coupling assembly

The passive transition shown in Fig 4-15 comprises of the following components:

- Microstrip line passive coupling circuit: Arlon AD250C [52]
- Alignment/compression plates: Polycarbonate
- Low PIM edge connector: Silver plated brass
- RG 142 cable
- Non-conductive fasteners: Nylon
- Low PIM 7/16 DIN Jack

If DC grounding of the coaxial interface is required, a short circuited parallel stub can be fitted to the low PIM connector as shown in Fig 4-15. This option may be required to protect the equipment from lightning or other static charge sources, such as areas designated intrinsically

4-134

safe areas in petro-chemical sites. This proposed coupler provides this performance as well as complete DC isolation to solve a mechanical issue when interfacing "Coplanar waveguide (CPW)" using a cable or connector.
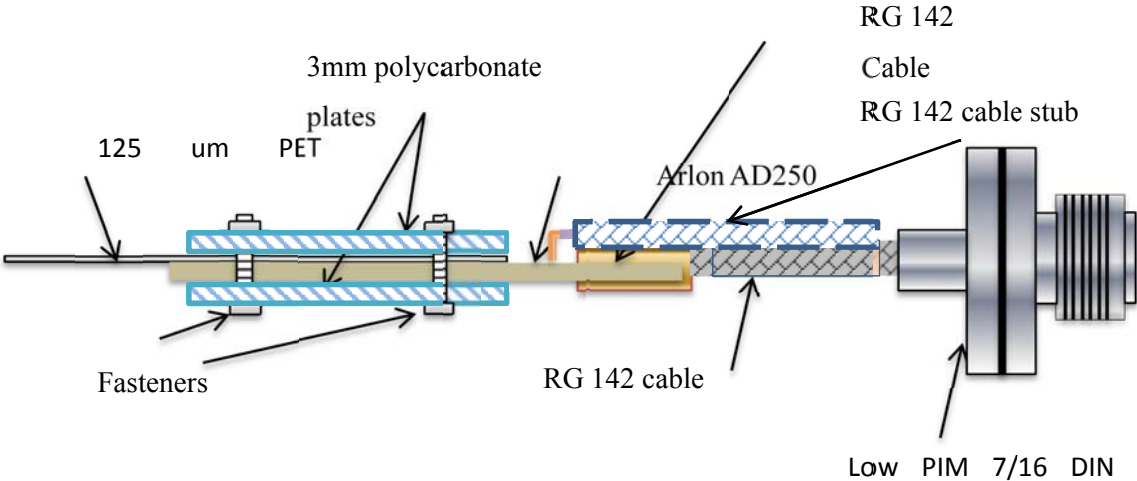
Fig 4-15 Side view of passive transition attached to the PET CPW feed PCB

The Arlon Microstrip circuit is secured to the PET collinear array substrate by polycarbonate alignment/compression plates and nonconductive fasteners. The fastener holes in the plates are aligned precisely to those on the PET array substrate, keying the alignment and ensuring consistent coupling performance. To test the impact of misalignment of the substrate layers, a parametric sweep of the longitudinal alignment was conducted. Fig4-16 depicts the test structure used. The substrates were offset by ± 3 mm whilst monitoring the reflection coefficient magnitude the passive coupling transition. The results of this simulation are shown in Fig4-17, where an offset of ± 3 mm changes the insertion loss value by a maximum of 0.15 dB. The reflection coefficient magnitude exhibits more significant change.
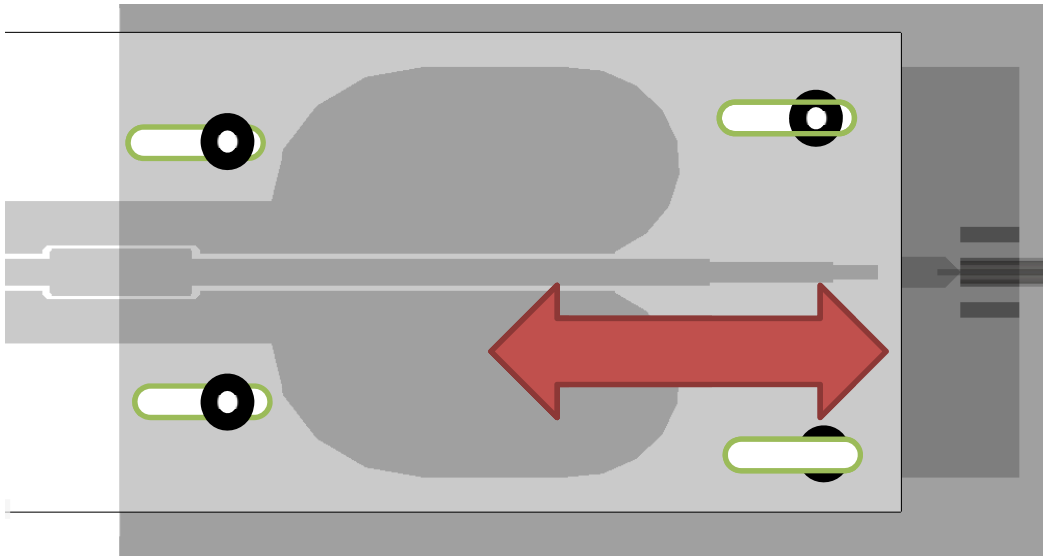
Fig4-16 Passive coupler alignment test configuration
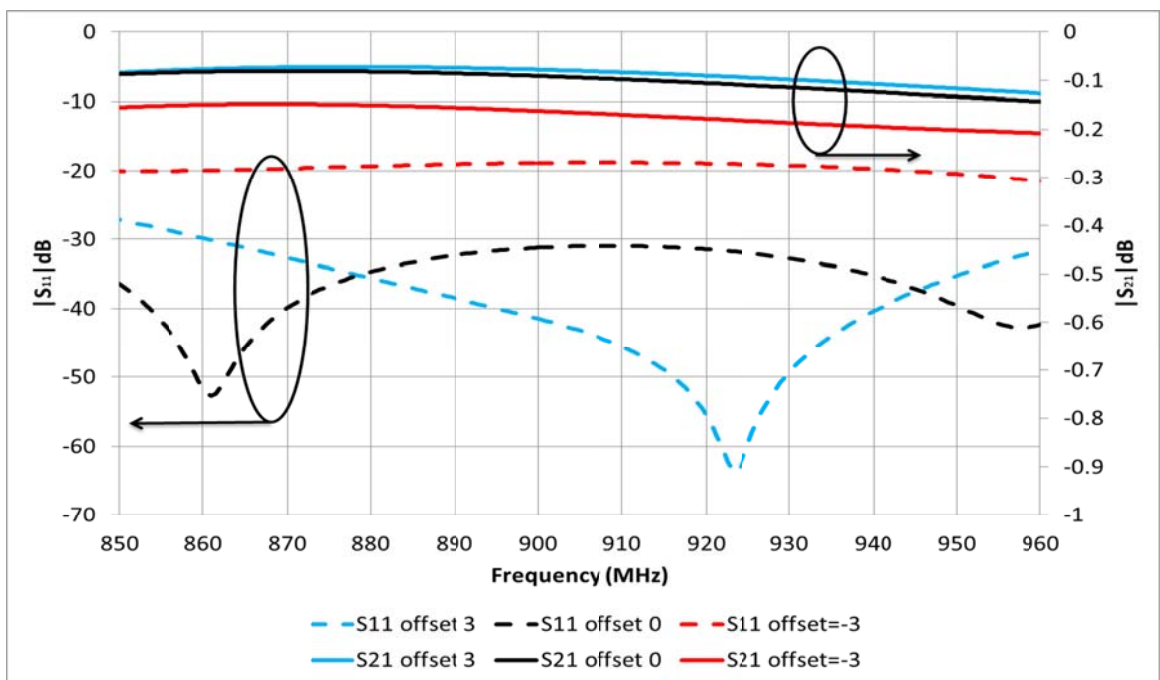
Fig4-17 Parametric sweep of the passive coupler substrate alignment

The PIM performance and PIP performance results for the passive coupling transition were tested as part of the complete collinear array, and are detailed in Chapter 5. As the low PIM connector is hand crafted from raw brass, it has only achieved a PIM value of -148dBc. This is expected to fall well below -150 dBc in the final professionally machined and finished product.

4-136

4.7 Summary

The majority of "Coplanar waveguide (CPW)" to microstrip transitions presented in the literature are aimed at frequencies above 1 GHz for MMIC ("monolithic microwave integrated circuit ") applications. In Section 4.2 the literature has shown that the transition topologies encountered had DC continuity in at least one of the conductors. In Section 4.3 a novel "Coplanar waveguide (CPW)" to microstrip transition is presented. The proposed transition was implemented in order to increase the mechanical strength of the cable connection and eliminate solder processes. This transition has low loss, low PIM, incidental impedance matching, and is totally DC isolated from the input to output transmission lines. It provides sufficient mechanical isolation to enable a robust coaxial cable connection.

In Section 4.4 the proposed coupler performance is determined using electromagnetic simulation. The insertion and reflection coefficient magnitude performance is explored with respect to key parameters that affect the coupling between the "Coplanar waveguide (CPW)" and microstrip transmission lines. As the output impedance of the "Coplanar waveguide (CPW)" is different to the VNA ("Vector Network Analyser") measuring equipment, a commonly used back-to-back measurement technique was explained in Section 4.5. The passive coupling transition performance was then verified by testing a realized prototype of the back-to-back structure, with reasonable congruence to the simulated results. An insertion and reflection coefficient magnitude of < 0.5 dB and > 15 dB respectively was achieved over the frequency band of 850-960 MHz.

The transition assembly was detailed in Section 4.6, which consists primarily of a flexible 0.125 mm "Polyethylene terephthalate (PET)" PCB laminated with the more substantial Arlon AD250 [52] rigid microstrip substrate. The lamination and alignment of the planar substrates was investigated to determine the effect of manufacturing tolerance. The coupling structure was shown to be relatively insensitive to small offsets of ± 3 mm. The solder-less assembly is expected to improve the PIM performance significantly. With complete passive coupling, the transition circuit is capable of coupling efficiently through dissimilar substrate dielectrics and thicknesses. This allows the collinear array described in this thesis fabricated on 0.125 mm thick "*Polyethylene terephthalate* (PET) "to be easily cabled during the assembly process.

Chapter 5 "Coplanar waveguide(CPW)" fed omnidirectional collinear array with frequency independent beam direction

In this chapter the planar feed network, dipole elements and passive coupler components introduced in previous chapters are integrated to form the proposed omnidirectional six element "coplanar waveguide (CPW)" fed collinear array. The array has unique attributes which expand the possible uses for a relatively low cost PCB based antennas, with pattern performance comparable to much more complex array designs.

Table 1-4 the characteristics of a selection of state-of-the-art omnidirectional antennas are compared with the advantages and disadvantages for each technology, and how they compare to the characteristics of the proposed array in TABLE 1-1.

In Section 5.1 the planar structured feed network, dipole elements and passive coupler components are reviewed, and then united to form an omnidirectional collinear array. The performance specifications for the array are also revisited in Section 5.2.

Section 5.3 details the simulated and measured array performance. Simulated and measured reflection coefficient magnitude results are compared. Base station array antenna performance is ultimately assessed by the analysis of the radiation pattern. Factors such as beam tilt, gain and side lobe level are the main characteristic measures discussed in this section.

The power handling performance is another important factor in base station array applications. Section 5.4 evaluates the maximum power handling of the array. The behaviour of the array when PIM (Passive Intermodulation) products are generated using an excitation of two carriers, and the PIP (Peak Instantaneous Power) as a result of the combination of a number of transmitters into the one antenna are also analysed.

Section 5.5 explores the mechanical limits that base station arrays are required to withstand in their installation environment. The calculated wind survival ratings and projected area are

presented, along with the design considerations put in place to protect the array from these stresses.

A discussion on the methods used to provide a pre-calculated beam tilt based on phase offset in base station arrays is presented in Section 5.6. Modelling results for a proposed array with a fixed 4 degree down tilt are provided, and the impact this modification has on the reflection coefficient magnitude performance is analysed. A comparison is made between the tilted and un-tilted array in terms of reflection coefficient magnitude, pattern shape and realized gain. Finally, the chapter is summarized in Section 5.7.

5.1   Structure of the omnidirectional array with beam stability

The array feed network based on coplanar transmission lines presented in Chapter 2 utilised a centrally located "Coplanar waveguide (CPW)" discontinuity, which in combination with the dual secondary coplanar strip transmission lines provides the phasing required for zero beam tilt functionality.   The dipoles elements used in the array are optimized for maximum bandwidth and compatibility with the feed network in Chapter 3. The specially designed cable connection interface described in Chapter 4 provides a low PIM interface from the attached cable to the edge of the coupling PCB. This coupler alleviates one of the most common causes of PIM in an array; the solder joints between the feeding coaxial cable and the array itself.

The proposed "coplanar waveguide(CPW)" fed omnidirectional array with frequency independent beam direction is depicted in Fig 5-1. The array can be described as two series fed dipole arrays placed back to back (Part A and Part B) for an upper sub-assembly and a lower sub-assembly with a lateral line of symmetry.   Each series fed array contains dipole antenna elements with the geometry shown in Fig 5-9 and has an offset cardioid azimuth radiation pattern. There is a 180 degree phase offset between each series fed array, resulting in near omnidirectional patterns from each sub-assembly.

The sub-assemblies are fed back to back with a line of symmetry through the centre axis of the array, creating the gable phase profile required for centre feeding and zero beam tilt. This phase profile results in the upper sub array assembly tilting in opposition to the lower sub array assembly when frequency is varied. In this configuration, the vertical omnidirectional main beam broadens rather than abruptly tilting (as it would in a series feed array) with change in frequency. "Coplanar waveguide (CPW)" is well known to provide very good cross

5-139

talk immunity in microwave circuits. This is primarily due to the ground tracks blocking the surface wave propagation between active lines. This attribute of "Coplanar waveguide (CPW)" has been exploited to provide a level of isolation between the main "Coplanar waveguide (CPW)" feed currents and the secondary parallel strip transmission line currents. The array would not function correctly if these signals were allowed to cross paths uncontrolled.

To maximize the PIM and PIP performance and to provide a gradual transition from "Coplanar waveguide (CPW)" to microstrip modes, the array is DC isolated by a specially designed "Coplanar waveguide (CPW)" to microstrip transition as shown in Fig 5-1 The transition uses capacitive coupling to both ground and source, and hence this coupler effectively DC isolates the array. Coupling is provided by mechanically laminating the specially modified interface of the array to the transition, providing a low loss connection to the array.
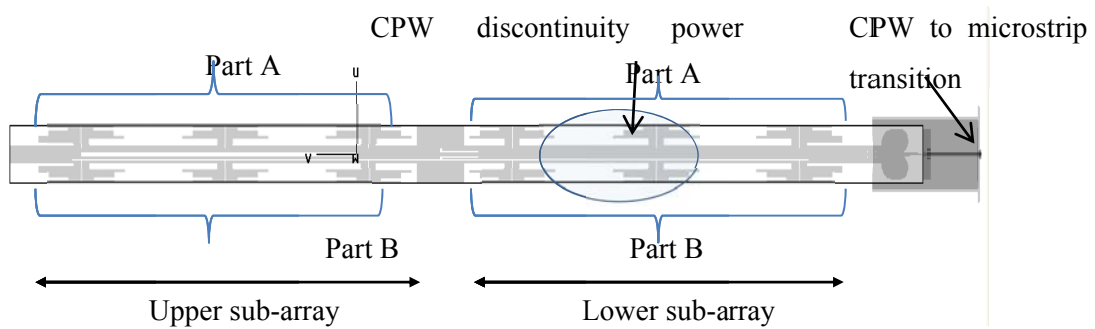
Fig 5-1 A schematic of the overall array components

5.2 Images of the six element "Coplanar waveguide (CPW)" array components.

The following images are showing the major components of the array

In Fig 5-2 The array is presented alongside an existing array antenna using the same radome.
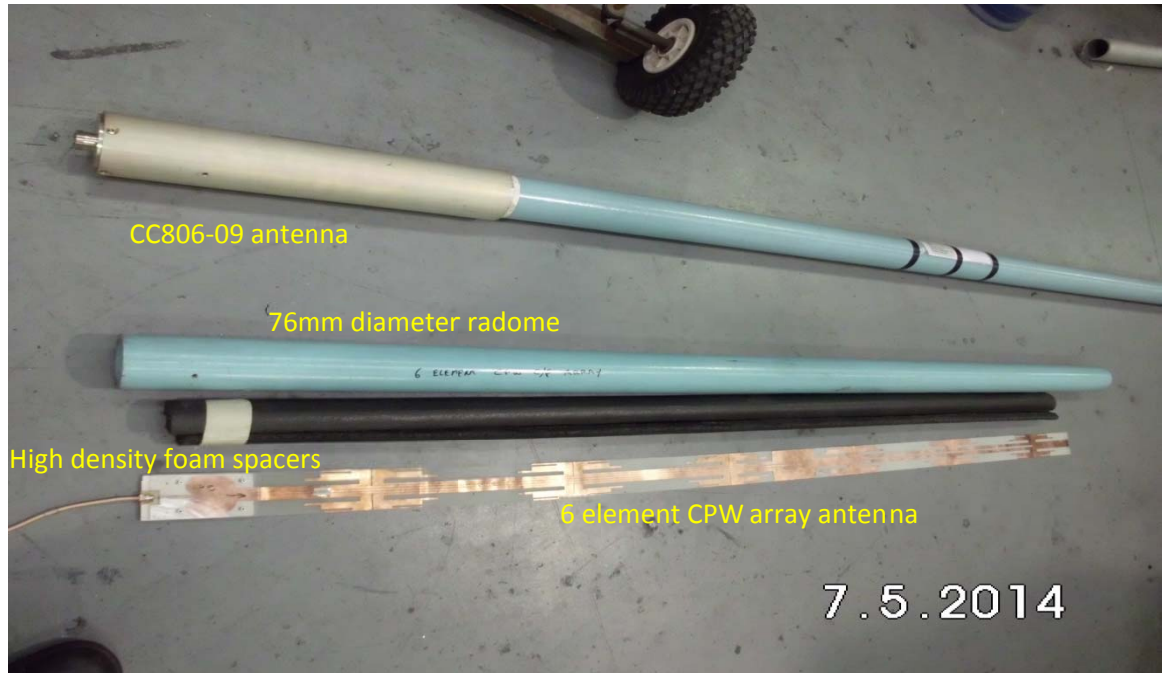
Fig 5-2 Components of the "Coplanar waveguide (CPW)" array with an antenna using the same radome

In Fig 5-3 The high density foam spacers are shown either side of the array PCB. The foam spacers are designed to support the PCB concentrically in the radome to prevent asymmetric loading and possible azimuth pattern distortion. The passive coupler circuit is shown attached to the array.

5-141
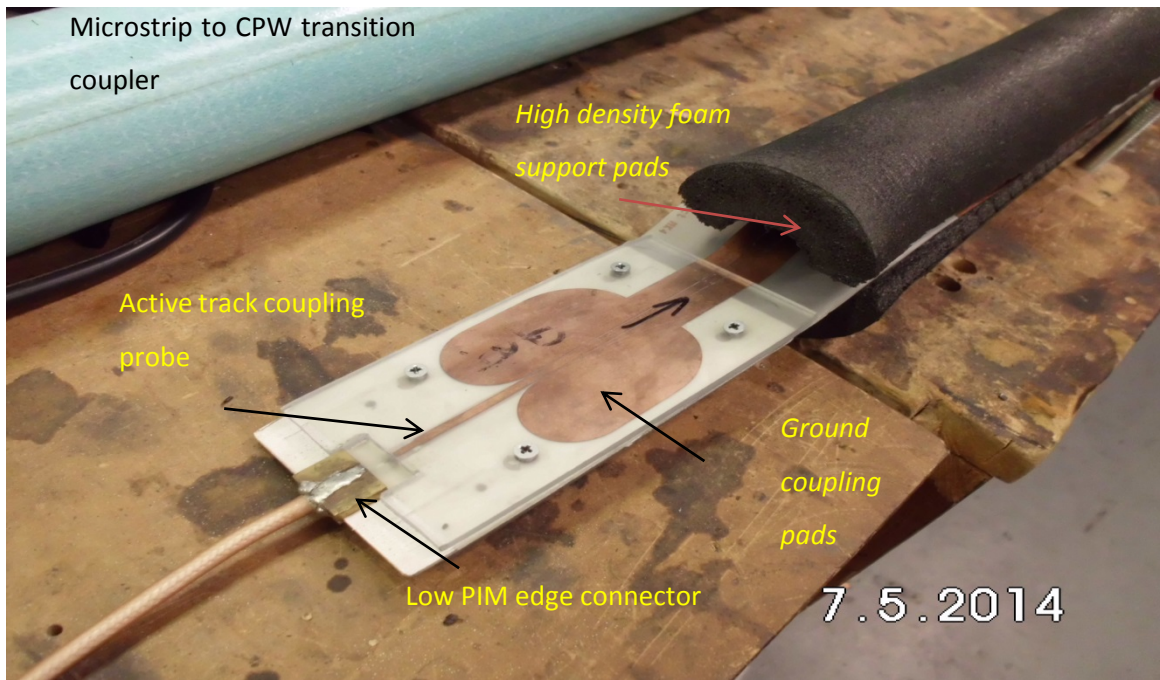
Fig 5-3 The foam spacers used to support the array PCB

In Fig 5-4 The passive coupling circuit attached to the array sandwiched between two polycarbonate plates and secured with four fasteners.
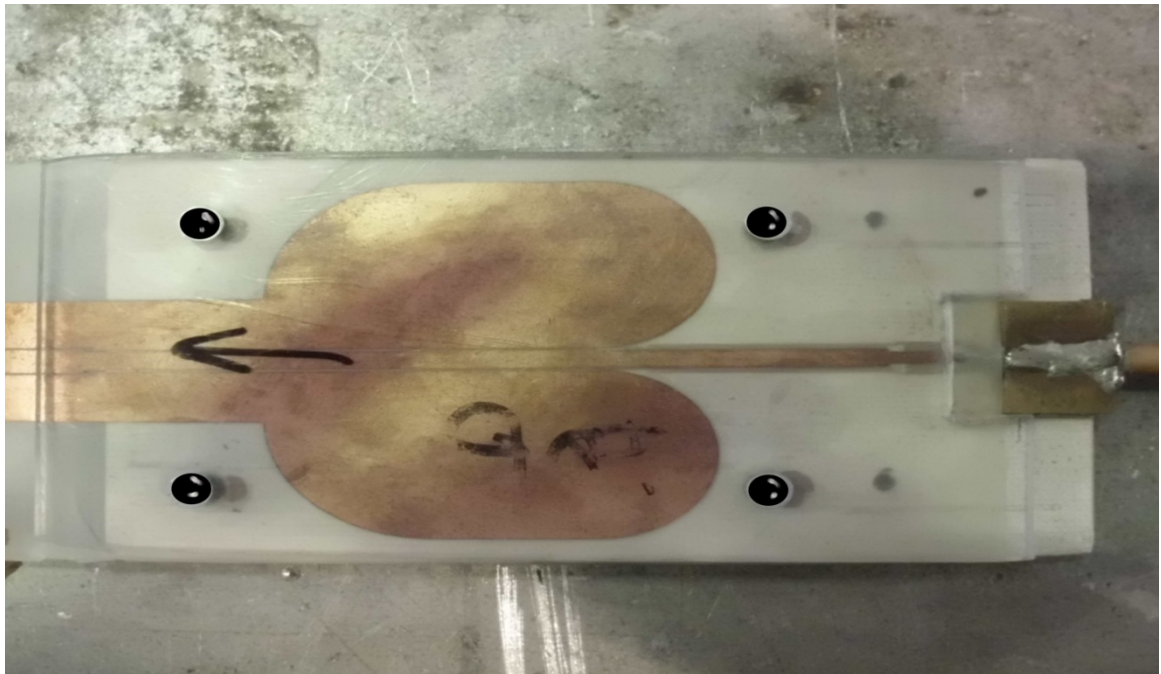
Fig 5-4 The passive coupler circuit attached to the array

5-142

In Fig 5-5 shows the full length of the array components. The cross section of the foam spacers is a "D" with a 12mm diameter core removed to prevent direct contact with the "Coplanar waveguide (CPW)" main line.

Fig 5-5 The full length of the "Coplanar waveguide (CPW)" array

In figures 5-6 to 5-8 are the impedance matching and phase control elements

Fig 5-6 close-up of "Coplanar waveguide (CPW)" transmission line

5-143

CPW and slotline

CPW phase reference shunt

2010.1.1
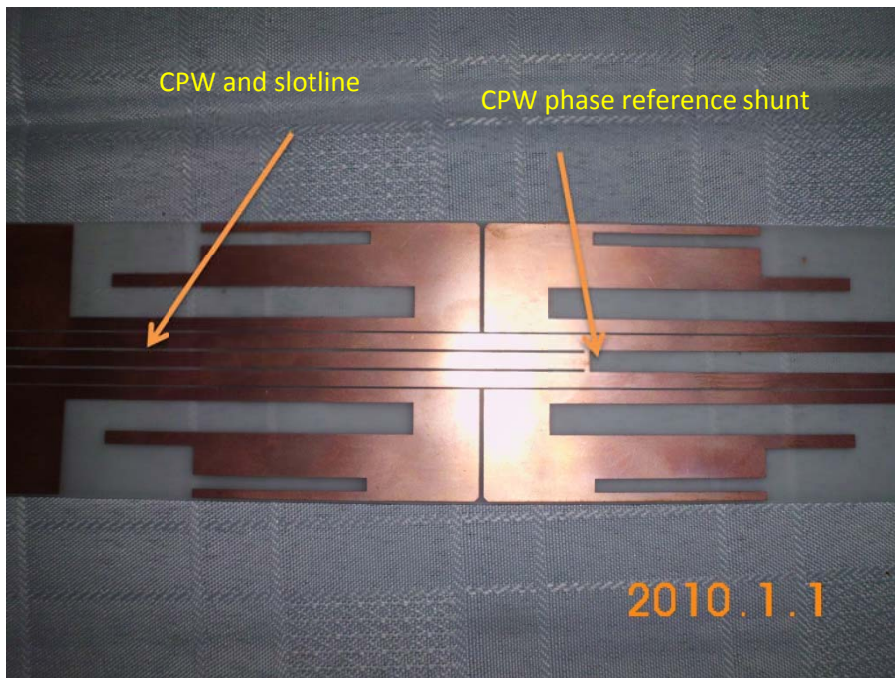
Fig 5-7 close-up of upper dipole

Slot line ground return stubs

2010.1.1

Fig 5-8 close-up of top element

5.2.1   Array construction

The array is enclosed in a pull-extruded fiberglass radome 76mm outer diameter with an internal diameter of 63mm. This radome has been selected as it is used for other array

antennas of a similar frequency band. The array has been fabricated on a low cost, flexible, 0.125 mm PET substrate clad with 0.035 mm copper. The passive coupling circuit uses Arlon AD250 high temperature PIM friendly substrate.   High density polyethylene (HD-PE) foam spacers are used to support the array concentrically inside the radome.   A mounting tube support is then fitted and secured to the radome. The array construction is detailed in Fig 5-10 . The complete technical drawings of the array are given in Appendix A through to E.

:ing

uth

feed

ince

ts for

ape

Integral choke

CPW   GROUND

Slot line feed

Fig 5-9 Planar dipole structure

5-145

Fasteners

Feed cable interface

Polycarbonate plates top and
bottom support the coupling circuit

cpw array main circuit
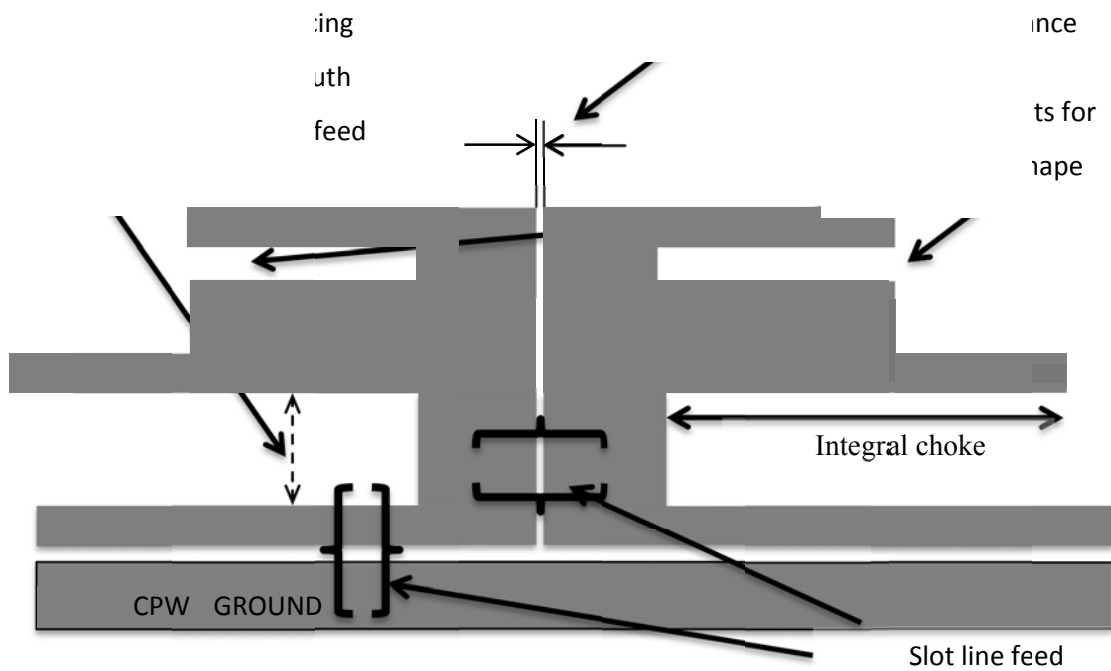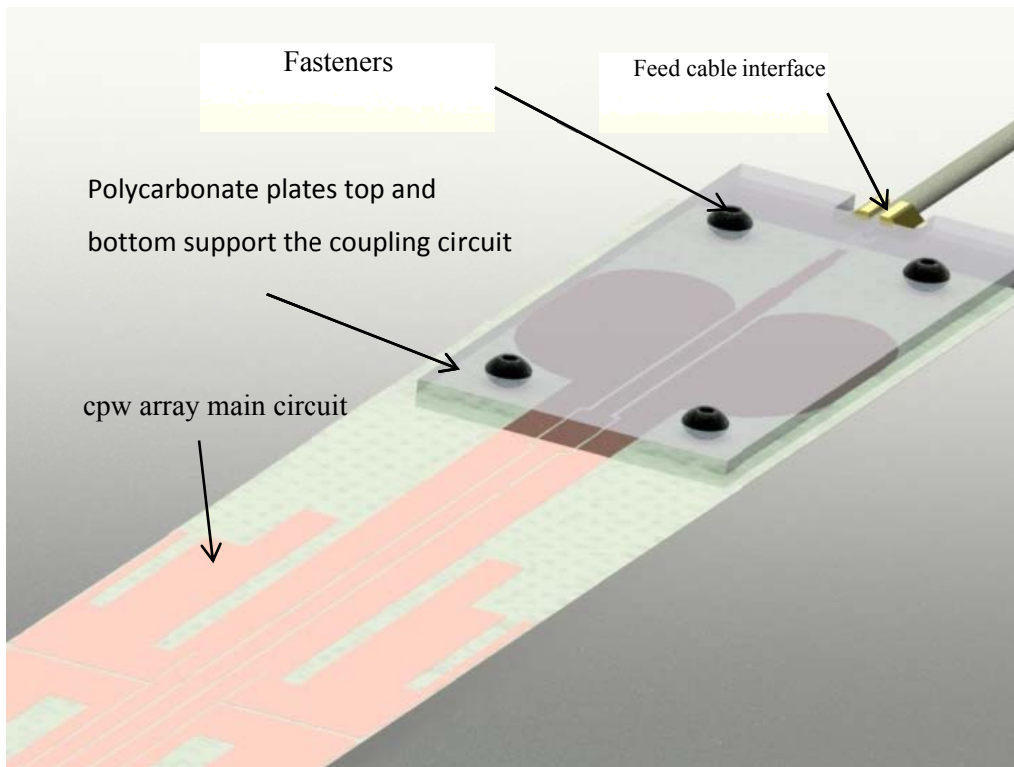
Fig 5.3 Passive coupling circuit laminated to the array PCB

ng

Radome

ɔr
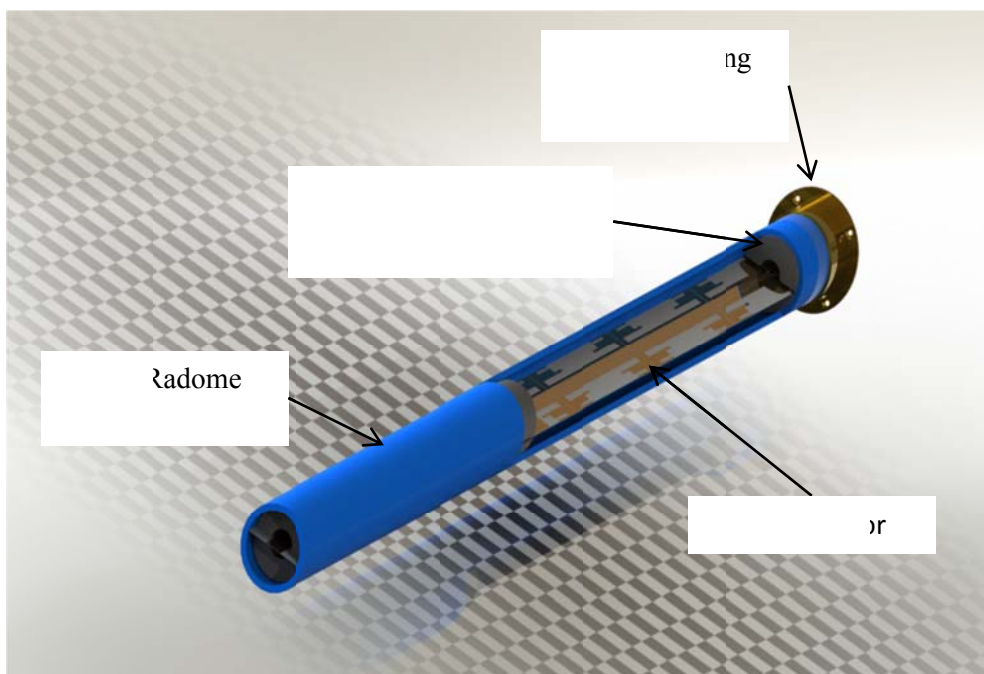
Fig 5-10 Cut away representation of the array

5.3 Performance expectations

Table 5-1 is the performance expected from this antenna based on low power applications. This antenna was not expected to handle high power levels, as the materials used in the prototype are intended for temperature controlled circuits. The specifications are suitable for low power (less than 100 Watts) cell extension and low power telemetry applications.

Table 5-1 Electrical specifications (from Chapter 1)

Characteristic	Specification
Frequency band	850 - 960 MHz
Gain	10.0 ± 1 dBi over 10% bandwidth
Side lobe suppression (typical)	-10 dB
Azimuth pattern stability	± 0.8 dB over 360˚ 10% bandwidth
Tilt	0 ± 1 degree over 10% bandwidth
Power rating	100 Watts maximum at 26˚ C
VSWR	< 1.5:1 over 10% bandwidth
Connector interface	7/16 Din jack
PIM	-150 dBc, 2 x 30dBm carriers
Peak Instantaneous Power	1 kW

A gain of 10 dBi is specified over a 10% bandwidth. A typical 6 element collinear array vertical beam width of 10 to 12 degrees allows for range of possible installation locations without the need for accurate placement. The power rating specified of 100 W enables multiplexing of transmitters with a maximum total combined power of 70 Watts at low duty cycle. A peak instantaneous power rating of 1 kW enables coincidental digital symbols when the array is

5-147

used with WCDMA or other digital modulation techniques. Zero beam tilt is required for broad band performance independent of operational frequency within the band 850 - 960 MHz. A 7/16 DIN connector is essential to obtain the associated PIM specification of -150 dBc.

Six collinear radiator elements are required with an element spacing of 0.881λ to achieve a gain of 10 dBi at centre frequency of 903 MHz referring to Eqn. 10. An element spacing of 0.881λ is used based on net dielectric loading offsets from substrate and radome loading.

Estimation of number of elements required

$$|N| \approx \frac{\lambda \frac{D}{2}}{d} \qquad (10)$$

N = number of elements,

D = directivity in dBi,

λ = wavelength,

d = distance between elements.

$$\lambda = \frac{3 \times 10^8}{903 \times 10^6} = 332mm$$

$$d = \lambda \times 0.881 = 291mm$$

$$N = \frac{332 \times \frac{10}{2}}{291} \approx 6$$

5.4 Array Antenna performance

The analysis of the collinear array is conducted using Finite Difference Time Domain solver [40]. An accurate model of the antenna dimensions has been constructed, including all material electrical properties. The final design artwork is exported to create a prototype PCB.

5-148

This PCB is then assembled into the complete antenna array, including the radome and mounting fixtures. The antenna reflection coefficient performance is then tested in free space using a Vector Network Analyser.

The simulated and measured results for the collinear array with frequency independent beam direction are shown in Fig 5-11. Both the numerical model and the fabricated prototype have a reflection coefficient magnitude in excess of 14 dB within the specified bandwidth from 850 - 960 MHz, Some minor discrepancies in the shape of the simulated and measured results can be observed. These were found to be due to tolerances in the manual fabrication of the coupling interface.
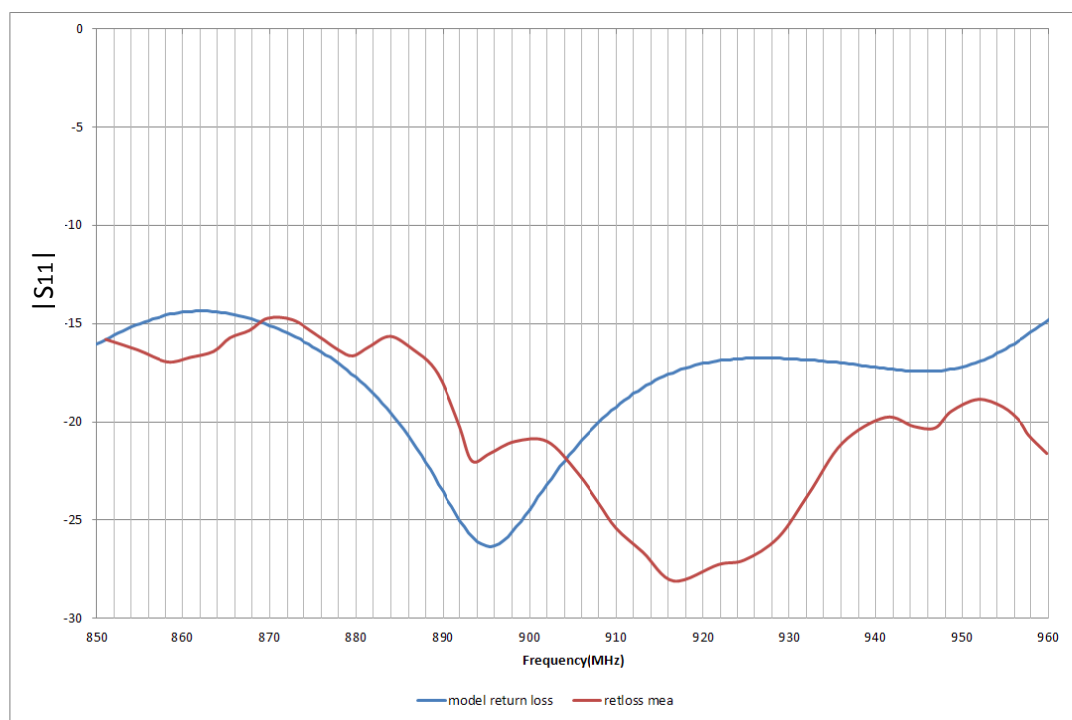
Fig 5-11 Measured and simulated reflection coefficient magnitude for the proposed collinear array

5.4.1 Radiation pattern measurement technique

Microwave arrays of small physical size and small aperture can be measured indoors in an anechoic chamber. The proposed array is 1900mm long, approximately 6 wavelengths at

903MHz. The range length is determined by the aperture size (D) at the wavelength of operation: using Eqn. 11

$$\text{Far field} = \frac{2D^2}{\lambda} \qquad\qquad (11)$$

For an array of this size the range length given by (10) is more than 40 meters. Due to this large range length, it is more practical to use a free space ground reflection range as shown in Fig 5-14 to test the proposed array. In this configuration, the ground reflection itself is used to cancel out the reflections on the range. The source array is mounted horizontally at a height where the specular ground reflection and the incident wave coincide at test position creating a reflection quiet zone. The array under test is tilted forward to be on bore sight to the base of the source support. To measure the radiation pattern of an array outdoors, it must be placed in relative free space to prevent reflections that may impact on the results. In this case the range area is located on 20 hectares of cleared farm land at Tooborac, North of Melbourne, Australia. Shown in Fig 5-12 is the typical radiation pattern logging equipment and rotation control.

Fig 5-12 range test control and logging equipment

The antenna under test is mounted on an insulated mount to measure the elevation pattern as shown in Fig 5-13 the antenna is mounted high above ground to prevent ground reflection, and requires an elevation platform to make adjustments.

5-150

Fig 5-13 setting up antenna for testing

To measure vertically polarized omnidirectional arrays, the array is placed horizontally on a non-metallic pedestal above the ground. To stimulate the array under test, a signal source is applied. Due to reciprocity, the array under test or the source array can be either active (TX) or passive (RX) in the system. The choice of active and passive antennas is normally based on elimination of interference from or to other services. The array is rotated on its central axis through 360 degrees. This angular transducer generates the X axis data. The amplitude of the received level output from the network analyser is the Y axis data. The radiation pattern is a representation of the X axis data with respect to Y axis data. It can be presented in either of two forms, Cartesian (in Fig 5-15), or polar (in Fig 5-16)
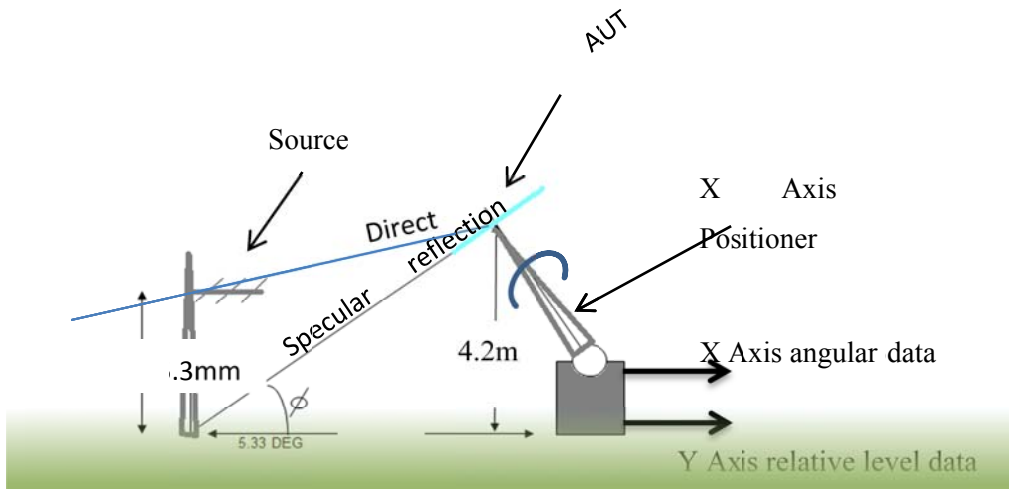
Fig 5-14 Ground reflection range
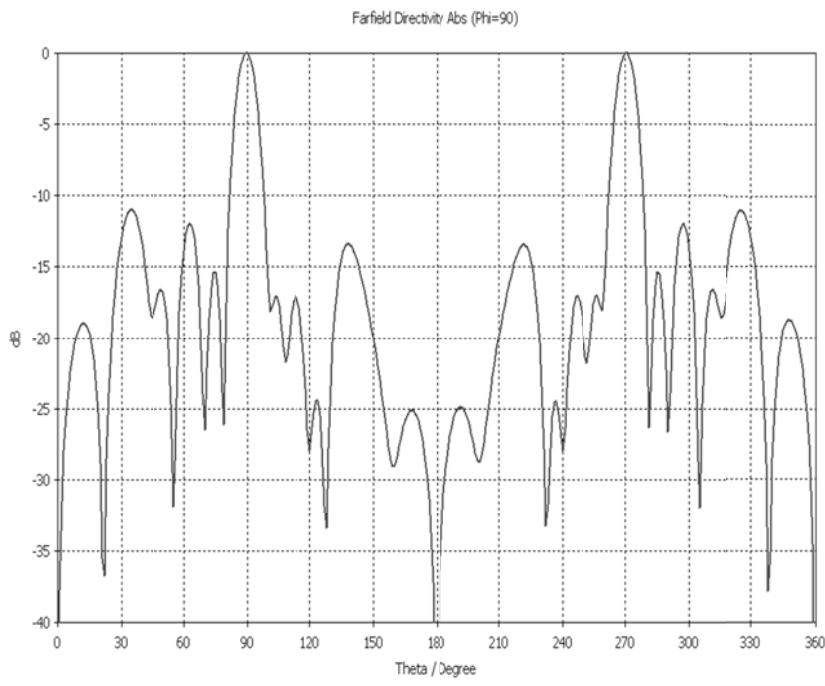
Fig 5-15 Cartesian plot of array elevation pattern
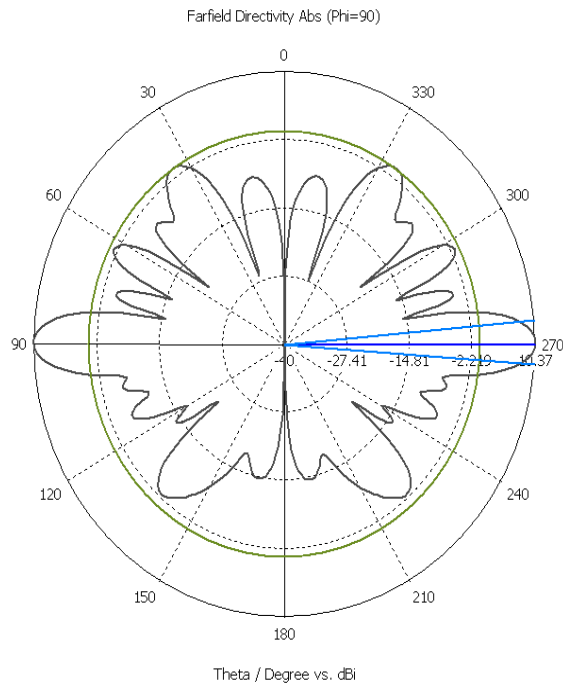
Fig 5-16 Polar axis plot of elevation pattern shown in fig 5.15

The directivity of the array is calculated by integration of the main lobe. The gain of the array (in dBd) is simply the directivity minus the gain of a dipole in free space which is approximately 2.14 dBi. The total gain of the array is this value minus the reflection and resistive losses. Another method to evaluate gain which complies with TIA 329C standard is the gain by comparison technique. In this case, a known standard gain array is measured by the same process as the array under test and received levels compared. The array under test gain is determined relative to the measured value of the standard gain array.

5-153

5.4.2 Simulated and measured radiations patterns

The measured and simulated radiation patterns for the collinear array with frequency independent beam direction are presented in Fig 5-17 to Fig 5-21. The results display very good similarity with the exception of slightly higher level side lobes at 960 MHz in the measured case. The main lobe elevation pattern is on the horizon within ± 1˚ over the 850 - 960 MHz bandwidth. The measured and simulated beam tilt and beam width characteristics are compared in Table 5-2 and Table 5-3.
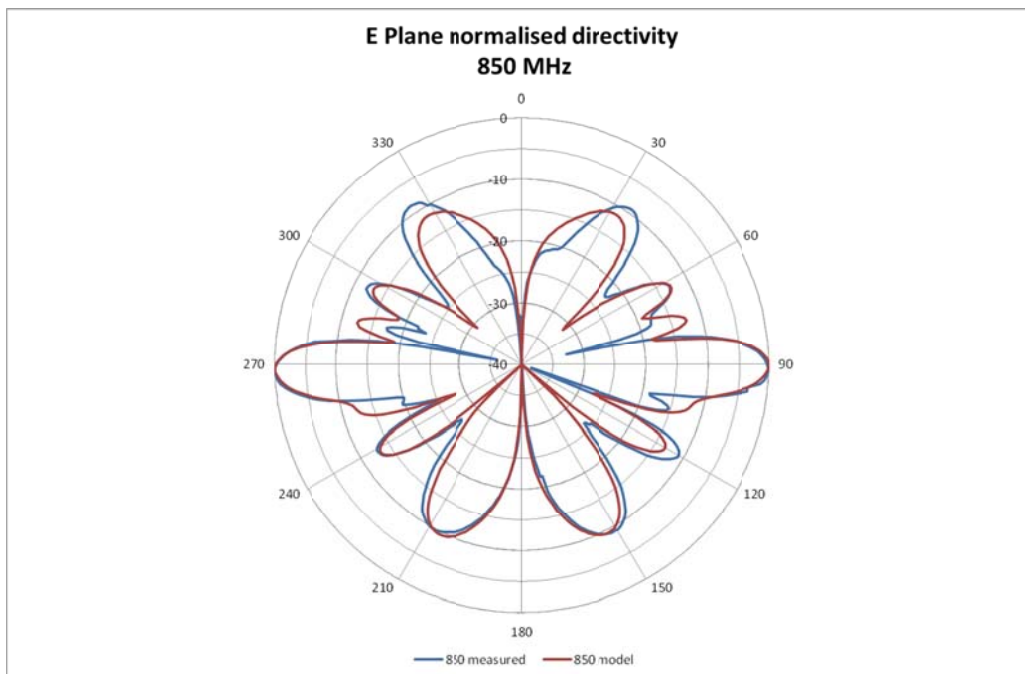
Fig 5-17 Model and measured elevation patterns 850 MHz
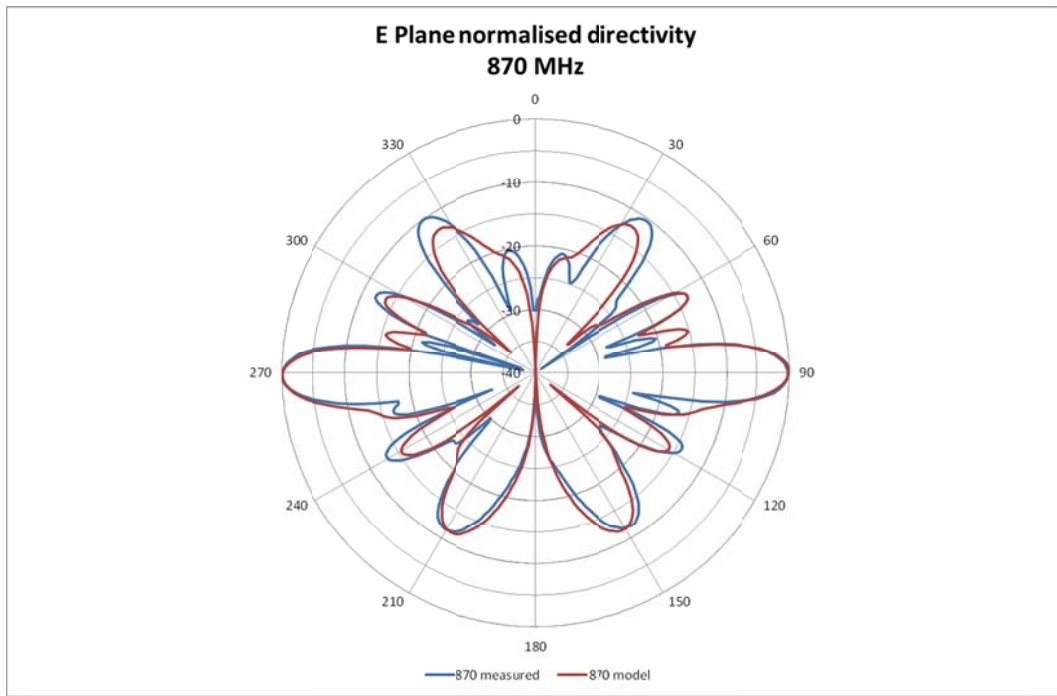
Fig 5-18 Model and measured elevation patterns 870 MHz
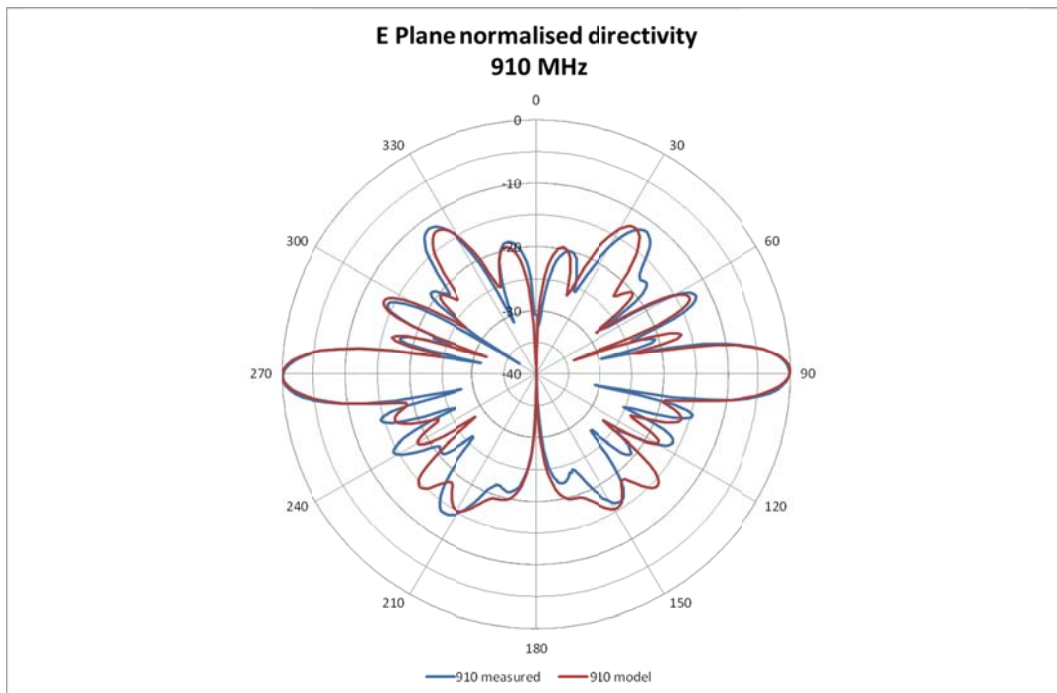
Fig 5-19 Model and measured elevation patterns 910 MHz

5-155
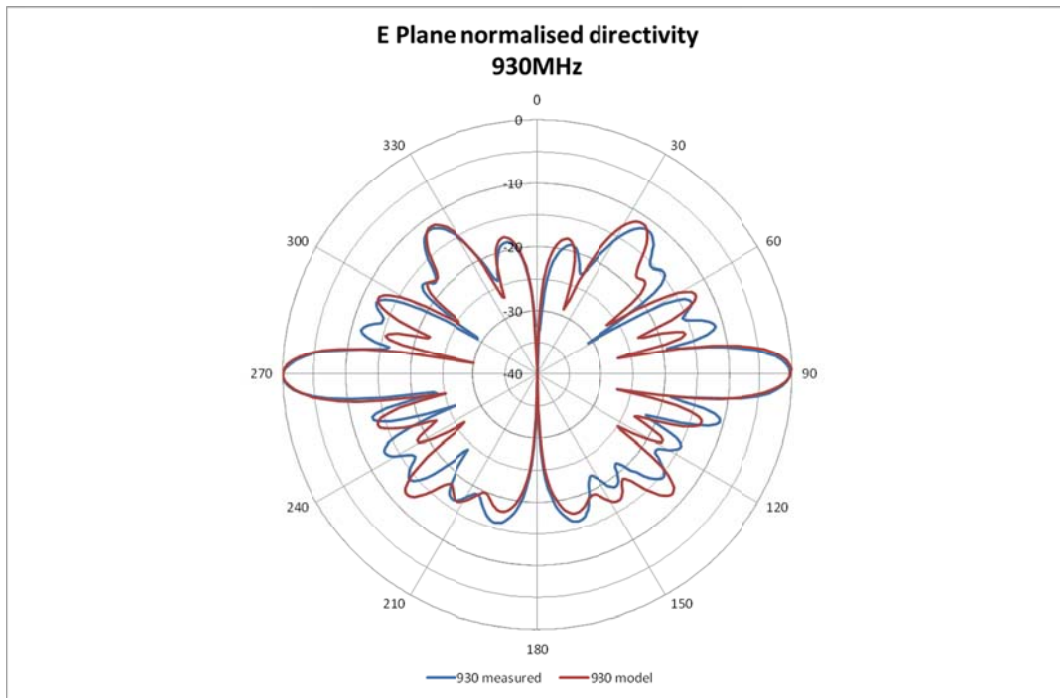
Fig 5-20 Model and measured elevation patterns 930 MHz
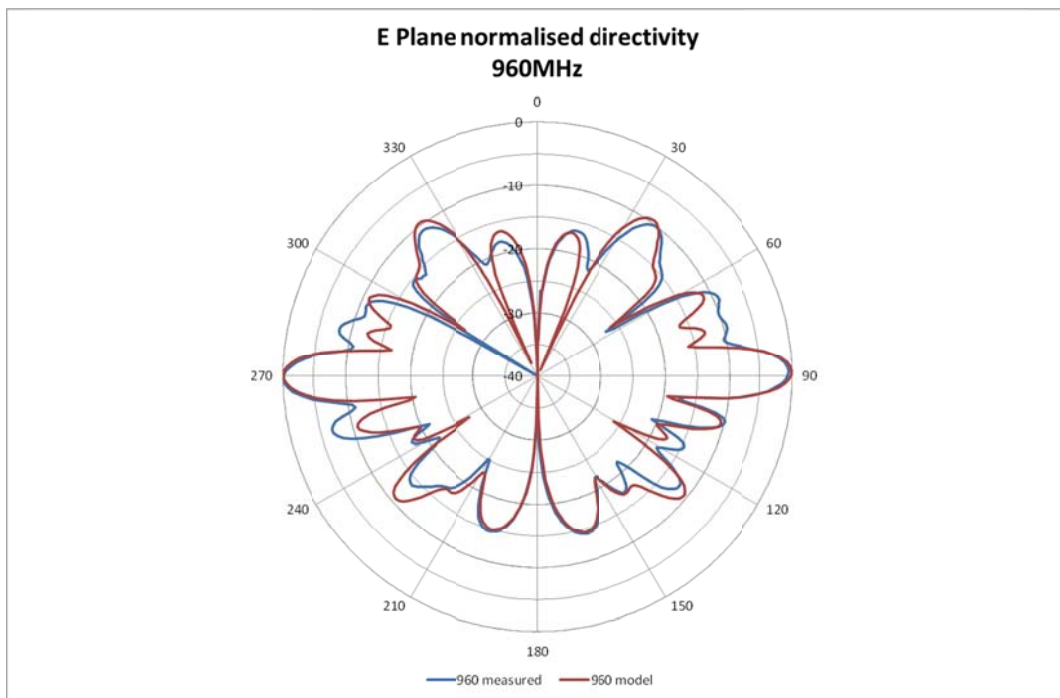
Fig 5-21 Model and measured elevation patterns 960 MHz

5-156

Table 5-2 Beam tilt characteristics (in degrees)

Frequency (MHz)	850	870	910	930	960
Model (Array)	-1.0	-1.0	0.0	0.0	1.0
Measured(Array)	-0.9	0.0	0.1	0.2	0.6

Table 5-3 Half power beam widths (in degrees)

Frequency(MHz)	850	870	910	930	960
Model (Array)	10.5	10.7	10.8	10.8	11.5
Measured (Array)	10.6	10.6	10.2	9.3	9.3

5.4.3 Gain characteristics

The gain of the prototype collinear array with frequency independent beam direction was evaluated using the gain by comparison technique, employing a pyramidal horn standard gain antenna (700-1200 MHz). The loss in the array was determined by comparing the calculated directivity and the measured gain of the array, and the efficiency of the array was thus calculated. Table 5-4 summarises the measured pattern characteristics of the prototype collinear array.

Table 5-4 Pattern characteristics for the six element array with frequency independent beam direction

5-157

Six element collinear array (measured)	HH, Path = 45 m, AUT height = 4.2 m, Po = +10dBm test range 45				
Frequency (MHz)	850	870	910	930	960
HPBW (°)	10.6	10.6	10.2	9.3	9.3
Beam Tilt (°)	-0.9	0.0	0.1	0.2	0.6
Directivity (dBi)	9.05	9.52	9.9	10.2	9.7
AUT gain by comparison (dBi)	9.0	9.4	9.9	10	9.5
Residual loss (dB) (coupling, resistive and VSWR losses)	0.05	0.12	0.0	0.2	0.2
Efficiency (%)	95.3	95.7	96.0	97.9	98.9

The peak measured gain is 10.2 dBi, and the results over the 850 – 960 MHz frequency band are within the 10 ± 1 dBi tolerance specified in Table 5.1. The realized gain from the CST simulation is plotted in Fig 5-22 and compared to the measured gain results. The results show good congruence, with a maximum difference of only 0.4 dB. The variation could be attributed to accuracy tolerances in the measurement technique.
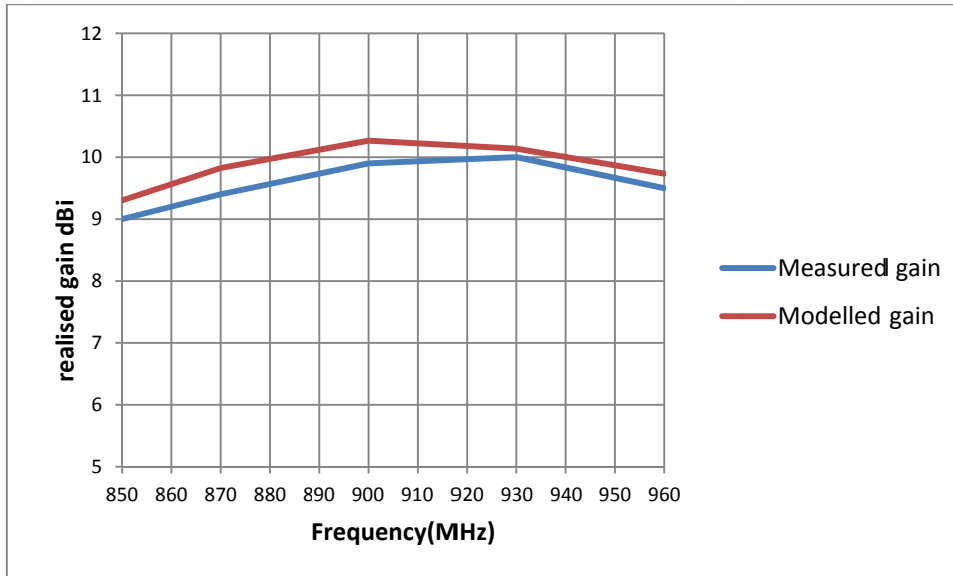
Fig 5-22 Measured gain and modelled realized gain for the six element array

In summary, the collinear array with frequency independent beam direction has a vertical beam stability of ±1° over the defined bandwidth, which is within the specifications. The side lobe level is typically 10 dB down on the main lobe, except for at the edge of the band (960 MHz) where it reaches 7.8 dB. The beam width is between 9 - 11° across the defined band. The maximum azimuth deviation for the array is ± 0.7 dB at 960 MHz. The azimuth pattern deviation is discussed in Chapter 3, where it was shown to be caused by geometric asymmetry commonly found in planar element arrays. Correction techniques for this azimuth deviation have not been implemented, as they would result in the array being too wide for the specified radome.

5.4.4 Peak instantaneous power performance measured

With advanced radio networks using multi-carrier digital schemes, there is a statistical chance that multiple transmitter carrier powers can combine in-phase to generate a high voltage gradient within an array combiner/feed network [2]. This voltage is capable of destroying the insulation components in an array, including coaxial cable dielectrics and insulators.

For all base station arrays that support multiple carrier systems, electrical acceptance testing should include a non-destructive high pot test at a peak level of approximately 2.1 kV [2]. This test places the components under working stress and can detects faulty solder joints or intermittent contacts, moisture and contaminated dielectrics. Failure to detect these quality points can result in early system failure.

5-159

For non-destructive device testing, the applied voltage is gradually increased towards the peak voltage whilst monitoring the leakage current as shown in Fig 1-12. If the current exceeds a pre-set threshold or an arc occurs before reaching the test voltage the device has failed and the applied voltage resets. The voltage spike associated with PIP is not readily detected by conventional power meters. It is normally seen as noise affecting the bit error rate. The measurement of PIP is not practical, and prevention is preferable. Eqn. 12 can be used to calculate the potential value for PIP based on the power, modulation index and the number of transmitters in use at a transmitter site. The proposed collinear array has been subjected to high pot testing and passed the 2.1 kV limit as shown in Fig 1-12, that validating the electrical performance of the prototype.

$$PIP = 2 \times 10^{\left[\frac{20\log_{10}(N)+10\log_{10}(P_{ca})+M}{10}\right]} \qquad (12)$$

M = modulation Peak to Average ratio dB

P_{ca} = Power per channel at antenna port in watts

N = Number of channels in use
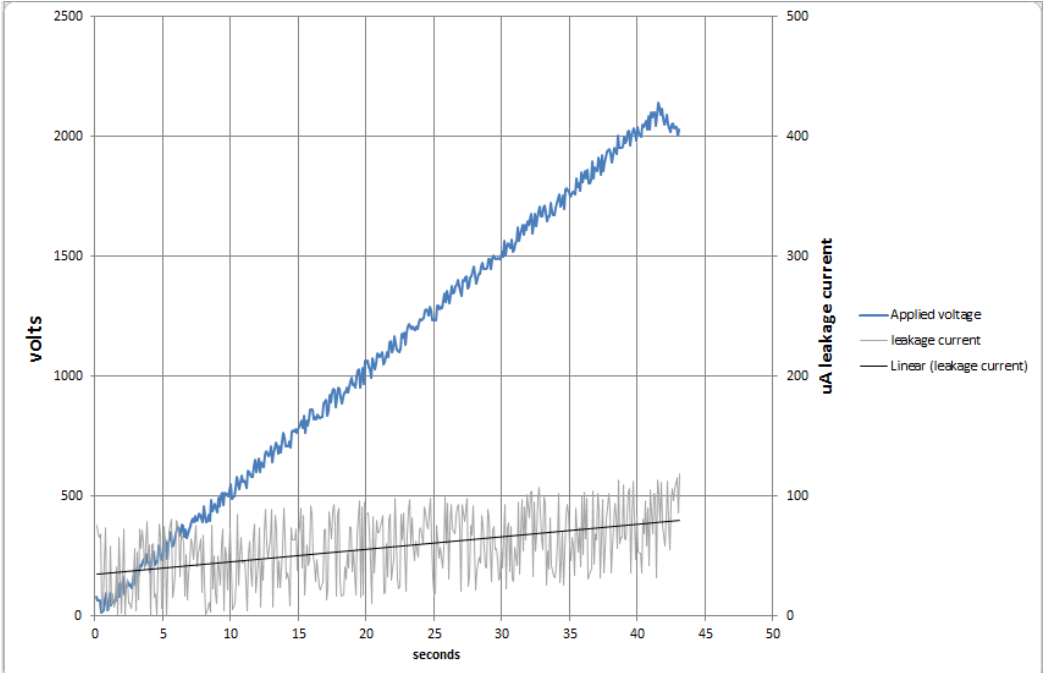
Fig 5-23 Non-destructive ionisation test of the passive coupler

5.4.5 Passive intermodulation performance measured

The PIM of the prototype collinear array with frequency independent beam direction was evaluated experimentally (refer to Fig 1-11 for a schematic of this experimental setup). The PIM Test Bridge consists of two transmitters combined using a low PIM diplexer set to frequencies that will generate a product in the pass band of the receiver channel. The receiver consists of a small amplifier connected to a spectrum analyser, which is filtered to prevent the fundamental TX carriers from de-sensitising the receiver. The PIM test equipment has residual PIM contribution; and this is accounted for in the results. The values of PIM are expressed as dBc, relative to the fundamental carrier levels. For example, if two 46 dBm carriers are applied to the device under test, and the measured level at the mixing frequency is -104dBm, then the difference between them is the PIM level = -150 dBc. Typical values for PIM are between -140 and -160dBc.

The PIM value measured for the prototype was -148 dBc, falling just short of the desired -150dBc. The substrate edge connection used in this prototype was machined by hand from brass and is not plated. It is expected that when this component is precision machined and silver plated the PIM value for the prototype collinear array with frequency independent beam direction will meet or exceed state-of-the-art value of less than -150dBc [10].

5.5   Power handling performance

The power handling capabilities of base station arrays must be determined to ensure they do not fail under peak load conditions. The governing factors related to power handling are:

- coaxial cable power rating,
- dielectric losses,
- VSWR,
- heat dissipation,
- material thermal properties,
- duty cycle and peak power.

For high power applications above 200 Watts at a frequency of 800 MHz, the conductor volume must be large in order to handle in excess of 70 amps of RF current. Ground connections are normally bonded directly to the mounting tube as it provides excellent heat dissipation.

One of the primary consequences of poor power handling is a gradual drift in the measured VSWR performance. Once the VSWR reaches approximately 1.8:1, the generated heat increases and can go into thermal runaway. This VSWR drift can be caused by dielectric heating or mechanical distortion which detunes the array with increased temperature. The end result can be VSWR shut down of a transmitter site.

5.5.1 Power measurement method

The maximum power handling capability of the collinear array feed network was determined by an actual power test. The transmitter source comprises of four Andrew feed forward cell extender transmitters, phase locked and combined to deliver a maximum power of 400 watts, as shown in Fig 5-24. The control combiner has an inbuilt VSWR bridge connected in series with each transmitter. This allows the monitoring of the VSWR performance of the antenna under load. A directional coupler connected to a spectrum analyser is used to verify the forward and reflected power levels of the combined output. The reflection coefficient magnitude is then calculated and recorded.

5.5.2 Power test results

The power testing results are summarized in configuration

Table 5-5 the starting power level for the test is approximately 80 Watts, and is held for one hour. At the completion of this stage, the temperature recorded by the thermal imaging camera is $54°$ C, or 27°C above ambient (27°C). The power is then increased to approximately 100 watts for one hour. At this level the array internal temperature is measured to be 70°C which is $43°$ C above ambient at the completion of the test. If the ambient temperature were to reach 40 degrees, this in combination with the $43°$ C internal temperature would increase

the net temperature to 83°C. Even at this high ambient temperature, the net temperature remains well short of the material working temperature of approximately 130°C.
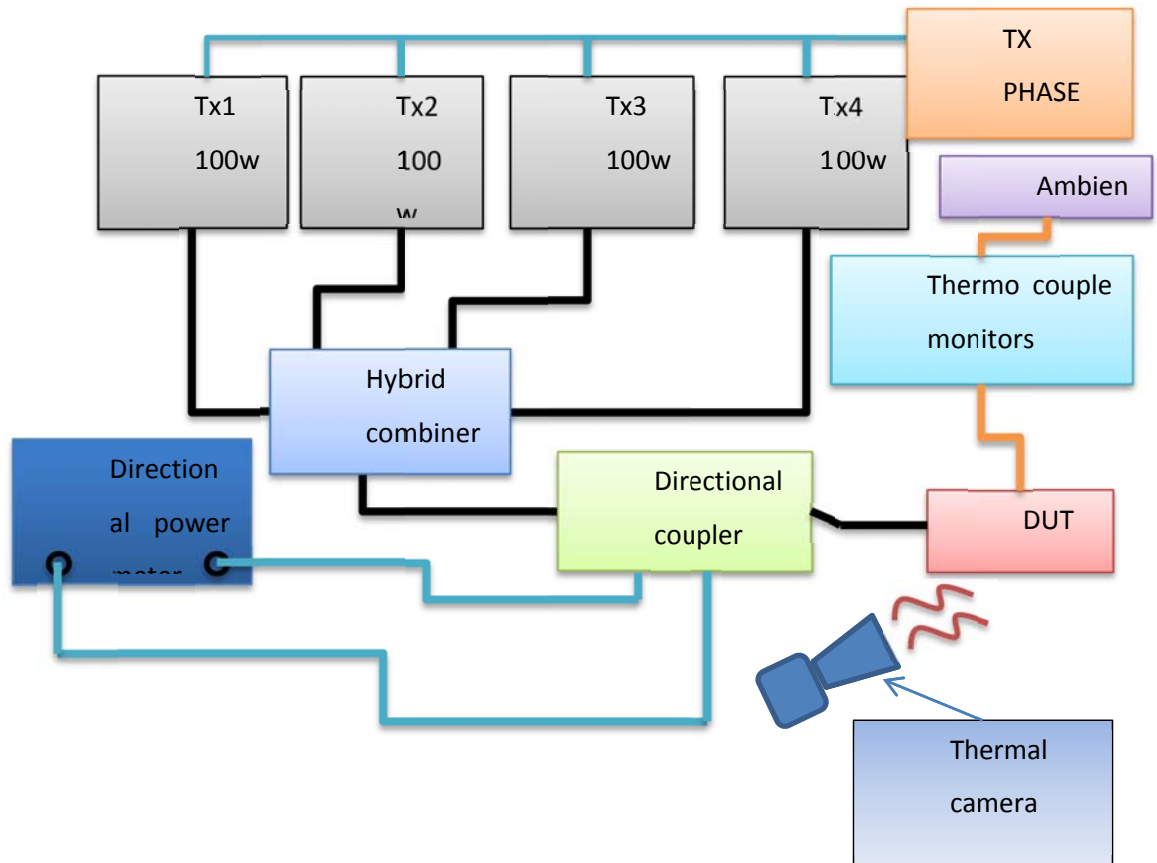
Fig 5-24 Power testing configuration

Table 5-5 Power measurement with thermal monitoring

Forward power dBm	Reflected power dBm	Forward power Watts	Reflection coefficient magnitude dB	Max recorded °C	Ambient chamber °C	above ambient °C	Total power applied Watts
-30.7	-43.2	85.1	-12.5	54	27	27	78.8
-29.5	-42.1	112.2	-12.6	(70)	27	(43)	(101.1)
-28.6	-41.5	138.0	-12.9	100	29	71	127.8
-27.5	-41	177.8	-13.5	136	29	107	161.9
-26.6	-37.3	218.8	-10.7	150	29	121	203.2

The VSWR did not change significantly during the power testing, and hence the printed collinear array can be rated to a maximum of 100 Watts. This rating is sufficient for many low

5-163

power applications. The use of the low cost PET substrate limits the power rating. If the substrate is changed to Kapton or Polyamide, the power rating would most likely increase but would also significantly increase the cost.

5.6 Mechanical Characteristics

To protect the collinear array with frequency independent beam direction against mechanical stresses, the radiator is supported by high density polyethylene foam pads and enclosed in a heavy duty 76mm OD radome with a 6mm wall. The array is mounted on a low profile radial flange affixed to the radome, using silicone sealant and grub screws.

As most collinear array antennas are installed high above ground, they are subjected to severe weather include large swings in temperature strong winds and rain. Wind survival speed is an important figure, as it allows the selection of an array type and construction that is suitable for a particular environment. Wind load is calculated as an equivalent flat plate projected area in accordance with TIA329C, and wind gust ratings in accordance with AS1170.2:2002. The Torque is the twisting moment applied to the mounting hardware.

The proposed printed collinear array has been designed to fit the internal dimensions of an off-the-shelf radome. This radome is a 1.9 m section of the normal 6.5 m stocked length used for high gain corporate fed collinear arrays. As such the mechanical strengths of this radome are well within what would be required for an antenna of this size (refer to Table 5-6). The wind gust rating for the proposed antenna array ensures it can survive in excess of 240 km/h wind gusts without failure.

Table 5-6 Mechanical characteristics

Projected area	1270 cm^2
Lateral thrust @160 km/h	160 N
Wind gust rating	> 240 km/h
Torque @ 160 km/h	73 Nm
Length	1850mm
Radome	76mm
Mounting	89 mm diameter
Weight	3kg

5.7   Fixed beam tilt array

Where an array is mounted high above the intended coverage area, a fixed beam tilt can be applied to prevent interference to other services beyond the radio horizon allowing for frequency reuse and efficient network planning. There are two primary options for tilting the main beam of an array antenna. A mechanical tilt is normally applied to directional panels. This is provided by physically tilting the antenna via the mounting hardware design. Electrical beam tilt can be applied by offsetting the phase balance in the antenna. Under this condition, the phase front of the array is now forced to a gradient rather than parallel, the tilt in an omnidirectional antenna is imposed on the elevation pattern and distributed radially in the azimuth pattern.

To achieve electrical tilt, delay sections are placed in the feed network. In a corporate fed array this shift can be integrated into each power divider arm, resulting in lower distortion to the side lobe structure than when only the first branch is offset, and as such allowing for a greater tilt range. For a centre fed array based on series feed sub-arrays the delay is simply placed at the central feed point. The upper sub array has a phase advance over the lower array. This change in phase has an impact on the matching circuit and the side lobe levels, and

smaller tilt ranges are realized when compared to a corporate fed array. Series fed arrays can be tilted over a wider range but can only hold the tilt angle at a single frequency. In

Table 5-7, a table of collinear arrays with various feed methods and the typical tilt stability over a 10% bandwidth is presented. The worst case is the series fed array where the beam tilt at the lowest frequency is more than $10°$.

Table 5-7 Tilt stability characteristics of omnidirectional array feed technologies

Frequency (MHz)	850	870	900	940	960
Centre fed array	-5°	-4°	-4°	-4°	-5°
Corporate fed array	-3˚	-4˚	-3˚	-4˚	-3˚
Series fed dipole array	-13˚	-10˚	-8˚	-6˚	-4˚

A fixed down tilt is created in a centre fed array by applying phase shift at the central feed distribution as shown in Fig 5-25 (the "Coplanar waveguide (CPW)" discontinuity in the feed network) where the feed slot has been re-positioned in order to produce a differential offset in the phase. The phase shift magnitude and sign controls the amount and direction of tilt in the main lobe. In the proposed collinear array, down tilt is controlled by the location of the "Coplanar waveguide (CPW)" discontinuity slots   relative to centre axis of the array. (13) is used to calculate the required phase delay, and (14) determines the physical length difference needed to present the correct phase offset. A fixed phase offset is used to introduce an electrical down tilt to the array which is independent of frequency.

$\beta = phase\ shift°$

$\theta = (tilt\ angle)$

$d = distance\ between\ sources\ in\ mm$

$\lambda_g = guided\ wavelength$

5-166

$$\beta = \frac{360° \cdot d \cdot \sin \Theta}{\lambda} \qquad (13)$$

$$\ell = \frac{\beta}{360} \cdot \lambda_g = \text{physical shift in mm} \qquad (14)$$
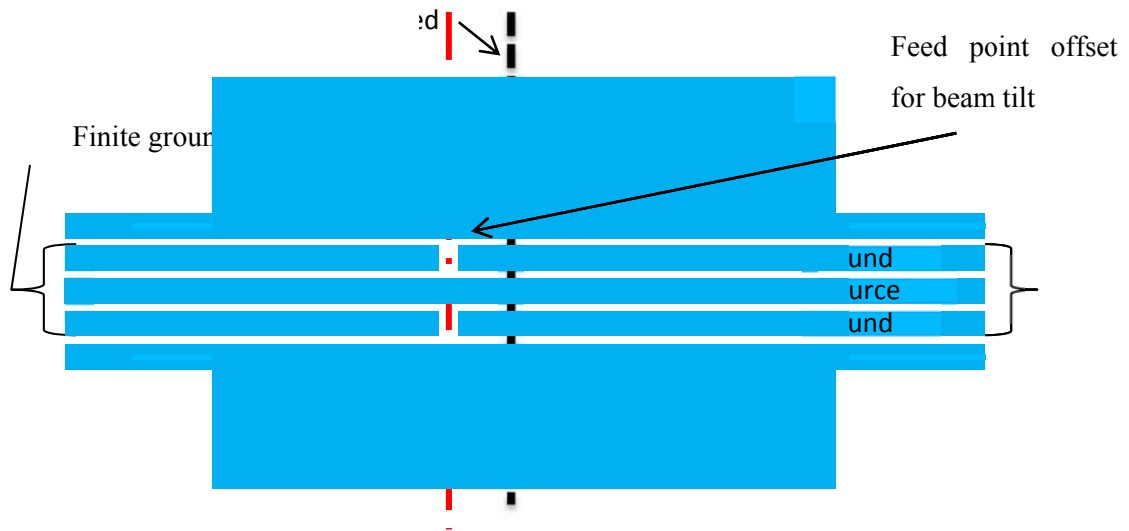
Fig 5-25   Adjustment of the "Coplanar waveguide (CPW)" feed point position to control tilt

5.7.1   Down tilt performance

The proposed planar array can be configured to provide fixed beam tilt by adjusting the position of the feed point. The limit for beam tilt is the upper side lobe level. Too much tilt will result in a side lobe equal in height to the main lobe and a loss in directivity assuming no other change in geometry. Practical centre fed arrays can tilt to approximately $4°$ from zenith before losing pattern stability.

To show the effectiveness of this method, a polar plot of a zero tilt collinear array of Fig 5-26 is compared to the same array with 4° down tilt shown in Fig 5-27   The 4° beam down tilt is stable within 4 ± 1°, and the first upper side lobe is 3 dB down from the main lobe at 960 MHz. A 4° down tilt is sufficient for most base station applications.

Having upset the phase balance, the application of beam tilt normally impacts on the reflection coefficient magnitude performance, as can be seen in Fig 5-28 for the 4° down tilt collinear array where the reflection coefficient magnitude has been reduced down to 9 dB. The realized broadband gain at beam maximum is also reduced by approximately 1 dB, as shown in Fig 5-29

It is possible compensate for the mismatch associated with beam tilt by optimizing the pattern shape to reduce the side lobes for a predetermined beam tilt. This can be achieved by reducing the element spacing.
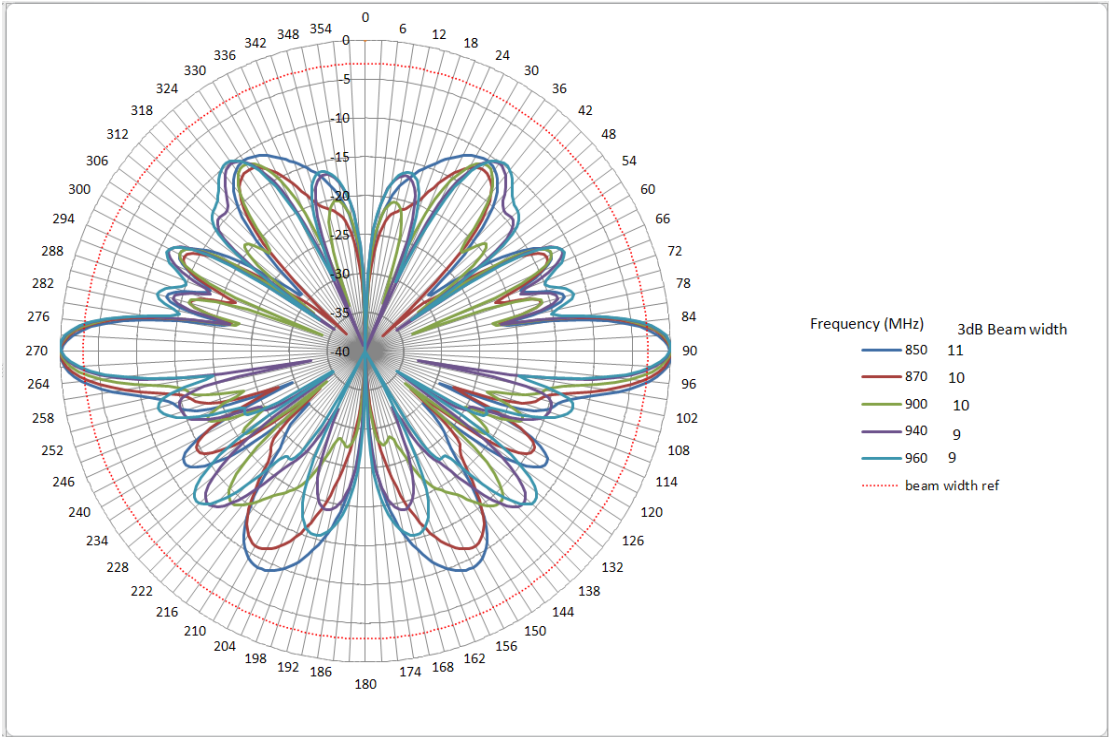
Fig 5-26 Vertical radiation pattern for the zero tilt collinear array
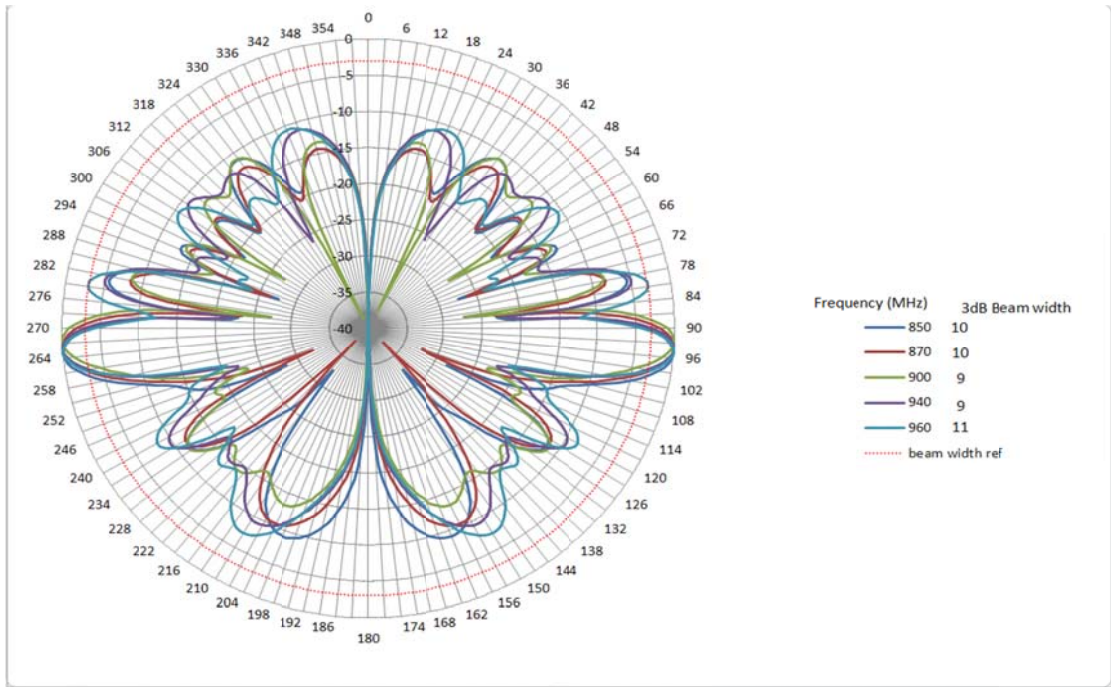
Fig 5-27 Vertical pattern for a 4° fixed beam tilt collinear array
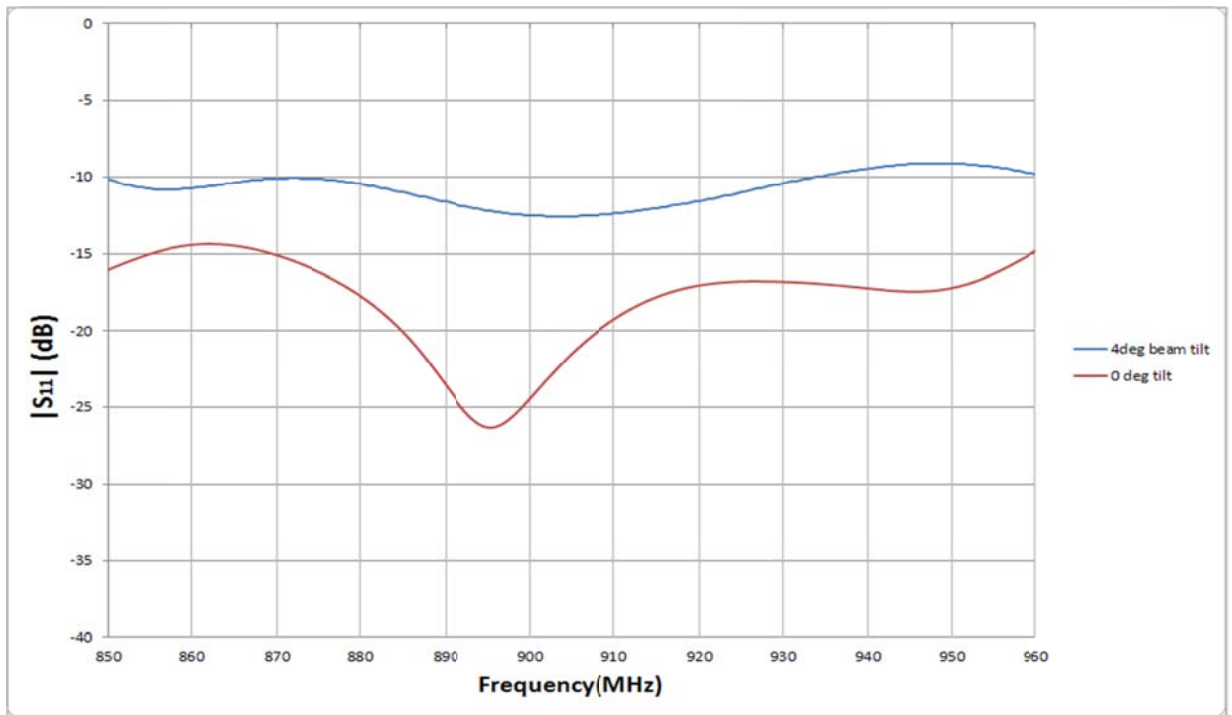
Fig 5-28 Reflection coefficient magnitude of array with 4°beam tilt compared to array with 0°beam tilt
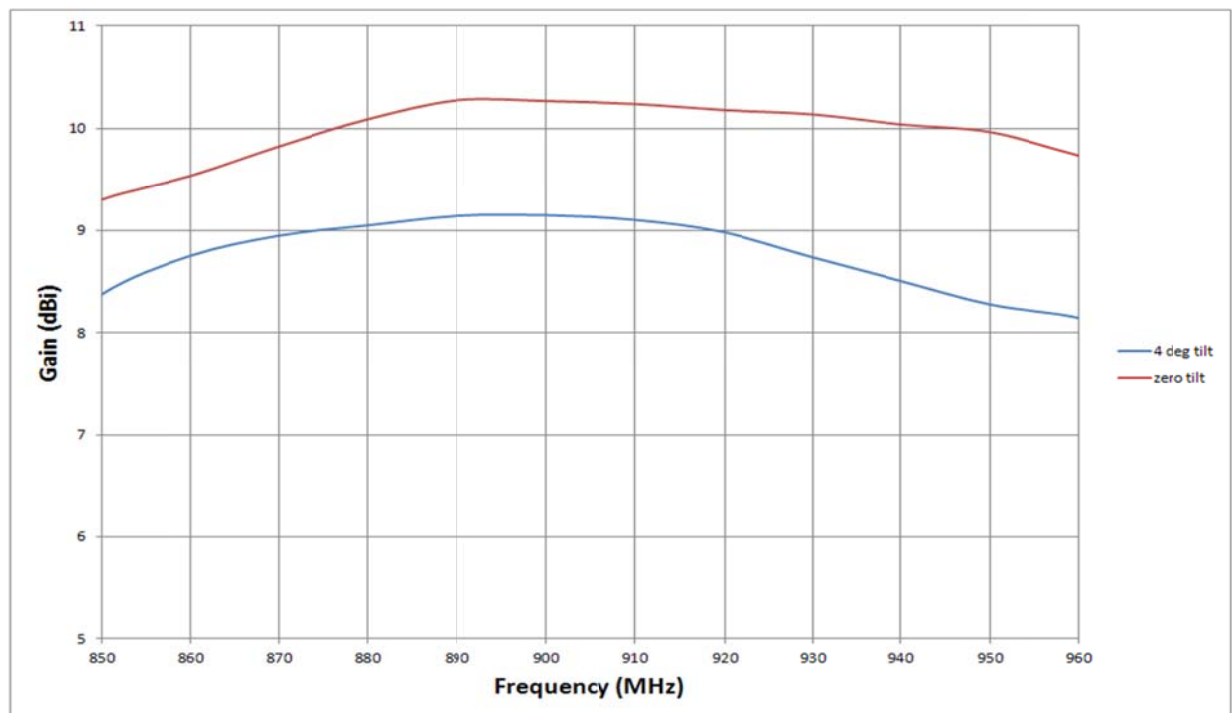
Fig 5-29 Gain comparison (pattern maximum) 4°tilted and 0° tilt array

5.8   Summary

In this chapter an omnidirectional six element "coplanar waveguide(CPW)" fed collinear array was assembled from the planar feed network, planar dipole elements and planar passive coupler components previously discussed in Chapters 2, 3 and 4. The array has the unique attributes wide band, effectively zero beam tilt over 10% bandwidth, and low passive intermodulation. It has been shown in simulation as well as experimentally that the "Coplanar waveguide (CPW)" based collinear arrays main objective of frequency independent beam direction has been achieved. The radiation pattern and gain of the array are typical for a six element centre fed array. The measured reflection coefficient magnitude performance is greater than 14 dB across the required bandwidth, although the measured response is slightly different to the simulation due to hand fabrication tolerances.

The intermodulation performance has been tested using passive intermodulation test equipment. The objective of low passive intermodulation has not been achieved, falling just short of the -150 dBc state-of-the-art levels. For low power systems, a PIM value of -140dBc is acceptable. It is expected that when the coaxial interface components are machined to higher tolerance and silver plated, the specified level of -150dBc can be met. The coupling interface has also been hi pot tested to 2.1 kV without failure. At this level the antenna can be used where PIP is expected to be less than 1 kW.

The mechanical specifications for the array have also been discussed. The array has been designed using a radome diameter commonly employed to support antennas greater than 5 meters long. The designed wind loading for the prototype collinear array is 240 km/h.

An example of a fixed down tilt in the proposed array has been presented. The impact of tilt on the critical parameters such as reflection coefficient magnitude, gain and side lobe level have been analysed and compared to the standard configuration of the "Coplanar waveguide (CPW)" fed collinear array with disturbance to the reflection coefficient magnitude observed and a gain reduction of approximately 1 dB recorded. The maximum tilt for a centre fed array is limited by two factors, side lobe level and reflection coefficient magnitude. The side lobe level must be low to prevent interference to other services, and the desired reflection coefficient magnitude performance must be maintained to minimize reflection losses that will have a negative impact on the realized gain.

Chapter 6   Thesis overview and proposed further work

The objective of this thesis is to investigate enhanced performance collinear antenna arrays with effectively zero beam tilt verses frequency. The array is to have comparable performance to the state of the art planar collinear arrays. To the author's knowledge, a high gain omnidirectional array of greater than two elements based on a "Coplanar waveguide (CPW)" centre feed architecture has not been reported. To progress this development, some guidelines and specifications were drawn against existing tubular metal construction antennas. The complete array including dipole elements is to be constructed on a single sided inexpensive flexible substrate. The design takes full advantage of modern reel-to-reel manufacturing techniques for large scale flexible printed circuits.

Electromagnetic simulation (using CST Microwave Studio) [40] is the key design method, providing a realistic representation of the array performance after initial circuit simulations. This accounts for the open and compact architecture of the feed network, which has a small level of interaction with the radiation pattern. As such the radiation pattern of the array is a key parameter for consideration during the design of the feed network and dipole elements.

6.1   Chapter 1 Summary - Background information

Chapter one reviews the state of the art in collinear array antennas. Performance comparisons between the fundamental collinear designs (i.e. centre fed, corporate fed and the lower cost series fed arrays) are presented. The key applications for each type of array are given, with a discussion on the limitations for each type of array.

6.2   Chapter 2 Summary - Feed Network

A "coplanar waveguide(CPW)" feed network architecture suitable for a centre fed planar collinear array is presented in Chapter 2. The feed design satisfies the dimensional and electrical requirements of the project. The theoretical circuit schematic of the feed network was devised, including all node impedances and transformer sections. The feed network characteristics have been analysed as a planar multi-port network with the aid of CST Design Studio and verified by an electromagnetic model using CST Microwave Studio.

In section 2.1, it was shown that by designing the "Coplanar waveguide (CPW)" main feed for higher impedance the overall width of the array can be reduced. This allows for a wider track spacing and relatively narrower width conductors to be used, resulting in an array that meets the mechanical constraints set by the selected radome tube. A secondary slot transmission line was used to distribute the energy from the main "Coplanar waveguide (CPW)" feed line to the dipole antenna elements of the array.

The limitations of the "Coplanar waveguide (CPW)" feed network was discussed in Section 2.2 related to the low effective thermal dissipation when compared to conventional metal tube construction. The minimum track spacing of 0.5mm imposed by standard reel to reel flexible printed circuit processing was also considered a constraint of this work. The method used to support the feed network with foam spacers is presented with a consideration for the RF transparency of this material.

A CST Design studio circuit model of the feed network has been created in Section 2.3 and port characteristics were analysed. The feed network is broken into its functional sections, and analysed to ensure appropriate amplitude and phase distribution to the antenna ports.

An electromagnetic model of the entire feed network was generated in Section 2.4 to verify the circuit simulations of Section 2.3. The feed network meets all of the electrical specifications, including operation in the desired frequency band, low transmission loss, and relatively stable phase profile.

6-173

6.3   Chapter 3 Summary - Planar dipole

Within an electromagnetic modelling environment, the operational parameters of the novel planar dipole element proposed for use in a collinear array have been analysed. The transition from a cylindrical dipole to a planar dipole was discussed, and further developed to allow for use in the collinear array proposed in this thesis. It was shown how this planar dipole is related to coaxially constructed dipoles in terms of current choking.

The proposed planar dipole is designed to meet the broad bandwidth and omnidirectional pattern specifications outlined in Chapter 1 by implementing augmentation techniques, namely slots and notches. The notches are used to compensate for reactance associated with the close proximity of the dipoles to the edge of the slotline feed. The slots augment the radiation pattern to improve directivity and reduce azimuth ripple, and to lesser extent assist in impedance matching. The proposed planar dipole is shown to be capable of a 15% bandwidth for VSWR < 2:1, whereas the conventional planar dipole shape typically achieves a 12% bandwidth. The novel planar dipole design meets the bandwidth required for base station applications, and is similar to a cylindrical dipole in terms of impedance and radiation pattern performance for the same volume.

6.4   Chapter 4 Summary - "Coplanar waveguide (CPW)" to Microstrip Passive coupler

In an effort to improve the mechanical stability of the coaxial cable connection to the feed network, a novel passive coupler transition was developed. A secondary feature of this transition is complete DC isolation of the array from the transmission equipment.

The majority of "Coplanar waveguide (CPW)" to microstrip transitions presented in the literature are aimed at frequencies above 1 GHz for*" monolithic microwave integrated circuit* (MMIC)" applications. In Section 4.2 a literature review indicated that the transition topologies generally have DC continuity in at least one of the conductors (signal and/or ground).

In Section 4.3 the novel "Coplanar waveguide (CPW)" to microstrip transition is presented. The proposed transition was implemented in order to increase the mechanical strength of the cable connection and eliminate solder processes. This transition has low loss, low PIM, incidental impedance matching, and is totally DC isolated from the input to output transmission lines. It provides sufficient mechanical isolation to enable a robust coaxial cable connection to the thin and flexible PET substrate employed.

In Section 4.4 the proposed coupler performance is determined using electromagnetic simulation. The insertion and reflection coefficient magnitude performance is explored with respect to key parameters that affect the coupling between the "Coplanar waveguide (CPW)" and microstrip transmission lines. As the output impedance (of the "Coplanar waveguide (CPW)") is different to the VNA measuring equipment, a commonly used back-to-back measurement technique was explained in Section 4.5. The passive coupling transition performance was then verified by testing a realized prototype of the back-to-back structure, with reasonable congruence to the simulated results. An insertion and reflection coefficient magnitude of < 0.5 dB and > 15 dB respectively was achieved over the frequency band of 850-960 MHz.

The transition assembly was detailed in Section 4.6, which consists primarily of a flexible 0.125 mm PET PCB laminated with the more substantial Arlon AD250 rigid microstrip substrate. The lamination and alignment of the planar substrates was investigated to determine the effect of manufacturing tolerance. The coupling structure was shown to be relatively insensitive to offsets of ± 3 mm. The solder-less assembly is expected to improve the PIM performance significantly. With complete passive coupling, the transition circuit is capable of coupling efficiently through dissimilar substrate dielectrics and thicknesses. This allows the collinear array described in this thesis fabricated on 0.125 mm thick PET substrate to be easily cabled and inspected during the assembly process.

6-175

6.5   Chapter 5 Summary - Complete array performance evaluation

In Chapter 5 an omnidirectional six element "coplanar waveguide(CPW)" fed collinear array was assembled from the planar feed network, planar dipole elements and planar passive coupler components previously discussed in Chapters 2, 3 and 4. The array has the unique attributes wide band, effectively zero beam tilt over > 10% bandwidth, and low passive intermodulation. It has been shown in simulation as well as experimentally that the "Coplanar waveguide (CPW)" based collinear arrays main objective of frequency independent beam direction has been achieved. The radiation pattern and gain of the array are typical for a six element centre fed array. The measured reflection coefficient magnitude performance is greater than 14 dB across the required bandwidth, although the measured response is slightly different to the simulation due to hand fabrication tolerances.

The intermodulation performance has been tested using passive intermodulation test equipment. The objective of low passive intermodulation has not been achieved, falling just short of the -150 dBc state-of-the-art levels. For low power systems, a PIM value of -140dBc is acceptable. It is expected that when the coaxial interface components are machined to higher tolerance and silver plated, the specified level of -150dBc can be met. The coupling interface has also been hi pot tested to 2.1 kV without failure. At this level the antenna can be used where PIP is expected to be less than 1 kW. The proposed collinear array has been subjected to high pot testing and passed the 2.1 kV limit as shown in Fig 1-12, that validating the electrical performance of the prototype.

The mechanical specifications for the array have also been discussed. The array has been designed using a radome diameter commonly employed to support antennas greater than 5 meters long. The designed wind loading for the prototype collinear array is 240 km/h.

An example of a fixed down tilt in the proposed array has been presented. The impact of tilt on the critical parameters such as reflection coefficient magnitude, gain and side lobe level

have been analysed and compared to the standard configuration of the "Coplanar waveguide (CPW)" fed collinear array with disturbance to the reflection coefficient magnitude observed and a gain reduction of approximately 1 dB recorded. The maximum tilt for a centre fed array is limited by two factors, side lobe level and reflection coefficient magnitude. The side lobe level must be low to prevent interference to other services, and the desired reflection coefficient magnitude performance must be maintained to minimize reflection losses that will have a negative impact on the realized gain.

6.6 Conclusion

A high performance centre fed collinear array with planar architecture has been presented. The modelled and measured radiation patterns show good congruence with a gain of 10 dBi and beam tilt less than one degree over a 10% bandwidth. A passive intermodulation value of -148 dBc has been achieved due mainly to the reduced number of electrical joints. A PIP test has shown that the transmission line can withstand an ionisation test at 2.1 kV.

This is as a result of increasing the line impedance and minimum track spacing >0.5mm.

The design constraint where the array must fit an existing 76mm diameter radome has been met. The array width has been restricted to 32mm. The passive coupling circuit has been effective with < 0.5 dB insertion loss with reflection coefficient <-14 dB over 10% bandwidth.

6.7 Proposed future work

Areas of further development for the enhanced performance collinear antenna array proposed in this thesis are based on the requirements for future communications networks.

6.7.1 Further development to improve radio site efficiency

As major network providers aim to increase the capacity for high speed digital communications and keep ahead of demand, the requirements for smaller cell sizes and high density lower power mesh networks are likely to increase [3].

This current development in printed circuit based collinear antennas allows for more elements to be fed without increasing the width of the assembly. This passive coupled architecture may also be developed to provide multiband performance as the CPW transmission line is not a frequency sensitive part of the array. Shorter slot lines could independently support other frequency bands interleaved or in series. In this case, the challenge will be to reduce mutual coupling detuning effects.

An increase in the directive gain is also possible as more elements are added. The challenge is to provide a suitable matching circuit and further improve the phase stability.

By increasing the number of fed elements to 12, results in a directivity of 15 dBi. This centre fed planar design allows for the expansion to greater numbers of elements an example of which is shown in APPENDIX E and radiation patterns in APPENDIX F through to M.

 Higher gain antennas with low power transmitters can improve the power supply consumption of a radio site, interference incidents can be reduced by decreasing the power of the transmitters and increasing the gain of the antenna.

The design can be scaled to higher bands where the physical size can be reduced.

The antenna bandwidth of the array can also be scaled to any frequency range between up to 1.2 GHz. The operational frequency is limited by the minimum track spacing of the printed circuit fabrication technique at 1.2 GHz.

6.7.2 Beam tilt control using new technology.

In chapter 5.7 there is an example of how beam tilt can be implemented in a planar architecture array. This was shown in modelling by shifting the feed point relative to the centre axis.

Recently there have been some encouraging developments into voltage variable dielectrics. These materials are potentially able to provide a remotely variable phase shift which could be used to control phase offset within the array antenna thereby controlling the amount of beam tilt. Currently the voltage required to shift the dielectric constant effectively is >=5 kV

6.7.3 Beam direction control to allow for frequency reuse

Another tool used by service providers to increase the capacity of a service is frequency reuse. This can allow a service to occupy the same channel frequency in a neighbouring cell. This can be provided by restricting the beam direction or by controlling the elevation beam angle. An example of beam direction control is shown in   APPENDIX M with the radiation patterns shown in APPENDIX O to. This could be of particular use to spatial diversity schemes such as MIMO services. A number of elements can be mounted to provide de-correlation suitable for MIMO applications.

An investigation into the use of high temperature substrates and thermal sinking in the design would allow for a power rating of up to 250 Watts.

REFERENCES

[1]   A. Jaybeam, "Global antenna solutions," 2012. [Online]. Available: www.amphenol-jaybeam.com. [Accessed 2012].

[2]   RF industries, "www.rfiemea.com/downloads/," 2011. [Online]. Available: http://www.rfiemea.com/downloads/PIP%20Ratingof%20Antenna.pdf. [Accessed 16 April 2012].

[3]   J. J. Fujimoto K, 'Mobile Antenna Systems Handbook, ' 1994'.

[4]   Stutzman, Warren L Thiel,Gary A , Antenna Theory and Design, First ed., John Wiley & Sons, Inc, 1981.

[5]   G. Wilson, "Electrical downtilt through beam steering versus mechanical downtilt," in *Vehicular Technology Conference 42nd vol 1 May 1992*, 1992.

[6]   H. Khodabakshi and J. A. Rashed-Mohassel, "Design of an electrical downtilt basestaion antenna," in *Microwave,Antennas,Propagation and EMC Technologies for Wireless Communications,IEEE International Symposium on*, 2005.

[7]   J. Hadzoglou, "Adjustable beam tilt antenna". USA Patent US 5,512,914, 30 apr 1996.

[8]   D. L. Runyon, "Vertical Electrical Downtilt Antenna". USA Patent US 6,864,837 B2, 8 March 2005.

[9]   R. Industries, "www.rfi.com.au," [Online]. Available: www.rfi.com.au. [Accessed 06 03 2012].

[10]   R. INDUSTRIES, "PIM and the effects it can have on your radio installation," 2011. [Online]. Available: media.wfonline.com.au/pdf/events/connect_rc11/presentation/pim-and-the-effects. [Accessed 03 May 2012].

[11]   Commscope, "PIM Happens," 2012. [Online]. Available: www.commscope.com. [Accessed 2012].

[12]   P. Lui and A. Rawlins, "Passive Non-linearities in antenna systems," in *IEE Colloquium on Passive Intermodulation Products in Antennas and related structures*, London, 1989.

[13]   R. C. Johnson, Antenna Engineering Handbook, third ed., United States of America: McGraw-Hill, Inc, 1993.

[14]   C. S. Franklin, "ANTENNA". Great Britain Patent 1,934,182, 7 November 1933.

[15]   TIA239.

[16]   C. Balanis, Antenna Theory Analysis and Design Third edition,, Wiley books, 2005..

[17]   H.Nakano, N.Chiba, "Numerical analysis of collinear monopole antennas with coils," *Electronic letters,* vol. Vol27, no. 12, 6 June 1991.

[18]   H. A. Wheeler, "A vertical antenna made of transposed sections of coaxial cable," *IRE Conv.Rec vol 4 pt 1 ,* pp. 160-164, 1956.

[19]   Akihide Sakitani, "Analysis of coaxial collinear antenna: Recurrence formula of voltage and admittances at connections," *IEEE Transactions on Antennas and Propagation,* vol. 39, no. issue, pp. 15-20, 1991.

[20]   G, J Bischak, "A new series of commercial base station antennas," *IRE Transaction on vehicular communications,* vol. 13, pp. 24-27, September 1959.

[21]   J. S. Brown, "An omnidirectional medium gain 460 MC base station antenna using simplified suppressors," *Vehicular Communications, IRE Transactions on,* vol. 9, no. 1, pp. 80-85, June 1957.

[22]   W. N. Caron, Antenna Impedance Matching, First ed., USA: The American Radio Relay League, 1989.

[23]   V.Stoiljkovic et al, "A Novel Dual Band Centre fed printed dipole antenna," *IEEE Antennas and Propagation Society International Symposium,* vol. 2, pp. 938-941, 22-27 June 2003.

[24]   Kin-Lu Wong. Fu-Ren Hsiao and Tzung-Wen Chiou, "Omnidirectional planar dipole array antenna," *IEEE Transactions on antennas and propagation,* vol. 52, no. 2, 2004.
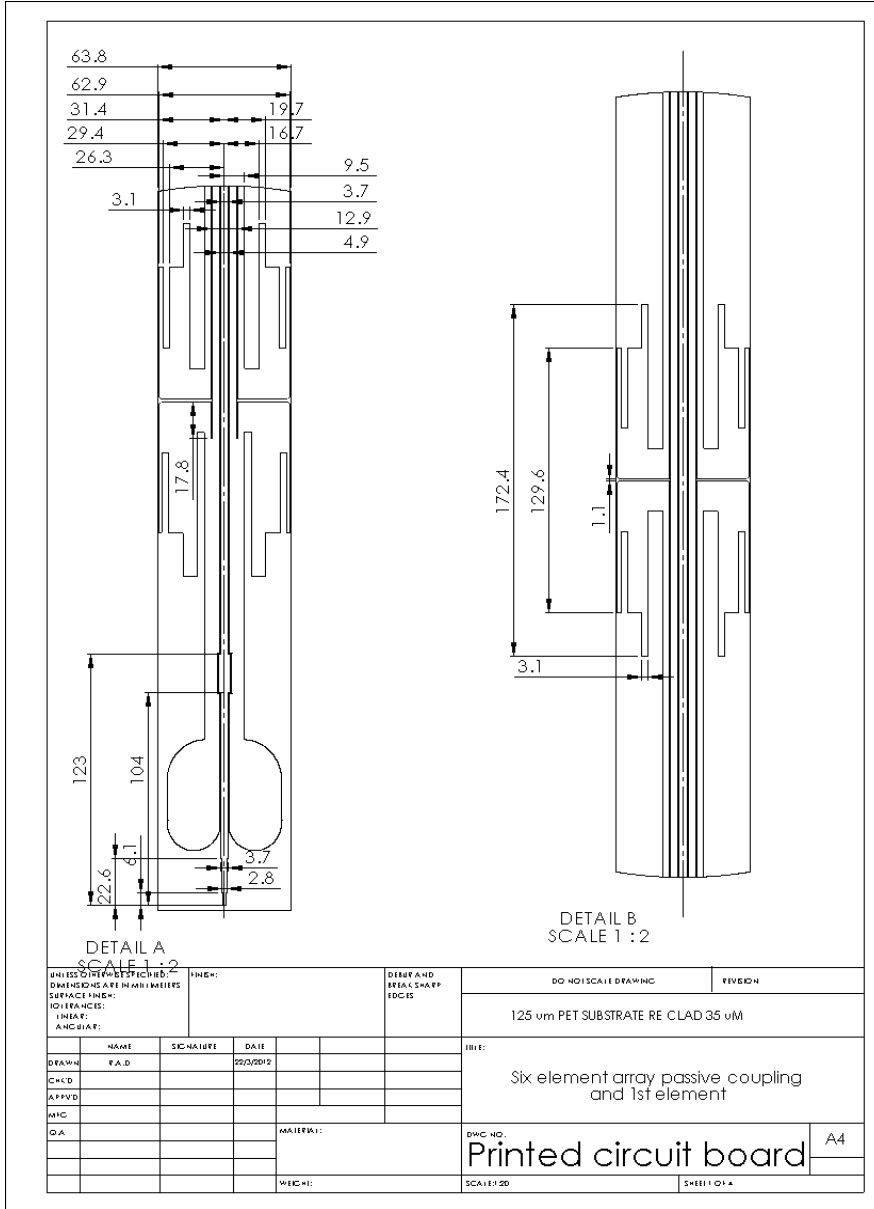
[25]   Yu Xiaole', Ni Daning2, Wang Wutul An Omnidirectional High-Gain Antenna Element for TD-SCDMA Base Station "Antennas, Propagation.

[26]   C. S. Franklin, "Antenna". Patent 1,957,949, 8 July 1929.

[27]   E. Harris, "Vertically polarised high frequency antenna array". USA Patent 2,750,859, 12 June 1956.

[28]   Lin, "Double skirt Omni directional dipole antenna". Patent US Pat No. US 4,963,879, 1990..

[29]   Akimoto, M.; Taga, T.;, "Characteristics of a bidirectional printed dipole antenna for street-microcellular systems," in *IEEE 46th Vehicular Technology Conference, 1996. 'Mobile Technologyfor the Human Race'.*, Akimoto, M.; Taga, T.;, 1996.

[30]   "rfs world antenna product finder," Radio frequency Systems, 03 July 2012. [Online]. Available: www.rfsworld.com. [Accessed 03 July 2012].

[31]   D. P. Kaegebein, "Parallel fed collinear antenna array". USA Patent 6057804, 10 Oct 1997.

[32]   Yoshihide Yamada,Hisahi Morishita,Yoshio Ebine, "A Multi-Frequency Base Station Antenna for Complex Cell Configurations," in *Vehicular Technology Conference 50th*, 2002.

[33]   Wei,Kunpeng et al., "A Triband Shunt-Fed Omnidirectional Planar Dipole Array," *Antennas and wireless Propagation Letters,* vol. 9, pp. 850-853, 2010.

[34]   McEwan, A.Z Jakal and N. J, "Collinear antennas based on coplanar waveguide," in *Antennas and propagation, Tenth International Conference on*, 1997.

[35]   I. Wolff, "Bismarckstr. 81,D-47048 design rules coplanar waveguides".

[36]   Nesic, Aleksandar Nesic and Dusan, "A new class of electromagnetically coupled printed antenna arrays," *Telecommunications in Modern Satellite, cable and broadcasting service, TELSIKS 2003 sixth international conference on,* vol. 1, pp. 206 - 209, 17 November 2003.

[37]   R. Brock and N. Safi, "PCB SPECS2," 10 April 2000. [Online]. Available: www.multiflexcircuits.com/documents/PCB_SPEC2.PDF.   [Accessed   Sunday
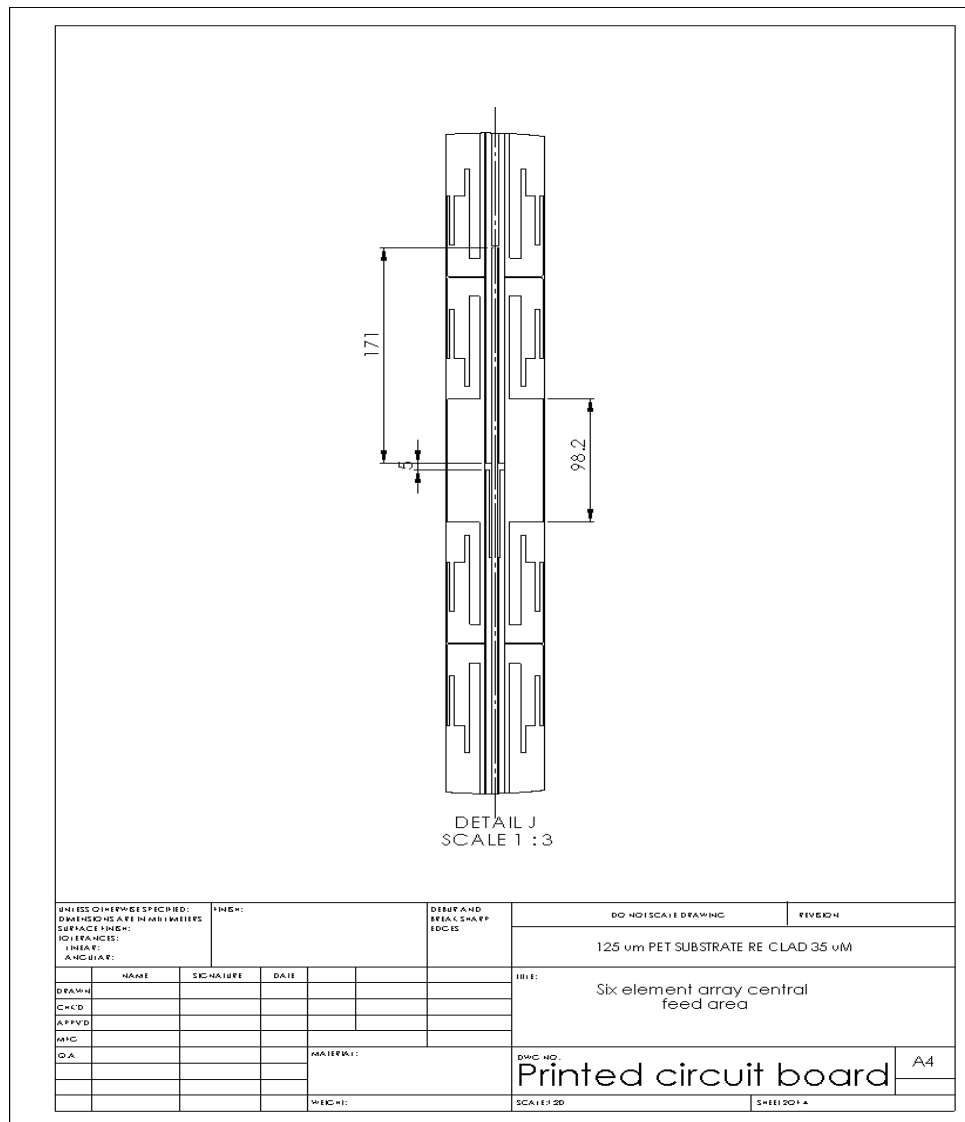
February 2012].

[38]   Corporation, Rogers, "Rogers corporation Advanced Circuit Materials," 2012. [Online]. Available: www.rogerscorp/documents/882/acm/Fabrication-Guidelines-Ultralam-3000-LCP-Materials.aspx. [Accessed 05 03 2012].

[39]   L. Zhu, "Characterisation of Finite-Ground CPW Reactive Series- connected elements for innovative design of Uniplanar M(H)MICs," *IEEE Transactions on microwave theory and techniques,* vol. vol50 NO 2, February 2002.

[40]   CST Microwave Studio.

[41]   R.A. Daly, W.S.T. Rowe, K. Ghorbani, ""Zero tilt omnidirectional collinear array antenna with coplanar feed."," *Electronics Letters, vol.47, no.6, pp.359-360, Mar.14 2011.,* vol. 47, no. 6, 17 March 2011.

[42]   C. Wen, "Coplanar Waveguide: A Surface Strip Transmission Line Suitable for Nonreciprocal Gyromagnetic Device Applications," *Microwave Theory and Techniques, IEEE Transactions on,* vol. 17, no. 12, pp. 1087- 1090, Dec 1969.

[43]   W. Heinrich, "Quasi-TEM Description of MMIC coplanar lines including conductor loss effects," *IEEE Microwave theory and techniques Transactions on,* vol. 41, no. 1, pp. 45-52, Jan 1993.

[44]   V.Deepu,S Mridula,R.Sujith,P.Mohanan, "Slotline fed dipole antenna for wide band applications," *Microwave and Optical Technology Letters,* vol. 51, no. 3, pp. 826-830, 2009.

[45]   L. Zhu, "Broad band microstrip to CPW transition via frequency dependent electromagnetic coupling," *IEEE Transactions on Microwave theory and techniques,* vol. 52, no. 5, pp. 1517-1520, May 2004.

[46]   Juno Kim, tatsuo Itoh, "A novel microstrip to Coplanar Waveguide transition for flip chip interconnection using electromagnetic coupling," in *28th European Microwave Conference*, Amsterdam, 1998.

[47]   Safwata ,A. M. E.; Zaki, K.A.; Johnson, W.;Lee, Chi H.,, "Novel transition between different configurations of planar transmission lines," *Microwave and Wireless Componenets Letters,* vol. 12, no. 4, pp. 128-130, April 2002.

[48]   C. Dengpeng, "A Broadband Microstrip-to-CPW Transition," *APMC 2005,* 2005.

[49]   Lin, T.H., ""Via-free broadband micro strip to CPW transition.","" *Electronics Letters" ,* vol. Vol. 37, no. No.15, pp. 960-961, 19th July 2001.

[50]   Gauthier,G.P.;Katehi, L.P and Rebeiz, G.M, "W-Band finite ground coplanar waveguide to microstrip line transition," in *Miicrowave Symosium digest IEEE MTT'S International*, 1998.

[51]   Liang Han; Ke Wu; Wei Hong; Xiao-Ping Chen, "Compact and Broad band Transition of Microstrip Line to Finite-Ground Coplanar Waveguide," in *Proceedings of the 38th European Microwave Conference*, Amsterdam, 27-31 Oct 2008.

[52]   A. LLC, "ARLON LLC," 2010. [Online]. Available: www.arlon-med.com/AD250C. [Accessed 05 03 2012].

[53]   Lin Zhu and Kathleen L. Melde., "On-Wafer Measurement of Microstrip-based circuits with a broad band vialess transition," *IEEE Transactions on advanced packaging,* vol. 29, no. 3, pp. 654-659, August 2006.
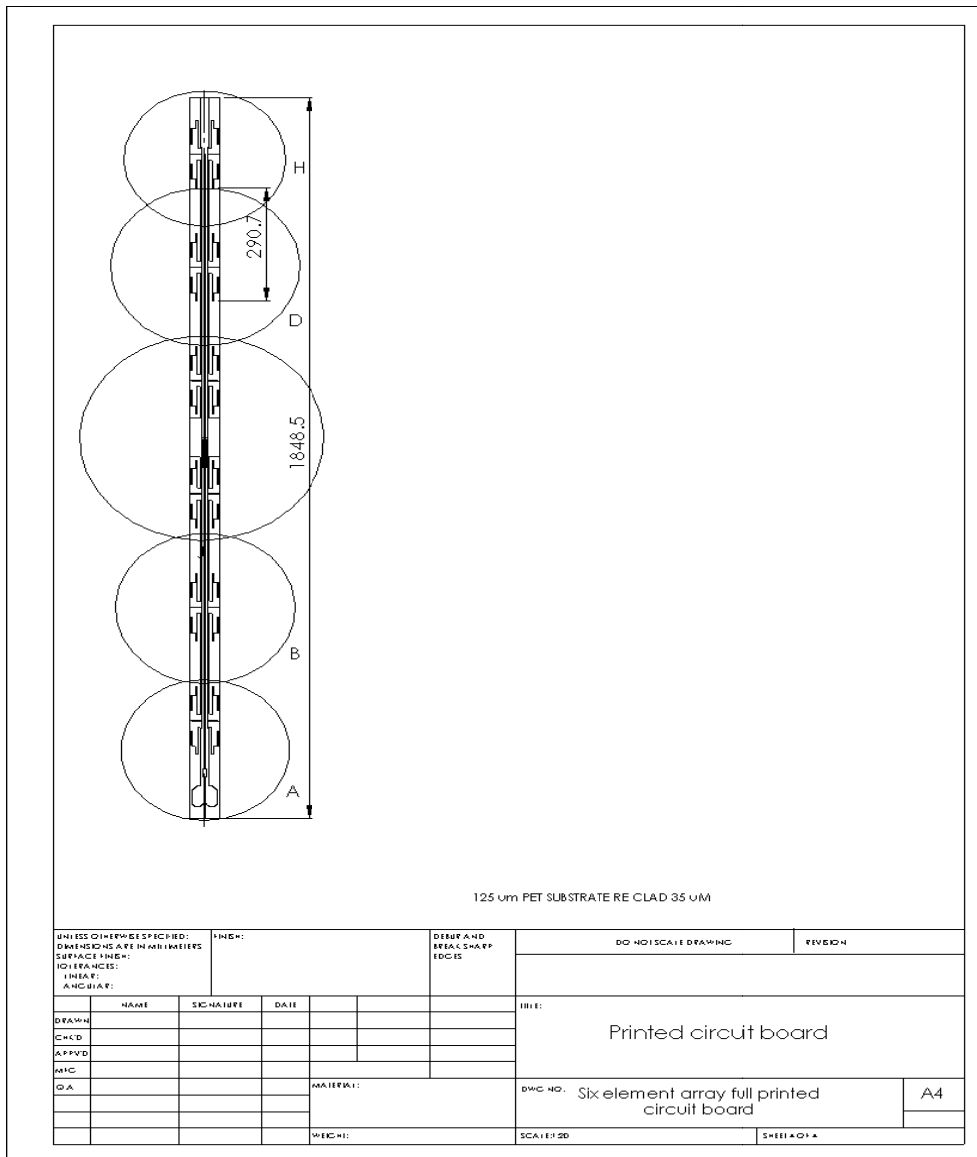
APPENDIX A The topology of the lower coupling and second dipole of the planar collinear array
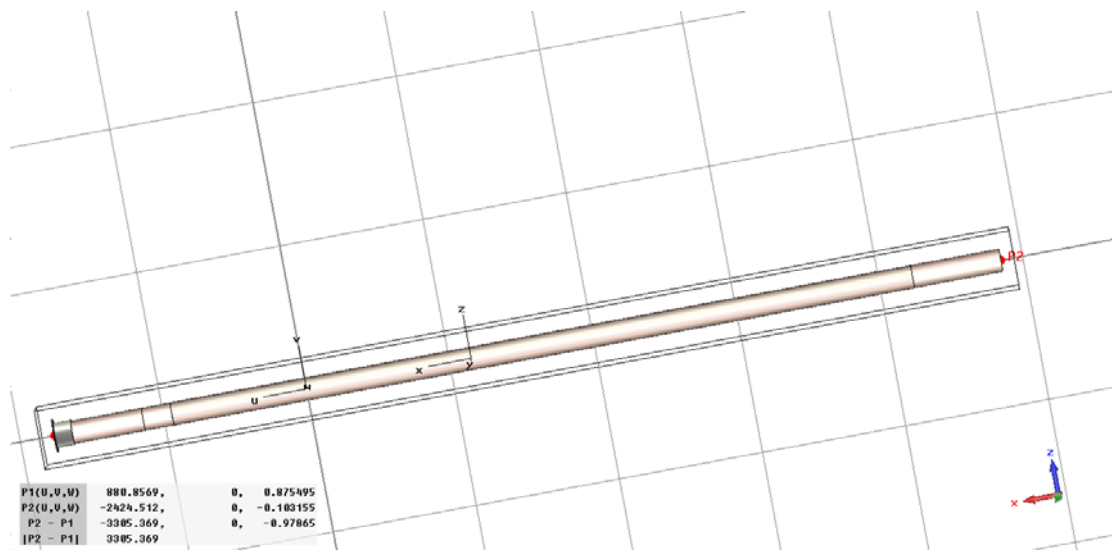

DETAIL A
SCALE 1 : 2

DETAIL B
SCALE 1 : 2

125 um PET SUBSTRATE RE CLAD 35 uM

Six element array passive coupling
and 1st element

Printed circuit board   A4

DETAIL J
SCALE 1 : 3

171

98.2

5

	NAME	SIGNATURE	DATE			TITLE:	
DRAWN							
CHK'D							
APPV'D							
MFG							
Q.A							

UNLESS OTHERWISE SPECIFIED:
DIMENSIONS ARE IN MILLIMETERS
SURFACE FINISH:
TOLERANCES:
  LINEAR:
  ANGULAR:

FINISH:

DEBUR AND
BREAK SHARP
EDGES

DO NOT SCALE DRAWING

REVISION

125 um PET SUBSTRATE RE CLAD 35 uM

Six element array central
feed area

MATERIAL:

WEIGHT:

DWG NO.

Printed circuit board

A4

SCALE:1:20

SHEET 20 > 4

DETAIL D
SCALE 1 : 2

DETAIL H
SCALE 1 : 2

	NAME	SIGNATURE	DATE			
DRAWN						
CHK'D						
APPV'D						
MFG						
Q.A						

UNLESS OTHERWISE SPECIFIED:
DIMENSIONS ARE IN MILLIMETERS
SURFACE FINISH:
TOLERANCES:
   LINEAR:
   ANGULAR:

FINISH:

DEBUR AND
BREAK SHARP
EDGES

DO NOT SCALE DRAWING   REVISION

125 um PET SUBSTRATE RE CLAD 35 uM

TITLE:

Six element array
5th and 6th element
Printed circuit board

MATERIAL:

WEIGHT:

DWG NO.   A4

SCALE: 1:20   SHEET 3 OF 4

APPENDIX E First model trial of a ten element array

APPENDIX F The broad band gain response of a ten element array
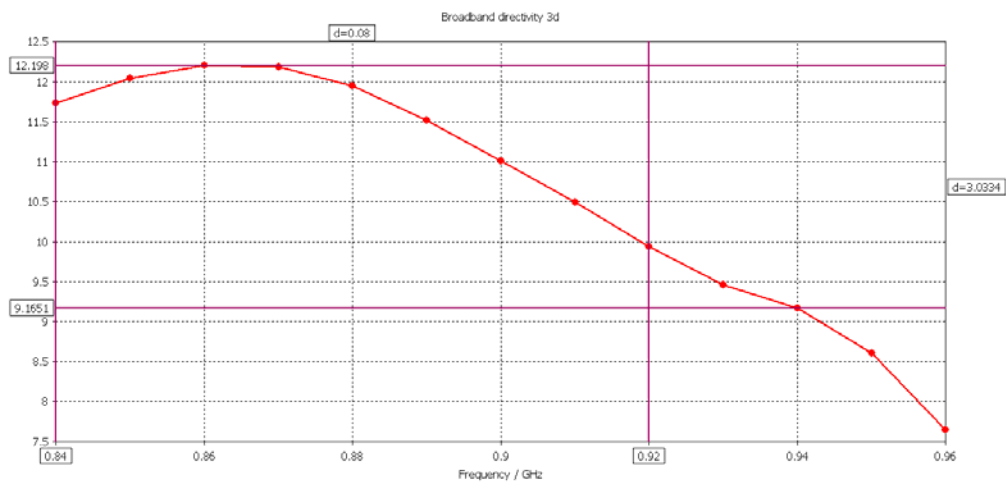
APPENDIX G The ten element "Coplanar waveguide (CPW)" array at 840 MHz

Farfield Directivity Abs (Epsilon=90)
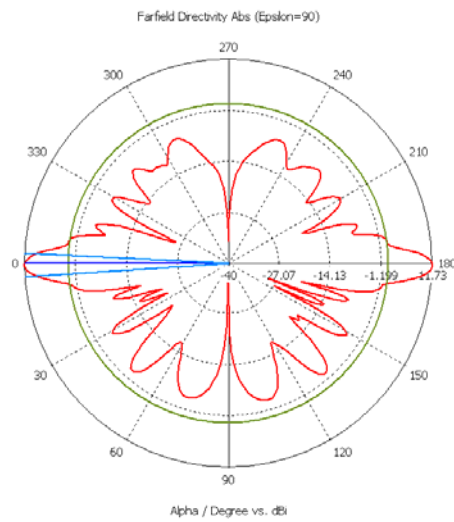
farfield (f=00.8400 GHz) [1]

Alpha / Degree vs. dBi

Frequency = 0.84
Main lobe magnitude = 11.7 dBi
Main lobe direction =   0.0 deg.
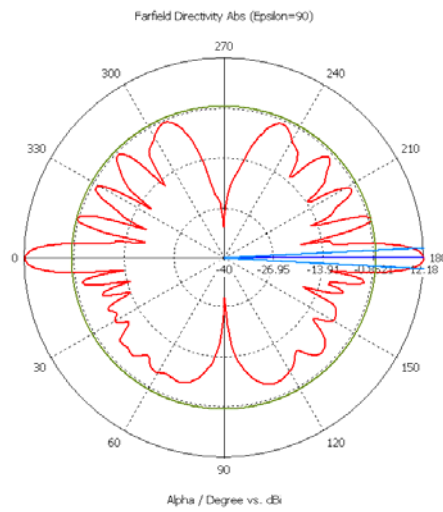Angular width (3 dB) =   6.7 deg.
Side lobe level = -11.1 dB

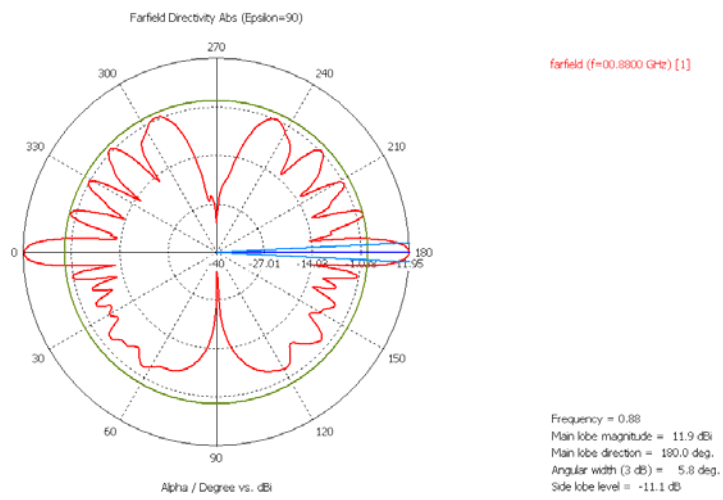APPENDIX H The ten element "Coplanar waveguide (CPW)" array at 850 MHz

Farfield Directivity Abs (Epsilon=90)
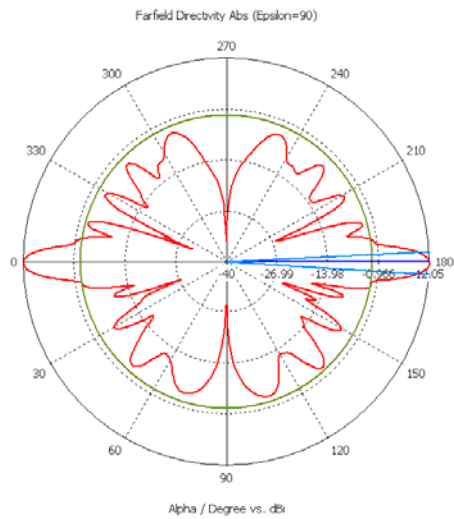
farfield (f=00.8500 GHz) [1]

Alpha / Degree vs. dBi

Frequency = 0.85
Main lobe magnitude = 12.0 dBi
Main lobe direction = 180.0 deg.
Angular width (3 dB) =   6.4 deg.
Side lobe level = -14.5 dB

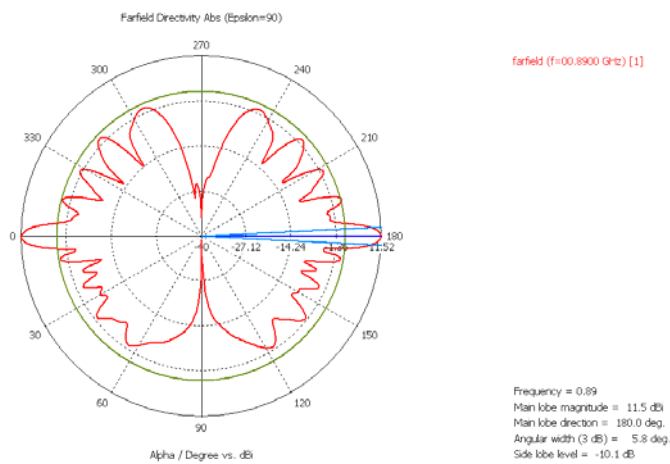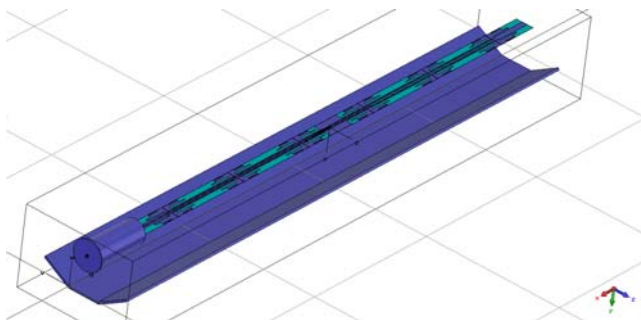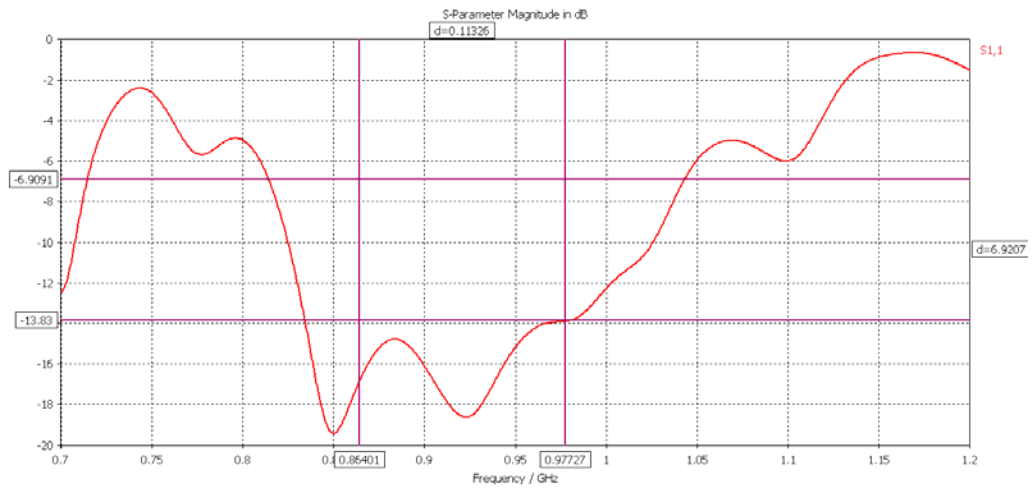APPENDIX I The ten element "Coplanar waveguide (CPW)" array at 860 MHz

Farfield Directivity Abs (Epsilon=90)
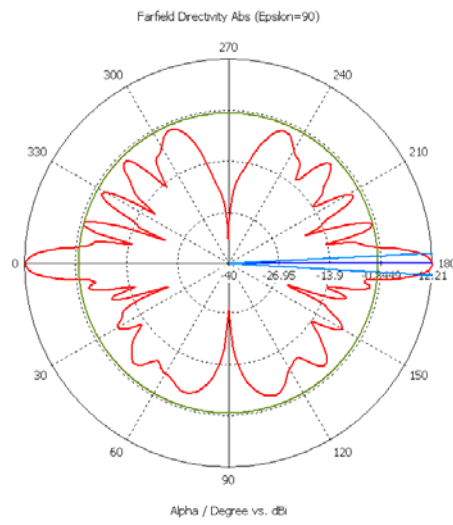
farfield (f=00.8600 GHz) [1]

Alpha / Degree vs. dBi

Frequency = 0.86
Main lobe magnitude = 12.2 dBi
Main lobe direction = 180.0 deg.
Angular width (3 dB) =   6.1 deg.
Side lobe level = -13.8 dB

APPENDIX J The ten element "Coplanar waveguide (CPW)" array at 870 MHz

Farfield Directivity Abs (Epsilon=90)

farfield (f=00.8700 GHz) [1]

Alpha / Degree vs. dBi

Frequency = 0.87
Main lobe magnitude = 12.2 dBi
Main lobe direction = 180.0 deg.
Angular width (3 dB) =   5.9 deg.
Side lobe level = -12.4 dB

6-191

APPENDIX K The ten element "Coplanar waveguide (CPW)" array at 880 MHz

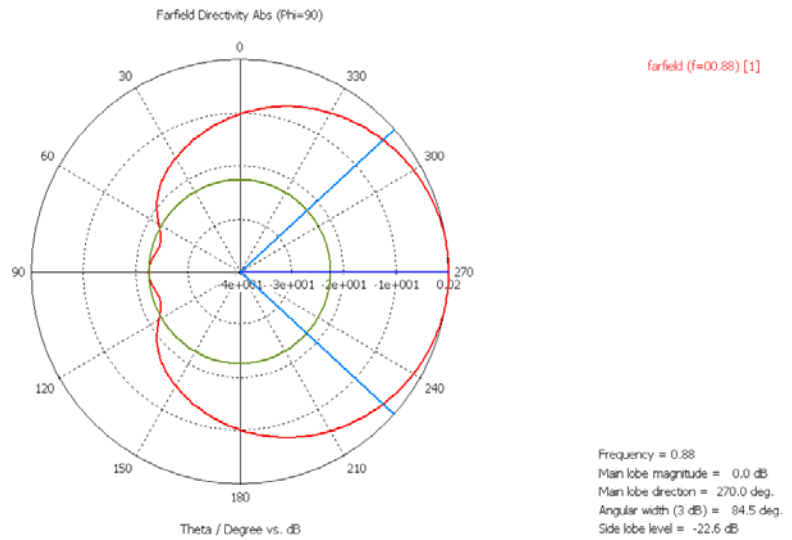APPENDIX L The ten element "Coplanar waveguide (CPW)" array at 890 MHz

APPENDIX M The "Coplanar waveguide (CPW)" panel array   (850-960 MHz, 15 dBi)
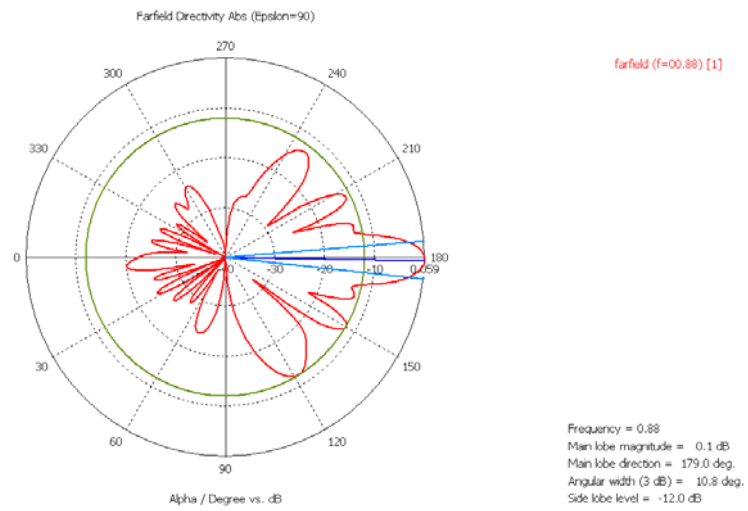
APPENDIX N The reflection coefficient for the "Coplanar waveguide (CPW)" six element panel array
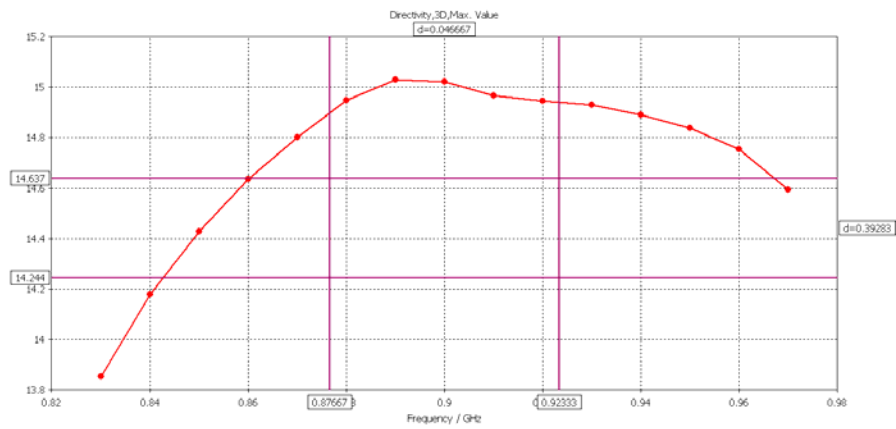

APPENDIX O The azimuth pattern for the "Coplanar waveguide (CPW)" six element panel array
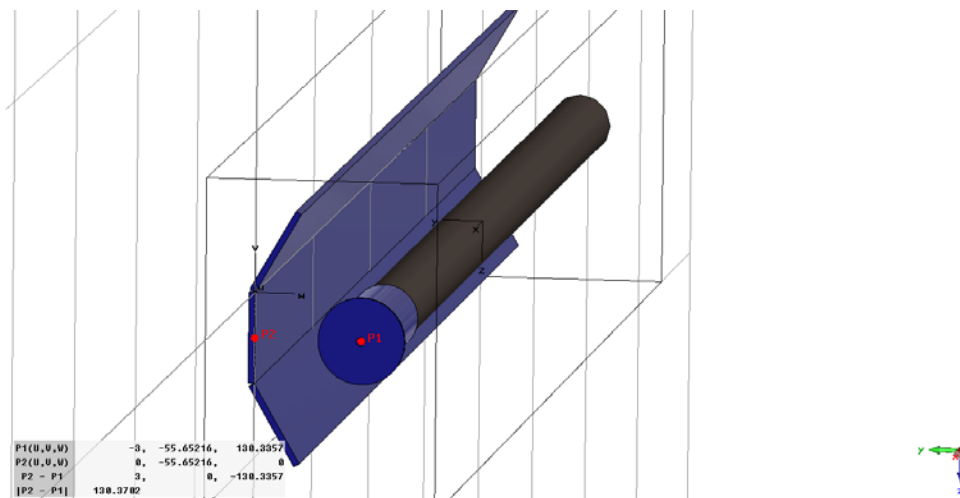
APPENDIX P The elevation pattern for the "Coplanar waveguide (CPW)" six element panel array
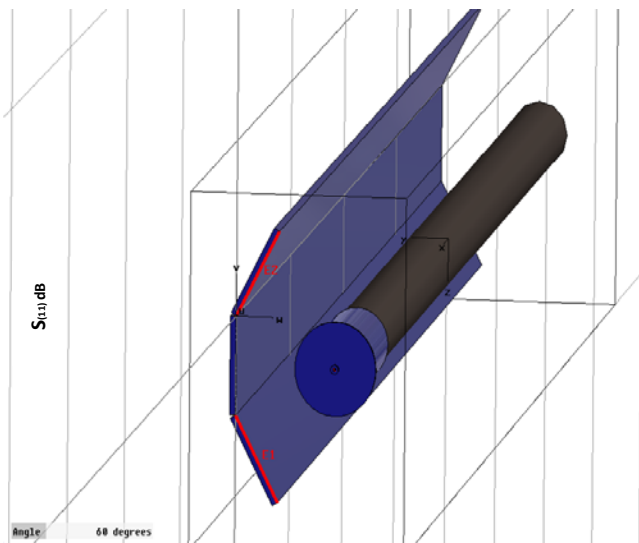

APPENDIX Q The broad band directivity response for the trough reflector array

APPENDIX R The spacing from the reflector to the array for the trough reflector array

APPENDIX S The angle of the trough reflector

APPENDIX T The reflection coefficient for omnidirectional and unidirectional array